Characterisation of a Rat Model of Post-herpetic Neuralgia

Wai Ling Kok

Thesis submitted for the degree of Doctor of Philosophy
University of Edinburgh
2006

Declaration

I declare that the work described herein is my own except where otherwise indicated. No part of this work has been submitted for any other degree or professional qualification.

Wai Ling Kok

Laboratory of Clinical and Molecular Virology
University of Edinburgh
Summerhall
Edinburgh
EH9 1QH

Acknowledgements

I would like to thank my supervisors Dr. Bob Dalziel and Professor Tony Nash for their useful advice, help, support and encouragement throughout this study. Special thanks go to Dr Margo Mark for her help and guidance particularly in *in vivo* experiments. Many thanks to Dr. Kevin Robertson for his help in the microarray study and data analyses. Also, Mr. Billy Smith and Mrs. Christine Forrest for their invaluable assistance.

I would also like to thank my labmates, Mrs Dawn Grant, Mr Colin Sharp, Dr Amanda Brass for their help and support. A big thank you to other PhD students and staffs in the department for their help and support along the way. I am also grateful to the Darwin Trust of Edinburgh for funding my studentship. Last but not least, thanks to my family and friends for all their love, motivation and encouragement.

Abstract

Varicella-zoster virus (VZV) is an alphaherpesvirus that causes childhood chickenpox, becomes latent in dorsal root ganglia (DRG) after primary infection and subsequently may reactivate to cause shingles (zoster). It is essential to understand the molecular mechanisms governing VZV latency and reactivation because approximately 20% of the human population will develop zoster and possibly experience post-herpetic neuralgia (PHN), a debilitating pain syndrome associated with zoster. Little is known about the pathogenesis of PHN mainly due to a previous lack of a good animal model and the cell-associated nature of VZV *in vitro*. An *in vivo* model of latent VZV in the adult rat was adapted. Foot reflex withdrawal responses has been shown to persist for longer than 60 days post infection similar to changes seen in PHN patients. The aim of this study was to further characterise this model so that it could provide a useful and unique opportunity to study the host-virus interaction involved in the pathogenesis of PHN. Nested PCR was able to detect viral DNA in the different lumbar DRG but the low level of latent gene expression gave no direct correlation of the observed behavioural changes with the pattern of gene expression in the infected DRG. Real-time PCR was developed, a quantitative assay, to investigate the low abundance of the latent genes. Viral DNA could also be detected in microdissected cells, which provide an alternative for investigating the gene expression in each subneuronal population in the DRG. Time course study showed that viral DNA was present in the infected DRG as early as 24 h post infection and viremia was not detected from 1 to 3 days post infection. This suggested that the spread of the virus is mainly through axonal pathway. Viral DNA could not be detected in other tissues like spleen, spinal cord and brain suggested that the latent virus was limited to the peripheral nervous system. RT-PCR was able to detect viral transcripts in infected cells but not in the latently infected DRG due to the low abundance of viral genome copy and limitation in detection of the assay. Therefore, a global approach was taken to look at the transcriptional activity in the latently infected neurones by carrying out a microarray experiment. The Rat Expression Set 230A GeneChip was used in this study. Of the 15,866 known rat genes represented on the RAE 230A, 5295 probe sets were not detected (33%). 9556 genes detected on both samples, of which 332 with altered expression and 57 of them has an increase in expression. Of the 57 increased in expression, 32 met the cut-off of 50 and only 5 had a fold change of greater than 2. Due to the tissue heterogeneity, only a small fraction of cells in the DRG harbours latent VZV. A small difference in expression might give rise to a large difference on a whole ganglion basis. Of the ten genes which were significantly regulated, prostaglandin D_2 synthase was validated by real time PCR and showed an upregulation of 2.7 fold corroborate with the results from microarray. PGD_2 was reported recently to have neuroprotective role in the nervous system. This study is in effect a pilot study giving a general overview of the changes within the DRG and thus provide a source of further characterisation of this model to understand the pathogenesis of the VZV induced allodynia.

Contents

Table of Contents

List of Figures

List of Tables

Abbreviations

AHV-1	Alcelaphine herpesvirus 1
ATP	Adenosine triphosphate
bp	Base pair
cDNA	Complementary DNA
cRNA	Complementary RNA
CSF	Cerebrospinal fluid
C_t	Cycle threshold
DIG-dUTP	Digoxigenin-labelled dideoxyuridine-triphosphate
DMEM	Dulbecco's modified Eagles medium
DMSO	Dimethyl sulphoxide
DNA	Deoxyribonucleic acid
dNTP	Deoxynucleoside triphosphate
DRG	Dorsal root ganglion
dsDNA	Double stranded DNA
DTT	Dithiothreitol
E.coli	*Escherichia coli*
EBV	Epstein-Barr virus
EDTA	Ethylenediaminetriacetic acid
ER	endoplasmic reticulum
EST	Expressed sequence tag
FCS	Foetal calf serum
HBV	Hepatitis B virus
HCMV	Human cytomegalovirus
HHV-6	Human herpesvirus 6
HSV-1	Herpes simplex virus 1
HSV-2	Herpes simplex virus 2
IE	Immediate early
IPKB	Ingenuity pathway knowledge base
IPTG	Isopropyl-β-D-thiogalactopyranoside
IVT	*In vitro* transcription
KSHV	Kaposi's sarcoma herpesvirus
LAT	Latency associated transcript
LB	Luria Bertani
LCM	Laser capture microdissection
M	Molar
MHC	Major histocompatibility complex
mM	Milimolar
mRNA	Messenger RNA
MW	Molecular weight
Oligo dT	Oligodeoxythymidine
ORF	Open reading frame
PBS	Phosphate buffered saline
PCR	Polymerase chain reaction
PHN	Post-herpetic neuralgia
PWT	Paw withdrawal threshold

RNA	Ribonucleic acid
rRNA	Ribosomal RNA
RT	Reverse transcriptase
RT-PCR	Reverse transcriptase PCR
SDS	Sodium dodecyl sulphate
SLR	Signal log ratio
SSC	Standard saline citrate
TAE	Tris acetate EDTA
TBS	Tris buffered saline
TE	Tris EDTA buffer
U	Unit
UV	Ultraviolet light
vol	Volume
VZV	Varicella zoster virus
X-gal	5-bromo-4-chloro-3-indoyl-β-D-galactoside

CHAPTER ONE

INTRODUCTION

1.1 Herpesviruses

Herpesviruses are ubiquitous in nature. Well over a hundred herpesviruses have been identified, infecting a range of vertebrates from humans to fish (Roizman et al. 1992) and at least one invertebrate, the Pacific oyster, *Crassostrea gigas* is host to a herpesvirus (Minson et al. 2000). In nature, each is closely associated with a single host species, and the most extensively studied hosts are infected by several distinct herpesviruses. The host-specific occurrence of herpesviruses indicates that they have evolved with their hosts over long periods of time and are exquisitely well adapted to them.

Herpesviruses are among the largest and most complex of viruses (Davison 2002). The virions are 200-250 nm in diameter, and consist of a linear double stranded DNA genome of 125-245 kbp, containing from around 70 to 200 genes. The DNA genome is packaged within an icosahedral capsid approximately 125 nm in diameter, embedded in a matrix known as the tegument which contains many virus-encoded proteins, wrapped in a lipid membrane containing several viral glycoproteins.

Most herpesviruses share four significant biologic properties (Roizman and Pellett 2001):

i) They encode enzymes for nucleic acid metabolism, DNA synthesis and processing of proteins.

ii) Viral DNA synthesis and capsid assembly occurs in the nucleus.

iii) The production of infectious progeny is invariably accompanied by cell death.

iv) All herpesviruses have a tendency to remain latent in their hosts.

1.1.1 Herpesviruses Classification

All herpesviruses are included in the family *Herpesviridae* based on their virion architecture. The members of the family *Herpesviridae* are classified into three subfamilies, the *Alphaherpesvirinae, Betaherpesvirinae* and *Gammaherpesvirinae*. The subfamilies are further classified into genera based on DNA sequence homology and similarities in genome sequence arrangement (see Table 1.1).

1.1.2 Alphaherpesviruses

Alphaherpesviruses as a group have a wide but variable host range with short reproductive cycles that cause rapid cytopathic effect and cell lysis (Roizman 1996). They have the ability to establish latent infections primarily but not exclusively in sensory ganglia. This subfamily contains the genera *Simplexvirus*, *Varicellovirus*, *Marek's disease-like virus*, and *infectious laryngotracheitis-like virus*.

1.1.3 Betaherpesviruses

Betaherpesviruses have a restricted host range, a long reproductive cycle and infection progresses slowly in culture (Pass 2001). Infected cells frequently become enlarged (cytomegalia) and carrier cultures are readily established. The virus can be

maintained in a latent state in secretory glands, lymphoreticular cells, kidneys and other tissues. This subfamily contains the genera *Cytomegalovirus*, *Muromegalovirus* and *Roseolovirus*.

1.1.4 Gammaherpesviruses

Gammaherpesviruses have a narrow host range. They are distinguished by their ability to establish latency in lymphocytes and are associated with malignancies, such as various B-cell lymphomas (Cesarman et al. 1995) and Kaposi's sarcoma (Chang et al. 1994). This subfamily contains the genera *Lymphocryptovirus* and *Rhadinovirus*.

1.1.5 Herpesvirus Sequence Arrangements

Based on their genome structure, herpesviruses can be divided into six groups arbitrarily classified A to F (Figure 1.1). In group A genomes, e.g. Channel catfish herpesvirus, sequence from one terminus is directly repeated at the other terminus. In group B genomes, such as herpesvirus saimiri, the terminal sequence is directly repeated many times at both termini. For those herpesviruses which infect humans (group C, group D and group E) unique structures are demonstratable. In the group C genomes, as exemplified by Epstein-Barr virus and Kaposi's sarcoma herpesvirus, a number of reiterations divide the genome into several well-delineated domains. The group D genomes, such as Marek's disease virus, have sequences from one terminus repeated in an inverted orientation internally. Thus, the DNA extracted from these virions consists

of two equal molar populations. For group E viral genomes, such as herpes simplex virus and cytomegalovirus, the genomes are divided into internal unique sequences whereby both termini are repeated in an inverted orientation. Thus, the genomes can form four equimolar populations, which differ in relative orientation of the two unique segments. Repeat sequences have not been identified in group F exemplified by tupaia herpesvirus.

Table 1.1 Herpesvirus classifications and some common disease(s)

Virus	Host	Disease(s)
Alphaherpesvirinae		
Simplexvirus		
Herpes simplex virus type 1 (HSV-1)	Human	Cold sores, keratitis
Herpes simplex virus type 2 (HSV-2)	Human	Genital lesions
Varicellovirus		
Varicella-zoster virus (VZV)	Human	Chicken pox, shingles
Simian varicella virus (SVV)	African Green monkey	Varicella
Equine herpesvirus 1 (EHV-1)	Horse	Spontaneous abortion
Equine herpesvirus 4 (EHV-4)	Horse	Rhinopneumonitis
Bovine herpesvirus 1 (BHV-1)	Cow	Infection of the upper respiratory tract
"Marek's disease-like viruses"		
Marek's disease virus type 1 (MDV-1)	Chicken	Marek's disease
Marek's disease virus type 2 (MDV-2)	Chicken	
Herpesvirus of turkeys (HVT)	Turkey	
Betaherpesvirinae		
Cytomegalovirus		
Human cytomegalovirus (HCMV)	Human	Mononucleosis, Congenital deformities, Ocular Disease
Muromegalovirus		
Murine cytomegalovirus (MCMV)	Mice	
Rat cytomegalovirus (RCMV)	Rat	
Roseolovirus		
Human herpesvirus 6 (HHV-6)	Human	Fever, rash in infants
Human herpesvirus 7 (HHV-7)	Human	
Gammaherpesvirinae		
Lymphocryptovirus		
Epstein-Barr virus (EBV)	Human	Burkitt's Lymphoma, Hodgkin's disease
Rhadinovirus		
Herpesvirus saimiri (HSV)	Squirrel monkey	Lymphoproliferative in heterologous hosts
Herpesvirus ateles (HVA)	Spider monkey	
Alcelaphine herpesvirus 1 (AHV-1)	Wildebeest	Malignant catarrhal fever
Human herpesvirus 8 (HHV-8)	Human	Karposi's Sarcoma
Rhesus rhadinovirus (RRV)	Rhesus monkey	Lymphoproliferative disease in immunosuppressed host
Murid herpesvirus 4 (MHV-4)	Mice	Lymphoma
Bovine herpesvirus 4 (BHV-4)	Cow	Conjunctivitis
Equine herpesvirus 2 (EHV-2)	Horse	Respiratory illness

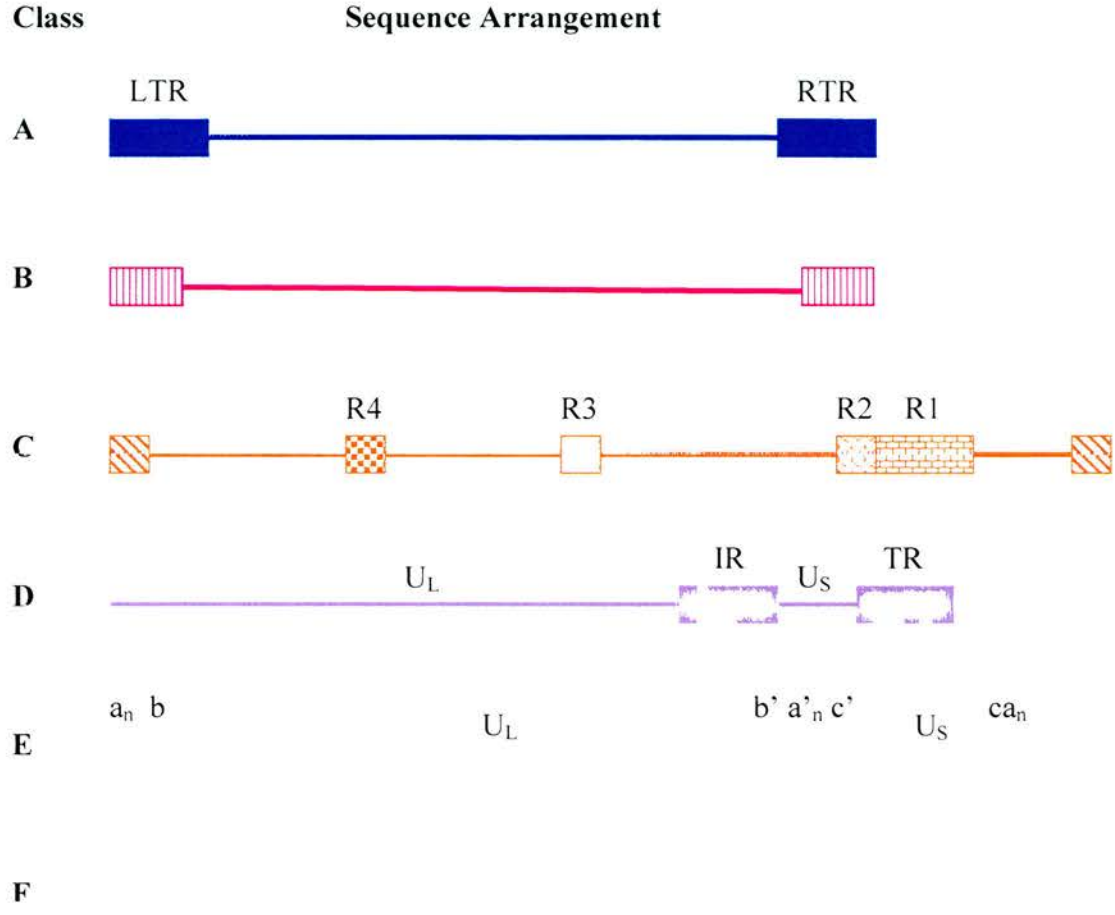

Figure 1.1 A schematic diagram of the sequence arrangements of *Herpesviridae*. The genomes A, B, C, D, E and F are exemplified by the channel catfish herpesvirus, herpesvirus siamiri, Epstein-Barr virus, Marek's disease virus, herpes simplex viruses, and tupaia herpesvirus, respectively. The horizontal lines represent unique or quasi-unique regions. The reiterated domains are shown as rectangles and are designated as left and right terminal repeats (LTR and RTR) for group A, repeats R1 to R4 for internal repeats of group C, and internal and terminal repeats (IR and TR) of group D. The termini of group E consist of two elements. One terminus contains n copies of sequence 'a' next to a larger sequence designated as 'b'. The other terminus has one directly repeated 'a' sequence next to a sequence designated 'c'. The terminal repeat 'ab' and 'ca' sequences are inserted in an inverted orientation (denoted by primes) separating the unique sequences into a long (U_l) and short (U_S) domains. Terminal reiterations in the genome of group F have not been described (adapted from Roizman and Pellett, 2001).

1.1.6 Herpesvirus Genes

Most herpesvirus genes contain a promoter or regulatory sequence spanning 50 to 200 bp upstream of a TATA box, a transcription initiation site 20 to 25 bp downstream of the TATA box, a 5' non-translated leader sequence of 30 to 300 bp, a single major open reading frame (ORF) with a translation initiation codon that meets the host requirements for efficient initiation, 10 to 30 bp of 3' non-translated sequence and a canonical polyadenylation signal with standard flanking sequences (Roizman and Pellett 2001). Exceptions do exist, e.g. HSV-1 $\gamma_1$34.5 gene has no TATA box and the promoter regulatory sequences of HSV late genes may be located 3' to the TATA box. Gene overlaps are common and ORFs can be expressed that are situated entirely antisense to the each other (e.g. HSV-1 $\gamma_1$34.5). A common feature of herpesvirus genomes is clusters of 3' co-terminal transcripts, each designed to express a different ORF. Most genes are transcribed by RNA polymerase II but EBERS of EBV, a set of small non-polyadenylated RNAs are synthesised by RNA polymerase III (Howe and Shu 1993). Most herpesvirus genes are not spliced. Nonetheless, every herpesvirus encodes at least some spliced genes to which splicing enable differential regulation of a gene at distinct parts of the virus life cycle. Herpesviruses also encode non-coding RNAs (e.g. latency-associated transcripts of HSV and the EBERs of EBV).

1.1.7 Herpesvirus Replication

As a prototype member of the *Herpesviridae*, observations made with HSV-1 can be applied to other members in the family in general, though details for individual

viruses can vary substantially. Like all herpesviruses, HSV displays both lytic and latent modes of interaction with its natural human host. Primary infection of epithelial cells produces the lytic response where virus replication occurs followed by cell death. Progeny virus particles then infect adjacent sensory neurons, establishing a lifelong latent infection, where by the virus genome persists in the cell as an episome, with no production of new virions and a restricted portion of the genome is transcribed.

Herpesvirus replication based on the HSV infection cycle can be divided into 8 stages, as illustrated in Figure 1.2. HSV entry into susceptible cells involves binding of the viral glycoproteins gC and or gB to heparan sulphate chains on the cell surface, followed by fusion of the viral envelope with a cell membrane (Spear et al. 2000). The fusion step requires four glycoproteins (gD, gB, gH and gL) and a cellular receptor that binds gD. Deletion of the genes for any one of these four glycoproteins is lethal and results in production of virions that can bind to cells, provided gC is present but cannot penetrate (Mettenleiter 2000). Binding of gD to one of these receptors triggers envelope-fusion and release of the viral nucleocapsid and tegument into the cell cytoplasm. At least four different membrane-bound molecules can serve as gD receptors (Spear and Longnecker 2003): HVEM (herpesvirus entry mediator), a member of the tumor necrosis factor receptor superfamily, nectin-1 and nectin-2, which are immunoglobulin (Ig) superfamily members and specifc sites in heparan sulphate generated by certain 3-O-sulfotransferases. After fusion of the envelope to the plasma membrane, some tegument proteins remain in the cytoplasm whereas others are either transported to the nucleus or remain associated with the capsid. The capsid with associated tegument structures is then transported through the microtubular network to the nuclear pore.

Upon entry into the nucleus, the viral DNA immediately circularises. Viral DNA is transcribed throughout productive infection by host RNA polymerase II, but with the participation of viral factors at all stages of infection. Viral gene expression is co-ordinately regulated and sequentially ordered in a cascade fashion and three broad classes of genes have been identified. These are the immediate early (IE or α), early (E or β) and late (L or γ). The IE genes, which do not need prior viral protein synthesis for their expression, are the first to be expressed in the nucleus following viral entry. Transcription of IE genes is activated by VP16, a major component of the HSV tegument (Campbell et al. 1984). VP16 acts through the target sequence TAATGARAT, which is present in at least one copy in all HSV IE promoters. TAATGARAT is a binding site for the cellular factor Oct 1, a member of a protein family initially characterised by the ability to bind the 'octamer' sequence ATGCAAAT (Sturm et al. 1988). Upon release from the tegument, VP16 binds to a cellular protein called host cell factor (HCF), which carries VP16 into the nucleus. The VP16-HCF complex binds to Oct 1/TAATGARAT, forming the activator complex to promote the expression of the IE genes.

Six HSV IE genes (ICP0, ICP4, ICP22, ICP27, ICP47 and $U_s1.5$) are expressed first, and five of these (ICP0, ICP4, ICP22, ICP27 and $U_s1.5$) encode regulatory proteins that stimulate expression of the E and L genes (Roizman and Sears 1995). The E genes are activated next, giving rise to proteins required for replication of the viral genome. Viral DNA replication then ensues, augmenting IE-dependent expression of the L genes that encode the structural components of the virion (Roizman and Sears 1995). The bulk

of viral DNA is synthesised by a rolling circle mechanism, yielding concatemers which, are cleaved into monomers and packaged into capsids. Replication of HSV-1 DNA requires seven virus gene products, comprising an origin binding protein, a single-stranded DNA binding protein, a DNA polymerase composed of two subunits and a helicase primase complex composed of three gene products. Homologues of all but the origin binding protein have been identified in all three herpesvirus subfamilies.

Assembly occurs in stages; after packaging of DNA into preassembled capsids, the virus matures and acquires infectivity by budding through the inner lamella of the nuclear membrane. However, the transit of virions from the space between the inner and outer nuclear membranes to the subcellular space is less well defined (Roizman and Pellett 2001). It has been suggested that the virus may become de-enveloped by fusion with the nuclear membrane and may then be re-enveloped in the Golgi compartment. The alternative theory is that the virion buds through the outer nuclear membrane, with the envelope intact and then enters the Golgi already enveloped. Whilst in the Golgi, the oligosacharrides of the virion glycoproteins are processed by Golgi enzymes. The enveloped virions are transported through the Golgi to the cell surface in vesicles, where they are released from the cell.

1.1.8 Herpesvirus Latency

Latent infections can be characterised by three general properties: i) expression of productive cycle viral genes is absent or inefficient; ii) immune detection of the cell harbouring the latent genome is reduced or eliminated and iii) the viral genome itself

persists intact so that at some later time a productive acute infection can be initiated to ensure spread of its progeny to a new host (Flint et al. 2004). The latent genome can be maintained as a non-replicating chromosome in non-dividing cells such as neurones e.g. herpes simplex virus (HSV) and varicella zoster virus (VZV) or become an autonomous, self-replicating chromosome in a diving cell e.g. Epstein-Barr virus (EBV) or be integrated into a host chromosome e.g. adeno-associated virus.

Such a 'long term parking' of a viral genome in the latent infection is remarkable for its stability. A balance among the regulators of viral and cellular gene expression must be maintained. Generally, only a restricted set of viral gene products is made (Millhouse and Wigdahl 2000). Viral proteins required for productive replication may not be produced at all, a pattern exemplified by HSV. In contrast, some herpesviruses's viral genome was not entirely quiescent during latency, as is the case for EBV. At least nine viral proteins important for modulating the host immune responses are expressed in latently infected cells (Crawford 2004).

Latent genomes retain the capacity to replicate and cause disease upon reactivation. If latency is to have any value as a survival strategy, there must exist a mechanism for reactivation so that infectious virions can spread to other hosts. The precise molecular mechanisms that lead to reactivation from the latent state are not fully understood and may differ from one virus to another. Reactivation may occur following a variety of local or systemic stimuli such as physical or emotional stress, fever, exposure to ultraviolet light, tissue damage and immune suppression. Although all herpesviruses remain latent in a specific set of cells, the exact cell in which they remain latent varies from one virus to another (Roizman and Pellett 2001). For example,

whereas latent HSV has been detected only in neurons, latent EBV has been found primarily in B lymphocytes.

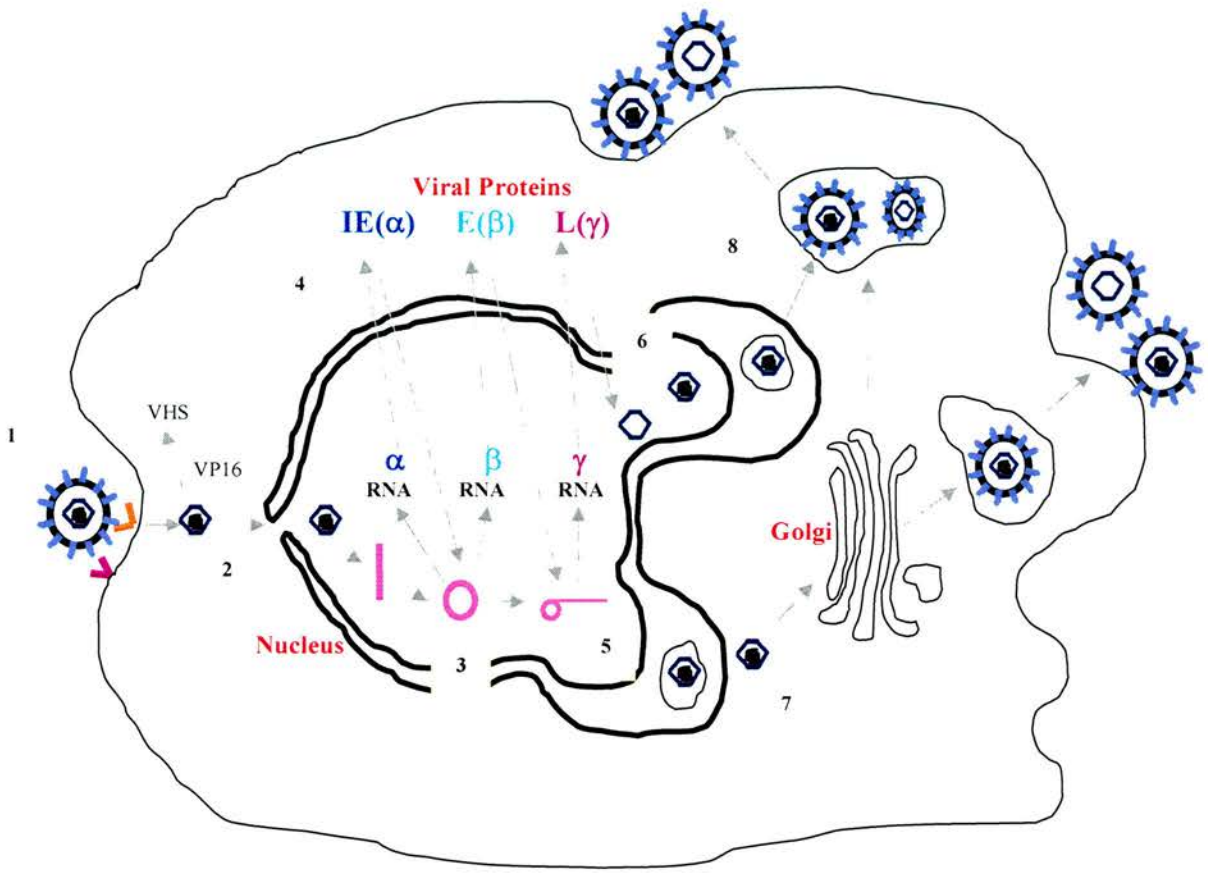

Figure 1.2 General overview of herpesvirus replication, based on HSV. 1: The virus initiates infection by the fusion of the viral envelope with the plasma membrane following attachment to the cell surface. 2: Fusion of the membranes releases two proteins from the virion: capsid and tegument proteins: VHS shuts off protein synthesis while VP16, which activates transcription of viral genome is transported to the nucleus. 3: The capsid is transported to the nucleus and immediately circularises. VP16 interacts with the host transcriptional components to stimulate transcription of the immediate-early genes. 4: A cascade of viral immediate-early (IE or α), early (E or β) and late (L or γ) transcripts and proteins are synthesised. 5: Viral DNA replication follows a rolling circle mechanism, which yields head-to-tail concatemers of unit-length viral DNA. 6: Nucleocapsids are assembled and package newly synthesised DNA. Controversy exists regarding the mode of nucleocapsid egress from the nucleus, the site of envelopment and the pathway leading to release of particles from the infected cell. Two general pathways of viral egress, 7: The envelope fuses with the outer nuclear membrane, de-enveloping the capsid and releasing it into the cytoplasm. The capsid buds into the Golgi apparatus, forming an enveloped virion, which is transported to the surface by vesicular transport. Alternatively, 8: The virion particle buds through the outer nuclear membrane and is transported by vesicular movement through the Golgi apparatus to the exterior of the cells (adapted from Cohen and Straus, 2001).

1.2 Varicella zoster virus

Varicella zoster virus (VZV) is a herpesvirus, classified in the subfamily alphaherpesvirinae. This subfamily also contains the human herpes simplex virus types 1 and 2 (HSV-1, HSV-2), which are members of the genus simplexvirus and the animal herpesviruses, pseudorabiesvirus (PRV), equine herpesvirus types 1 and 4 (EHV-1, EHV-4) and simian varicella virus (SVV), which have been grouped with VZV into the genus varicellovirus (Davison 2002). VZV is often compared to closely related and better-studied herpesviruses for insights into its molecular biology, particularly HSV-1.

VZV is a ubiquitous human herpesvirus and is the causative agent of two diseases, varicella (chicken pox) following primary infection and herpes zoster (shingles) following reactivation from a latent infection in sensory ganglia of affected dermatomes (Weller 1996). Primary VZV infection is associated with a cell-associated viremia and a diffuse cutaneous rash. A variety of stimuli can induce this latent virus to reactivate, travel back down the axons and produce a new round of productive infection at the site of initial infection.

Herpes zoster is a pressing medical problem possibly because it may be followed by severe neuropathic pain, post herpetic neuralgia (PHN), which is resistant to therapy (Gann and Whitley 2002). The seriousness of VZV as a public health hazard has been ameliorated by the development of an effective vaccine (Arvin and Gershon 1996). Nevertheless, VZV persists as a problem because of the existence of a large pool of

potentially infectious VZV in adults that could serve as a long-lasting reservoir from which the sporadic reactivation of VZV provides a persistent source of wild-type VZV.

1.2.1 Morphology

The VZV particle, like all other herpesviruses, is comprised of four major elements: the core, the nucleocapsid, the tegument and the envelope (Figure 1.3). Existing data regarding VZV structure and morphology are consistent with the models developed for HSV. Recent advances in electron-cryomicroscopy and three-dimensional image reconstruction techniques have led to many studies that have greatly extended our knowledge of herpesvirus architecture (Butcher et al. 1998), (Trus et al. 1999). These studies reveal a high degree of conservation in overall herpesvirus capsid structure. All herpesvirus capsids studied to date are organised in a T=16 icosahedral lattices composed of 150 hexamers and 12 pentamers. Heterotrimeric structures known as triplexes are located between these hexamer/pentamer structures at local 3-fold symmetry axes. Whereas HSV nucleocapsids have electron-dense cores, VZV nucleocapsids obtained from virus grown in cell culture often lack dense cores, perhaps reflecting the low infectivity of VZV released from cultured cells. The tegument, which has long been considered an amorphous mass of proteins, has been shown to have an ordered structure and forms an asymmetric cap in mature HSV-1 virions (Grunewald et al. 2003). The product of VZVORF10 was found in its tegument together with IE proteins encoded by VZVORFs 4, 62 and 63 (Kinchington et al. 1992). The enveloped particle has a pleomorphic to spherical shape with a diameter of 180-200 nm. Spikes

interspersing the envelope are made up of glycoproteins, which are approximately 8 nm. The VZV particle is fragile, its lipid envelope renders VZV susceptible to disinfection by organic solvents and the particle is subject to degradation by physical and chemical treatments (Cohen and Straus 2001).

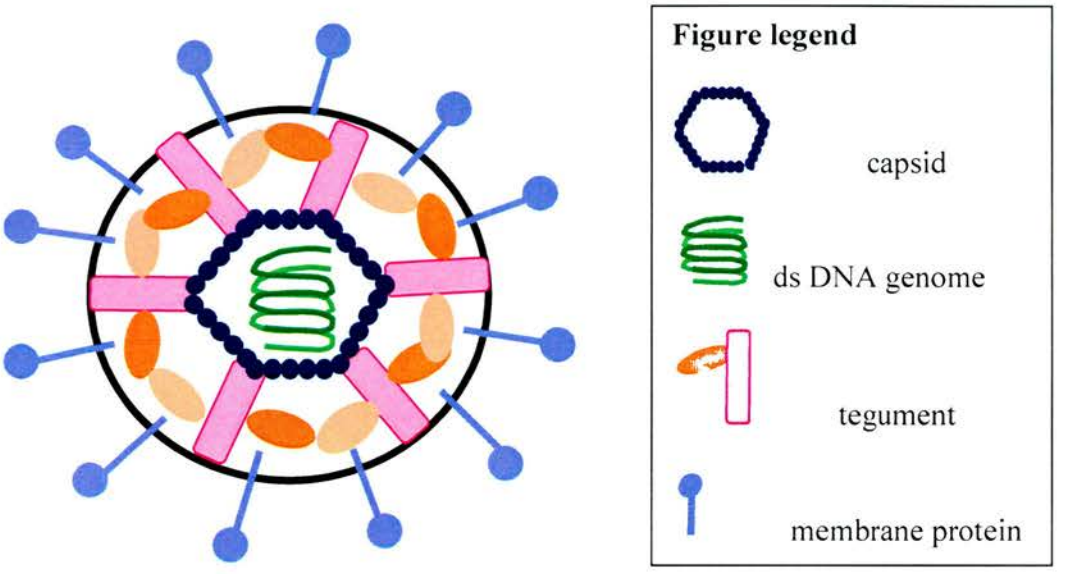

Figure 1.3 A schematic diagram of VZV. The VZV virion consists of a nucleocapsid surrounding a core that contains the linear double-stranded DNA genome. A protein tegument separates the capsid from the lipid envelope, which incorporates the major viral glycoproteins presumed to mediate cell entry.

1.2.2 Genome Organisation

The complete DNA sequence of the VZV Dumas strain was first reported in 1986 (Davison and Scott 1986). The VZV genome is a linear double-stranded DNA of about 124 884 bp with an average G + C content of 46%. The VZV genome organisation shows distinct similarities and sequence homology with HSV DNA but there is a substantial variation in the extent of this homology, most notably in the almost complete loss of the repeats around the long unique sequence in VZV. The VZV genome is arranged into two unique sequences U_L (ca. 100 kbp) and U_S (ca. 5200 bp), surrounded by small inverted repeats IR_L/TR_L (88bp) and large inverted repeats IR_S/TR_S (ca. 7300 bp), respectively as shown in Figure 1.4.

The genomic organisation of the virion DNA contains two major and two minor arrangements with different orientations of the U_L and U_S segments. The U_S segment exists equally in its two orientations. In contrast, one orientation of the U_L segment predominates in approximately 95% of molecules and the other in only 5%. The VZV genome contains approximately 70 unique open reading frames (ORFs) and three genes that are duplicated in the repeats (ORFs 62/71, 63/70, 64/69) (Ruyechan and Hay 2000). The VZV genome also has five regions in which a series of nucleotides is repeated, which are designated R1 (ORF 11), R2 (ORF 14), R3 (ORF 22), R4 (U_S repeat regions, 2 copies) and R5 (within an intragenic region of U_L).

VZV is considered to be genetically stable around the world not until the unexpected isolation of two VZV strains with a D150N missense mutation within the gE glycoprotein in North America in 1998 (Santos et al. 1998) and 2002 (Tipples et al.

2002). The mutant viruses reveal a reduction in affinity to the 3B3 monoclonal antibody, which is commonly used in diagnostic immunostaining. It appears to spread rapidly in tissue culture and in the SCID-hu mouse model. The complete DNA sequences of the two mutant viruses revealed that the increased cell spread phenotype was dependent substantially on the single D150N polymorphism in glycoprotein gE (Grose et al. 2004).

Recently, the DNA sequence of the varicella vaccine virus (vOka) and its parental virus (pOka) were completed (Gomi et al. 2002). Comparison of the sequences revealed 42 base substitutions, which led to 20 amino acid conversions and length differences in tandem repeat regions (R1, R3 and R4) and in an origin of DNA replication. Amino acid substitutions existed in 12 ORFs (6, 9A, 10, 21, 31, 39, 50, 52, 55, 59, 62, 64) of which 15 base substitutions, leading to eight amino acid substitutions, were in the gene 62 region alone.

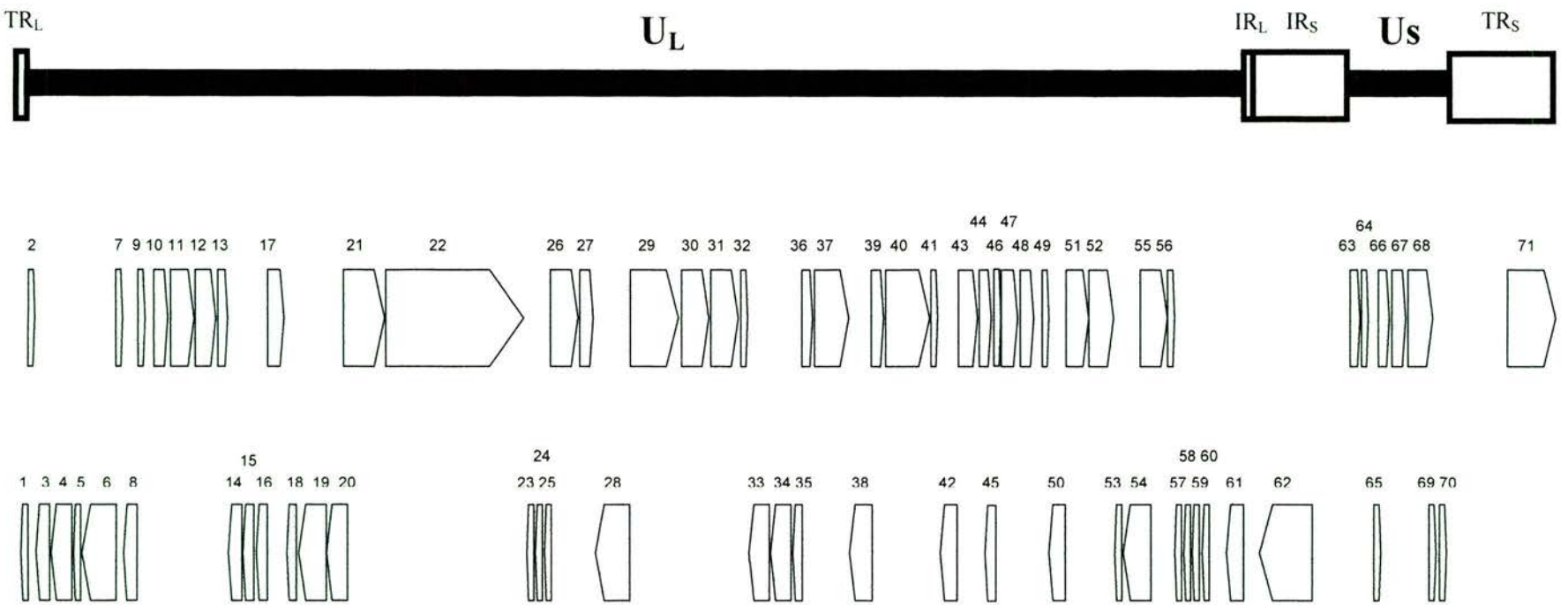

Figure 1.4 Organisation of VZV genome. The linear double-stranded DNA genome consists of long unique (U_L) and short unique (U_S) sections, each of which is flanked by terminal repeats (TR_L/TR_S) and inverted repeat regions (IR_L/IR_S). TR_L and IR_L are 88 bp, TR_S and IR_S are 7300 bp long (adapted from Cohrs et al., 2003a).

1.2.3 VZV Replication

VZV replication is highly cell-associated and very few viruses are released at any phase of replication in cell culture (Grose and Ng 1992). VZV readily infects human fetal diploid cells and melanoma cells and also replicates in Vero cells and primary African green monkey kidney cells. Replication is associated with expression of viral proteins within 4 to 10 h and formation of multinucleated giant cells and other cytopathic changes within 2 to 7 days. EM studies show that most VZV virions are enclosed in cytoplasmic vacuoles; defective particles are numerous and virions appear to disintegrate in the cytoplasm before reaching extracellular spaces. Degradation appears to occur as a result of virus entry into acidic prelysosomal vacuoles in the cytoplasm (Gershon et al. 1994). VZV is highly temperature sensitive, with inactivation occurring at 56°C to 60°C and it is not infectious if the virion envelope is disrupted.

1.2.3.1 Attachment, Entry and Uncoating

Precise analysis of VZV replication kinetics is hampered due to the highly cell-associated nature of VZV when grown *in vitro* and only few infectious virions are released. However, the kinetics of replication of VZV is presumed to follow the cascade of alpha, beta and gamma gene activation that characterises HSV replication as shown in Figure 1.2. Previous studies have revealed that oligosaccharides derived from glycoproteins of the VZV envelope contain mannose 6-phosphate (Man-6-P) (Gabel et al. 1989). At least four viral glycoproteins (gB, gE, gH and gI) contain N-linked complex oligosaccharides with Man-6-P groups and thus are ligands for the large cation-

independent Man-6-P receptor (MPR^{Ci}). Man-6-P and other phosphorylated monosaccharides protect cells from the cytopathic effect (CPE) of VZV with an order of potency that parallels their affinity for binding to the MPR^{Ci}. Treatment of cells with chloroquine, which reduces the expression of MPR^{Ci} at cell surfaces, also protects against infection by VZV. Electron microscopic immunocytochemical observations have revealed that enveloped virions are associated with MPR^{Ci} at the cell surface and that newly enveloped virions are incorporated into MPR^{Ci} containing vesicles in the trans-Golgi network (TGN) (Gershon et al. 1994). These observations are compatible with the hypothesis that an interaction of viral glycoproteins with a MPR^{Ci} is important in viral entry. MPR^{Ci} also plays a role in the diversion of VZV to late endosome (Chen et al. 2004), where virions are inactivated prior to exocytosis. Biopsies from VZV-infected human skin supported the idea that because MPR^{Ci} expression is naturally lost in maturing superficial epidermal cells when epidermal cells mature to form squames, these cells do not divert VZV to endosomes and constitutively secrete infectious VZV (Chen et al. 2004).

Since VZV does not possess a gD homolog, the virus may not utilise any of the known herpesvirus entry mediators. Following the interaction of gD with its receptor, HSV gB, gH and gL are required for fusion of the viral envelope with the cell membrane. VZV possesses homologues of all three of these glycoproteins, however, their roles in fusion of the viral envelope and subsequent penetration of the nucleocapsid into the cell are unproven. It is plausible that the uptake of VZV, like that of HSV, involves more than a single step and more than one type of receptor. The adsorption of VZV is mediated by heparan sulfate proteoglycan (Zhu et al. 1995) and that a receptor

for which Man-6-P is a ligand plays a subsequent role in viral entry. Once penetration has occurred, the nucleocapsid is transported to the nuclear surface, through which it penetrates and releases its genomic contents. It is not known whether cellular cytoskeletal elements facilitate centripetal movement to the nucleus or in what form the viral core arrives there (Cohen and Straus 2001).

1.2.3.2 Viral Gene Expression

While it has been assumed that each VZV gene is temporally regulated in the same transcriptional group as HSV-1 homolog, this may not be the case, particularly for IE gene expression. VZV contains homolog to four of the five HSV-1 IE genes (VZV ORFs 4, 61, 62, 63). However, the VZV genome is more homologous to PRV and EHV-1 than to that of HSV-1 and these animal herpesviruses only express a single IE gene, the respective homolog of VZVORF62 (Kinchington et al. 2000). Activation of VZV IE gene expression also appears to differ from the mechanisms used by HSV-1, PRV and EHV-1. In the latter viruses, all IE genes contain an upstream TAATGARAT sequence motifs, through which a virion transactivator protein (homologous to VZV ORF10) activates transcription. Only VZVORF62 promoter contains such an element, the VZV IE genes ORF4 and ORF63 do not (Moriuchi et al. 1994b). Maybe, the latter genes are activated directly by other transactivators in the virion, such as VZVORF62 protein.

1.2.3.3 The Immediate Early Phase

The initiation of the VZV replicative cycle leads to transcription of α genes by cellular RNA polymerase II. The transcripts are transported to the cytoplasm where they are translated and give rise to IE proteins. The latter migrate back to the nucleus where they regulate further gene expression. Due to their homology with HSV α genes ICP 27, 0, 4 and 22, respectively, VZV proteins encoded by ORFs 4, 61, 62 and 63 are considered as IE proteins, although this has only been demonstrated for ORFs 4 (Defechereux et al. 1997), 62 (Forghani et al. 1990) and 63 (Debrus et al. 1995).

ORF62

ORF 62 is a diploid gene, which encodes a 140 kDa protein of 1310 amino acids which, is expressed as a nuclear IE phosphoprotein (Forghani et al. 1990) and is also a major component of the virus tegument (Kinchington et al. 1992). IE62 is a functional homologue of HSV-1 ICP4 as demonstrated by its ability to complement ICP4 mutants (Disney and Everett 1990). HSV-1 ICP4 is essential for replication, it is required for transcriptional activation of β and γ genes and for repression of α genes (Dixon and Schaffer 1980). IE62 could stimulate the transcription of all VZV genes studied to date in transient transfection assays (Perera et al. 1992), (Moriuchi et al. 1994b). IE62 can also repress its own transcription (Disney and Everett 1990), although in neural cells IE62 can enhance transcription from its own promoter (Perera et al. 1992). IE62 probably does not act on its own, but in synergy with other IE proteins or even with cellular proteins. Immunofluorescence analyses have shown that IE62 can mediate the

nuclear localisation of IE4, another IE protein that also possesses regulatory functions (Spengler, et al. 2000). Coprecipitation experiments suggest that IE62 may also interact with, and be phosphorylated by, the ORF47 protein kinase *in vitro* (Kinchington et al. 2001). IE62 also cooperates with the cellular transcription factor USF to activate the promoters of ORF28, ORF29 (Meier and Straus 1995), and ORF4 (Michael et al. 1998). Only ORF62 has an upstream TAATGARAT sequence homologous to the HSV-1 TAATGARAT elements known to be essential for stimulation by VP16 (McKee et al. 1990). The upstream region of VZVORF62 contains three TAATGARAT elements important for transactivation of the ORF62 promoter by the VZVORF10 protein in the tegument (Moriuchi et al. 1995). The ORF10 protein forms a complex with two of the TAATGARAT elements in the ORF62 promoter that lack an overlapping octamer-binding motif. Two cellular proteins, Oct 1 and host cell factor (HCF) form a complex with the ORF10 protein and at least one of the TAATGARAT elements on the ORF62 promoter.

ORF4

VZV ORF4 encodes a 51 kDa phosphoprotein present largely in the viral tegument (Kinchington et al. 1995). Its localisation is mostly cytoplasmic and produced very early on in infected cells, however, when coexpressed with ORF62, ORF4 protein is primarily located in the nucleus (Defechereux et al. 1996). Although it has a high homology with HSV-1 ICP27, in the carboxy-terminal region, IE4 appears to be functionally distinct from its HSV-1 homolog (Perera et al. 1994). VZV ORF4 deletion mutant could not be complemented in cells expressing HSV-1 ICP 27 (Cohen et al.

2005). In transient expression assays, IE4 transactivates VZV promoters, either on its own or in synergy with IE62 (Defechereux et al. 1993) but has no demonstrable transrepressing activity (Perera et al. 1994). For example, ORF4 does not transactivate expression of the ORF63 IE or ORF28 putative early gene promoter. In transient expression assays, VZV ORF4 synergises with VZVORF62 to transactivate expression of putative IE, E and L promoters. It has been shown to be effective both at transcriptional and posttranscriptional levels. Transcriptional activation requires dimerisation of the ORF4 protein. It acts as a transactivator when brought close to DNA but transactivation probably requires the simultaneous presence of other functional proteins interacting with the transcription complex, such as the TATA-binding protein, the transcriptional factor IIB or the nuclear factor κB (Spengler et al. 2000).

ORF63

ORF63 is a diploid gene, encodes an IE protein of 45 kDa (Sadzot-Delvaux and Rentier 2001) and is present in the virion tegument. This protein is encoded by VZV ORFs 63 and 70 and is the putative homologue of HSV ICP22. IE63 is strongly expressed during lytic infection in cell culture as well as in skin lesions (Debrus et al. 1995). IE63 is abundantly produced at the first stage of infection and is essential for VZV replication (Sommer et al. 2001). Its activity as a potential transcription factor is subject to controversy. It has been shown that ORF63 protein upregulates the VZV thymidine kinase promoter and downregulates the IE62 promoter in transient transfection assays (Jackers et al. 1992). Nevertheless, IE63 has recently been shown in

transient transfection assay to downregulate the expression of the VZV DNA polymerase gene (Bontems et al. 2002). More recently, the same laboratory has also reported that IE63 is a transcriptional repressor of some VZV and cellular promoters and its activity is directed towards the assembly of transcription pre-initiation complex (Di Valentin et al. 2005). An interesting feature of the VZV IE63 protein is its cellular localization during the different phases of VZV infection. Indeed, at the first stage of infection, IE63 is predominantly present in the nucleus (Debrus et al. 1995), along with products of other latency associated genes, namely IE4, ORF21, ORF29 and IE62 while during latency, the protein exhibits an exclusive cytoplasmic localization (Lungu et al. 1998, Grinfeld and Kennedy 2004). These genes can be found both in the cytoplasm and the nucleus when reactivation occurs. The presence of IE63 protein and its cellular localization modification might reflect an important role in the latency process. ORF63 protein has been detected in animal (Debrus et al. 1995), (Sadzot-Delvaux et al. 1995), (Fleetwood-Walker et al. 1999) and human ganglia (Mahalingam et al. 1996), suggesting a role in latency. Kennedy et al., (2001) has reported that expression of VZV gene 63 appears to be the single most consistent feature of VZV latency.

ORF61

ORF61 encodes a 62-65 kDa phosphoprotein that localises to the nucleus of infected cells. Unlike the other VZV IE genes, ORF61 is not present in the viral tegument (Kinchington et al. 1995). VZV ORF61 is homologous to HSV ICP0 and can functionally complement an HSV-1 ICP0 deletion mutant. VZVORF61 protein transactivates putative VZV IE, E and L promoters in transient expression assays

(Moriuchi et al. 1993a). Depending on its cellular concentration and on host cell lines, IE61 can either repress or transactivate the functions of IE4 and IE62 on VZV gene promoters (Moriuchi et al. 1993a). The amino terminus of ORF61 contains a RING finger domain that binds zinc and is required for the transactivating activity of the full length protein (Moriuchi et al. 1994a). Deletion mutants of VZVORF61 can replicate, but they are impaired for syncytia formation and growth in cell culture (Cohen and Nguyen 1998). Cells infected with these mutants show reduce expression of gE but normal levels of ORF62 protein. HSV-1 ICP0, the homolog of ORF61 shows different patterns of activities in transient expression assays. Whereas ICP0 activates the HSV-1 TK promoter in transient expression assays, ICP0 does not activate the VZVORF36 promoter (Inchauspe and Ostrove 1989). Unlike ORF61, ICP0 does not show repressing activity in transient expression assays.

1.2.3.4 The Early Phase

Once the IE proteins have been synthesised and transported to the nucleus, they allow the expression of β genes that are only expressed at very low levels in their absence. VZV has a homologue for each of the seven core proteins involved in origin-dependent DNA replication of HSV (Wu et al. 1988). These are encoded by VZV ORF28 (DNA polymerase), ORF29 (single-stranded DNA binding protein), ORF16 (polymerase accessory protein), ORF51 (origin-binding protein) and ORFs 6, 52 and 55 (helicase/primase complex). The VZV origins of replication are located within the short repeat regions of the genome, between ORF62 and ORF63 (and ORFs70 and 71).

1.2.3.5 The Late Phase

After VZV genome replication, L proteins are assembled into nucleocapsids and the viral genome is wrapped inside. VZV ORF10 encodes a 410 amino acid protein incorporated into the virion tegument. This protein is the homolog of α-TIF, the HSV-1 virion-associated transactivator (VP16) directly involved in the induction of IE gene expression. VZV ORF10 transactivates the VZV ORF62 but not the putative IE ORF61 and ORF4 promoters (Moriuchi et al. 1993b). Surprisingly, ORF10 is dispensable for VZV replication in cell culture (Cohen and Seidel 1994), while its HSV counterpart VP16 is essential for HSV replication and assembly of virus. However, cell lines expressing ORF10 protein complement an HSV-1 VP16 mutant that lacks transactivating activity.

The VZV major nucleocapsid component is a 155 kDa protein encoded by ORF 40, homologous to the HSV-1 UL19. It is detected in the nucleus of infected cells where the capsids are assembled. VZV nucleocapsids also contain a complex made of a 32 kDa phosphoprotein and a 36 kDa nonphosphorylated protein possibly encoded by ORFs 33 and 33.5. The VZV genome encodes at least eight glycoproteins named gE, gB, gH, gI, gC, gL, gK and gM encoded by ORFs68, 31, 37, 67, 14, 60, 5 and 50, respectively. Viral glycoproteins are involved in interactions with target cells and play a crucial role in eliciting the host's immune response.

1.2.3.6 Assembly and Egress

At the end of the replicative cycle, expression of the three classes of viral genes has occurred and assembly of large amount of nucleocapsid is observed in VZV-infected nuclei. Two similar models of VZV replication have been suggested. One model stipulates that nucleocapsids are enveloped as they exit and traverse the nuclear membrane and then become incorporated into large cytoplasmic vesicles (Harson and Grose 1995). The nucleocapsid passes through the inner nuclear membrane and acquires its initial envelope. The enveloped particle travels through the perinuclear space where it is engulfed within a vacuole. A vacuole containing one or more viral particles is pinched off and resides within the cytoplasm. Viral glycoproteins are released from the trans-Golgi network (TGN) in microvesicles and fuse with the cytoplasmic vesicles containing viral particles. Virion laden vesicles fuse with one another to form a larger vacuole. These vesicles migrate to the cell surface where fully enveloped virions with functional glycoproteins are released by exocytosis.

Gershon, et al., (1994) proposed a slightly different scenario for VZV maturation and release. In their views, nucleocapsids first acquire and then lose their envelopes as they traverse the nuclear membrane. Nucleocapsids assemble in the nuclei of infected cells, acquire an envelope from the inner nuclear membrane as they bud into the perinuclear cisterna and fuse with the RER (rough endoplasmic reticulum) to release nucleocapsids into the cytosol. Viral glycoproteins are synthesised in the RER independently of the nucleocapsids and are targeted to the TGN (Zhu et al. 1995). Within the TGN, vacuoles form 'envelopment' sacs with concave and convex faces. Viral and cellular glycoproteins are separated in the envelopment sacs of the TGN so

that viral glycoproteins sort to the concave face, while cellular proteins, including the mannose 6-phosphate receptor (MPR^{ci}), sort to the convex face. The concave face becomes coated with tegument, envelopment sacs encircle nucleocapsids and ultimately fuse to enclose them with trapped tegument (Wang et al. 2001). The original concave face becomes the viral envelope, while the convex face becomes a transport vesicle. The vesicles that contain newly enveloped VZV transfer virions to late endosomes where VZV is degraded and released to the external medium by exocytosis.

1.2.4 VZV Latency

The study of VZV latency is fraught with obstacles. Little information exists on the molecular mechanisms leading to latency and to reactivation of VZV. Based on the Fenner mousepox model, VZV is thought to access sensory nerve tissues and establish latency via two mechanisms: i) direct hematogenous spread to sensory ganglia; ii) retrograde axonal transport from infected epidermal and dermal tissues. The concept of viremia is supported by the finding that PBMC are productively infected during varicella and the number of cells latently infected in the ganglion (Ozaki et al., 1994). In support of this hypothesis also, simian varicella virus (SVV) DNA can be detected in ganglia of experimentally infected monkeys on day 6 before the onset of rash and also in ganglia of monkeys that never develop rash (Kennedy et al. 1998).

On the other hand, retrograde transport along neuronal pathways was supported by evidence that the sites of zoster manifestations resembles the distribution of varicella lesions (Hope-Simpson, 1965). Also, longitudinal clinical trials revealed that episodes of

vaccine-associated zoster often occur at or near the prior site of inoculation, suggesting latency had been established preferentially within the sensory ganglion serving that single dermatome. If VZV spread to ganglia solely by a hematogenous route, then other body sites should have been well represented among the post vaccination zoster cases (Gershon et al., 1996). Further support of the latter mechanism is shown by the recent guinea pig enteric ganglia model (Chen et al. 2003). Latent VZV infection of isolated enteric neurons was established when culture mainly consist of neurons and exposed to cell free virus.

The mechanism by which HSV establishes and maintains latency is different from that of VZV. The differences are readily evident when considering the clinical patterns of infection with each of these viruses. Three features of zoster suggest an unusual mechanism of VZV latency and reactivation. First, the restricted geography of zoster, which is scattered in grape-like clusters but limited to a single dermatome, suggests that the peripheral lesions originate from multiple nerve endings rather than from one or a few focal sites of peripheral infection. This implicates an extensive neurone to neurone spread of VZV at the site of latency upon reactivation (Croen and Straus 1991), (Meier et al. 1993). For comparison, reactivated HSV-1 lesions tend to be small and focal, suggesting that few neurones become involved and reactivation of latent HSV-1 in the latent neurone is all that is required for peripheral access.

A second unusual feature is zoster-associated pain that often complicates clinical zoster. PHN is the most common complication manifestation of zoster and may last for weeks, months or even years following resolution of clinical disease (Gilden et al. 1992), (Rowbotham and Fields 1996). The mechanism of PHN is unknown but it is

likely a result of necrosis and inflammatory responses to demyelination and cell damage during ganglionic replication. For comparison, such a long-term pain is not usually experienced with reactivated HSV-1 and pain associated with lesions normally resolves 3-4 days after their appearance.

Finally, the frequency of zoster is unusual in that some 80% of VZV seropositive individuals never show clinical evidence of reactivation. This suggests that either entry into latency or reactivation from it are highly inefficient processes or, alternatively, that reactivations of VZV are more frequent but are well controlled by the immune surveillance mechanisms prior to the development of peripheral disease. With HSV-1 infection, reactivation can occur multiple times in the presence of active and fully functional immunity and asymptomatic reactivation often occurs. Moreover, while HSV-1 incidence decreases with age, zoster incidence increases dramatically, suggesting triggers for reactivation are quite different for these two viruses.

No viral proteins have been detected in HSV latently infected cells and the only transcripts detected are the latency-associated transcripts (LATs) (Wagner and Bloom 1997). There is no evidence that these RNAs representing stable introns are translated into protein and their precise role in the life cycle of HSV remains controversial. LATs are present as several non-polyadenylated collinear RNAs, including a major 2-kb LAT and a 1.5-kb splice variant (Farrell et al. 1994). The 2-kb LAT is believed to be a stable intron spliced from a low-abundance 8.3-kb primary transcript. It has been suggested that the LAT plays a crucial role in viral reactivation. LAT mutant viruses show reduced ability to reactivate in the mouse model (Sawtell and Thompson 1992) and have decreased spontaneous and induced reactivation frequencies in the rabbit model (Perng

et al. 1994). The LAT also has an important role in promoting the establishment and maintenance of the latency (Maggioncalda et al. 1996), (Sawtell 1997) even though earlier studies found no evidence to support this idea (Sederati et al. 1989). It has been observed that LAT mutant viruses express viral productive cycle genes in greater numbers in mouse neurons (Garber et al. 1997) and establish latent infection in fewer neuronal cells than parental viruses (Sawtell 1997). It has been proposed that the LAT may repress viral replication in neuronal cells by reducing IE gene mRNA levels and facilitate the establishment of HSV-1 latency in neuronal cells (Mador et al. 1998). In addition, the LAT may promote neuronal survival through an anti-apoptotic mechanism (Ahmed et al. 2002), (Branco and Fraser 2005).

Far less is known about the nature and mechanisms regulating VZV latency but what is known suggests a process that is very different from HSV latency. Current major issues involving VZV latency have been the cell-type localisation of latent VZV, the frequency with which VZV establishes latency and the nature and extent of VZV gene expression during latency (Kennedy 2002), (Cohrs et al. 2004). Each will be discussed individually in the following sections.

1.2.4.1 Cell Type Localisation of Latent VZV

Identification of the cell type harbouring latent VZV is important since the pathogenesis of initial infection and reactivation may depend on the number and type of cells initially infected (Steiner 1996), (Kennedy and Steiner 1994). Initially, *in situ* hybridisation (ISH) revealed that VZV was latent exclusively in neurons (Hyman et al. 1983), (Gilden et al. 1987). These findings were later disputed by the apparent detection

of VZV in non-neuronal satellite cells (Croen et al. 1988), (Meier et al. 1993) and by a single report that found VZV in many neurons and non-neuronal cells (Lungu et al. 1995). However, ISH results of autopsy samples containing low amounts of latent virus DNA are unpredictable and prone to misinterpretation (Mahalingam et al. 1999). Improvements in ISH that incorporated polymerase chain reaction (PCR) and amplified low copy number latent virus DNA revealed VZV DNA predominantly, if not exclusively, in neurons (Dueland et al. 1995), (Kennedy et al. 1998), (Kennedy et al. 1999), (Kennedy 2000), (Kennedy et al. 2001). A similar finding was also reported by Levin et al., (2003) and they found that latent VZV DNA is present primarily in large neurones.

1.2.4.2 The Burden of Latent VZV DNA

Analysis of an animal model of HSV-1 latency suggests that latent genome copy number may be an important parameter for subsequent induced reactivation *in vivo* (Sawtell et al. 1998). Latent VZV DNA is present in low copy number as routine Southern and northern blot hybridisation analyses did not succeed in detecting them in extracts of human ganglia (Meier et al. 1993). Semi-quantitative PCR showed that 10^3-10^5 copies of latent VZV DNA were present in 10^5 ganglionic cells (Clarke et al. 1995) which is similar to the amount of latent HSV-1 found in human ganglia by Southern analysis (Efstathiou et al. 1986). However, Mahalingam et al., (1993) only detected 6-31 copies of VZV genome per 10^5 cells. LaGuardia et al., (1999), reported 5.5 copies of VZV DNA per 10^5 ganglionic cells, assuming 100 non-neuronal cells per neuron. Real-time quantitative PCR analysis detected 258 ± 38 copies of VZV DNA per 10^5

ganglionic cells (Pevenstein et al. 2000). Recently, quantitative competitive PCR detected an average of 4.7 copies of VZV DNA per latently infected neuron (Levin et al. 2003). The large variation in the virus load in these studies might reflect the differences in the natural history of the infection in the individuals from whom the samples were obtained or discrepancies in the techniques used to estimate copy numbers.

1.2.4.3 Latent VZV Gene Expression

There have been several published studies of latent VZV gene expression using a variety of different techniques on pooled and individual human ganglia, including northern blot analysis, *in situ* hybridisation (ISH) and cDNA library construction (Kennedy 2002). Most studies have reported the presence of RNA for VZV genes 21, 29, 62 and 63 (Cohrs et al. 1994), (Cohrs et al. 1995), (Cohrs et al. 1996), (Kennedy 2002) with conflicting results for the presence of RNA for gene 4, which has been reported by some workers (Croen et al. 1988), (Kennedy 2000) but not others (Meier et al. 1993). However, a more recent work has shown that ORF4 is indeed important for establishment of latency, besides ORF63 (Cohen et al. 2005). Analysis of latently infected human trigeminal ganglia by reverse transcriptase-dependent nested PCR, *in situ* hybridisation, and immunohistochemistry, revealed that VZVORF66 to be a previously unrecognised latently expressed virus gene (Cohrs et al. 2003a). IE 62 is a major transcriptional activator, which can drive transcription from all kinetic classes of virus genes and enhances the infectivity of transfected VZV DNA (Moriuchi et al. 1994b). To maintain latency, the effect of IE62 on subsequent virus gene expression

must be controlled. Cohrs et al., 2004 suggested three models of the control of IE62 function as illustrated in Figure 1.5.

The first model of modulating IE62 activity is based on cellular location (Figure 1.5A). IE62 localises to the nucleus early in virus infection and later accumulates in the cytoplasm (Kinchington and Turse 1998). Interestingly, this protein has been shown to localise predominantly in the cytoplasm during latency (Lungu et al. 1998). Later, it was found that the protein kinase encoded by VZVORF66 (VZV66pk) phosphorylates IE62, resulting in cytoplasmic accummulation of IE62 (Kinchington et al. 2000), (Kinchington et al. 2001). While the phosphorylation of IE62 late in VZV lytic infection appears to be a mechanism by which IE62 is incorporated into progeny virions, the cytoplasmic location of IE62 during latency that results perhaps from VZV66pk phosphorylation mitigates IE62 dependent gene transactivation (Cohrs et al. 2003a). Thus, this mechanism allows IE62 remains within a cell without stimulating gene transcription.

A second mechanism of regulating IE62 activity is through the control at the promoter level (Figure 1.5B). Consistent with this hypothesis is the finding that the protein encoded by VZV gene 29 binds to a 40 bp region on the glycoprotein I promoter (He et al. 2001). This protein was found to increase IE62 induced gI expression in permissive cells and reduce IE62 transactivation in non-permissive cells (Ito et al. 2003). VZV gene 29 and 21 proteins were tested to find out if they have the same function as their HSV-1 homologues which can form a DNA binding complex in the nucleus of virus infected cells (Shelton et al. 1994) and modulate IE62 functions (McNamee et al. 2000). However, it was reported that VZV gene 29 and 21 proteins had no significant

effect on IE62-induced activation of gene 20, 21, 28 or 29 promoters in tissue culture system (Cohrs et al. 2002).

A third mechanism of modulating IE62 activity is through transcriptional control (Figure 1.5C). The HSV-1 homologue of the VZV gene 63 protein (ICP22) has been shown to alter phosphorylation of cellular RNA polymerase II, thereby reprogramming the cellular transcription apparatus to more readily transcribe viral genes. By analogy, VZV gene 63 protein might modify gene expression by interacting with transcription factors but conclusive evidence is lacking. However, VZV gene 63 protein can complex with IE62 and phosphorylated forms of VZV gene 63 protein reduce IE62-induced promoter activation. Since the effect of ICP22 on RNA polymerase II is dependent on its phosphorylation, the possibility exists that phosphorylated forms of VZV gene 63 protein can alter cellular transcription to reduce the effect of IE62 on virus gene activation.

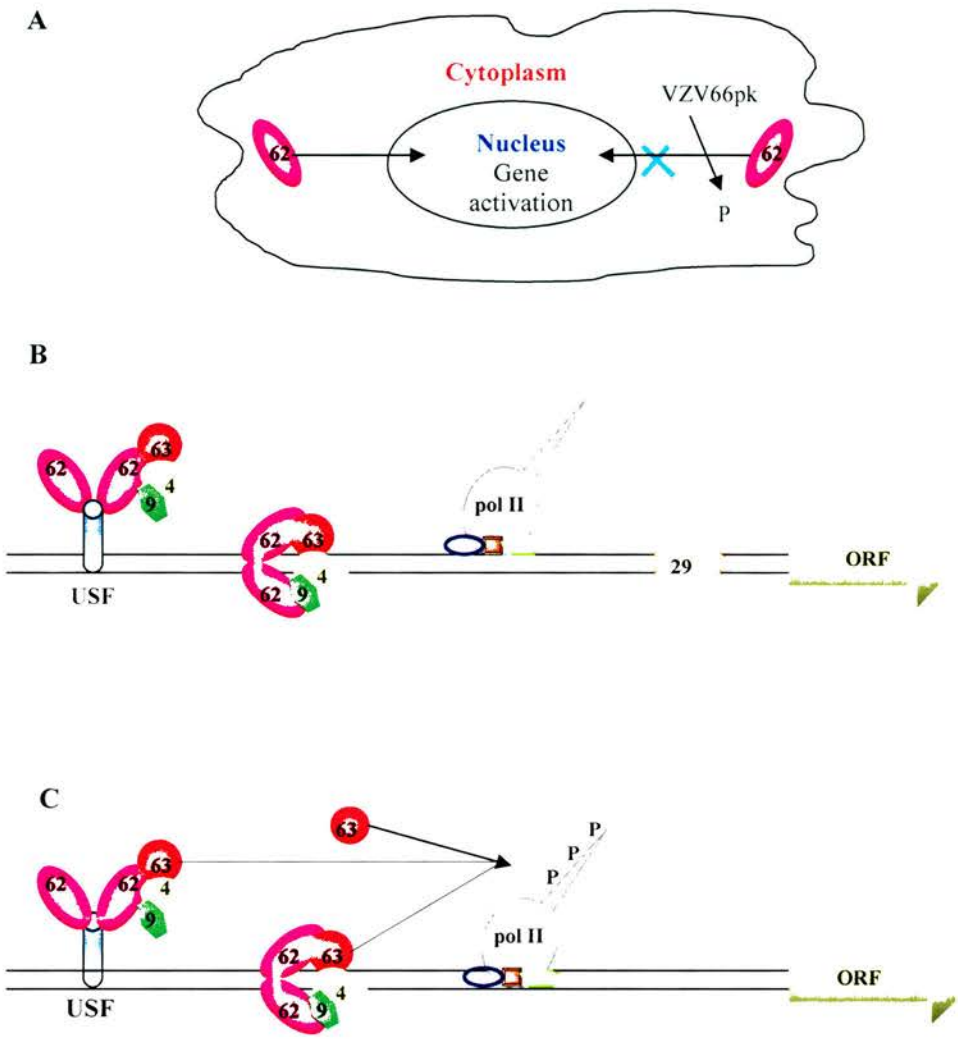

Figure 1.5 Regulation of IE62 function. Model A: regulation by location. Cytoplasmic VZV IE62 is translocated into the nucleus where gene activation in trans is initiated. Phosphorylation of IE62 by VZVORF66pk halts IE62 nuclear import, IE62 is restricted to the cytoplasm and gene activation does not occur. Model B: regulation at the promoter. Nuclear IE62 is associated with at least 3 virus proteins encoded by open reading frames 4, 9 and 63. The complex binds to VZV gene promoters either through cellular transcription factors, in this case the previously identified upstream stimulating factor (USF), or directly to the promoter itself. The IE62 complex further associates with cellular RNA pol II and its associated transcription factors. However, RNA transcription is blocked by downstream binding of VZV gene 29 protein. Model C: regulation by transcription factor modification. As in Model B, nuclear IE62 and the associated VZV and cellular proteins bind to gene promoters. However, transcription is blocked by modification of the cellular RNA pol II complex. In this model either free or bound VZV gene 63 protein alters the phosphorylation pattern of the C-terminal domain of cellular RNA pol II, resulting in transcriptional control (adapted from Cohrs et al. 2004).

1.2.5 Reactivation

VZV reactivation is associated with activation of transcription of all kinetic classes of viral genes (Lungu et al. 1995). It is still not clear how alphaherpesviruses move, assemble, and spread in the nervous system. Recent work by Tomishima and Enquist (2002) suggested that viral egress can occur sporadically along the length of infected axons and is not confined solely to axon terminals. They also reported that extracellular particles are not involved in nonneuronal cell infections. Lungu et al. (1998) have reported that five VZV encoded proteins (ORFs 4, 21, 29, 62, 63) exhibit cytoplasmic localisation during latent infection and a nuclear and cytoplasmic localisation during reactivation.

The guinea pig enteric ganglia model has demonstrated that presence of non-neuronal cells is a critical determinant of whether VZV would establish a latent or lytic infection of cultured enteric neurons (Chen et al. 2003). The nature of the influence of non-neuronal cells is not understood. It is hypothesised that they amplify VZV and that the determination of whether infection will be latent or lytic depends on the number of VZV to which the neurons are exposed. This might happen when VZV infected cells fuse with neurons and introduce VZV gene products that are not present in the virion. Only certain VZV proteins that are produced by infected cells are incorporated into viral particles. However, all viral proteins in the cytosol of infected cells will enter a target cell by diffusing through the fusion pore, whether or not these proteins are incorporated into virions. Such proteins might play a role in lytic infection. If this were to be the case, then latent infection would be established in neurons when they become infected by free

extracellular particles, but lytic infection would result when neurons become infected by fusion with VZV infected cells.

1.2.6 Immune Evasion Mechanism of VZV

Both cell-mediated and humoral immunity are elicited during the course of primary VZV infection. The early host responses to VZV are non-specific and involve natural killer (NK) cells and interferons (IFN) that function to restrict virus replication and spread (Arvin, 1996). VZV specific T cell recognition is critical for host recovery from varicella and both major histocompatibility complex (MHC) class I restricted $CD8^+$ T cells and MHC class II restricted $CD4^+$ T cells are sensitised during primary VZV infection (Sharp et al. 1992).

MHC I molecules are heterodimers consisting of a membrane bound heavy chain (αC) and a light chain β_2 microglobulin (β_2m) which present peptides derived from cytosolic proteins to $CD8^+$ T lymphocytes. Antigenic peptides generated by cytosolic proteases are transported into the endoplasmic reticulum (ER) by the ATP-dependent transporter associated with antigen processing (TAP), where they associate with MHC I heterodimers. The resulting trimolecular complex is transported from the ER through the Golgi compartment to the cell surface where it presents the peptide to cytotoxic T lymphocytes (Lehner and Trowsdale 1998). Each step in the MHC I biosynthesis and assembly pathway has been shown to be a potential target for viral interference and the subsequent modulation of MHC I expression on cell surfaces.

VZV was found to down-regulate cell-surface MHC I expression on infected human fibroblasts and T lymphocytes (Abendroth et al. 2000) by impairing the transport of MHC I molecules from the Golgi compartment to the cell surface. This effect may enable the virus to evade $CD8^+$ T-cell immune recognition during VZV pathogenesis, including the critical phase of T-lymphocyte-associated viremia. Inhibition of late viral gene expression by treatment of infected fibroblasts with phosphonoacetic acid (PAA) did not influence the modulation of MHC I expression, nor did transfection of cells with plasmids expressing immediate early viral proteins. However, cells transfected with a plasmid carrying the early gene VZVORF66 did result in a significant down-regulation of MHC I expression, suggesting that this gene encodes a protein with an immunomodulatory function.

$CD4^+$ T cells that recognise VZV are almost exclusively of the Th1 type, and IFN-γ is a major cytokine product of these memory T cells. The ability of VZV to inhibit MHC class II expression in most infected cells, despite exposure to high concentrations of IFN-γ, provides a mechanism by which the virus can limit the antiviral activity of $CD4^+$ T cells. MHC class II are polymorphic heterodimers with α and β chains which present exogenous peptides to $CD4^+$ T lymphocytes. The α and β chains form a heterodimer in the ER. This complex associates with the invariant chain (Ii) and is transported through the Golgi and trans-Golgi reticulum to endosomes in the cytoplasm. The Ii chain is degraded in these endosomes, allowing antigenic peptides, which are produced by proteolysis of endocytosed proteins, to bind to the a/b heterodimer. The peptide-MHC II complex then presented on the cell surface (Pieters, 1997). In contrast

to MHC class I, MHC class II proteins are expressed constitutively only on B cells, monocytes, dendritic cells and thymic epithelium. IFN-γ has an important function in $CD4^+$ T cell recognition of infected cells because it is a potent inducer of MHC class II expression on many cell types.

The ability of VZV to inhibit MHC class II expression in most infected human fibroblasts, despite exposure to high concentrations of IFN-γ, provides a mechanism by which the virus can limit the consequences of immune surveillance by $CD4^+$ cells (Abendroth et al. 2000). VZV inhibits MHC class II expression by interfering with the Jak/Stat signal transduction pathway by reducing steady-state Jak2 and Stat1α but not Jak1 protein expression in IFN-γ treated cells as shown in Figure 1.6. Stat1α is a component of the Jak/Stat signal transduction pathway, which includes Jak1 and Jak2. CIITA and IRF1 expression is induced after IFN-γ treatment by Stat1α. The failure to detect CIITA and IRF-1 RNA in VZV infected IFN-γ treated cells suggested that these cells may have a disruption of the Jak/Stat pathway.

A third immune evasion mechanism for VZV was reported whereby the virus is able to productively infect mature dendritic cells (DCs) (Gavin et al. 2003). Dendritic cells (DCs) are potent antigen-presenting cells critical for the initiation of a successful antiviral immune response through the stimulation of immunologically naïve T lymphocytes (Banchereau and Steinman 1998). DCs located in the periphery exist as immature cells, expressing low levels of MHC class I and MHC class II molecules and costimulatory molecules such as CD80 and CD86. Immature DCs readily take up antigen and are induced to migrate to the secondary lymphoid organs, where they

undergo maturation and present processed antigens to antigen-specific T lymphocytes. VZV interference with mature DC function resulted in a selective downregulation of cell surface expression of MHC class I, CD80, CD83, and CD86 but did not alter MHC class II expression (Gavin et al. 2003). More importantly, VZV infection of mature DCs significantly reduced their ability to stimulate the proliferation of allogeneic T lymphocytes.

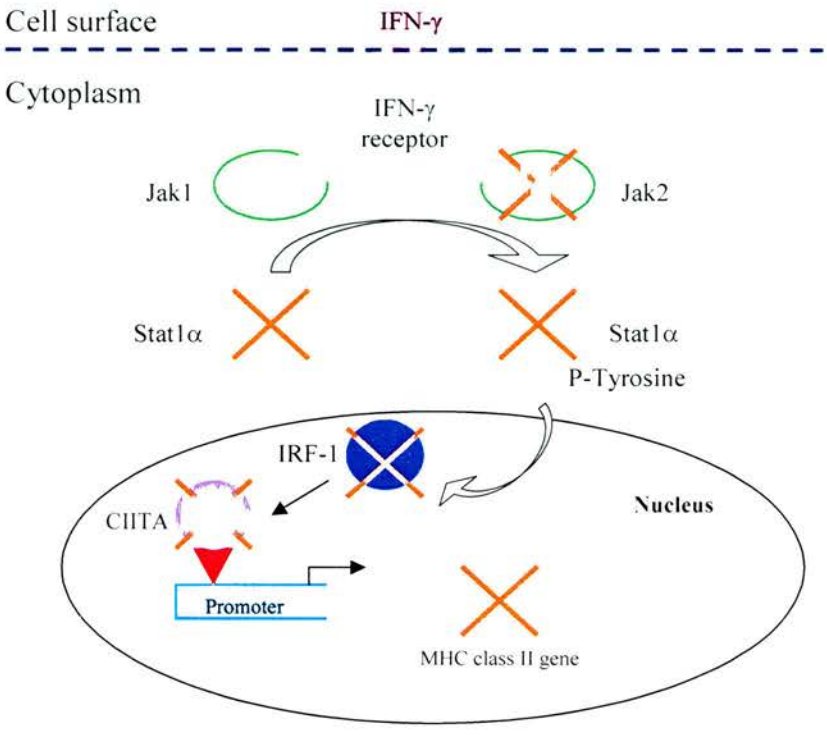

Figure 1.6 Interference by VZV with IFN-γ induced up-regulation of MHC class II expression via Jak/Stat signal transduction pathway. CIITA and IRF-1 expression is induced after IFN-γ treatment by Stat1α, which includes Jak1 and Jak2. The various proteins that are affected in VZV-infected cells are crossed out (adapted from Abendroth et al. 2000).

1.3 Clinical Manifestations of Varicella

A primary infection with VZV causes varicella, or chickenpox, a highly contagious disease of childhood (Arvin 1996). Virus is spread by the airborne route from the skin lesions and oropharynx of infected individuals to susceptible contacts. The first symptoms of varicella are often a prodrome consisting of fever, malaise, headache and abdominal pain typically begin about 24-48 h before rash (Arvin 1999). Each lesion evolves within a few hours from an erythematous macule to the formation of a vesicle surrounded by erythema, the classic 'dew drop on a rose petal'. The vesicle fluid becomes cloudy and may develop an umbilicated appearance as the lesion begins to crust. As the initial lesions progress through these stages, crops of new lesions continue to form, usually in a 'centrifugal' pattern, i.e., from the face and trunk to the extremities. Hypopigmentation of the underlying skin may be seen as the crusts resolve, but extensive scarring is unusual unless secondary bacterial infection occurs. Skin lesions appear on the trunk, face, scalp and extremities, with the greatest concentration on the trunk. A hallmark of varicella is the presence of lesions in all stages of development at the same time (LaRussa 2000). Healthy children develop an average of approximately 300 lesions. The average duration of lesion formation is three to five days in the normal child, however, it is usually longer in adolescents and adults and certainly in the immunocompromised. Fever often accompanies the rash. Body temperature usually parallels the severity of rash and may range from normal to greater than 105°F. As the appearance of new lesions slows, fever begins to decline. Other common symptoms

include pruritus that may be severe when skin lesions are extensive, headache, malaise and anorexia (Arvin 1999).

1.3.1 Pathogenesis

Primary VZV infection is presumed to be initiated by inoculation of the mucous membranes of the respiratory tract with infectious virus transferred in respiratory droplets or by contact with infectious vesicular fluid from an infected individual (Arvin et al. 1996). In the absence of experimental data, early events in VZV pathogenesis have been compared to mousepox (Grose 1981), (Grose et al. 2000) as shown in Figure 1.7. According to this model, VZV is presumed to infect mononuclear cells in regional lymph nodes after inoculation of mucous membranes, causing a primary viremia that carries the virus to reticuloendothelial organs such as the liver and spleen for a phase of virus replication. A secondary lymphocyte mediated viremia delivers systemically to the cutaneous epithelial cells, where replication causes deep necrotic lesions of the epidermis and dermis. The incubation period is usually 14-16 days, with a range of 10-21 days.

A recent experiment in severe combined immunodeficiency mice with human skin grafts (SCIDhu mice) supported the concept that infected T cells have the potential to mediate VZV transfer to skin immediately after entering the circulation during the primary viremia (Ku et al. 2004). It was suggested that the prolonged interval between exposure and the appearance of varicella skin lesions reflects the time required for VZV

to overcome previously unrecognised but potent innate immune barriers, especially alpha interferon production, mounted directly by epidermal cells *in vivo* (Ku et al. 2004).

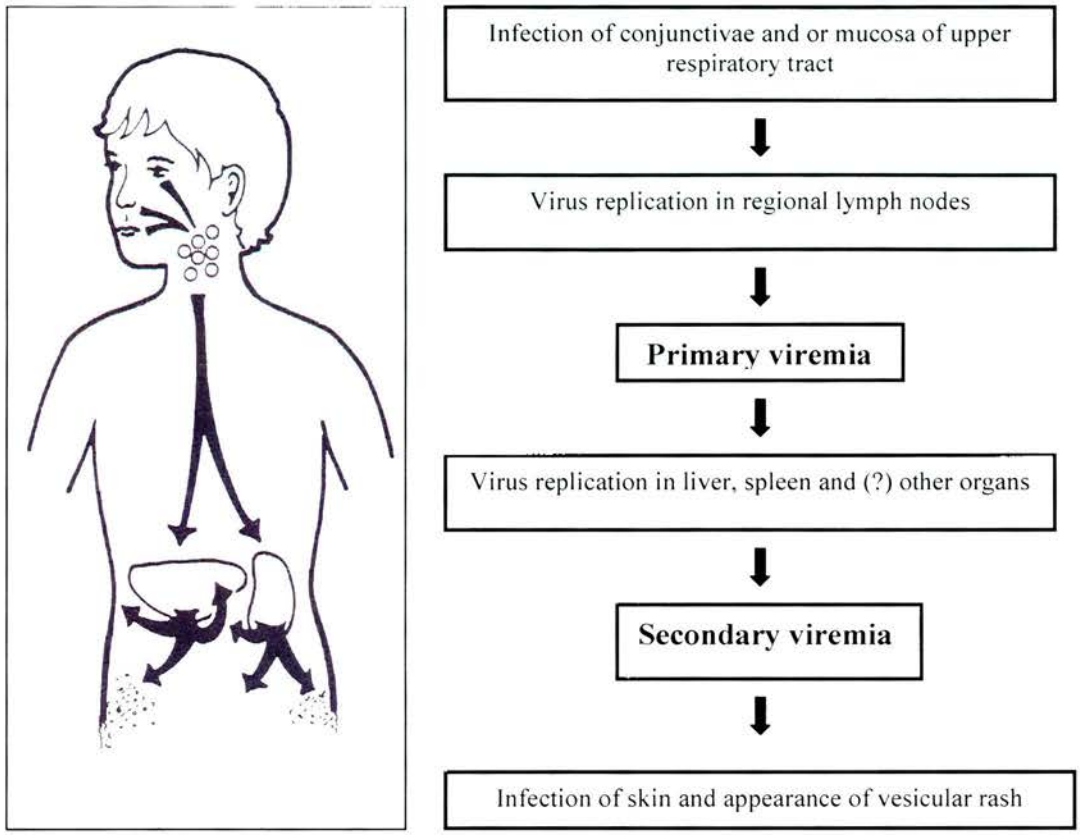

Figure 1.7 Diagrammatic representation of the pathogenesis of chicken pox infection based on mousepox. There are two viremias during the 14 days incubation period. The first viremia occurs after local replication at the site of infection. At the end of the second viremia, the typical chicken pox rash appears (adapted from Grose, 1981).

1.3.2 Complications

While chicken pox in the normal child is usually a benign illness, this infection in the adult or immunocompromised individual is of increased severity, as evidenced by enhanced morbidity and mortality. For example, in children receiving cancer chemotherapy, nearly one third have progressive involvement of multiple organs, including lungs, liver and the central nervous system (LaRussa 2000). The overall mortality of chicken pox in the immunocompromised host has been reported to be 8 to 10%. The most serious complication of varicella is pneumonitis, which is characterised by progressive tachypnea and cough (Choo et al. 1995). Secondary bacterial infection of the skin, which is usually caused by *Streptococcus pyogenes* or *Staphylococcus aureus* is also a common infectious complication of varicella (Peterson et al. 1996). These can range in severity from impetiginised lesions and bullous impetigo to cellulites and erysipelas. The common neurologic complications of varicella are meningoencephalitis and cerebellar ataxia (Arvin 1999).

1.3.3 Treatment

A live attenuated varicella zoster virus vaccine was developed in Japan at the beginning of the 1970s (Takahashi et al. 1975) and was introduced into the routine infant immunisation schedule of the United States in 1995. The vaccine virus was generated by serial passage of a clinical VZV isolate, the parent Oka (pOka) virus, in human and guinea pig embryo fibroblasts. Varicella vaccine virus (vOka) is attenuated and immunogenic in susceptible healthy children (Krause and Klinman 1995). Concerns have been raised about a potential age shift with the effects of varicella vaccination, i.e. an increase in the number of varicella cases in older age groups, which generally results in a more severe disease outcome (Wagenpfeil et al. 2004). A further concern is the potential initial increase in herpes zoster incidence resulting from a decrease in the spread of wild-type VZV following vaccination. Recently, Oxman et al., (2005) have reported that the live attenuated Oka/Merck VZV vaccine markedly reduced morbidity from herpes zoster and postherpetic neuralgia.

Medical management of chicken pox in the normal host is directed toward prevention of avoidable complications. Meticulous care and good hygiene can avoid secondary bacterial infection of the skin. Antiviral therapy was first shown to be efficacious for the management of varicella in the late 1970s and early 1980s using the non-specific inhibitors of viral replication, vidarabine and interferon (Whitley 2000). Acyclovir, a synthetic acyclic purine nucleoside analogue which is a selective inhibitor of VZV replication was then proven useful and has become the drug of choice. Additionally, foscarnet, a pyrophosphate analogue, is available for intravenous therapy

of varicella infections in high-risk immunocompromised hosts who are presumed to have an infection caused by an acyclovir or penciclovir resistant virus (Enright and Prober 2003).

1.4 Clinical Manifestation of Herpes Zoster

Herpes zoster (HZ or shingles) is a common disease caused by reactivation of latent VZV that has an estimated annual incidence of 2 to 3 cases per 1000 persons (Portenoy et al. 1986), rising with age and a lifetime prevalence as high as 20% (Stankus et al. 2000). The age-specific incidence of HZ was shown by a rapid increase during infancy and adolescent from 0.79/1000/annum to reach about 2.2 and remain around that rate from 20 to 50 years of age (Hope Simpson 2001). Thereafter, the incidence rate increases as steeply as in the first 20 years of life, to reach 12.2/1000 in octogenarians, a 15 fold that in those under 10 years old and 5.5 times that of persons between 20 and 50 years old (Hope Simpson 2001). It was found that the severity of the disease increased with age but the condition did not occur in epidemics and there was no characteristic seasonal variation.

HZ is a localised disease characterised by unilateral radicular pain and vesicular eruption that is generally limited to the dermatome innervated by a single spinal or cranial nerve (Ragozzino et al. 1982). Thoracic and lumbar dermatomes are most commonly involved. HZ may involve the eyelids when the first or second branch of the fifth cranial nerve is affected but keratitis heralds a sight threatening condition, herpes zoster ophthalmicus. Early in the disease course, erythematous, macropapular lesions

appear that rapidly evolve into a vesicular rash. Vesicles may coalesce to form bullous lesions. In the normal host, these lesions continue to form over a period of 3 to 5 days, with the total duration of disease being 10 to 15 days (Whitley 2001). Unusual cutaneous manifestations of herpes zoster, in addition to ophthalmic disease, include the involvement of the maxillary or mandibular branch of the trigeminal nerve, which results in intraoral involvement with lesions on the palate, tonsillar fossa, floor of the mouth and tongue. Neuromuscular disorders associated with HZ include the Guillain-Barre syndrome, transverse myelitis and myositis.

The prodomal symptoms of HZ are usually acute segmental neuralgia with pain and paresthesia in the involved dermatome (Wood et al. 1996). This generally precedes the eruption by several days, occasionally by a week or more and it varies from superficial itching, tingling, or burning to severe deep boring or sharp, stabbing, lancinating pain (Oxman et al. 2000).

1.4.1 Pathogenesis

Hope-Simpson proposed that immunity to VZV plays a pivotal role in the pathogenesis of herpes zoster (Hope-Simpson 1965) and subsequent observations support the hypothesis that cell-mediated immunity to VZV is a major determinant of the risk and severity of herpes zoster (Kost and Straus 1996). Whereas levels of antibody to VZV remain relatively constant with increasing age, the increased incidence and severity of herpes zoster and PHN among older adults are closely linked to a progressive age related decline in cell-mediated immunity to VZV. The concept that VZV takes

advantage of waning immunity to ensure its persistence in the population by causing herpes zoster is supported by correlations between age and a diminished capacity of peripheral blood T cells from persons who are immune and therefore latently infected, to proliferate and produce interferon-γ when stimulated with VZV antigens *in vitro* (Arvin 2005). VZV specific T cell immunity is elicited by primary VZV infection and is required for the resolution of varicella. Memory $CD4^+$ and $CD8^+$ T cells that recognise VZV proteins remain readily detectable in younger adults, in whom herpes zoster is relatively rare. Robust memory T cell immunity to VZV may reflect either the extent of the initial expansion of VZV-specific T cells elicited during primary infection or periodic boosting on exposure to varicella or on abortive, subclinical reactivation. Loss of VZV-specific T cell responses also defines periods of susceptibility to herpes zoster in immunocompromised patients. In contrast, anti-VZV IgG antibodies persist and persons who are at risk for herpes zoster because of declining T cell responses continue to be protected from varicella. Functionally, VZV-specific memory T cells probably control the later stages of reactivation that produce the typical signs of herpes zoster, rather than preventing latent VZV genomes in the ganglia from beginning to replicate. Over time, waning VZV-specific T cell immunity may place a person in a 'danger zone' for symptomatic VZV reactivation. Recurrences of herpes zoster are uncommon among immunocompetent persons, presumably because an episode of herpes zoster boosts immunity to VZV, effectively immunising against a subsequent episode (Oxman et al. 2005).

1.4.2 Complications

Complications of HZ have different manifestations and reflect different pathogenic mechanisms such as direct viral invasion, sensory or motor neuropathies and vasculopathy (Gilden et al. 2000). These complications depend on the localisation and include ocular, neurologic, visceral (pneumonitis, esophagitis, enterocolitis, myocarditis, pancreatitis) and other complications such as myositis and cystitis. HZ starts and ends with pain of varying degrees. During its course different stages of pain can be distinguished: the acute pain before and during the skin lesions and the chronic pain after the rash has healed (Arvin 1999). Today, both the acute and chronic pain of HZ are termed zoster-associated pain (ZAP) by the International Herpes Management Forum. The most common complication of HZ is postherpetic neuralgia, a chronic ZAP, which will be discussed in more detail in a separate section. HZ in the trigeminal ganglion is associated most often with clinical manifestations in the first division of trigeminal nerve, i.e. the ophthalmic branch (Arvin 1999). Clinical manifestations of this infection among others include conjunctivitis, dendritic keratitis and optic neuritis. Other complications of HZ involving cranial nerves include facial palsy, herpes zoster oticus and Ramsey-Hunt syndrome. Motor paralysis due to inflammation and necrosis in the anterior horn cells is also reported in HZ patients.

1.4.3 Treatment

The localised skin rash is not a serious problem but the prodromal pain associated with herpes zoster is a sign of the active infection of sensory ganglia. The syndrome of

zoster sine herpete also suggests direct involvement of the ganglia and autopsy studies have suggested the destruction of neurons and satellite cells during VZV reactivation (Gilden et al. 2000). As a consequence of this pathogenic process, the benefit of antiviral therapy with acyclovir and related agents is limited in patients with herpes zoster. Neurologic damage begins before the characteristic dermatomal rash appears and PHN can be prolonged and intractable despite early antiviral therapy and aggressive pain management.

Over the last 20 years, a series of effective and well-tolerated antiviral compounds have been licensed for treatment of HZ (Balfour 1999). Three oral antiviral drugs (acyclovir, valaciclovir, and famciclovir) are currently approved in the United States and United Kingdom for treatment of HZ in immunocompetent host. Acyclovir was the first oral antiviral compound marketed for treatment of HZ (Whitley 2001). While widely and successfully prescribed, the efficacy of acyclovir for HZ is somewhat limited by its poor oral bioavailability. Valaciclovir the prodrug of acyclovir has been developed to provide an orally administered drug with an improved efficacy. Famciclovir, a prodrug of penciclovir was also developed as the oral formulation because penciclovir is poorly absorbed (Wood 2002). In double-blind placebo controlled trials, acyclovir reduces the overall duration of pain and the incidence of PHN, defined as pain at 3 or 6 months after enrolment (Wood et al. 1996). Famciclovir reduces the duration of PHN, defined either as pain beyond rash healing or as pain beyond 30 days or 3 months from enrolment (Tyring et al. 1995). In a comparative study of acyclovir and valaciclovir, valaciclovir reduced the overall duration of pain considered as a continuum. Besides antiviral therapy, steroids e.g. corticosteroids were shown to be beneficial to reduce acute zoster

pain (Wood 2002). Nerve blocks, analgesics and antidepressants also have some efficacy towards relieving acute pain.

1.5 Post-herpetic neuralgia

Zoster in immunocompetent patients most often resolves without sequelae. However, many elderly patients have prolonged, often debilitating pain, known as post-herpetic neuralgia (PHN). PHN has been defined as severe pain occurring 1 month after rash onset or that persists for greater than 3 months (Dworkin 1996). PHN is classed as a neuropathic pain that is associated with mechanical allodynia (Watson 1989).

Increasing age is the most important predictor of PHN, where older age has been consistently associated with an increase risk of developing PHN in patients with herpes zoster. Hope-Simpson (Hope-Simpson 1975) reported that the incidence of PHN was 3-4% in the 30-49 age group but rose to 29% in those 70-79 and 34% in the over 80 year old age group. In addition to age, 4 risk factors for PHN have been identified which are greater acute pain severity, greater rash severity, sensory dysfunction in the affected dermatome during acute herpes zoster and the presence of painful prodrome preceding the rash (Dworkin 1996). Patients with prolonged PHN often have ongoing disturbances in physical and psychosocial functioning. In severe cases, PHN can lead to drug dependency, depression, and even suicide (Chidiac et al. 2001).

A complete history and physical examination continue to be the standard for making the diagnosis of PHN. Pain is typically localised to the dermatome affected by the rash and most often described as burning, throbbing, or sharp and shooting in nature

(Kanazi et al. 2000). Allodynia, the presence of pain in response to a normally innocuous stimulus, is common in PHN and often causes patients great distress.

1.5.1 Pathogenesis

The pathogenesis of PHN remains unknown. Clinical virological correlations suggest that virus persistence in ganglia, which produces a chronic ganglionitis, is the cause. VZV specific DNA (Mahalingam et al. 1995) and VZV specific late glycoproteins (Vafai et al. 1988) have been found in blood MNCs of PHN patients 1-8 years after zoster. In zoster patients who did not develop PHN, VZV DNA was only found in MNCs up to 38 days, or not at all, after disappearance of zoster pain (Gilden et al. 1988). Further evidence that the longstanding radicular pain of PHN reflects a chronic ganglionitis has come from the detection of VZV DNA in blood MNCs and cerebrospinal fluid (CSF) of two patients with zoster sine herpete (pain without rash) (Gilden et al. 1994). It was reported that the pain disappeared after both patients were treated with intravenous acyclovir. However, PHN is resistant to opioid and non-steroidal anti-inflammatory drugs (NSAIDS), which are the mainstay of treatments for acute and inflammatory pain states. This suggests that inflammatory responses alone are not sufficient to induce PHN. Neuropathic pain such as PHN is characterised by neuronal hyperexcitability in damaged areas of the nervous system (Rowbotham 2001). This hyperexcitability is due to molecular changes (e.g. abnormal expression of sodium channels, changes in γ-aminobutyric acid (GABA) inhibition at the level of the

peripheral nociceptor, in the DRG. The mechanism in which latent VZV infection interacts with the neurone to induce such molecular changes is unclear.

1.5.2 Treatment

Like zoster, PHN has no universally accepted treatment. Furthermore, PHN often does not respond well to medications that are used to treat nociceptive pain, including acetaminophen (APAP), nonsteroidal anti-inflammatory drugs (NSAIDs) and opioids (Kost and Straus 1996). In the US, only Lidoderm (topical lidocaine) and Neurontin (gabapentin) have been approved by the US Food and Drug Administration for the treatment of PHN (Stankus et al. 2000). Current antiviral agents such as acyclovir, valaciclovir or famciclovir have been shown to reduce pain resulting from VZV and the overall duration of pain (Whitley 2001) providing treatment is given within 72 h after onset of the rash. Oral steriods may add to the benefit of antiviral therapy for reducing the acute pain of herpes zoster but have no effect on the development of PHN (Stankus et al. 2000). Tricyclic antidepressants e.g. amitriptyline, nortriptyline and desipramine remain an important treatment for patients with PHN because they have an analgesic effect in chronic pain that is independent of their antidepressant effect (Johnson 2002). Anticonvulsants like gabapentin has been shown to reduce pain severity by 66% in PHN patients in a randomised double-blind study (Berry et al. 2005). Opioids such as morphine, oxycodone and methadone are in routine use for PHN in which they help in pain relief and reduction in allodynia and disability (Watson et al. 1998). Although sympathetic nerve blocks maybe effective in relieving pain during acute zoster, these

blocks do not appear to provide prolonged relief in patients with long standing PHN (Watson et al. 1998). Topical capsaicin treatment is licensed for the treatment of PHN and was more efficacious than placebo in two of three small studies (Volmink et al. 1996). However, many patients experience local stinging and burning. Two small placebo controlled studies have indicated a beneficial effect of lidocaine patches in PHN (Rowbotham et al. 1996), (Galer et al. 1999).

1.6 Animal Models of VZV

The predominant obstacle to immunopathological studies of VZV is the lack of an animal model that could mimic the clinical events observed during human infection. Both *in vitro* and *in vivo*, VZV is remarkably species-specific to its primary host, humans. In addition to its cell-associated characteristic in tissue culture, it has been difficult to achieve sufficiently high titers of virus for use as inocula in the experimental animal and to manipulate *in vitro* to enhance the susceptibility of other species.

Non-human primates can be infected but usually remain asymptomatic, with the exception of gorillas and chimpanzees (Myers and Conelly 1992), (Cohen et al. 1996). When African green monkeys, *Erythrocebus patas*, and pygmy marmosets were infected with VZV, no infectious virus was recovered but VZV IgG antibodies were induced. Other models that have been used include the guinea pig (Myers et al. 1985), (Myers et al. 1991), common marmoset (Provost et al. 1987), rat (Sadzot-Delvaux et al. 1990), (Sadzot-Delvaux et al. 1995), mouse (Wroblewska et al. 1993) and rabbit (Dunkel et al. 1995).

The guinea pig model reproduces some critical events in VZV pathogenesis, including viremia and ganglion infection, and can be used to evaluate the host response to viral antigens (Myers and Conelly 1992), (Lowry et al. 1992), (Sabella et al. 1993). Animals remain asymptomatic, although some hairless weanling animals developed a very short-term exanthematous rash (Myers et al. 1991).

The common marmoset appears to be similar in many aspects to the guinea pig, in that infection leads to short-lived viremia, shedding of virus and seroconversion but with few clinical signs of disease (Provost et al. 1987). The ocular model in the rabbit eye was considered at one time as a potential model for herpes zoster ophthalmicus, but some highly variable parameters renders its acceptance (Dunkel et al. 1995). Ocular inoculation in mice resulted in detection of viral DNA but no viral protein found (Wroblewska et al. 1993).

Adult rats inoculated subcutaneously into the footpad with VZV caused a long-term persistence of virus in DRG where both RNA and protein could be detected (Sadzot-Delvaux et al. 1995). Fleetwood-Walker et al., (1999) have previously reported adaptation of this model and described the development of allodynia and hyperalgesia in infected rats up to day 35 post-infection. This model was further characterised and showed that infected rats develop chronic mechanical allodynia, which remains for longer than 60 days post infection and resolves by 100 days post infection (Dalziel et al. 2004). Although ganglionic infection can be established in this model after peripheral inoculation of VZV but the drawbacks of the rat model as a model of VZV latency in humans are that VZV does not reactivate, non-ganglionic tissues have not been shown to be free of VZV and VZV in rats is not restricted to ganglionic neurons (Cohrs et al.

2004). Since PHN is caused by a reactivation of VZV and no reactivation has been shown in the rats, there is concern of this model as a model of PHN in humans. However, ganglia of PHN patients cannot be studies during life, therefore, the rat model is so far the best studied model that could mimic the clinical situation of PHN in human.

VZV tropism for certain human cell types can be examined in the SCID-hu mouse model (Ito et al. 2005), (Baiker et al. 2004). These animals have allografts of human thymus/liver, containing CD4+, CD8+ and dual positive T cells or human skin implants that can be inoculated with VZV. The closely related simian varicella virus (SVV) of primates might also be a model to which human VZV latency can be compared due to their similarities at the level of antigenic similarity, genome organisation and DNA sequence (White et al. 1997), (Gray et al. 2004).

1.7 Project Aims

Investigating the molecular mechanisms of VZV pathogenesis has been difficult because of VZV's restricted infectivity for non-human species *in vivo* and the highly cell-associated nature of VZV replication *in vitro*. VZV latency also remains poorly understood partly due to the previous lack of a good animal model system. These obstacles have been addressed by the development of a rat model of VZV latency (Sadzot-Delvaux et al. 1990). This model was further adapted and able to demonstrate striking changes in behavioural reflex responses similar to changes seen in PHN patients (Fleetwood-Walker et al. 1999). Thus, the model provides an excellent system to study

the interactions of VZV with both the immune and nervous systems during a latent infection.

Using the rat model, we would like to test the hypothesis that presence of some or all of the genes found expressed in VZV latently infected neurones, results in an increased sensitivity to noxious stimulus. It may affect the physiological function of that neurone by either directly via a change in the nociceptive pathways and transcriptional activity of the neurone or in response to a chronic immune response directed to these proteins. The virus-host interactions that lead to development of the sensory changes similar to PHN could be measured by well-established tests of mechanical allodynia.

The objectives of this study are:

i) to correlate between the observed altered sensory behaviour with the pattern of gene expression in infected DRG

ii) to study the viral spread in the rat model

iii) to investigate which components of the virus are responsible for eliciting allodynia

The development and further characterisation of this model could serve as a useful and unique opportunity to study the host-virus interactions involved in the pathogenesis of PHN. Ultimately, by exploiting the rat model, a better insight into understanding the virus and cellular factor, which govern VZV latency and how the latent virus interacts with the sensory neurone harbouring it could be gained. This is essential if advances towards a treatment for PHN are to be made.

CHAPTER TWO

MATERIALS AND METHODS

2.1. Materials

2.1.1. Chemicals

All chemicals purchased were of molecular grade and obtained from Sigma (Sigma-Aldrich Ltd., UK) unless otherwise stated.

2.1.2. Common Media, Buffers and Solutions

The media, buffers and standard solutions used in this study are listed in Table 2.1. Broth was stored at room temperature and all agar plates were kept at 4°C. Broth and plates were used within 1 month or 2 weeks if antibiotics were added.

Table 2.1 Common Media, Buffers and Solutions

Media, Buffers, Solutions	Recipes, per litre
Luria-Bertani (LB)	Bacto-tryptone (10 g), Bacto-yeast extract (5 g), NaCl (5 g)
LB agar	LB broth, bacto-agar (15 g)
1× PBS	NaCl (0.1 M), KCl (2.7 mM), Na_2HPO_4 (4 mM), KH_2PO_4 (1.8 mM)
10× TAE	Tris-acetate (40 mM), EDTA (1 mM; pH 8.0)
TBS	Tris-HCl (50 mM; pH 7.5), NaCl (150 mM)
20× SSC	NaCl (3 M), Sodium citrate (0.3 M), adjust to pH 7.0 with NaOH
TE	Tris-Cl (10 mM; pH 8.0), EDTA (1 mM)

2.2. General Molecular Techniques

2.2.1. DNA Extraction from Animal Tissues

DNeasy Tissue kit (QIAGEN) was used to extract DNA from tissues. Small tissue pieces (~ 25 mg) were placed in a microcentrifuge tube with Buffer ATL (180 µl). Proteinase K (20 mg/ml; 20 µl) was added and the reaction incubated at 55°C for 3 h or overnight until the tissue was completely lysed. The sample was vortexed for 15 s and Buffer AL (200 µl) was added, mixed thoroughly and incubated at 70°C for 10 min. Ethanol (96-100%; 200 µl) was added to the sample and mixed. The mixture was transferred to the DNeasy spin column and centrifuged for 1 min at 6000 × g and the flow-through discarded. The DNeasy spin column was placed in a new collection tube (2 ml). Buffer AW1 (500 µl) was added and centrifuged as described above. The process was repeated with Buffer AW2 (500 µl) but with centrifugation for 3 min at 13,000 × g to dry the DNeasy membrane. For elution, the DNeasy spin column was placed in a clean microcentrifuge tube (1.5 ml) and Buffer AE (100 µl) was pipetted directly onto the membrane. The column was incubated for 1 min at room temperature before being centrifuged for another minute at 6000 × g. The elution was repeated with the first eluate. The DNA was kept at -20°C until use.

2.2.2. DNA Extraction from Animal Cells

An appropriate number of cells (5×10^6) were trypsinised and centrifuged for 5 min at 300 × g. The pellet was resuspended in PBS (200 µl). Proteinase K (20 mg/ml; 20 µl) and Buffer AL (200 µl) was added to the sample, mixed thoroughly and incubated at 70°C for 10 min. The remainder of the protocol was similar to DNA extraction from animal tissues (section 2.2.1).

2.2.3. DNA and Total RNA Extraction from Animal Cells or Tissue

Simultaneous isolation of DNA and total RNA from animal cells or tissues could be performed in QIAGEN RNA/DNA kit according to the manufacturer's instruction. A T175 flask of virus infected cells were trypsinised and collected as a cell pellet prior to lysis. In order to trypsinised cells, medium was removed and cells were washed with PBS. PBS was removed and cells were trypsinised with 0.1-0.25% trypsin in PBS. After cells were detached from the flask, medium was added and cells were transferred to a polypropylene centrifuge tube and centrifuged at 300 × *g* for 5 min. Supernatant was removed, cell pellet was loosen by flicking the tube and lysis Buffer QRL1 with pre-mixed β-mercapthoethanol (1:100) were added. Buffer QRV1 (0.5 ml) was added, mixed and centrifuged at 15,000 × *g* for 20 min at 4°C. The supernatant was carefully transferred into an RNase-free 2 ml collection tube. Ice-cold isopropanol (0.8 ml) was added and the tube was incubated on ice for 5 min followed by centrifugation at 15,000 × *g* for 30 min at 4°C. In the meantime, the QIAGEN-tip was equilibrated with Buffer

QRE (1 ml) by allowing the buffer to enter the column by gravity flow. The supernatant was discarded after the centrifugation and Buffer QRL1 (0.15 ml) was added. The nucleic acid pellet was dissolved by heating the tube for 3 min at 60°C followed by vortexing for 5 s and flicking sharply the tube. This step was repeated at least twice. Buffer QRV2 was added (1.35 ml), mixed thoroughly by vortexing and centrifuged at 5000 × *g* for 5 min at 4°C. Sample was then applied to the equilibrated QIAGEN-tip and allowed to enter the resin by gravity flow. Flow-through was collected for subsequent DNA isolation and placed at room temperature. Buffer QRW (2 ml) was pipetted onto the QIAGEN-tip and allowed to enter the resin by gravity flow. Buffer QRU (1 ml) pre-heated to 45°C was added onto the QIAGEN-tip and the RNA was eluted by gravity flow into a 2 ml collection tube. Ice-cold isopropanol (1 ml) was added to the eluate, mixed and placed on ice.

For isolation of genomic DNA, the flow-through from above was pipetted onto the same QIAGEN-tip and was allowed to enter the resin by gravity flow and this process was repeated with the same flow-through. Buffer QC (3 ml) were added to the QIAGEN-tip and was allowed to enter the resin by gravity flow. The genomic DNA was eluted with preheated Buffer QF (1 ml). Isopropanol (0.7 vol) at room temperature was added to the eluate, mixed and incubated for 10 min at room temperature. The isopropanol precipitated RNA and DNA were centrifuged at 15,000 × *g* for 30 min at 4°C and the supernatant was carefully removed. Ice-cold 70% ethanol was added, vortexed briefly and centrifuged at 15,000 × *g* for 20 min at 4°C. The supernatant was removed and this step was repeated once. The RNA and DNA pellets were air-dried

approximately 10 min at room temperature with the tubes resting upside down on a paper towel. The DNA and RNA were dissolved in TE buffer (100 µl) and RNase-free water (20 µl), respectively, by heating the tube for 3 min at 60°C, followed by vortexing for 5 s and flicking sharply the tube and repeated at least twice. The DNA was then stored at -20°C and the RNA was kept at -80°C until use.

The isolation method used for animal tissues was the same except in the starting material where approximately 20 mg of tissues were used.

2.2.4. DNA Extraction from Whole Non-nucleated Blood

Proteinase K (20 mg/ml; 20 µl) followed by anti-coagulated blood (100 µl) was added to a microcentrifuge tube (1.5 ml) and the volume was adjusted to 220 µl with PBS. Buffer AL (200 µl) was added and mixed thoroughly. The reaction was incubated at 70°C for 10 min. The rest of the protocol was similar to DNA extraction from tissues (section 2.2.1).

2.2.5. Quantitation of Nucleic Acids

DNA and RNA concentrations were determined by the measuring of their absorbance at 260 nm in a spectrophotometer (Cecil). An A_{260} of 1 corresponds to 50 µg DNA and 40 µg RNA per ml water.

2.2.6. Agarose Gel Electrophoresis

PCR products were resolved by electrophoresis in 2% (w/v) agarose gel containing ethidium bromide (0.5 μg/ml). 15 μl of the PCR products were added with Blue/Orange 6× loading dye [Promega, 15% (w/v) Ficoll 400, 0.03% (w/v) Bromophenol blue, 0.03% (w/v) Xylene Cynol, 0.4% (w/v) Orange G, Tris-Cl (10 mM, pH 7.5), EDTA (50 mM); 3 μl]. The electrophoresis was carried out at constant voltage (13 cm × 15 cm gels at 110 V) for 60 min in a horizontal gel apparatus (Bio-Rad) with 1× TAE buffer. Fragments were sized using a 100 bp DNA ladder (Invitrogen). DNA was visualised on a UV transilluminator and the gel photographed with a UVP camera.

2.2.7. Restriction Endonuclease Digestion

Restriction enzymes were purchased from New England Biolabs. Reactions were carried out in a volume of 10-20 μl with 1 U enzyme per μg DNA and incubated at the optimum temperature with the appropriate buffers following the manufacturer's instruction.

2.2.8. Ligation using the pGEM-T Easy Vector System

Ligation reactions containing 2× Rapid Ligation buffer [Tris-Cl (60 mM, pH 7.8), $MgCl_2$ (20 mM), DTT (20 mM), ATP (2 mM), 10% (w/v) polyethylene glycol (MW8000); 5 μl], pGEM-T Easy vector (50 ng; 1 μl, Promega), T4 DNA ligase (3 W; 1

μl, Promega) and PCR products were set up in a total volume of 10 μl, mixed and incubated at 4°C overnight.

2.2.9. Sequencing

All plasmid inserts into pGEM-T Easy vector were identified and confirmed by sequencing which was carried out by Mr. Ian Bennet using an automated LI-COR DNA sequencer model 4000L (MWG-Biotech). Primers used were M13 reverse sequencing primer (5'-GGA TTA CAA TTT CAC ACA GG-3') and M13 universal primer (5'-GTA AAA CGA CGG CCA GT-3').

2.2.10. Southern Blot Analysis

Southern blot analysis was carried out in this study to confirm the identity of the nested-PCR products. A 20-mer oligonucleotide (5'-CGT GCT GGG AGG AAT TGT TA-3') specific to VZV gene 63 was synthesised to be used as a probe in Southern blot. The oligonucleotide was ezymatically labelled at the 3' end by incorporation of a single digoxigenin-labelled dideoxyuridine-triphosphate (DIG-dUTP) terminal transferase. 100 pmol of the oligonucleotide was added to 20 μl reaction mixtures containing 5× reaction buffer [Potassium cacodylate (1 M), Tris-HCl (0.125 M), bovine serum albumin (1.25 mg/ml), pH 6.6; 4 μl], $CoCl_2$ solution (25 mM; 4 μl), DIG-dUTP (1 mM; 1 μl), dATP (10 mM; 1 μl) and terminal transferase (400 U; 1 μl). The reaction was mixed, incubated

at 37°C for 15 min and placed on ice for 5 min. The reaction was terminated by adding EDTA (0.25 M; 1 µl). The probe was stored at -20°C until use.

PCR products were electrophoresed in a 2% (w/v) agarose gel with DIG labelled DNA molecular weight marker VIII (Roche) and a photograph of the gel was taken. A small triangular piece was cut from the bottom left-hand corner of the gel to simplify orientation during the succeeding operations. The gel was then incubated in denaturation buffer (0.5 M NaOH, 1.5 M NaCl) twice for 20 min with gentle agitation and rinsed briefly with dH_20. The gel was transferred to neutralisation buffer (1 M Tris-Cl, 1.5 M NaCl) for 20 min and repeated twice.

A support larger than the gel was placed in a tray containing 10× SSC and covered with a Plexiglas plate. Two lengths of Whatman 3 MM paper wider than the gel and long enough to reach the bottom of the dish on either side were placed on the glass plate. When the blotting paper on top of the support was thoroughly wet, air bubbles were removed by rolling with a pipette. Two sheets of blotting papers and a positively charge nylon membrane (Roche) were cut 1 mm larger than the gel in each dimension. The membrane was first wet in dH_20 and then in 10× SSC for 5 min. The gel was placed up-side down on the platform and any air bubbles removed. The gel was surrounded with parafilm to ensure the buffer moved only through the gel and not around it. The pre-cut membrane was then placed on top of the gel so that the cut corners were aligned. A pipette was rolled across the surface of the membrane to remove any air bubbles. Two sheets of Whatman 3MM papers were briefly wet in 10× SSC and placed on top of the nylon membrane. A stack of paper towels (10-15 cm) were cut just smaller than the

blotting papers were put on top of the papers. A second Plexiglas plate was placed on top of the paper towels and weighed down with a 1 kg weight. The transfer of DNA was allowed to proceed overnight.

The next morning, paper towels and blotting papers above the gel were removed. The gel and the attached membrane were turned over, gel side up on a dry sheet of blotting paper. The positions of the gel slots were marked with a soft lead pencil. The gel was peeled from the membrane and discarded. The membrane was put into a UV stratalinker to crosslink the DNA to the membrane.

The membrane was prehybridised in prewarmed hybridisation buffer (DIG Easy Hyb, Roche) at 50°C for 30 min with gentle agitation. The hybridisation buffer was discarded and new prewarmed hybridisation buffer containing DIG labelled probe (0.002 pmol) was added. The hybridisation process was continued overnight at 50°C with gentle agitation. The membrane was washed twice for 5 min each in 2× SSC 0.1% (w/v) SDS at room temperature under constant agitation. The membrane was washed twice more stringently for 15 min in 0.1× SSC, 0.1% (w/v) SDS at 50°C.

The DIG Luminescent Detection kit (Roche) was used to detect the DIG-labelled oligonucleotides using anti-digoxigenin, alkaline phosphatase conjugates and visualised with chemiluminescence substrate CSPD (Disodium 3-{4-methoxyspirofl, 2-dioxetane-3,2'- [5'-chloro] tricyclo [3.3.1.13,7] decan] 4-yl} phenyl phosphate). All incubations were performed at room temperature with agitation. Following post hybridisation washes, the membrane was rinsed briefly in washing buffer [0.1 M Maleic acid, 0.15 M NaCl, 0.3% (v/v) Tween 20, pH 7.5]. The membrane was incubated for 30 min in 10×

blocking solution [10% (w/v) propriety blocking reagent in Maleic acid buffer {Maleic acid (0.1 M), NaCl (0.15 M), pH 7.5}] and then for another 30 min in antibody solution (anti-DIG-AP conjugate diluted 1:10,000 in 1× blocking solution). The membrane was washed twice in washing buffer, 15 min each and equilibrated in detection buffer (0.1 M Tris-Cl, 0.1 M NaCl, pH 9.5) for 5 min. The membrane was placed on a development folder, DNA side facing up and 2 ml of diluted CSPD solution were applied. The membrane was covered immediately with the second sheet of folder to spread the substrate evenly and without air bubbles and incubated for 5 min. Excess liquid was squeezed out and the edges of the development folder was sealed. The damp membrane was incubated for 15 min at 37°C to enhance the reaction. The membrane was exposed to Lumi-film (18 × 24 cm, Roche) for 3 h or longer if required.

2.3. Bacterial Work

2.3.1. Growth and Maintenance of *Escherichia coli*

Bacterial cultures for plasmid preparation were grown from a single colony picked from a freshly streaked ampicillin (100 µg/ml) plate. A single colony was inoculated into LB medium (5 ml) containing ampicillin (100 µg/ml), and grown with vigorous shaking at 225 rpm at 37°C for 12-16 h.

2.3.2. Transformation of *E.coli* cells with Plasmid DNA

The ligation reactions were centrifuged briefly and placed on ice. One vial of One Shot Top10F' competent cells was thawed for each ligation. Transformation was carried out by adding the ligation mixture (5 µl) directly to the competent cells and mix gently by tapping. The cells were incubated on ice for 30 min and then 30 s at 42°C and quickly placed them on ice for 5 min. Pre-warmed SOC medium (250 µl) was added to each vial and incubated at 37°C for 1 h with shaking at 225 rpm. Different volumes of transformation mixtures (50 µl, 100 µl and 150 µl) were spread on separate LB agar plates containing ampicillin (100 µg/ml), X-gal (80 µg/ml) and IPTG (0.5 mM). The plates were inverted and incubated at 37°C overnight. Single white colonies were selected for further analysis by plasmid isolation, PCR, restriction enzyme digestion or sequencing.

2.3.3. Small-scale Preparation of Plasmid DNA

Small-scale extraction of plasmid DNA was carried out using QIAprep Miniprep kit (QIAGEN) following the manufacturer's instruction. Overnight cultures (1.5 ml) were centrifuged at 12,000 × g for 10 min and the supernatant removed. The bacterial cells pellet were resuspended in ice-cold Buffer P1 [Tris-Cl (50 mM, pH 8.0), EDTA (10 mM), RNase A (100 µg/ml); 250 µl]. Buffer P2 [NaOH (200 mM), 1% (w/v) SDS; 250 µl] was added and the tube was inverted gently 4-6 times to mix. Buffer N3 [KAc (3 M, pH 5.5); 350 µl] was added and the tube was inverted gently 4-6 times. The suspension was centrifuged for 10 min at 12,000 × g in a microcentrifuge. The supernatant was then

applied to the QIAprep Spin Column and centrifuged for 1 min. The flow-through was discarded. The QIAprep Spin Column was washed by addition of Buffer PE (750 µl) and centrifuged for 1 min. The flow-through was discarded and the column was centrifuged for an additional 1 min to remove residual wash buffer. The QIAprep Spin Column was put in a clean 1.5 ml centrifuge tube. Buffer EB [Tris-Cl (10 mM, pH 8.5); 50 µl] was added to the centre of each column and centrifuged for 1 min to elute DNA. Recombinant plasmids were screened by PCR, restriction enzyme digestion and sequencing.

2.4. RNA Work

2.4.1. RNA Stabilisation in Tissues

Fresh tissue samples less than 0.5 cm thick were immersed in 10 volumes of RNAlater RNA Stabilisation Reagent (Ambion).

2.4.2. Total RNA Extraction from Animal Tissues

Total RNA extraction from tissue was performed using the RNeasy Mini kit (QIAGEN). Stabilised tissues were removed from RNAlater. Approximately 30 mg of tissue was placed into 1.5 ml microcentrifuge tubes and disrupted in Buffer RLT with β-Mercaptoethanol (500 µl) using a disposable pestle (Sigma). The lysate was then homogenised immediately in a QIAshredder spin column (QIAGEN) at 12,000 × g for 2

min. The supernatant was transferred to a new microcentrifuge tube and 70% (v/v) ethanol (500 µl) was added and mixed. The samples were then applied to RNeasy mini columns and centrifuged for 15 s at 12,000 × g. The flow-through was discarded and Buffer RW1 (350 µl) added. The columns were centrifuged for 15 s at 12,000 × g and the flow-through discarded. DNase I (2.727 Kunitz; 10 µl) were added to Buffer RDD (70 µl) and gently inverted to mix. The DNase I solution was applied directly onto the RNeasy silica-gel membrane, and incubated for 15 min at room temperature. Buffer RW1 (350 µl) was added to the column and centrifuged for 15 s at 12,000 × g and the flow-through discarded. Buffer RPE (500 µl) was added and the columns centrifuged at 12,000 × g for 15 s. Another aliquot of Buffer RPE (500 µl) was added to the columns and centrifuged at 12,000 × g for 2 min to dry the RNeasy silica-gel membrane. The columns were transferred to new 1.5 ml microcentrifuge tubes for elution. RNase-free water (30 µl) was placed directly on the membrane and centrifuged for 1 min at 12,000 × g. A second elution was performed with the first eluate to obtain a higher total RNA concentration. The RNA was then reverse-transcribed immediately (section 2.4.4) or kept at -80°C.

2.4.3. Total RNA Extraction from Mamalian Cells

Cells grown in a monolayer in cell-culture vessels were trypsinised and collected as a pellet prior to lysis. Medium from the flask was aspirated and cells washed with PBS. PBS was decanted and 0.25% (v/v) trypsin was added. After cells were detached

from the flask, medium containing serum was added to inactivate the trypsin. Cells were transferred to polypropylene centrifuge tubes and pelleted by centrifugation at 1000 × g for 5 min. The supernatant was completely aspirated and disruption of the cells was followed by addition of Buffer RLT. The remaining of the extraction steps were the same as the protocol used for total RNA extraction from animal tissues (section 2.4.2).

2.4.4. Reverse-Transcriptase Polymerase Chain Reaction

Template RNA was thawed on ice. Up to 2 µg of RNA was used with the Omniscript Reverse Transcription kit (QIAGEN). A master mix containing 10× Buffer RT (2 µl), dNTP mix (2 µl; 0.5 mM each dNTP), Oligo-dT primer (2 µl; 1 µM), RNase inhibitor (1 µl; 10 U), Omniscript Reverse Transcriptase (1 µl; 4 U) and RNAse-free water in a total volume of 20 µl for one reaction was prepared. The reaction was mixed thoroughly and centrifuged briefly to collect residual liquid from the wall of the tube. The appropriate volume of master mix was distributed into individual tubes and kept on ice. Template RNA was added into tubes containing the master mix and mixed. The reaction was incubated at 37°C for 1 h. An aliquot (2-4 µl of the RT product) of the finished reverse-transcription reaction was added to the PCR mix for RT-PCR.

2.5. Mammalian Cells and Viruses

2.5.1. Cells and Viruses

CV-1 (Monkey African Green Kidney Fibroblast) cells were grown and maintained in Dulbecco's modified Eagles medium (DMEM; Gibco) supplemented with L-glutamine (2 mM) and 10% (v/v) foetal calf serum (FCS) in a 5% CO_2 incubator at 37°C. VZV strain Ellen (VR-568 mycoplasma free strain from ATCC, VA, USA), VZV parental Oka (pOka) strain and VZV vaccine Oka (vOka) strain were all propagated on CV-1 cells. VZV strain Dumas was propagated on Mewo cells. POka, vOka and Mewo cells were kind gifts from Dr. Marvin Sommer and Professor Ann Arvin of Stanford University.

2.5.2. Long Term Storage of Cells and Viruses

For long term storage, cells and viruses were frozen down in freezing mix [90% (v/v) FCS, 10% (v/v) DMSO] and kept in liquid nitrogen.

2.5.3. Recovering Cells and Viruses from Liquid Nitrogen

Vials of cells or viruses from the liquid nitrogen were thawed quickly in a 37°C water bath. A few drops of pre-warmed media were added carefully to the vials to equilibrate the osmotic pressure slowly. The cell were then aspirated into universal tubes containing 20 ml prewarmed media and centrifuged at 1000 × g for 5 min at room

temperature. The cell pellet was resuspended in 5 ml of media and put into a T25 flask. The flask was incubated overnight at 37°C in a 5% CO_2 incubator and growth was checked the next day. If cells were growing well, they were split into fresh medium and moved into the next sized flask.

2.5.4. Virus Propagation and Harvesting of Virus

Early log phase CV-1 cells were always used for VZV infection. A vial of virus was recovered from liquid nitrogen as mentioned in section 2.5.3 but the cell pellet was resuspended in 10 ml of pre-warmed media. The virus suspension was added to the flask containing cells where the media has been aspirated and incubated at 37°C. After an hour, 2% (v/v) DMEM was added (40 ml) to the flask. The virus was harvested when cells showed 80% cytopathic effect. The cells were then scraped from the flask using a cell scraper and centrifuged at 1000 × g for 10 min. The pellet was mixed well until no sign of cell clumps were visible, and the suspension of virus was used to infect new batches of log phase cells.

2.6. Animals and Behavioural Testing

2.6.1. The Rat Model of VZV Latency

In this project, all tissues used for study were obtained from rats infected with VZV and tested for allodynia. Briefly, the model is as follow: VZV was propagated in

CV-1 cells and harvested when cells exhibited approximately 80% cytopathic effect. Male Han Wistar rats were anaesthetised and injected subcutaneously in the left (ipsilateral) glabrous footpad with approximately 4×10^6 infected cells per animal in 50 μl medium. Behavioural test was carried out at specific days post infection to test for the development of allodynia with a calibrated set of von Frey filaments. Figure 2.1 shows a simplified diagram of the rat model. During testing, rats were removed from their cages and placed in lidded wire mesh cages that allowed full access to the paws. The rats were left to acclimatise for 10-15 min until they were quite settled and had all paws flat on the wire mesh cage (Figure 2.2A). Care was taken during the testing procedure to ensure that the animals were not putting their weight on the hind paws. Animals showed no obvious signs of discomfort and phenotypic changes only evident on formal testing. Details of assessment of allodynia with a set of von Frey filaments (Figure 2.2B) are described in section 2.6.4.

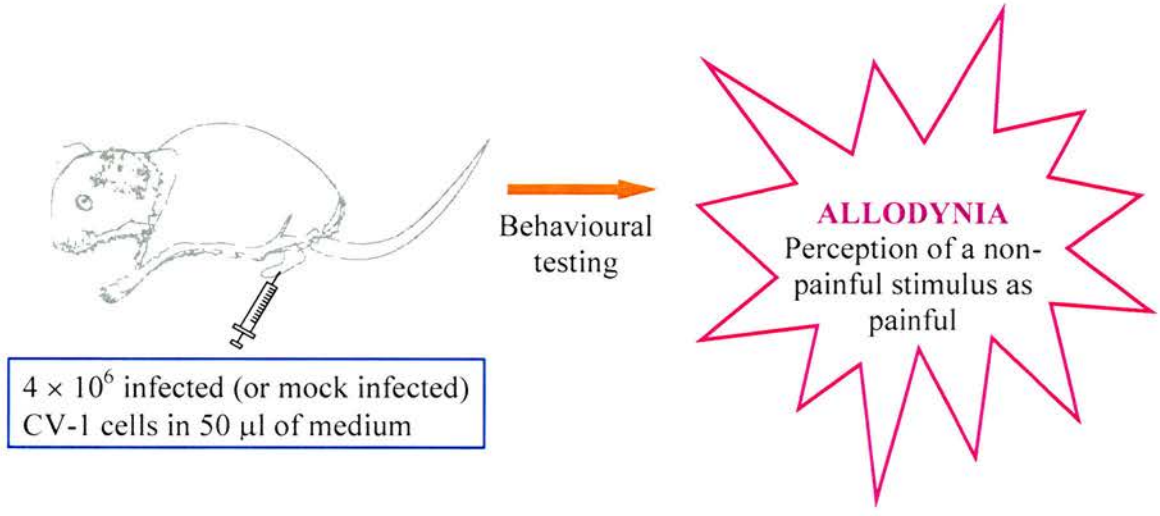

Figure 2.1 A diagram of the rat model. Male Han Wistar rats were injected subcutaneously with 4×10^6 infected (or mock infected) CV-1 cells in 50 µl medium into the left hind paw. Animals were tested on specific days post infection for development of allodynia.

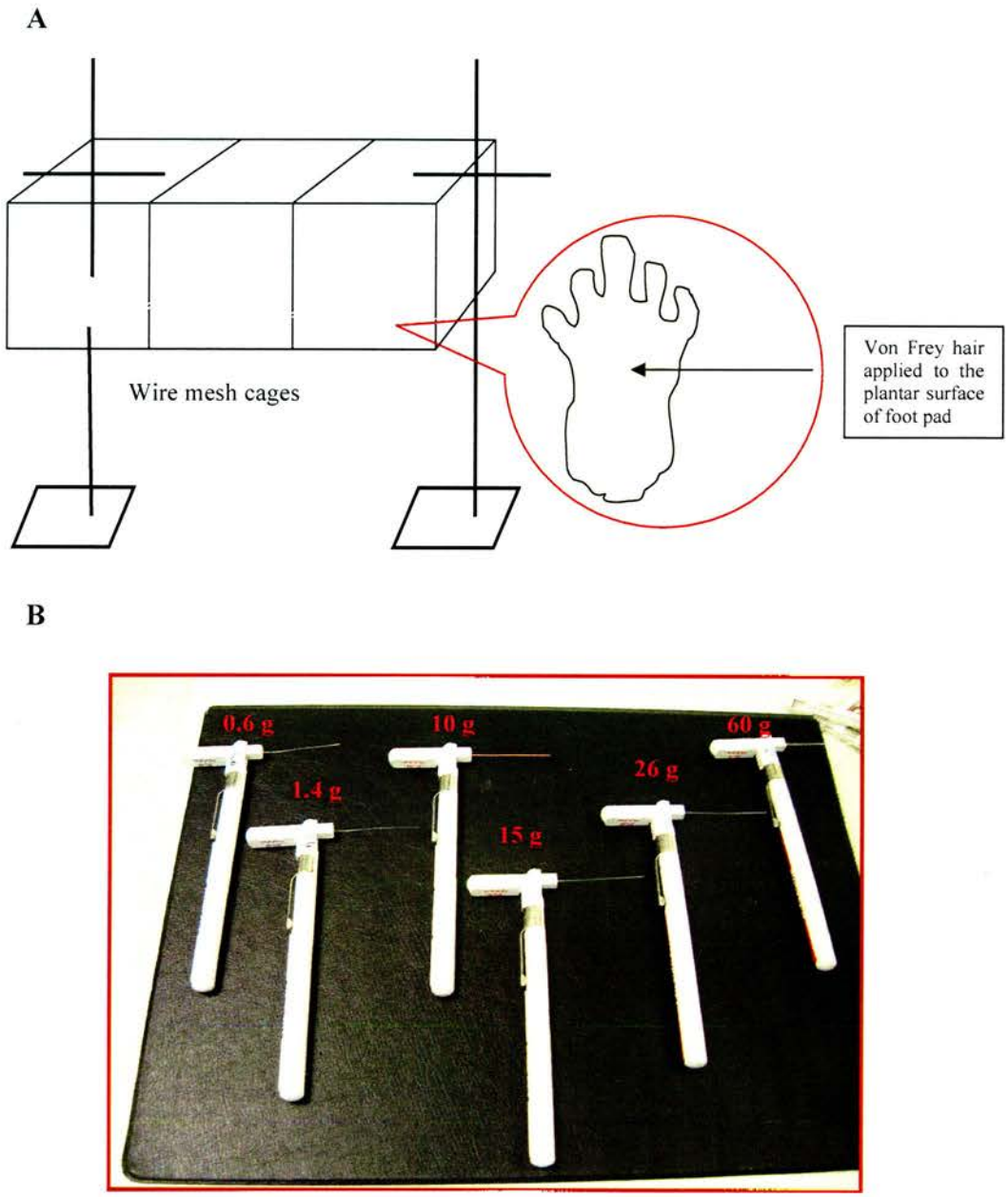

Figure 2.2 A diagram of the acclimatisation of rats in wire mesh cages and von Frey filaments. A) Acclimatisation of animals in wire mesh cages before testing. B) Von Frey filaments with different target forces (g) (note the difference thickness of the hair, 0.6 g is the lowest force and 60 g is the highest force) when applying to the footpad of rats during behavioural testing.

2.6.2. Source of Animals

Male Wistar rats (150-200 g; Harlan) were housed under standard light conditions and food and water allowed *ad libitum*. All animal experiments were carried out under the provision of Home Office project license (60/2760) and personal license (60/8842).

2.6.3. Inoculations

Animals were anaesthetised with Halothane prior to footpad injections. The glabrous skin of the left footpad was injected subcutaneously with approximately 4-8 × 10^6 VZV infected cells following previous experience (Dalziel et al, 2004) that on average these amount of cells were present in a near confluent T175 flask. Control rats were injected with uninfected cells and housed separately from the virus infected animals.

2.6.4. Assessment of Allodynia

Behavioural tests were carried out prior to infection and at the specified times post infection. Animals were randomised into groups according to their weight and mean paw withdrawal threshold (PWT) based on the readings from pre-testing sessions. The rats were placed in wire mash cages which allowed full access to the paws and were allowed to acclimatise prior to testing for about 10 to 15 min. PWT were measured using an ascending series of von Frey filaments. These hairs were applied manually to the

middle region of the left hind paw plantar surface. The hairs were applied with sufficient force to cause buckling of the filaments. Vertical elevation of the paw was considered as a positive withdrawal response. Whenever two positive responses out of five applications of the same hair were recorded, the next smaller von Frey hair was applied. Whenever a negative response occurred, the next higher force was applied. Triplicates of the ascending series were performed and the average was recorded.

2.6.5. Tissue Collection and Preservation

At the end of a study, animals were euthanised in a CO_2 chamber. Autopsy was performed whereby lumbar L1-L6 DRGs ipsilateral and contralateral to the site of injection were removed. Other tissues removed included foot pads, sciatic nerves, spleen, spinal cord, brain and blood. The tissues were either snap frozen in cooled isopentene bath kept in dry ice for DNA extraction (section 2.2.1) or immersed directly into RNAlater for RNA extraction (section 2.4.2).

2.7. Polymerase Chain Reaction

DNA was extracted from VZV infected CV-1 cells (section 2.2.2) as a template or positive control in polymerase chain reaction (PCR). Routinely, a nested or hemi-nested PCR was carried out in a total volume of 50 µl in a Hybaid PCR Sprint thermal cycler.

A master mix was prepared which contained all the components needed for PCR except the template DNA. The primary (1^0) reaction mixtures composed of

deoxynucleotide mix (10 mM each dNTP; 1 µl), 10× PCR reaction buffer with $MgCl_2$ [100 mM Tris-HCl, 15 mM $MgCl_2$, 500 mM KCl, pH 8.3; 5 ml], sense primer (100 ng; 1 µl), anti-sense primer (100 ng; 1 µl), HotStarTaq DNA polymerase (QIAGEN, 2.5 U; 0.25 µl) and dH_2O. 100-500 ng of genomic DNA or equivalent volume of sterile nuclease-free water (Sigma) as negative control was added finally to the individual tubes containing the master mix.

A 15 min initial incubation at 95°C was required to activate the HotStarTaq DNA polymerase followed by 35 PCR cycles (94°C, 30 s; 55°C, 30 s; 72°C, 60 s) and a final elongation at 72°C, 10 min. Nested or hemi-nested PCR (2^0) mixtures and conditions were identical to the 1^0 reaction except an aliquot of 1-2 µl of the 1^0 amplification product was used as the template and different sets of internal primers (P2 + P4 or P2 + P3). All oligonucleotides were synthesised by MWG-Biotech and their details are listed in Table 2.2.

Table 2.2 Oligonucleotide Primers

Gene	Name	Sequence (5' to 3')	Location
*ORF-63	VZV63P1	GCG AGA TTC ACG AAG ATT GCG	110817[a]
	VZV63P2	TTA TCT AAT GGG TCG CAC C	110856[a]
	VZV63P3	TCA ATT ACA TCC GAT GGC G	111092[b]
	VZV63P4	GCT ATC GTC TTC ACC ACC	111058[b]
*ORF-10	VZV10P1	GAT ATT ATC GTG AGG TGG	12821[a]
	VZV10P2	TTT CCT GGC GTT TGT ACG	12884[a]
	VZV10P3	CTT TTG CGT AAG GAT GAT CCG	13249[b]
	VZV10P4	CTTG AGG ATG TTT GAC CGC	13213[b]
*ORF-21	VZV21P1	ACA AGG CAG CAG TTT CAT TCG	33589[a]
	VZV21P2	CCG ACG CTG ATA ATA GGA CAA	33771[a]
	VZV21P3	GGT CAC TCC CAC TTG TAT TCC	33872[b]
ORF-62	VZV62P1	CCG AGG ATT CGT AAG ACC AA	122033[a]
	VZV62P2	GCG CCA GAG ACA GAA ATC A	122074[a]
	VZV62P3	GCT CTC ACA GCC TCA TCC TC	122262[b]
β-actin	ActinP1	GGC ACC ACA CTT TCT ACA	257[c]
	ActinP2	CTG TGT TGT CCC TGT ATG	413[c]
	ActinP3	GAG GTC TTT ACG GAT GTC	798[d]
	ActinP4	AAG GAA GGC TGG AAG AGA	879[d]

[a] Sense, same (5' to 3') direction as the ORF following VZV Dumas strain sequence (Davison and Scott, 1986)

[b] Antisense, opposite (5' to 3') direction from that of the ORF following VZV Dumas strain sequence (Davison and Scott, 1986).

[c] Location of 5' nucleotide with respect to the rat β-actin sequence (Nudel et al., 1983)

[d] Antisense location of 5' nucleotide with respect to the rat β-actin sequence (Nudel et al., 1983)

* Oligonucleotide sequences adapted from Cohrs et al. 1996

2.7.1. Nested-PCR Optimisation

Optimisation of the annealing temperature was performed for every set of primers to obtain the best amplification of the target with the least unspecific products. PCR was carried out as mentioned in section 2.7 but instead of DNA being added to each individual tubes, it could be added to the master mix preparation and distributed evenly to each microcentrifuge tubes. The PCR was performed in a gradient thermal cycler with temperature ranging from 42°C to 64°C with a step of 2°C (Robocycler, Stratagene).

2.8. Developing Real-time PCR Assay

2.8.1. Optimisation of Real time PCR Assay

Optimisation of the reagents used to perform PCR is critical for reliable and reproducible results. The following criteria were optimised: magnesium chloride concentration, primer concentration, template concentration and SYBR Green I concentration.

2.8.2. Standard Curve Construction

Assays were performed with 10-fold serial dilutions from 1 to 10^8 copy numbers of a plasmid containing a 294 bp insert of the IE63 gene. For plasmid construction, the corresponding sequence of the IE 63 region was amplified using primers VZV63P1 and VZV63P3 (Table 2.2) and ligated into pGEM-T Easy vector (Promega, section 2.2.8),

according to the manufacturer's instructions. Plasmid was extracted from selected positive clones, its concentration was determined (section 2.2.5) and the corresponding copy number was calculated using the formula below:

$$\frac{6.02 \times 10^{23} \text{ (copies/mol)} \times \text{concentration (g/µl)}}{\text{MW (g/ mol)}} = \text{Amount (copies/µl)}$$

MW = Molecular weight (g/mol)

1 mol = 6.02×10^{23} molecules (copies)

Average MW of dsDNA = (number of base pairs) x (660 Daltons/base pairs)

Example:

For pGEM-T Easy-63 plasmid that has a concentration of 215 ng/µl = 2.15×10^{-7} g/µl and a total size of 3309 bp:

MW = 3309 (bp) x 660 (Daltons/bp) = 2.18×10^{6} Daltons

1 mol = 2.18×10^{6} g

Also 1 mol = 6.02×10^{23} molecules (=copies)

$$\frac{6.02 \times 10^{23} \text{ (copies/mol)} \times 2.15 \times 10^{-7} \text{ (g/µl)}}{2.18 \times 10^{6} \text{ (g/mol)}} = 5.9 \times 10^{10} \text{ (copies/µl)}$$

The standard curve was plotted with fluorescence threshold (Ct) versus template concentration and concentrations of the samples were determined by interpolation.

2.8.3. Melting Curve Analysis

Melting curve analysis must be carried out at the end of the PCR amplification when using SYBR Green I format to identify specific PCR products from artefacts. Temperature dependent fluorescence measurements were made whilst slowly increasing the temperature of the reaction products from 65°C to 95°C. A graph of the first negative differential of the fluorescence signal with respect to temperature was plotted against temperature.

2.9. Laser Capture Microdissection

2.9.1. Preparation of Slide

Cryostat sections of snap frozen tissues were prepared on non-coated slides by Ms. Deborah Hall at the Department of Pathology, Easter Bush Veterinary Centre. The sections were stained with haematoxylin-eosin for better visualisation of the tissue architecture.

2.9.2. Lifting of Single Cell

LCM was carried out using a PixCell LCM system (Arcturus Engineering, Santa Clara, CA). A haematoxylin-eosin stained slide was examined under the microscope and area of interest was selected using a joystick to move the slide easily until the cells of interest were in the centre of the optical field. A thermoplastic polymer coating, ethylene vinyl acetate (EVA), attached to a rigid support was placed in contact with the tissue section with a transport arm. Then, with the simple push of a button, an infra red laser, focused to the size of the desired target, was pulsed which melts the film directly above the targeted cells. The focally melted polymer expanded and impregnated the voids in the targeted tissue and then solidified as it rapidly cooled. At this point, the tissue-containing polymer had become a mechanically strong, 5 μm thick, solid composite bonded onto the surface of the pure polymer film. In this manner, multiple identical cells was separately targeted and bonded to the polymer film. When the film and the cap were lifted off the tissue section, the tissue sheared at the edges of the polymer/tissue composite, leaving all the untargeted and unimpregnated tissue still attached to the glass slide. Only the selected cells that were targeted by the laser and captured by the polymer film transferred with it, while the rest of the tissue remained intact and ready for further dissection. The LCM process was repeated over and over on the same section until sufficient cells were collected. The cells on the cap were lysed in Buffer ATL (100 μl) containing Proteinase K (10 mg/ml) at 55°C overnight. DNA was extracted from approximately 30-40 cells using the DNeasy Tissue Kit (Qiagen) following the protocol

described in section 2.2.2. Nested-PCR was performed using primers specific for VZV 63 (VZV63P1 + VZV63P3; VZV63P2 + VZV63P4, Table 2.2).

2.10. Microarray

2.10.1. RNA Preparation

Tissues from 9 DRGs spanning lumbar segment L4, L5 and L6 ipsilateral to the site of injection were pooled from 3 VZV infected rats. Only animals showing the highest allodynia response were selected in this study. Animals were also mock-infected with CV-1 cells to serve as control in the study. Total RNA was extracted with RNeasy Mini kit (QIAGEN, section 2.4.2). The RNA was eluted with 30 µl RNase-free water, quantitated by UV spectrophotometer (Cecil) and quality checked with an Agilent 2100 Bioanalyser (Agilent Technologies) according to the manufacturer's instruction. Briefly, 1.0 µl of RNA was heat denatured at 70°C for 2 min and cooled on ice for at least 5 min in order to minimise secondary structure. Meanwhile, the RNA Agilent chip was prepared by loading gel and markers as per manufacturer's instructions. Each chip was loaded with up to twelve 1 µl samples of total RNA. Concentrations were determined by comparison to RNA ladder (150 ng) and integrity determined with visualisation of 18S and 28S ribosomal peaks and lack of small, degraded RNA fragments.

2.10.2. Affymetrix Hybridisation and Staining

GeneChip hybridisation and staining were carried out by Dr. Kevin Robertson at the Scottish Centre for Genomic Technology and Informatics (GTI) following the standard Affymetrix protocol. In brief, double-stranded cDNA was synthesised from the total RNA using the T7-Oligo (dT) Promoter Primer Kit. An *in vitro* transcription (IVT) reaction was performed to produce biotin-labelled cRNA from the cDNA. The cRNA was cleaned up and fragmented before hybridisation to the array. Following hybridisation, the probe array underwent an automated washing and staining protocol on the fluidics station. The probe array was then scanned with the Affymetrix GeneChip Scanner controlled by the Affymetrix Microarray Suite software. The software defines the probe cells and computes intensity for each cell.

2.10.3. Affymetrix Microarray Data Analysis

Pairwise comparative analysis were carried out using the Affymetrix Microarray Suite 5.1. During the comparison analysis, each probe set on one array (i.e. uninfected) was compared with its counterpart (i.e. infected) on the other array. A Wilcoxon's signed rank test was used to generate a p-value (probability that the two probe sets are different). From this p-value, threshold values have been set which define whether the level of a transcript has increased or decreased or unchanged.

2.10.4. Microarray Data Validation with Real-time PCR

Due to time limitation, validation was only performed on prostaglandin D_2 synthase (Ptgds) that showed to be the most highly up regulated gene from the microarray data. Primers Ptgds_for (5'-GGAGAAATTCATCACCTTTAGC-3') and Ptgds_rev (5'-CCACATCACCATGTGTTACCTG-3') were designed to amplify a 136 bp fragment of the Ptgds transcripts. After reverse-transcription, the Ptgds cDNA was cloned into pGEM-T Easy vector (section 2.2.8) and sequence confirmed to serve as a positive control in real-time PCR. Total RNA was extracted from infected and control animals using RNeasy Mini kit (QIAGEN) as detailed in section 2.4.2. RT-PCR, quantitation and melting curve analysis was performed on a Rotorgene 3000 machine (Corbett Research). Standard curves for Ptgds and beta actin were established to quantify the experimental samples. The cycling conditions were as followed: 10 min at 95°C, 20 s at 94°C, 20 s at 57°C and 20 s at 72°C repeated 40 times. Melting curve analysis was performed wherein the annealing temperature was decreased by 0.5°C during each step. Each sample was compared to the standard curve in order to determine the original starting amount of a particular transcript and to a melting curve to ensure the production of a specific product.

CHAPTER THREE

RESULTS AND DISCUSSION

3.1. Introduction

Little information exists on the molecular mechanisms involved in VZV latency and reactivation. This has indirectly hampered the knowledge of the mechanisms of post herpetic neuralgia (PHN) that often follows viral reactivation. Although the latent virus can be detected in human dorsal root ganglion (DRG), the difficulties encountered in obtaining ganglia from autopsy explain the slow progression of knowledge (Kennedy 2002). To circumvent this limitation, it is necessary to reproduce experimentally the events observed during human latency, a difficult endeavour when working with a virus known to be species-specific and to remain cell-associated *in vitro*. Many attempts have been made to induce VZV latency either *in vitro* by infection of dissociated DRG cells from human or non-human origin or *in vivo*, using mice, rats or guinea pigs (Sadzot-Delvaux and Rentier 2000). Even though none of the animal models described so far is satisfactory to evaluate all aspects of VZV pathophysiology in humans, many of them are useful to investigate acute infection, the immune response or latency. Different models help to answer different questions.

The rat model of VZV latency has been used to study many aspects VZV latency such as modelling latency establishment (Sadzot-Delvaux et al. 1990), (Sadzot-Delvaux et al. 1995) and viral gene expression during latency (Kennedy et al., 2001), (Grinfeld et al. 2004). The adaptation of this rat model and the ability to show striking changes in behavioural reflex responses represents a useful and unique experimental setting to investigate the cellular and molecular mechanisms involved in the establishment of PHN (Fleetwood-Walker et al. 1999), (Dalziel et al. 2004).

To date, transcripts encoding VZV open reading frames (ORFs) 4, 21, 29, 62, 63, 66 have been detected in human ganglia (Cohrs et al. 2003a), (Kennedy et al. 2000), (Cohrs et al. 2000). All but one of these viral transcripts i.e. ORF66 have also been detected in the rat model of VZV latency (Kennedy et al. 2001), (Sadzot-Delvaux et al. 1995). ORF21 and ORF66 have been shown to be dispensable for the establishment of latency (Xia et al. 2003), (Sato et al. 2003) while ORF4 and ORF63 are important for latent infection (Cohen et al. 2005), (Cohen et al. 2004). There have been fewer studies of VZV gene translation, although expression of VZV gene 63-encoded protein is well established in both human and rat (Kennedy et al. 2000), (Kennedy et al. 2001). One report, published by Lungu et al. (1998) described the localisation of proteins encoded by VZV genes 4, 21, 29, 62 and 63 in the cytoplasm of latently infected neurones in DRG of human subjects who had died without clinical evidence of herpes zoster. This observation has been confirmed by a recent report by Grinfeld and Kennedy (2004).

The aim of this work was tried to correlate the altered behavioural changes in the rats, i.e. showing allodynia, with gene expression in the infected DRG. The approaches taken to achieve this objective included:

- Analysis of gene expression in infected whole DRG by nested-PCR and real-time PCR.
- Analysis of purified populations of neurones as an alternative approach to whole DRG.

- Utilisation of microarray technology to investigate the global gene expression in DRG of infected and uninfected rats. Details of this experiment will be discussed in Chapter 4.

3.2. Results

3.2.1. Development of nested-PCR for VZV Genes 63 and 10

A nested-PCR involving two rounds of amplification reactions was established for the identification of VZV DNA in the latently infected DRG. The first round of PCR was performed with a pair of external primers specific to VZV genes 63 and 10 (VZV63P1 + VZV63P3, VZV10P1 + VZV10P3 (Cohrs et al. 1996); Table 2.2). Subsequently, an aliquot (1 μl) of the first round of PCR product was subjected to a second round of PCR. The second round of PCR was performed with two new primers (VZV63P2 + VZV63P4, VZV10P2 + VZV10P4 (Cohrs et al. 1996), Table 2.2) that hybridised to sequences internal to the first round primer-target sequences. In this way, only specific first round PCR products will be amplified in the second round. Gene 63 was chosen due to its frequent expression during latency in both human and rat (Kennedy et al. 2001) and it was intended that this PCR would be adopted to analyse mRNA expression. Likewise, gene 10, which is a late gene would serve as a control for productive viral gene transcription, as it has not been shown to be expressed in latently infected cells.

In order to confirm that the primer pairs worked, they were first tested with DNA extracted from VZV infected cells (section 2.2.2). The nested-PCR was performed with 100 ng of the template DNA as described (section 2.7). Figure 3.1 shows a nested-PCR amplification of genes 63 and 10 in VZV infected cells. Single distinct bands were obtained from each primer pair, indicating that the primers were specific.

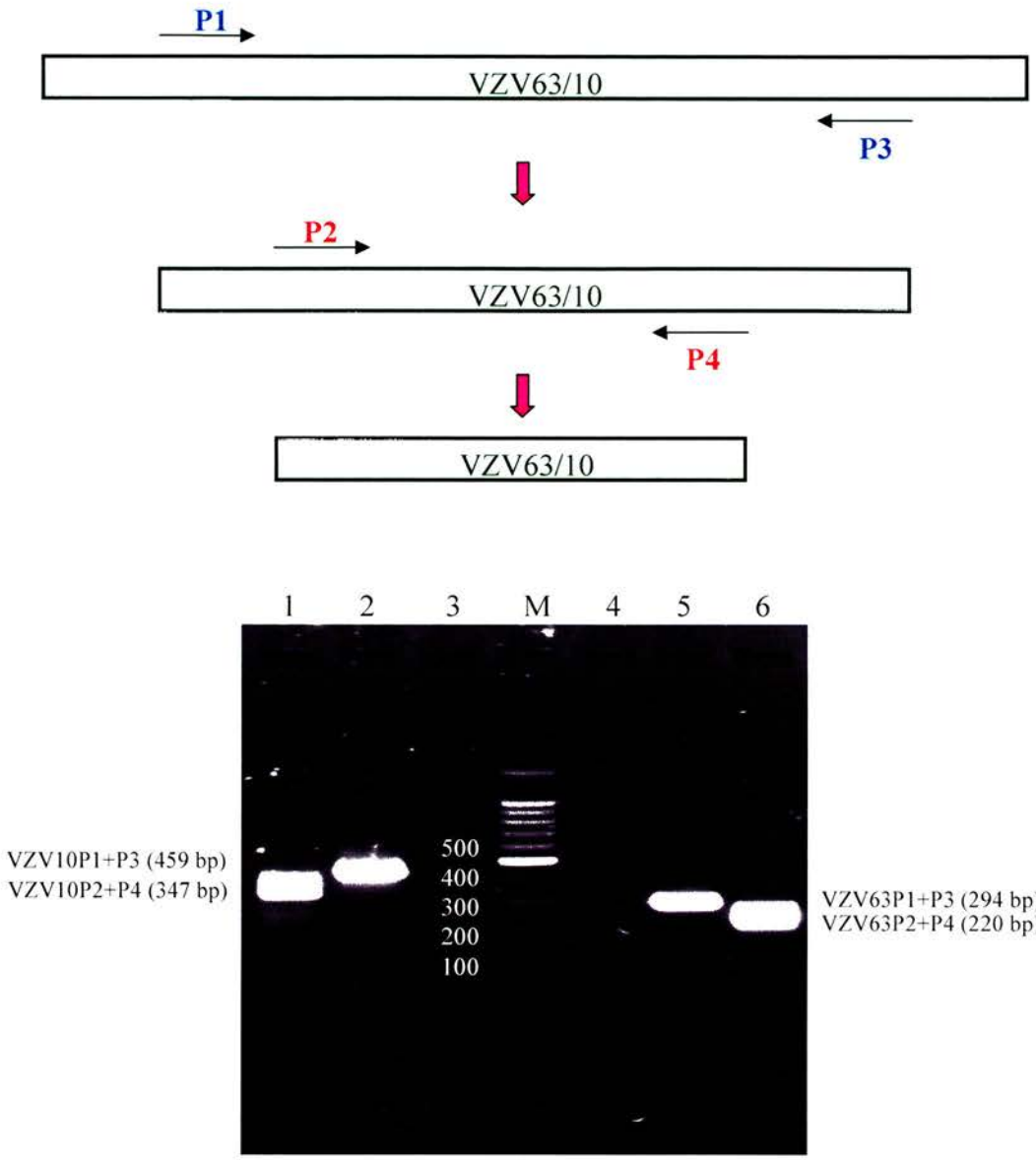

Figure 3.1 Amplification of VZV genes 63 and 10 with nested PCR. Amplified PCR products were analysed by electrophoresis in an 1.5% (w/v) agarose gel. Lanes 1, nested PCR product of VZV10P2+VZV10P4; 2, primary amplification with VZV10P1+VZV10P3; 3, negative control without template; M, 100 bp marker; 4, negative control without template; 5, primary PCR product of VZV63P1+VZV63P3; 6, nested PCR product of VZV63P2+VZV63P4.

3.2.2. Sensitivity of nested-PCR

In order to test the sensitivity of the nested PCR assay, a plasmid control was constructed. The corresponding sequence of the VZV63 region was amplified using primers VZV63P1 + VZV63P3 (Table 2.2) and ligated into the pGEM-T Easy vector (Promega), according to the manufacturer's instructions (section 2.2.8). Positive recombinants were confirmed by restriction enzyme analysis with *EcoR*1 (section 2.2.7) at 37°C with 1 μg of the plasmid in 10 μl reaction mixtures as shown in Figure 3.2A. PCR was also performed with primers VZV63P1 + VZV63P3 (Figure 3.2B). One of the positive clones was further confirmed by sequencing and named pGEM-T Easy-63.

The concentration of pGEM-T Easy-63 was determined with a spectrophotometer (section 2.2.5). Serial 10-fold dilutions of pGEM-T Easy-63 containing 10^9 to 10 copies were prepared. 2 μl of each dilution was used and 100 ng of CV-1 DNA was added into each 50 μl reaction mixture. Nested-PCR was carried out as described in section 2.7. 1 μl of the primary PCR product was used as a template for the secondary amplification. Figure 3.3 shows the sensitivity of the nested-PCR assay with VZV63 primers. Primary PCR could only detect down to 100 copies per 100 ng DNA, however the sensitivity of detection was improved to below 10 copies per 100 ng DNA after a second round of PCR. The results from this experiment showed that the detection limit of the VZV63 nested-PCR assay was below 10 copies per 100 ng DNA.

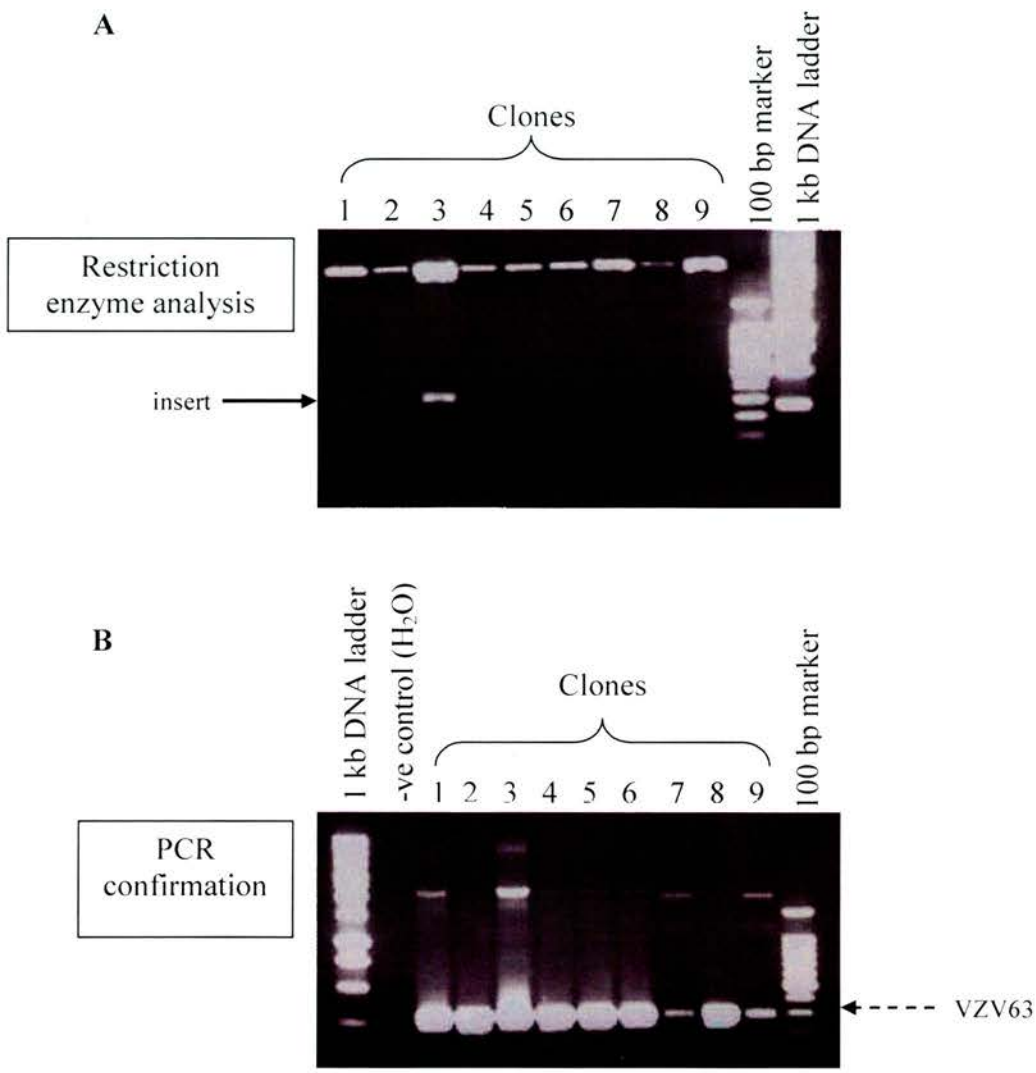

Figure 3.2 Restriction enzyme analysis and PCR to confirm VZV63 positive clones. (A) Recombinant plasmids were digested with *EcoR*I to confirm the presence of insert (full arrow). (B) PCR was performed with VZV63P1 + VZV63P3 on the positive clones and gene 63 products of the right size were detected (dotted arrow).

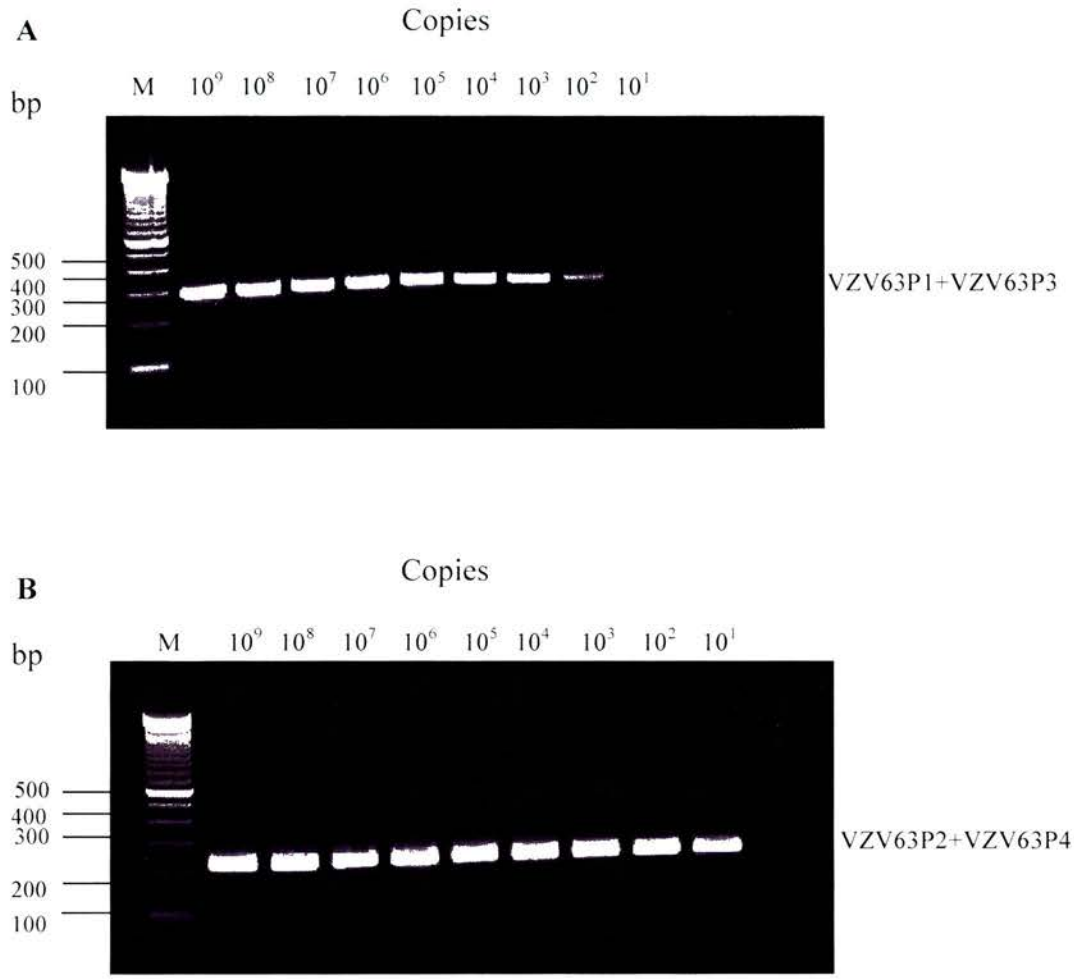

Figure 3.3 Sensitivity of the nested PCR assay. A) Primary PCR with serial 10-fold dilutions of the plasmid containing 10^9 to 10 copies of gene 63. B) 1μl of the primary PCR reaction was used in the secondary PCR. Sensitivity of PCR was 100 copies and below 10 copies per 100 ng DNA for primary and secondary PCR, respectively.

3.2.3. Detection of VZV DNA in Whole DRG by nested-PCR

In order to maximise efficient use of animal resources, tissues for the preliminary PCR analysis were taken from animals tested previously and stored in the tissue bank of the laboratory. DNA was extracted individually from L1 to L6 lumbar DRG from both ipsilateral and contralateral to the side of injection (section 2.2.1). 100 ng of DNA was used in the PCR amplification following the conditions used for gene 63 in order to investigate the presence of VZV DNA in the DRG. No products were seen on the agarose gel for the DRG samples after the first round of 35 cycles of PCR despite a band for the positive control (DNA from VZV infected cells). It was speculated that the copy number of the latent viral genome in the DRG was very low since in VZV infected cells viral DNA could be detected after one round of PCR. Therefore, a nested PCR would have to be performed. Indeed, PCR products with the correct size were seen after the nested-PCR. Figure 3.4 shows an example of a nested-PCR of infected DRGs positive for VZV DNA.

Due to a limitation in detection, the concentration of the starting DNA template was increased to 500 ng. With this cut-off concentration, a '+' in the nested-PCR indicated the presence of VZV DNA and a '-' meant that it is not detected. During the PCR analyses, contamination of the negative controls (H_2O or AHV-1 DNA) occurred frequently and thus made the results unreliable and had to be repeated. Steps taken to overcome this contamination problem included preparing the PCR reaction mixtures in a separate PCR room where no access of any form of DNA was allowed. All the PCR components including primers were aliquoted into small volumes. QIAGEN HotStarTaq

DNA polymerase was used to minimise hands-on time and the likelihood of introducing contaminants into the reaction mixtures when hot start method was performed. Another advantage of using QIAGEN HotStarTaq DNA polymerase was that the modified recombinant *Taq* polymerase could be added together into the PCR master mix but it will not be activated at temperature below 95°C, therefore preventing the formation of mis-primed products and primer-dimers at low temperatures. Separate sets of pipettes with hydrophobic filtered tips were also used.

Table 3.1 shows the nested-PCR analysis of DRG from infected animals analysed with the VZV63 primers. Shown are results for ten animals euthanised at different time points post infection with a mean of 30 days and with different paw withdrawal thresholds. VZV DNA could be detected in most of the animals especially those with high to marginal response to allodynia. No virus was found in animals, which had resolved to the baseline, e.g. 1267 and 1794. Viral DNA could be detected not only on the ipsilateral but also on the contralateral side to the injection. As there was no control uninfected tissues available at the time of this experiment being carried out, non-specific control DNA (AHV-1) and water were used as negative controls in the PCR. Both negative controls did not show any VZV63 specific amplification in the DRG samples tested. However, no correlation has been found as to which DRG along the lumbar segment harbours the viral DNA. The finding of VZV DNA in a particular DRG segment is probably affected by the individual viral load and the efficiency of viral spread to the DRG.

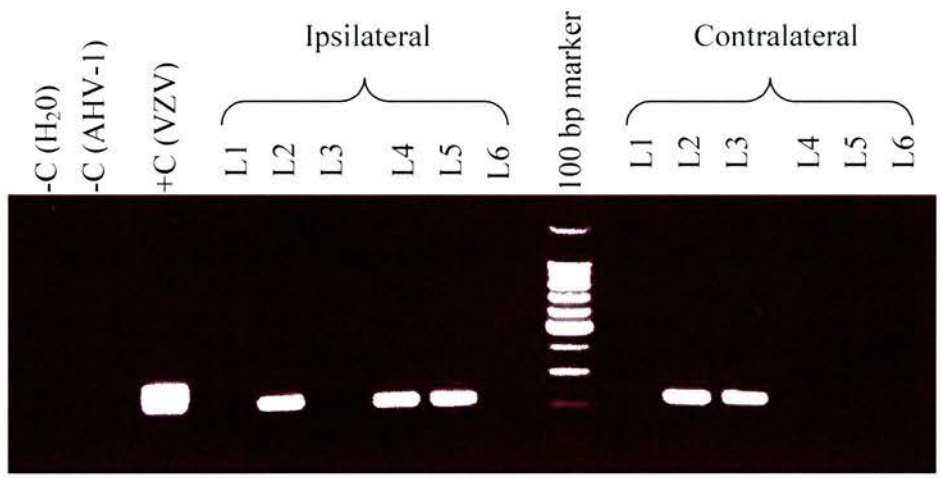

Figure 3.4 An example of the VZV63 nested-PCR on lumbar DRG tissue from an infected animal. A nested PCR was performed and products at the right size for VZV63 were detected in some of the DRGs. Negative controls with $H_2$0 and AHV-1 DNA showed no specific VZV63 amplification. DNA from VZV infected cells was positive. L1-L6 = lumbar DRG.

Table 3.1 Detection of VZV63 DNA in the VZV-infected DRG by nested PCR. PCR analysis was carried out on L1-L6 lumbar DRGs from both ipsilateral and contralateral side to injection with gene 63. PWT denotes paw withdrawal threshold. - = negative; + = positive.

Animal	Days post infection	VZV Gene 63													
		Ipsilateral							Contralateral						
		PWT	L1	L2	L3	L4	L5	L6	PWT	L1	L2	L3	L4	L5	L6
944	24	22.3	-	-	+	-	+	+	48.7	-	+	+	+	-	-
947	36	22.3	-	+	-	-	-	-	48.7	-	-	-	+	-	-
943	36	30	-	-	-	-	-	-	26	-	+	-	-	-	-
935	37	32	+	+	-	-	-	-	48.7	-	-	-	-	-	-
932	37	15	+	-	-	-	-	-	48.7	-	-	+	-	+	-
1267	36	60	-	-	-	-	-	-	60	-	-	-	-	-	-
1284	19	37.3	-	-	-	-	-	-	60	-	-	-	+	+	+
1277	28	11.7	-	-	-	-	-	+	48.7	+	-	-	+	-	-
1606	30	2	-	+	-	+	+	-	7.3	-	+	+	-	-	-
1794	30	60	-	-	-	-	-	-	60	-	-	-	-	-	-

3.2.4. Southern Blot Confirmation of the Presence of VZV DNA

In order to confirm the results from the nested PCR, an oligonucleotide specific to gene 63 was synthesised and labelled with DIG-dUTP at the 3' end to be used as a probe in Southern blot analysis. Figure 3.5 shows that positive results in nested PCR are confirmed by Southern blot with a band at the correct size for the gene 63 amplified products. Negative results were confirmed to be true negatives, indicating that Southern blot was no more sensitive than nested PCR and the results from nested-PCR were reliable within the detection limit. Beta actin was positive for all the negative samples tested indicating that the DNA was intact.

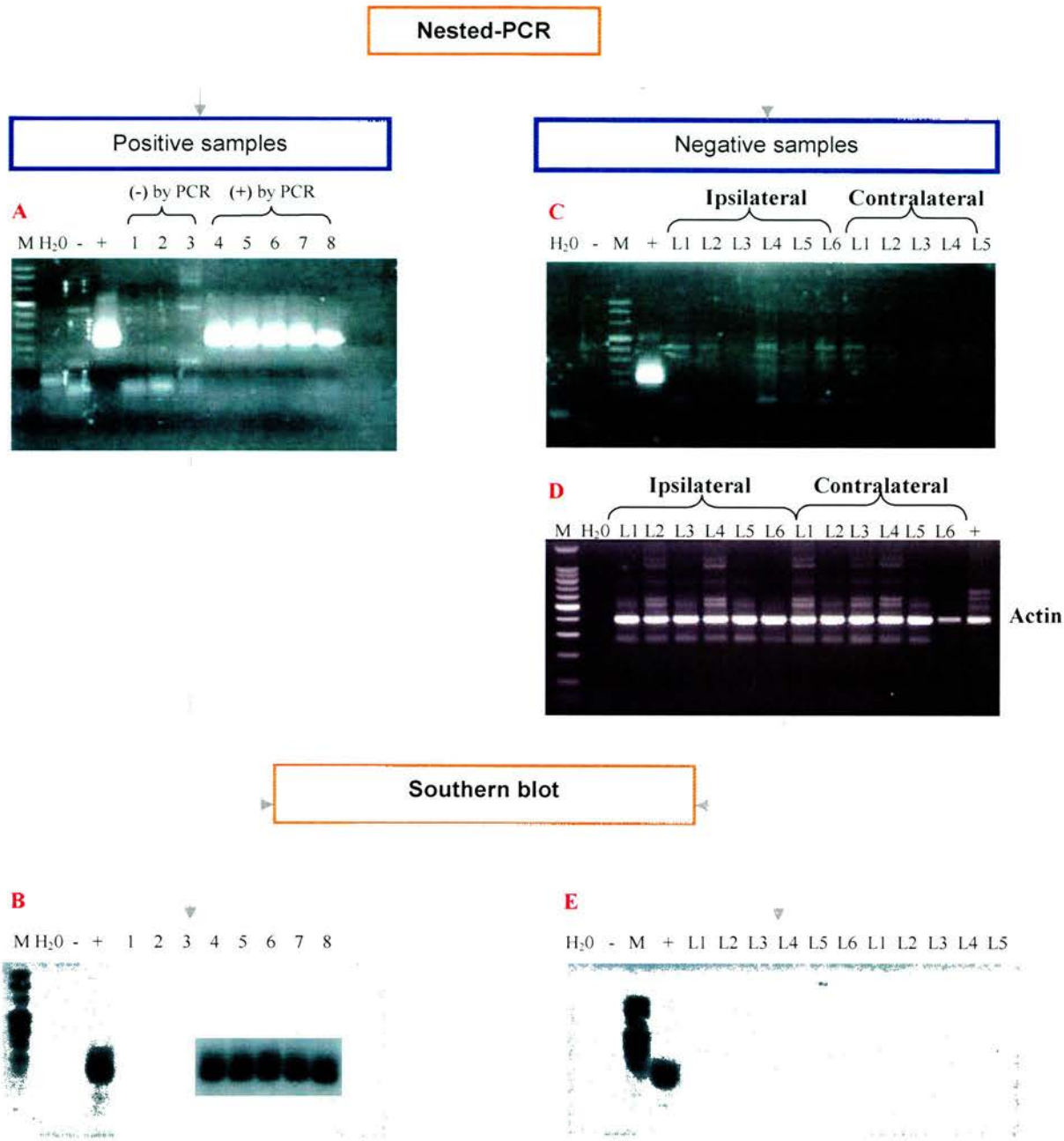

Figure 3.5 Southern blot confirmation of nested PCR results. Samples positive for gene 63 in nested PCR (A) was confirmed with corresponding positive bands in Southern blot (B). (C) Samples negative for gene 63 in nested PCR. (D) Beta actin was detected in all negative samples. (E) Southern blot confirmed the negative samples in nested PCR were true negatives. + = positive control with VZV DNA from infected cells; - = negative controls with AHV-1 DNA; M = marker.

3.2.5. Detection of VZV DNA in Microdissected Cells

An alternative approach was attempted to investigate the presence of VZV DNA in the DRG by looking at a single population of neurones. Laser capture microdissection (LCM) is a method used to select and isolate cell clusters from tissue sections (Emmert-Buck et al. 1996), (Suarez-Quian et al. 1999). Once captured, the cell clusters can be analysed with respect to their DNA, RNA or protein content.

Details of the LCM protocol were described in section 2.9. After dissection, the cap containing the targeted cells was removed using a transport arm and automatically placed on to a microcentrifuge tube that contains the extraction buffer. DNA was extracted from approximately 30 to 40 neurones and analysed by nested PCR with primers specific for VZV63. However, since no quantitative method was used to determine the viral load in these microdissected cells, the results shown here was qualitative and not able to compare with other reports on VZV burden in the ganglion. Figures 3.6A and B show photos of tissue pre- and post-microdissection, respectively. Figure 3.6C shows that viral DNA could be detected and beta actin was positive in all samples tested. The PCR samples were processed in duplicate but due to the sensitivity of detection, one of the two replicates (L4C and L5I) did not show the same results. These results proved that LCM could be used to isolate single population of cells in the DRG in which viral DNA could be retrieved for further study.

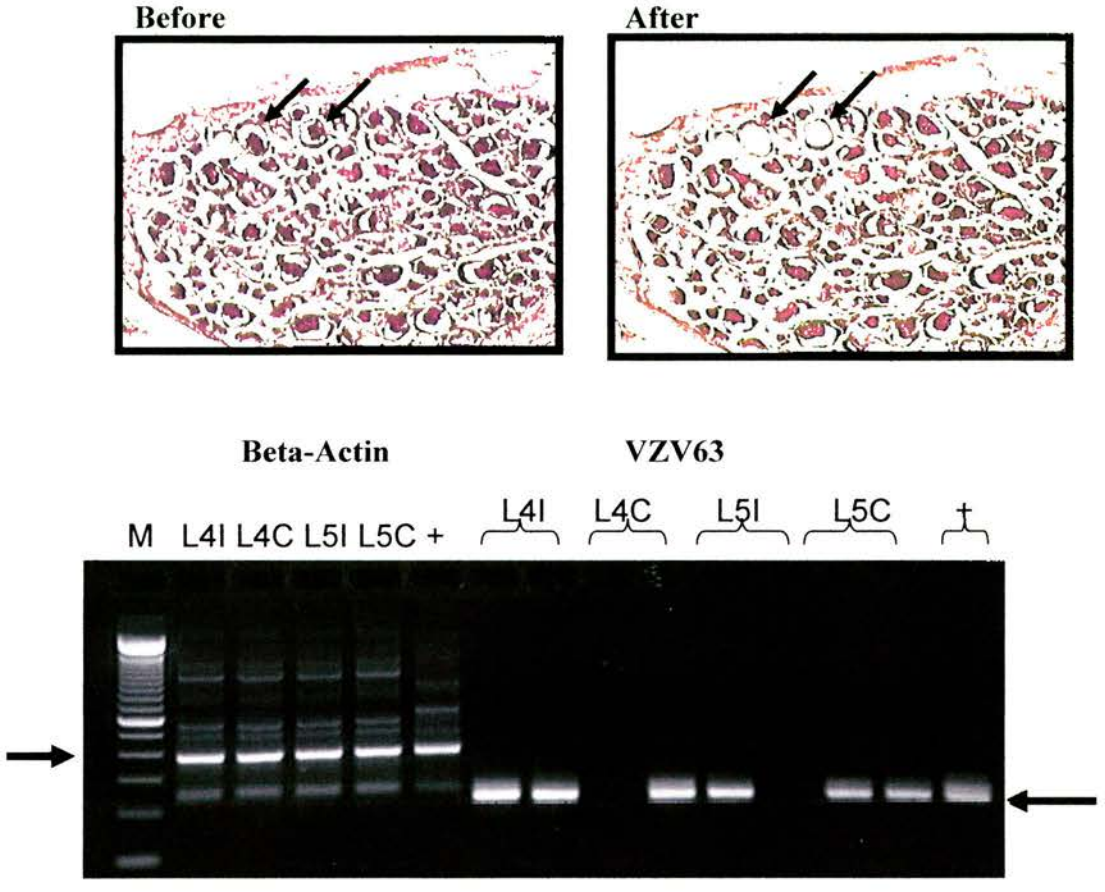

Figure 3.6 Single cell lifted by laser capture microdissection (LCM) and PCR analysis. A) Two single neurons are highlighted (arrows) before LCM; B) the same section after LCM where the two cells were being lifted; C) PCR analysis of the DNA extracted from microdissected cells with VZV63. Approximately 30 microdissected neurones were lifted and lysed in the microfuge tube for DNA extraction. L4I, L5I, L4C, L5C = lumbar DRG L4, L5 ipsilateral (I) or contralateral (C).

3.2.6. Real-time PCR

In order to overcome the sensitivity problem in nested-PCR, a quantitative and more robust assay was developed. Real-time PCR (qRT-PCR) has become one of the most powerful analytical tools for quantification of defined nucleic acid sequences. Since only minute amounts of template are required, applications include the evaluation of gene copy number and mRNA expression and the diagnosis of pathogens and mutations. The principle of qRT-PCR is that the recurring measurement of a fluorescent signal is proportional to the amount of amplification product. Several detection systems are now available and are either based on hybridisation probes such as Taqman probes (Holland, 1991), Molecular Beacons (Tyagi and Kramer 1996) and Scorpions (Whitcombe, 1999) or on intercalation by fluorescent dyes, such as the dsDNA binding dye SYBR Green 1 (Wittwer, 1997). While hybridisation probes offer the advantage of target sequence specificity, a specific probe is required. Given that the synthesis of fluorescence-labeled probes is still a major cost factor, the availability of a general detection method is of great benefit to those studies that aim at the quantification of a high number of genes.

Optimisation prior to carrying out the qRT-PCR assay with experimental samples will generate data that reflect on the quality of the assay design and produce valuable information to indicate where problems may lie. By using the minimum primer and probe concentration to give the best assay conditions, it is often possible to reduce the concentration of oligonucleotides included in the assays and so increase the specificity of the assay as well as saving costs. The template chosen for the optimisation

process can be derived from any convenient source where there is an excess supply. The most common sources include: cDNA, synthetic single stranded DNA amplicon, purified PCR fragment and cloned fragment within a plasmid. For purpose of optimisation here, the pGEM-T Easy-63 plasmid was used as a template with VZV63P1 + VZV63P3 primers (Table 2.2). The following parameters were optimised: magnesium chloride ($MgCl_2$), SYBR Green I, template and primer concentration. Melting curve analysis was carried out to check for product specificity.

3.2.6.1 $MgCl_2$ Titration

The PCR reaction was carried out in the presence of different $MgCl_2$ concentration ranging from 1-5 mM. The optimal $MgCl_2$ concentration is the one which has the lowest threshold cycle (C_t), the highest fluorescent intensity and the steepest curve slope. C_t value is the number of the first cycle at which the measured fluorescent signal exceeds the threshold limit. Therefore, in the example shown in Figure 3.7A, the optimum $MgCl_2$ concentration is 3 mM. The melting curve shows that primer-dimer only formed in the no template control (in the presence of 5 mM $MgCl_2$). At 1-5 mM $MgCl_2$, a specific product was shown by a sharp melting curve (Figure 3.7B).

3.2.6.2 SYBR Green I Concentration

Different dilutions (1: 1000 to 1: 40000) of SYBR Green I (Biogene) was prepared from the stock solution following the manufacturer's instructions. The SYBR

Green I dilutions were used to optimise the PCR reaction mixtures in order to get the best fluorescent intensity and amplification. As shown in Figure 3.8A, only a dilution of 1:1000 gives amplification and a specific product (shown by melting curve, Figure 3.8B).

3.2.6.3 Template Concentration

The template concentration tested was at 100 ng and 10 ng. The C_t for DNA working template dilutions should be 10-30. Higher dilutions are used if initial $C_t < 10$ or higher concentrations if initial $C_t > 30$. A high template concentration can lead to an early reaction plateau and results that are difficult to interpret. Figure 3.9 shows that template concentration indeed makes a difference in the C_t value. A higher concentration leads to earlier C_t and a lower concentration has a delayed C_t.

3.2.6.4 Primer Concentration

A matrix of different concentration of the forward and reverse primers encompassing the range from 0.05 μM to 0.9 μM was tested. As shown in Figure 3.10 the optimal primer concentration was 0.3 μM for forward and reverse primers given their lowest C_t and a specific product in the melting curve analysis.

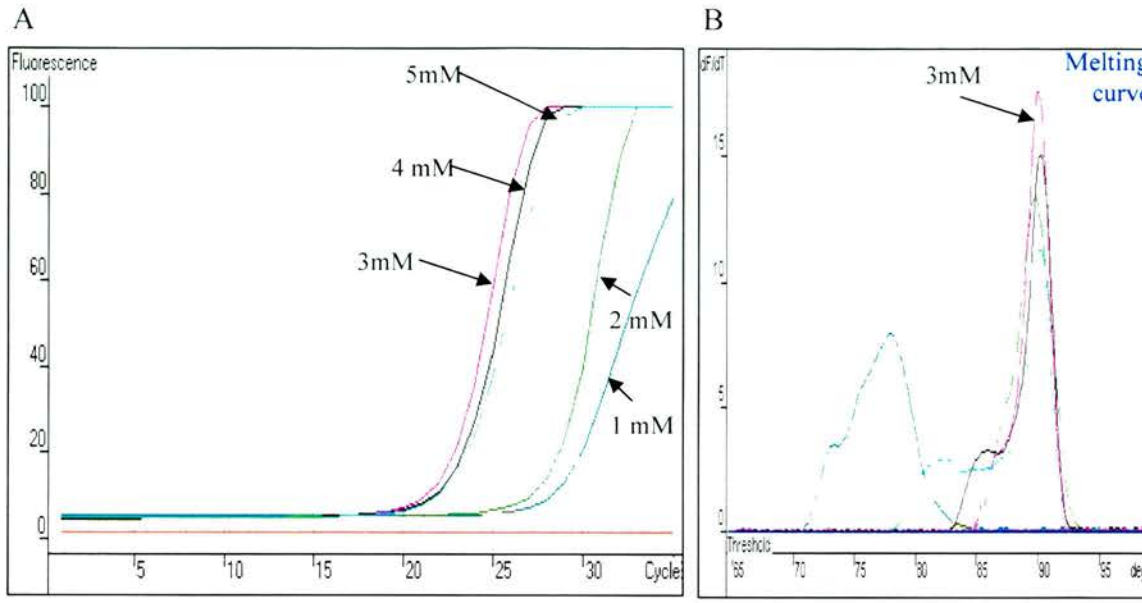

Figure 3.7 Effect of $MgCl_2$ concentration. (A) Different concentrations of $MgCl_2$ ranging from 1-5 mM were used to optimise the real-time PCR reaction. 3 mM of $MgCl_2$ gives the highest fluorescence and best amplification. (B) Melting curve showed a specific product and primer dimer only appeared in no template control at 5 mM $MgCl_2$.

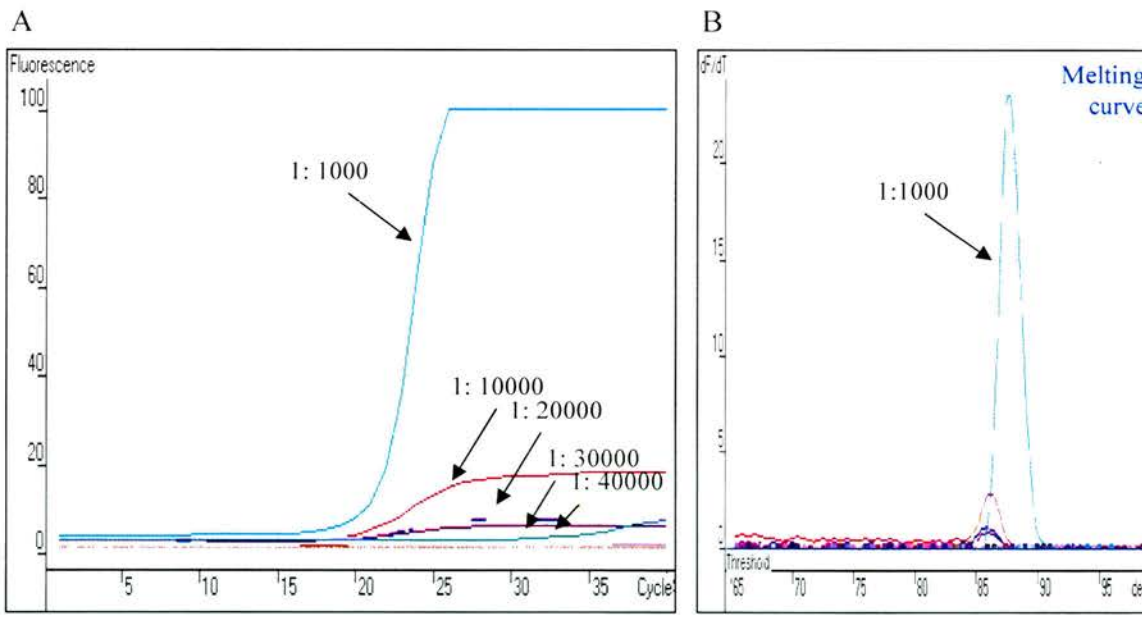

Figure 3.8 Effect of SYBR Green I. (A) The concentration of SYBR Green I did make a difference in the fluorescence intensity of the assay. Only dilution at 1: 1000 gave a specific product as shown in the melting curve analysis (B).

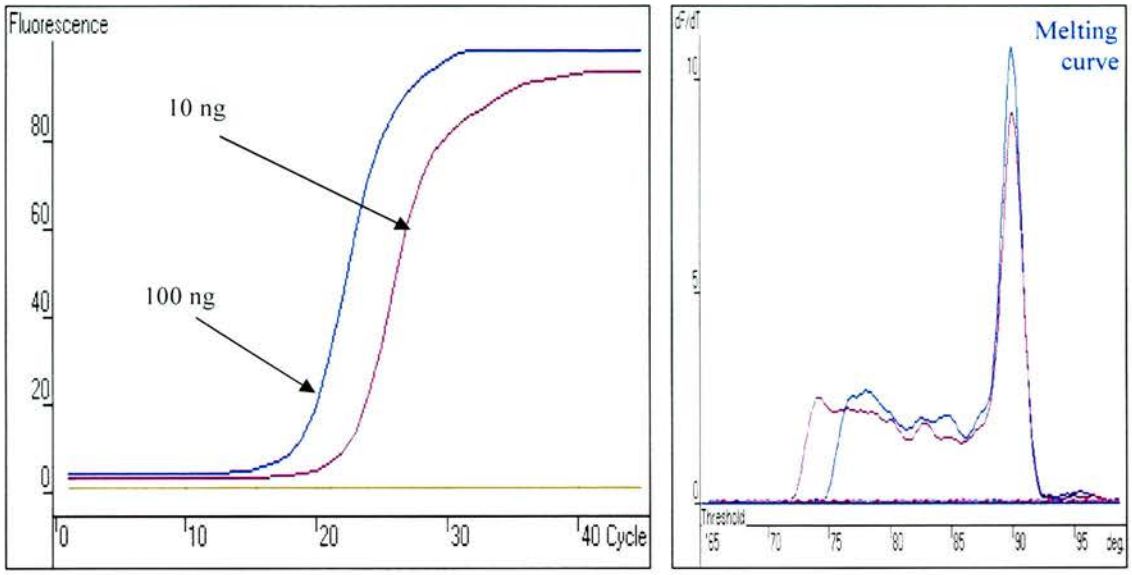

Figure 3.9 Effect of template concentration. Different concentrations of template did affect the C_t of the assay. Higher concentration (100 ng) resulted in an earlier C_t while lower concentration (10 ng) resulted in a later C_t.

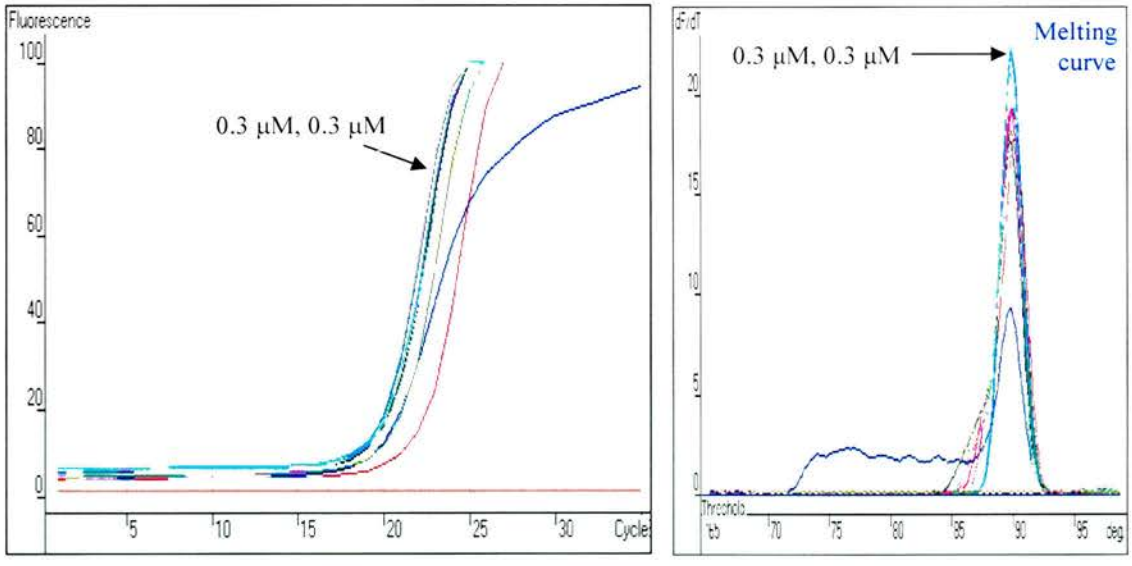

Figure 3.10 Effect of primer concentration. Concentration of 0.3 µM for both forward and reverse primers gave the best amplification and specificity of all the other combinations tried in the primer optimisation matrix set up.

3.2.7. Construction of a Standard Curve

Having chosen the optimum concentration for the primers, SYBR Green I and $MgCl_2$, it is important to determine the efficiency of the qRT-PCR reaction. A standard curve is a useful tool for examining the quality of the overall qRT-PCR assay and it should encompass as large a dynamic range as possible of a 10-fold dilution series over 5 to 7 logs. A miniprep of pGEM-T Easy-63 plasmid was prepared (section 2.3.3). The plasmid was linearised with *Nco*I and its concentration determined (section 2.2.5) in order to calculate the corresponding copy number using the formula given (section 2.8.2). A standard curve was constructed by preparing ten-fold serial dilutions of plasmid containing from 1 to 10^8 copies of VZV63. Uninfected rat dorsal root ganglion tissue DNA (500 ng) was added to the plasmid standard to compensate for the potential inhibition of amplication reactions by the added DNA. Each standard was run in triplicate using the optimised conditions as outlined below. The optimised PCR reaction mixtures contained H_2O (11.7 µl), 10 × PCR buffer without Mg (2 µl), Mg (3 mM; 2.4 µl), dNTP mix (10 mM each dNTP; 0.4 µl), forward primer (0.3 µM; 0.4 µl), reverse primer (0.3 µM; 0.4 µl), FastStart Taq (2 U, 0.2 µl), SyBr Green I (1:1000; 0.5 µl) and template DNA (2 µl) in a 20 µl reaction. Figure 3.11 shows an amplification plot with a large dynamic range of the measurement from 10^8 to 1 copy of the plasmid and the specificity of the assay were shown by a sharp melting peak in the melting curve analysis. The post real time PCR products could be analysed on an agarose gel for the correct size when there were doubts about the identity of the specific product, but often

it was unnecessary if the melting curve analysis showed a single melt curve consistently with the positive control.

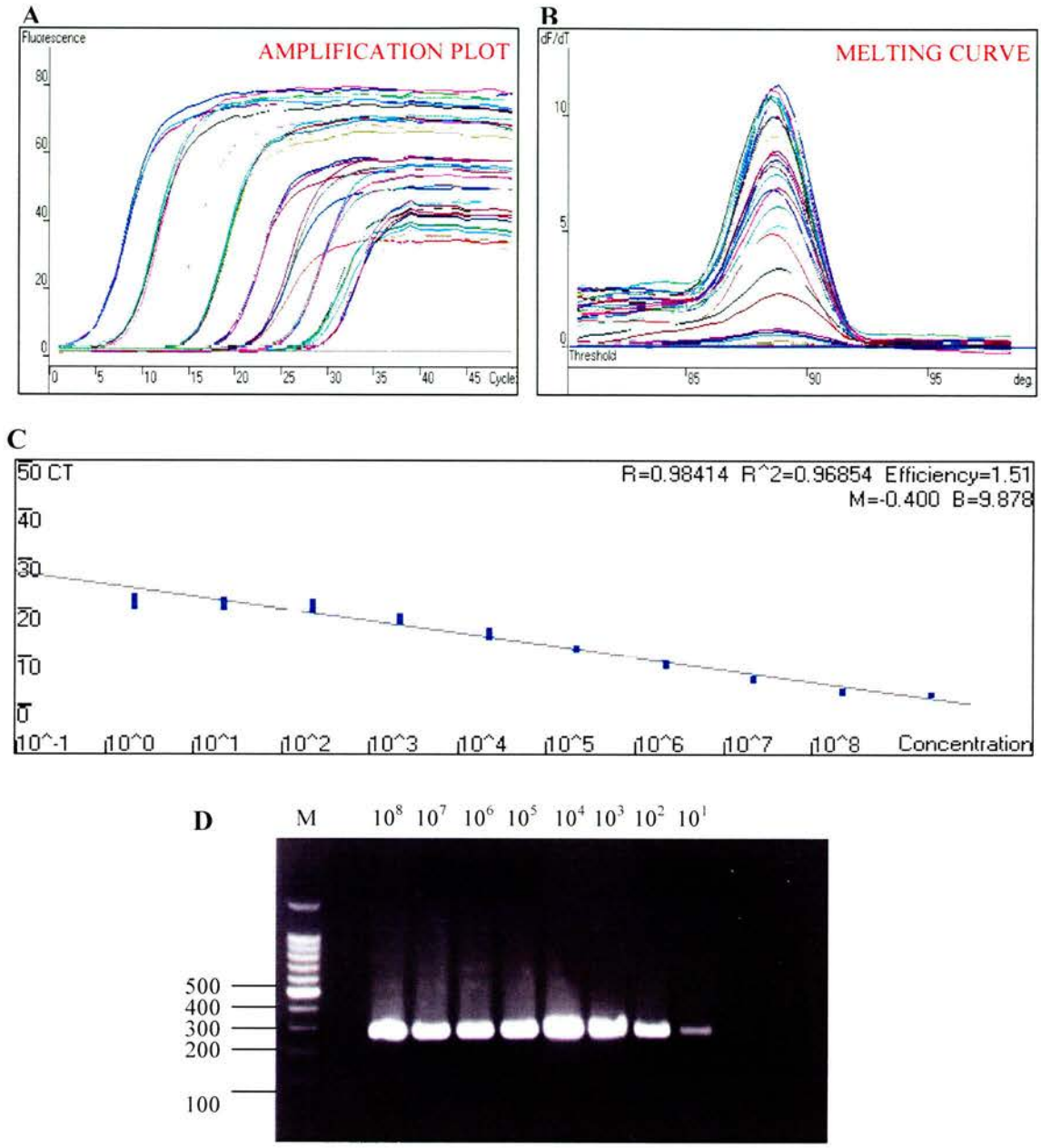

Figure 3.11 An example of a standard curve experiment in the Rotorgene 3000 machine. (A) The dynamic range of the assay was shown in the amplification plot. (B) The melting curve showed a specific product. (C) The standard curve showed that there was a linear correlation between the plasmid concentration and the threshold cycle (C_t). (D) The post real time PCR products of serial dilutions of plasmid copy numbers were analysed on an agarose gel showing products of the right size.

3.2.8. Quantitation of VZV DNA Viral Load with Real-time PCR

The viral load in the infected DRG could now be quantitated with the established standard curve constructed for VZV63. DRG samples were run in triplicate and quantitation was only considered valid if their values were within the linear range of the standard. Figure 3.12 shows the viral load in 12 DRGs from single animal. The viral load in the DRG ranged from 42 ± 24 (standard error of the mean) to 795 ± 459 copies per μg DNA.

The calculations for equivalent number of cells containing VZV genome were as follow:

The size of a haploid rat genome which contains the number of nucleotide pairs in one set of 23 chromosomes is ~ 2.75×10^9 bp

Therefore, a diploid genome contains ~ 5.5×10^9 bp

Ignoring the differences in AT vs GC composition, the average base pair weighs ~ 660 Dalton (660 g /mol)

So, the weight of one mole of diploid genome:

5.5×10^9 bp x 660 bp = 3.63×10^{12} g

And 1 mole = 6.02×10^{23} copies = 3.63×10^{12} g

Therefore, a diploid genome will contain 3.63×10^{12} g / 6.02×10^{23} = 6.0×10^{-12} g = 6 pg DNA per cell

Assuming there is 6 pg DNA per cell,

∴1 μg DNA ~ 1.7×10^5 cell equivalents

Therefore, it was estimated that there were between 42 ± 24 to 795 ± 459 VZV genomes per 1.7×10^5 cell equivalents.

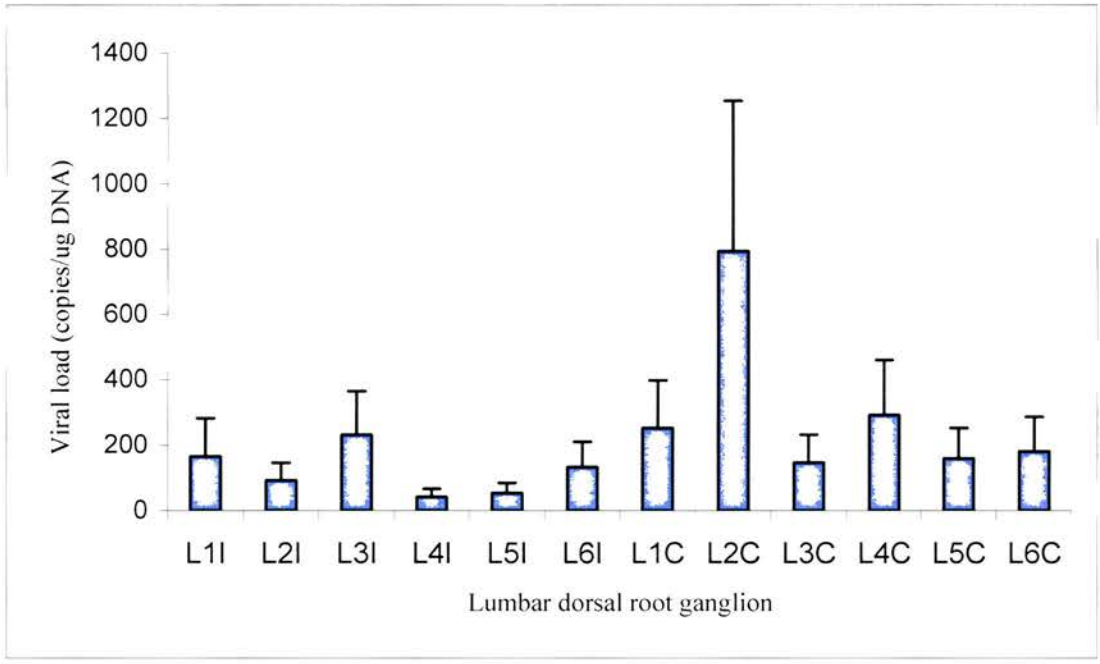

Figure 3.12 An example of viral load in the infected DRGs of an animal. Viral load in the different lumbar DRG was quantitated by real-time PCR. This animal was euthanized 10 days post infection and had developed a high degree of allodynia. Each bar represents the mean viral load ± SEM. L1I-L6I = ipsilateral lumbar DRG; L1C-L6C = contralateral lumbar DRG.

3.2.9. Detection of Viral Transcripts in Infected Cells

The detection of VZV DNA in the DRG suggests that the virus is present in the DRG of infected animals. The next step taken to gain a better understanding of the viral transcription was to study gene expression in the DRG. In order to study the gene expression in the DRG, reverse-transcriptase PCR (RT-PCR) assay was first optimised in an *in vitro* system due to the abundant expression of all classes of viral transcripts. RNA was extracted from VZV infected cells (section 2.4.3) and reversed transcribed (section 2.4.4). 2 μl of the reversed transcription reaction was used in PCR. A nested RT-PCR was performed with 35 cycles for each round of amplification. Transcripts for gene 63 and 10 were readily detected in the first round of RT-PCR. Beta actin was positive in all the samples tested. Negative controls with H_2O and without reverse transcriptase (-RT) were also negative, these confirmed that there was no genomic DNA contamination.

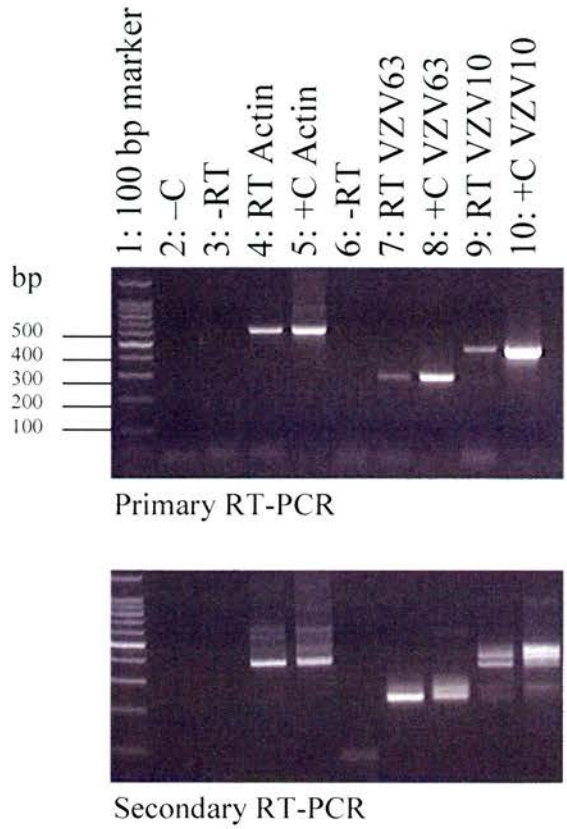

Figure 3.13 RT-PCR assay of VZV infected cells *in vitro*. 1 µg of the RNA was reverse-transcribed and 2 µl of the reverse transcription reaction were used to perform RT-PCR. Lane 1, 100 bp marker; 2, negative control (H_2O) without template; 3, -RT reaction (omitting reverse transcriptase enzyme); 4, RT-PCR with beta actin primers; 5, positive control for beta actin; 6, -RT reaction; 7, RT-PCR with VZV63 primers; 8, positive control for VZV63; 9, RT-PCR with VZV10 primers; 10, positive control for VZV10.

3.2.10. Detection of Viral Transcripts in Infected DRG

After establishing the RT-PCR assay in the *in vitro* system, the next step was to try to use the assay to detect latent viral transcripts in the infected DRG. Figure 3.14 shows that no transcript of VZV63 could be detected in any infected DRG even after a nested RT-PCR. Southern blot was carried out on these samples and they were proved to be true negatives. The RT step was working since the beta actin gene was amplified and there was no specific amplification for –RT reactions. RT-PCR of individual ganglia or pooling several DRGs did not result in detection of transcripts.

3.2.11. Detection of DNA and RNA Transcripts Simultaneously in the infected DRG

One way to ensure that the difficulty in detecting the viral transcript was not caused by the virus not getting to the DRG was to be able to analyse the same samples for their DNA and RNA content. A different method of isolating DNA and total RNA from the same sample was used here. The details of this protocol are described in section 2.2.3. This method allows the simultaneous isolation of genomic DNA and total RNA from animal cells or tissue samples with the QIAGEN RNA/DNA kit. The principle of the QIAGEN RNA/DNA kit is based on selective purification of RNA and genomic DNA by anion exchange on QIAGEN resin in a QIAGEN-tip. Figure 3.15 shows that both DNA and total RNA could be successfully isolated from VZV infected cells. PCR and RT-PCR were able to amplify specific regions of the VZV62 and VZV63

sequences. RNA obtained from this isolation method had to be DNase treated with care to remove all traces of genomic DNA.

When this method was repeated by pooling a group of six DRGs, both DNA and total RNA were obtained (Figure 3.16). However, when RT-PCR was performed on these samples, the viral transcripts could not be detected and only bands for beta actin were seen. VZV62 and VZV63 DNA were amplified in these samples. Therefore, these results proved that the non-detection of RNA transcripts in the samples was not a matter of the virus not getting to the DRG but instead it was likely due to a very low expression below the detection limit of the RT-PCR assay.

3.2.12. RT-PCR Optimisation

Many approaches have been tried to detect the transcripts in the infected DRG by optimising the RT-PCR assay. A different cDNA priming method using gene specific primers was tried as it has been reported that this method synthesised the most specific cDNA and provided the most sensitive method of quantification (Lekanne Deprez et al. 2002). Different RT systems were tried, annealing temperature and $MgCl_2$ concentration for the PCR were optimised. None of this worked even the pooling of more DRGs. The cDNA samples were also analysed by real-time PCR using the optimised VZV63 PCR conditions. However, there was no specific amplification seen in the melting curve analysis. Since the viral load has been found to be presence in low copy numbers in the DRG, it might suggest that the mRNA expression would also be low, resulting in the transcripts not being detected in the RT-PCR and real-time PCR assays.

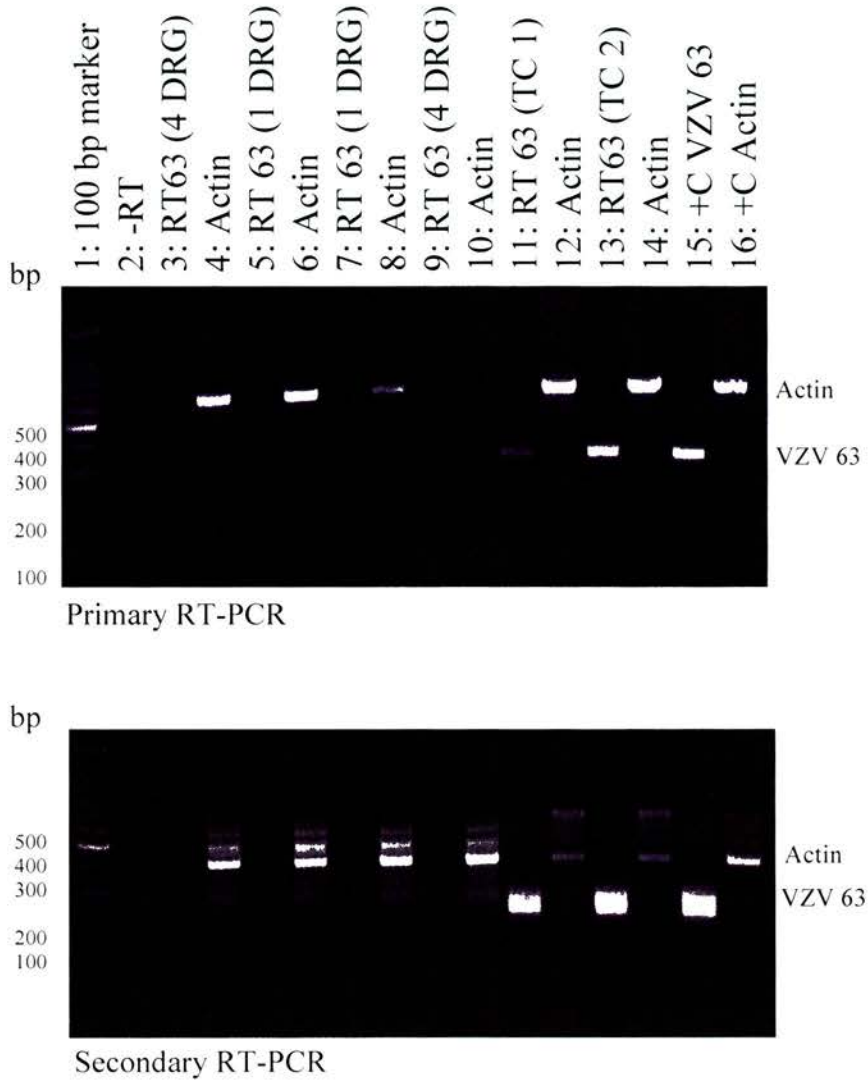

Figure 3.14 Detection of viral transcripts using primers specific for VZV63. VZV63 transcripts were not detected in the infected DRGs but beta actin was positive for all these samples. Lane 1, 100 bp marker; 2, -RT (omitting reverse transcriptase enzyme); 3, RT-PCR (4 DRGs); 5, RT-PCR (1399); 7, RT-PCR (1398); 9, RT-PCR (4DRGs); 11, 13, RT-PCR (cDNA from infected cells); 15, positive control (VZV63); 16, positive control (beta actin); 4, 6, 8, 10, 12, 14, RT-PCR with beta actin.

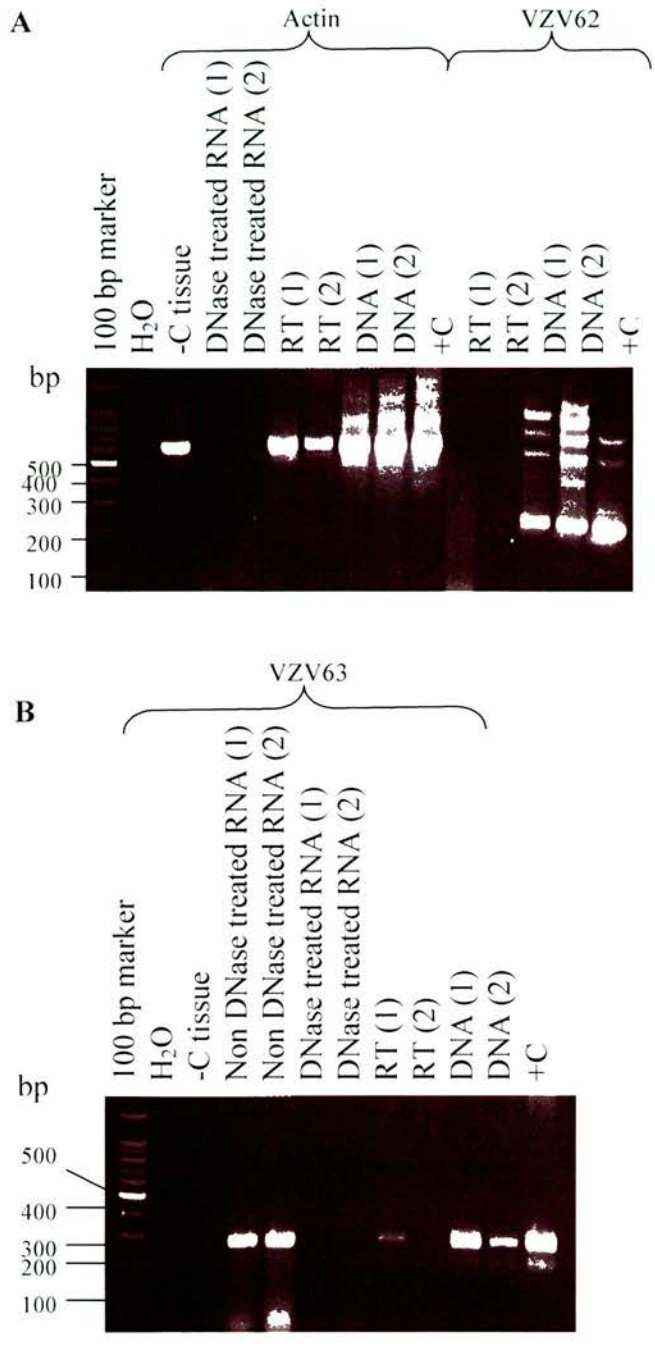

Figure 3.15 Simultaneous isolation of DNA and total RNA from VZV infected cells. A) PCR and RT-PCR analyses of DNA and RNA with primers specific for VZV62 and beta actin. B) PCR and RT-PCR analyses of DNA and RNA with VZV63. Both the VZV62 and VZV63 DNA and transcripts were detected in the cells. Genomic DNA was removed after DNase treatment. Beta actin was amplified in all samples. 1, 2 = cDNA from infected cells; +C = positive control.

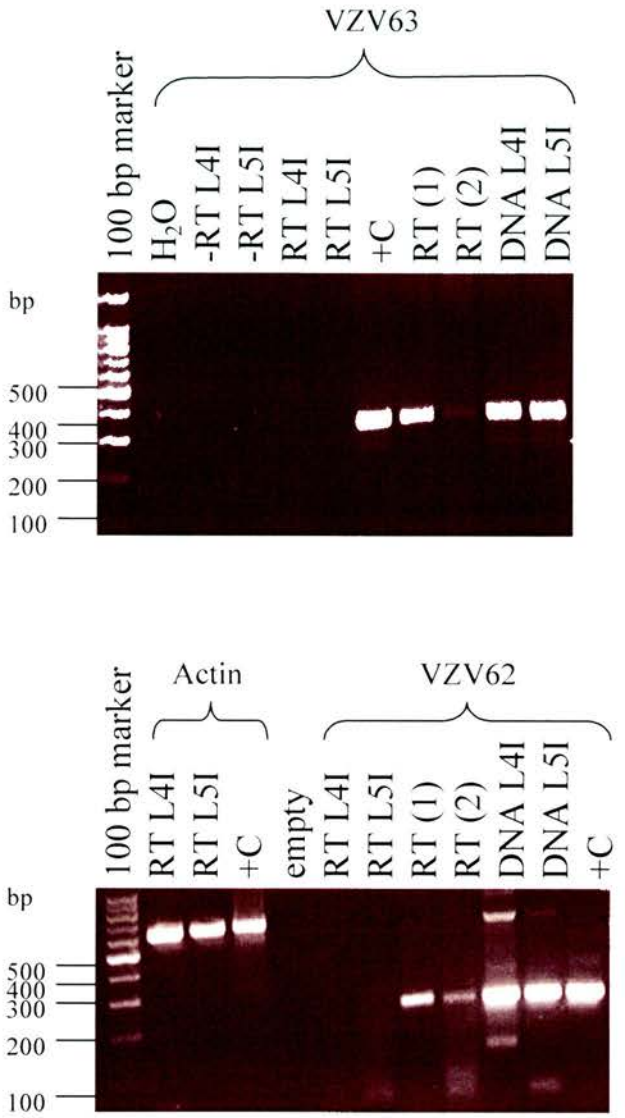

Figure 3.16 PCR and RT-PCR analysis of the DNA and total RNA isolated simultaneously from the infected DRG. DNA and RNA were isolated from infected DRG simultaneously. Only VZV62 and VZV63 genes were detected but not their transcripts. Beta actin was positive in both DRG samples analysed. L4I, L5I = infected lumbar DRG L4 and L5 ipsilateral; 1, 2 = cDNA from infected cells; +C = positive control.

3.2.13. Viral Spread in the Rat Model of VZV Latency

In order to investigate how the virus spread in the rat model after VZV injection into the footpad, an experiment was carried out to analyse the viral load in DRGs and other tissues at early time points (24 h, 48 h and 72 h) post infection. Two animals were studied at each time point and tissues analysed were DRG, footpad, sciatic nerve, spinal cord, brain, spleen and blood.

Table 3.2 shows the presence of VZV63 DNA by nested-PCR at 24 h, 48 h and 72 h. Viral DNA could be detected as early as 24 h after the infection in both ipsilateral and contralateral DRG to the side of injection. As expected, viral DNA could be detected at the ipsilateral footpad, which is the initial route of infection but not on the contralateral footpad. Both ipsilateral and contralateral sciatic nerves contained viral DNA at all the time points investigated. In order to check if there was a haematogenous dissemination of the virus in the rats, blood specimens from these animals were analysed. No viral DNA was detected in the blood of any of the animals at 24 h to 72 h. There was also no VZV DNA found in the spinal cord (whole cord analysis) and brain at any of the time points studied. This result suggests that latency is limited to the peripheral nervous system as is the case in humans.

Figure 3.17 shows a schematic diagram of viral spread in the rat model. VZV injected into the left footpad is predicted to travel via axonal transport to the DRG along the sciatic nerve which is the main nerve innervating the leg. This hypothesis is supported by the finding of viral DNA in the sciatic nerve. The virus then reaches the DRG, the site for VZV latency. We have show that the virus does spread to the

contralateral DRG and in the contralateral sciatic nerve, the mechanism by which this occurs is not clear. However, the results suggest that the hematogenous route is not likely.

Table 3.2 Detection of viral nucleic acids in the DRG at the early time point of infection (24 h, 48 h, 72 h) in the rat model. Two animals were studied at each time point. '+' denotes presence of viral gene 63; '-' denotes viral gene 63 not detected. L1I-L6I = lumbar DRG ipsilateral to the side of injection; L1C-L6C = lumbar DRG contralateral to the side of injection.

Tissues	Time post infection (h)		
	24	**48**	**72**
L1I	+	-	+
L2I	+	-	+
L3I	+	-	+
L4I	-	-	+
L5I	-	+	+
L6I	-	-	+
L1C	+	+	+
L2C	+	-	-
L3C	-	+	-
L4C	-	-	-
L5C	+	+	+
L6C	-	-	-
Footpad I	+	+	+
Footpad C	-	-	-
Sciatic I	+	+	+
Sciatic C	+	+	+
Blood	-	-	-
Spinal cord	-	-	-
Brain	-	-	-
Spleen	-	-	-

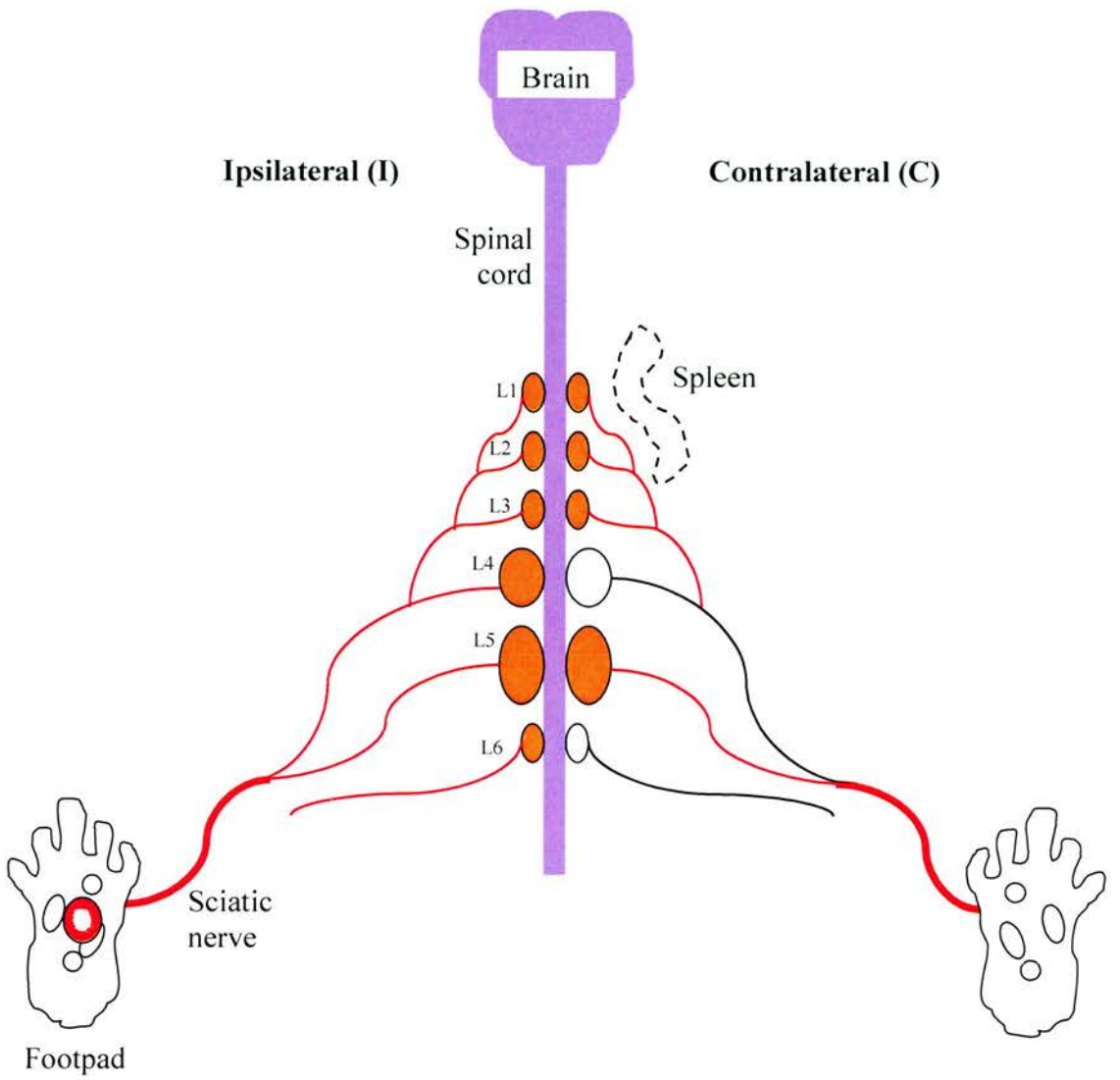

Figure 3.17 A schematic diagram of the viral spread in the rat model. VZV was injected subcutaneously into the left footpad of the rat. Viral DNA was found in the footpad (I), sciatic nerve (I and C) and in the lumbar DRG, L1-L6. Tissues found positive for VZV63 were in red. VZV63 was not detected in brain, spinal cord, L4C, L6C, spleen and the right footpad. The central nervous system is coloured in purple.

3.3. Discussion

In this study, the distribution and viral load of VZV DNA in the latently infected dorsal root ganglion (DRG) obtained from animals developing allodynia were studied with nested-PCR and real-time PCR. An alternative approach of isolating single populations of neurons was also investigated. A viral spread experiment was carried out to provide a better insight of the viral dissemination in the rat model.

3.3.1. Detection of VZV DNA in Infected Whole DRG

The nested PCR for VZV63 developed in this study has the ability to detect down to 10 copies of plasmid DNA. When fewer than 10 copies of plasmid DNA was analysed, the nested-PCR detected the samples infrequently and therefore replicates had to be included. A similar sensitivity of detection was also reported in a recent study comparing a TaqMan real-time PCR assays with nested PCR assays to detect HSV-1, HSV-2 and VZV in clinical samples (Weidmann et al. 2003).

In order to investigate the gene expression in the infected DRG and to correlate it with the altered behavioural changes in the rats, the first thing was to confirm the presence of viral gene in the DRG. VZV63 DNA was detected in the ipsilateral DRG of infected rats with the nested PCR system. Others have reported on the detection of VZV gene expression in the DRG in a similar rat model (Kennedy et al. 2001), (Grinfeld et al. 2004) with *in situ* hybridisation and *in situ* PCR techniques, respectively. However, in this study, virus was not only found in the ipsilateral DRG but also in the contralateral DRG concurrent to a 'contralateral effect' seen in some of the rats following infection of

only one footpad. This bilateral allodynia was reported by Dalziel et al., (2004). They proposed that the altered bilateral effects were related to the dose of VZV injected into the hindpaw and hypothesised that virus spread to the contralateral side was the cause of the allodynia. Animal studies of neuropathic pain states following unilateral nerve constriction have also reported bilateral effects (Attal et al. 1990), (Colvin et al. 1996). The contralateral effect could also be explained by an alternative hypothesis that pain is not only generated by the injured nerve fibres themselves but also by intact nerve fibres in the vicinity of injured nerve fibers (Schaible and Richter 2004). It has been shown that after an experimental lesion is introduced in the L5 DRG, spontaneous action potential discharges are observed in C-fibres in the uninjured L4 DRG. These fibres might have been affected by the Wallerian degeneration (Wu et al. 2001). Nevertheless, the finding of VZV DNA in the contralateral DRG suggested that the presence of virus indeed has contributed to the 'bilateral effect', however this possibility has to be further investigated.

3.3.2. Viral Load in the Latently Infected DRG

Even though nested PCR was sensitive to the point whereby viral DNA could be detected within its detection limit in the DRG, however it was still a qualitative assay. In order to quantitate the viral load in the DRG, a real-time PCR assay was developed. It has been shown that in some animal experiments, the latent viral genome levels in the sensory ganglia influence the reactivation frequency of HSV-1 and HSV-2, suggesting that the quantity of latent viral genome copies per ganglion (or latent viral load) may be

a significant determinant of herpesvirus reactivation from the nervous system (Sawtell et al. 1998), (Sawtell 1998).

Within the sensitivity of the real-time PCR assay, it was estimated that there were 42 ± 24 to 795 ± 459 copies of VZV genome per 10^5 cell equivalents. This means that there are only 0.02% to 0.5% of cells in the rat DRG containing VZV genome. This low abundance of viral DNA in the DRG could imply a low level of mRNA transcripts and this could have explained the difficulties in the detection of the viral transcripts in the DRG. Latently infected rabbits were found to contain on average 16.8 copies of HSV-1 DNA per 100 cells equivalents (Hill et al. 1996) while latently infected mice contained on average 50 copies of virus per 100 cell equivalents (Katz et al. 1990). At the single cell level, the HSV-1 DNA burden was shown to range from 10 to 1000 copies per individual latently infected mouse neuron (Sawtell et al. 1998). The amount of VZV DNA present in human ganglia was determined to be 557 to 55543 per 10^5 ganglion cell equivalents (Cohrs et al. 2000). At the single cell level, VZV DNA was found at a rate of two to five copies per 100 neuronal cells (LaGuardia et al. 1999). A recent report using LCM and real-time PCR to estimate the copy numbers of HSV-1 gG and VZV gene 62 from human trigeminal ganglion has reported 6.9 VZV genomes per positive cell (Wang et al. 2005). The estimated number of latent genomes per ganglion reported in the literature varies widely, in part depending on the method used to calculate that number and also different tissues used.

3.3.3. Detection of VZV DNA in Microdissected Cells

Laser capture microdissection (LCM) technique has proved to be a useful tool to isolate single cells from a mixed population in the DRG. The ability to detect VZV DNA in the microdissected cells will allow the study of gene expression in subpopulation of neurones in which VZV polypeptides are being expressed. It is important to study the neuronal subtypes as it has been shown that there is differential gene expression within DRG neurons (Luo et al. 1999). In the DRG, there is small-, medium- and large-sized neurons. Within the small neurons itself for example, there is heterogeneity in gene expression, which, presumably reflects, at least in part, the different sensory modalities transmitted. However, the LCM technique developed in this work could be refined further by integrating immunocytochemistry with LCM in order to approach the complicated heterogeneity. For example, cells could be stained for specific VZV markers so that cluster of cells of interest could be selected and captured. These cells could then be used for similar studies discussed here or in Chapter 4.

3.3.4. Detection of VZV Transcripts in the Infected DRG

Precise estimates of the number of VZV transcripts in human ganglia do not exist. That routine RT-PCR assays on unselected total RNA from human ganglia have not been reported to be positive suggests that the number of viral transcripts in latently infected tissues is low (Silverstein and Straus 2000). This contrasts with the data regarding HSV-encoded LATs, which are estimated at 100 or more copies for every latent viral genome (Ramakrishnan et al. 1994). Thus, the quantity of VZV RNA in

latently infected human ganglia must be substantially below this level, since HSV LATs are readily detected by Northern blot hybridisation and RT-PCR assays (Stevens et al. 1987), (Croen et al. 1988).

Since the viral DNA load in the DRG is very low, this suggests that not many copies of VZV genome are present in the DRG. Therefore, this may also reflect a limited mRNA expression, which hampers the detection of these RNA transcripts in the RT-PCR. Due to the limitation in sensitivity of the RT-PCR assay, a method of simultaneous isolation of the DNA and RNA from the same sample was adopted. This method has allowed the study of the DNA and gene expression in the same sample. However, results shown that RNA transcripts were not detected even in samples where the viral genome was found to be present. This again has suggested that a low level of RNA transcription due to the low abundance of VZV DNA in the DRG. The viral transcripts could not also be quantitated by real-time PCR has indicated that the level of expression of the latent virus was very low in the infected DRG and it was beyond the sensitivity of detection of the assay.

Due to the fact that SYBR Green I binds to any double-stranded DNA, the assay used might not be as specific as the probe based system. A sequence-specific probe was reported to provide better sensitivity for low copy number detection without the need to worry about unspecific products or primer dimers (Wittwer et al. 1997). A different nested real time PCR approach claimed to be able to overcome the limitation in sensitivity in order to quantitate Hepatitis B virus (HBV) DNA in serum (Brechtbuehl et al. 2001). The nested assay was sensitive to the level of a single HBV genome in the

PCR reaction. This approach might be applicable in future in order to quantitate the viral gene expression in the DRG.

3.3.5. Viral Spread in the Rat Model

This experiment was carried out with the aim of investigating the virus dissemination in the rat model after VZV infection. The finding of VZV DNA in the DRGs as early as 24 h post infection had suggested that the virus reaches the DRG possibly via the sensory nerve terminals present in the richly innervated glabrous skin of the footpad. The virus was predicted to ascend the neuronal pathway to the DRG, the site of VZV latency. However, the mechanism of spread of virus from the ipsilateral side to the contralateral side was not clear.

The finding of VZV DNA in DRG contralateral to the side of inoculation suggests that there might be another route apart from axonal transport where the virus travels in the rat model. The simplest explanation for this finding is that these animals develop viremia but in this study viremia was not detected in the VZV-infected rats from 24 h to 72 h. A similar finding was reported by Annunziato et al., (1998) where they could not detect viremia by PCR in the VZV infected rats two weeks after inoculation into the footpad with cell-free virus, however these rats developed antibody to VZV. Since virus inoculation is expected to elicit an immune response to viral antigens, they concluded that virus replication did not occur. They also suggested the likelihood that the blood samples were not obtained at the appropriate time point to detect VZV viremia in the rat model since in the guinea pig model, viremia occurs 2-5 days after inoculation (Lowry et

al. 1993). It may also be that viremia occurred but at a level below the level of detection of the PCR assay. Another alternative explanation for the finding of VZV infection contralateral to the inoculation sites is that virus spreads via the cerebrospinal fluid (CSF). VZV has been found in human CSF in the absence of clinical indications of encephalitis or meningitis (Annunziato et al. 1998).

No viral DNA was detected in the spleen, brain and spinal cord (taken from the cervical enlargement region) at all time points studied in this experiment. A similar finding was reported by Grinfeld et al., (2004), where they found no peripheral tissues (spleen, liver, lung and kidney) were positive for VZV genes 62 and 63 in VZV infected rats. This and our finding suggest that VZV infection in the rats mainly restricted to the peripheral nervous system.

3.4. Conclusion

In agreement with previous findings, rats inoculated subcutaneously with VZV into the footpad harbour the VZV DNA in their DRG. However, due to only a small fraction of cells in the DRG harbours latent VZV and due to the low-level expression of the viral transcripts, they were beyond the level of detection of the RT-PCR and real-time PCR assays developed. It is not possible to draw any correlation between the altered behavioural changes with the gene expression in the DRG from the results as there is no clear pattern observed. VZV DNA was also detected in DRG contralateral to the site of inoculation but viremia was not able to be demonstrated. The viral spread experiment

has confirmed that VZV injected into the footpad of rats primarily used a retrograde axonal route to reach the DRG where it remained latent.

CHAPTER FOUR

RESULTS AND DISCUSSION

4.1. Introduction

The ability to study thousands of genes simultaneously at one time was impractical until microarray technology was introduced in the mid 1990s (Brown and Botstein 1999), (Dhiman et al. 2002). Many studies have used microarray analysis to examine the host response to infection with herpesviruses, including HHV-6 infection of transformed T cells (Mayne et al. 2001), Epstein-Barr virus (EBV) infection of transformed B cells (Carter et al. 2002), human cytomegalovirus (HCMV) infection of primary human fibroblasts (Browne et al. 2001), Kaposi's sarcoma-associated herpesvirus (KSHV) infection of dermal microvascular endothelial cells (Moses et al. 2002), HSV-1 infection of mouse trigeminal ganglia (Kramer et al. 2003) and VZV infection in human T cells, fibroblasts and SCIDhu skin xenografts (Jones and Arvin 2003). Viral gene transcription has also been investigated by microarray analysis in BSC-1 cells infected with VZV (Cohrs et al. 2003) and viral and cellular gene transcription in fibroblasts infected with small plaque mutants of VZV (Jones and Arvin 2005). These studies have demonstrated many commonalities in host cell responses to herpesviruses. For example, interferon response genes were modulated by all herpesviruses that have been evaluated by microarray analysis. Herpesvirus infections tend to affect the regulation of other immune system genes as well, including interleukins and other cytokines. Genes involved in basic cellular processes such as cell cycle control, transcription and translation also tend to be altered by herpesvirus infection.

The study presented here was designed to investigate changes in host cell gene transcription in dorsal root ganglion following VZV-induced allodynia. The hypothesis

we wished to address was the presence of VZV proteins in latently infected or reactivating neurons results in an increased sensitivity to noxious stimulus via a change in the transcriptional activity of the neurone.

Two forms of microarray currently in wide use are the cDNA array format (Pease et al. 1994) and the oligonucleotide array format (Schena et al. 1995). cDNA arrays are commonly developed using protocols introduced in the Brown laboratory at Stanford University (http://cmgm.standford.edu/pbrown/mguide/index.html). cDNA arrays are made by robotic deposition of DNA spots 50-150 μm in diameter onto a coated glass surface. These moderate sized DNA arrays typically have around 10,000 spots on an area of 3.6 cm^2. This technology allows the comparison of fluorescently labelled cDNA populations from control and experimental samples in dual colours requiring less than 600 ng of mRNA per sample for a 10,000 spot DNA chip. High-density oligonucleotide arrays are readily available from a number of commercial supplier included for example from Affymetrix, Santa Clara, CA (www.affymetrix.com) and Agilent Technologies (www.chem.agilent.com) (Lipshutz et al. 1999).

4.1.1. Affymetrix GeneChip Array

The Affymetrix GeneChip technology platform consists of high-density microarrays and tools to help process and analyse those arrays. The advantages of Affymetrix GeneChips included high specificity and sensitivity. It is possible to get rapid results, it has the capability to monitor the expression of a large number of genes in the genome and it is the most widely used commercial microarray platform. However,

the disadvantages are that it is significantly more expensive than custom microarrays, demands stringent quality control and Affymetrix only makes GeneChip arrays for common experimental animals.

Affymetrix combines oligonucleotide synthesis and photolithography to produce DNA arrays that contain 65,000-400,000 DNA oligonucleotides on a 1.6 cm^2 glass surface (Ramsay 1998), (Lockhart et al. 1996). In DNA photolithography, ultraviolet light shines through holes in masks in order to direct parallel and stepwise synthesis of oligonucleotides. At each step in the synthesis, oligonucleotides are deprotected by light at the appropriate positions by the mask. The chip is then flooded with activated nucleotides, which couple to the deprotected positions. Uncoupled residues are then washed away, another mask is applied and the deprotection steps are carried out with the next nucleotide. Repetition of the cycle approximately 70 times, with 70 different masks, allows synthesis of the complete array of thousands of 25-mer oligonucleotides in parallel.

Once fabricated the gene chip probe arrays are ready for hybridisation. The nucleic acid to be analysed is isolated, amplified and labelled with a fluorescent reporter group and incubated with the array. The array is read on a scanner and the patterns of hybridisation are detected including measure of fluorescence intensity. This approach to gene expression monitoring is advantages because it allows the user to avoid genes that are repetitive or homologous to other known genes. Typically 20 pairs of oligonucleotides are arrayed to represent each gene, which improves the quantification, specificity and reliability of gene expression data (Lockhart et al. 1996).

4.1.2. Rat Expression Set 230A

In this study, Affymetrix Rat Expression Set 230A GeneChip arrays were used to analyse gene expression in mock (non-infected) and VZV infected DRG tissue. This array contains oligonucleotide probes specific for around 15,866 known rat genes present in the mouse unigene database. The array also contains probes representing around 10,400 Expressed Sequenced Tags (ESTs) sequences. ESTs are single pass sequence from either end of a cDNA clone. Figure 4.1 shows the overall workflow for the microarray experiment.

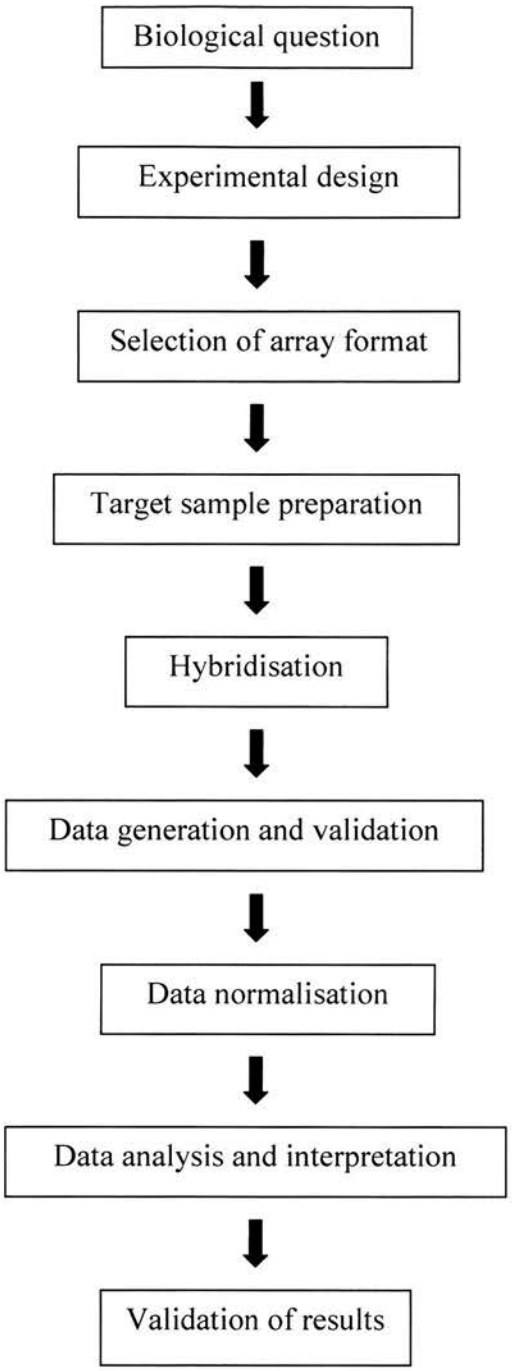

Figure 4.1 The workflow of the microarray experiment is outlined. Shown here are the standard steps involved in the workflow processes.

4.2. Results

4.2.1. Experimental Design

Experiments were undertaken in which DRG were obtained from VZV infected rats, which showed altered behavioural changes after infection. The experimental procedure was as described in section 2.6. Control animals were injected with non-infected CV-1 cells and following testing showed no significant changes in behavioural response compare to paw withdrawal threshold (PWT) from pre-inoculation testing. Figure 4.2A shows the VZV-induced altered behavioural changes in the infected and control rats. A drop in PWT was observed at day 3 for both infected and uninfected groups. This is commonly observed and may be attributed to an injection trauma at the site of injection (Fleetwood-Walker et al. 1999). It is notable that the PWT of the infected animals remained low compared to the control group, which returned almost to the baseline values at day 7. The experiment was terminated at day 10 when the infected animals were still sensitive but the control animals were back to the baseline ($p<0.05$). Only individual animals that showed allodynia (PWT less than 15 g) were used for tissue collection on post infection day 10 (Figure 4.2B).

4.2.2. Preparation of Target Sample

The extraction of high quality RNA for labelling and subsequent microarray hybridisation was essential in this study to ensure the success of reverse transcription and further verification analysis. Lumbar L4-L6 DRG, ipsilateral and contralateral to the

site of injection, were dissected from the animals and immersed immediately in RNAlater (Ambion) to prevent degradation of the RNA in the tissues prior to RNA extraction. In the microarray experiment only DRG from the ipsilateral side were used. 9 DRGs from the three animals showing the highest allodynia response (average PWT at 0.8 g, 1 g and 1.4 g) were pooled, disrupted and lysed in lysis buffer followed by homogenisation in a QIAshredder spin column to obtain a clear lysate (section 2.4.2). Total RNA extraction was carried out with the RNeasy Mini kit (QIAGEN) and the RNA was eluted with 30 µl of RNase-free water. The elution was repeated with the first eluate in order to increase the yield of the RNA. For this study, due to the limitation of the labelling process, at least 5 µg of total RNA was needed for labelling and hybridisation.

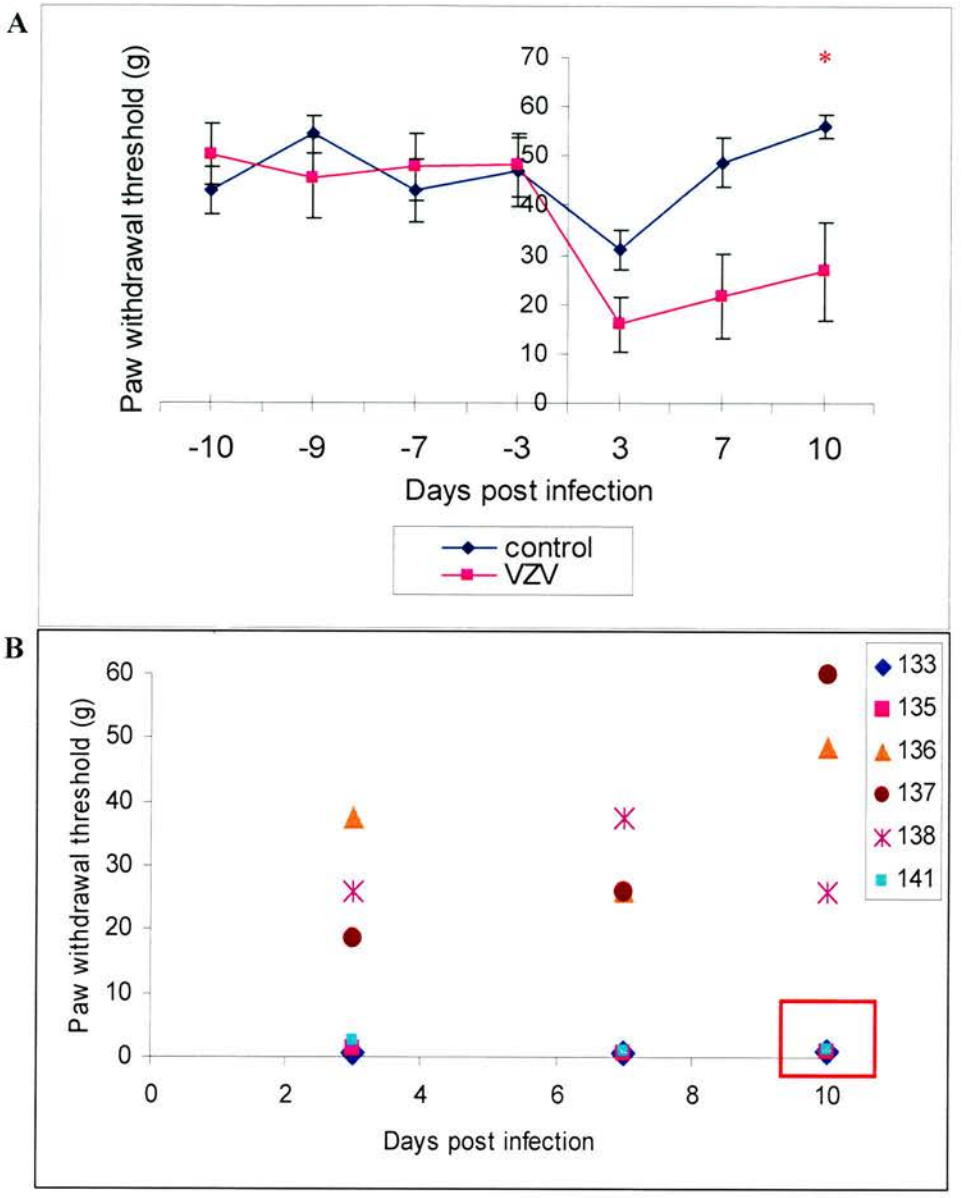

Figure 4.2 ***In vivo*** **experiment.** (A) Graph shows VZV-induced allodynia in animals to be used in the microarray experiment. Animals were injected in the left hindpaw on day 0 with either 4 x 10^6 VZV infected CV-1 cells (VZV, n=6) or uninfected CV-1 cells (control, n=6). The mean withdrawal thresholds in grams for ipsilateral paws were determined and plotted against time post infection in days for each group and SEM shown. Statistically significant differences between injected and non-injected hind paws (*P < 0.05, Mann-Whitney U test, n=6). Mock-infected control animals did not show significant behavioural changes before and after VZV infection. (B) Individual animals were shown. Tissues from the 3 animals showing the highest allodynia response (in red box) were pooled for RNA extraction.

4.2.3. Integrity and Quality of RNA

Messenger RNA (mRNA) typically comprises only 1-3% of total RNA samples and it is not easily visualised even with the most sensitive of methods. In contrast, ribosomal RNA, makes up > 80% of total RNA samples, with the majority of that comprised by the 28S and 18S rRNA species in mamalian systems. Traditionally, mRNA quality has been assessed by denaturing agarose gel electrophoresis of total RNA followed by staining with ethidium bromide. This method relies on the assumption that rRNA quality and quantity reflect that of the underlying mRNA population. If the 28S and 18S rRNA bands are discrete with no significant smearing and the 28S rRNA band is approximately twice as intense as the 18S rRNA band, then the mRNA in the sample is of good quality. The primary drawback to this method is that microgram amounts of RNA must be sacrificed.

In recent years, successful attempts have been made to improve on this approach and in this study an Agilent 2100 Bioanalyser and RNA6000 Nano LabChip Kit were used to measure nanogram quantities of total RNA. The bioanalyser fractionates RNA molecules according to size and the amounts of 18S and 28S rRNA are automatically calculated. Theoretically, intact RNA will have a 28S:18S rRNA ratio of 1.7-2.0. However, in practice, this ratio is rarely obtained with samples extracted from animal tissue and variation from source to source is observed (Robertson, K., personal communication).

Figure 4.3 shows an example of the electropherograms of the purified RNA samples extracted from the mock and infected tissues. The RNA was intact as shown by

relatively low number of small peaks in the profile and a ratio of 28S:18S of approximately 1.0 for both samples. In this study, once the RNA samples quality had been confirmed, samples were labelled and hybridised to the Affymetrix gene chip following the standard protocols which were carried out by Dr. Kevin Robertson at the Scottish Centre for Genomic Technology and Informatics.

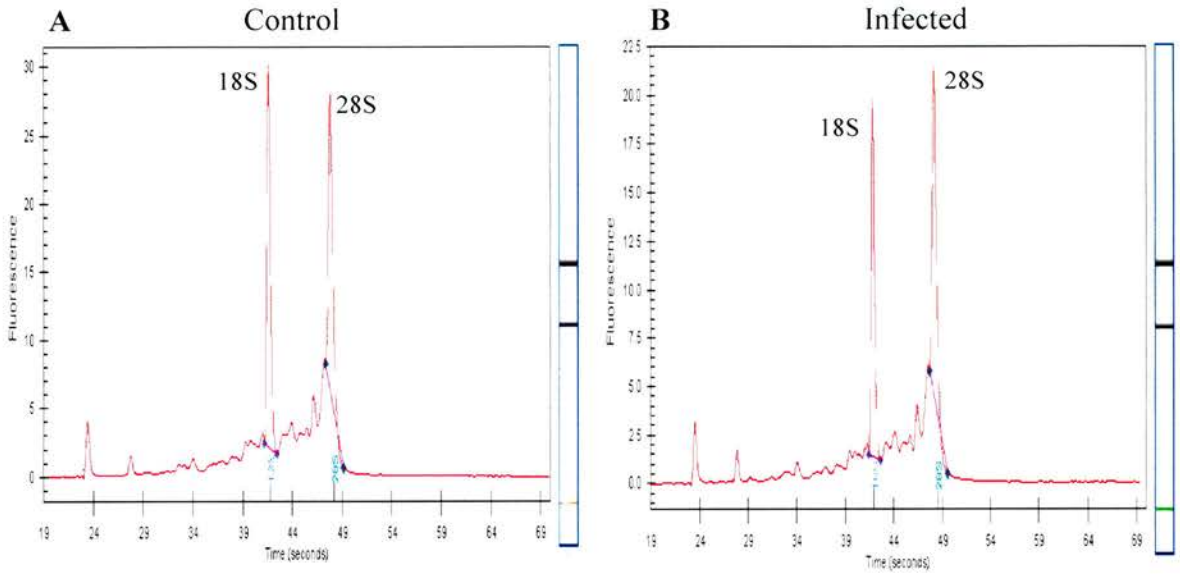

Figure 4.3 RNA quality and integrity check with the Agilent 2100 Bioanalyser. Panel A and B show gel-like images and electropherograms of RNA samples from control and VZV infected animals, respectively. RNA from these samples was of good quality as seen by very few small peaks and a good 28S:18S ratio.

4.2.4. Microarray Data Analysis

After hybridisation of the biotin labelled cDNA, arrays were washed and stained with streptavidin-phycoerythrin as outlined in the Affymetrix expression analysis technical manual. The arrays were then scanned using the Affymetrix GeneChip scanner 2500 and image analysis and quantitation were undertaken using Affymetrix MAS 5.1 software according to standard Affymetrix protocols. In brief, each transcript on the array is represented by a set of 13 to 20 probe pairs (depending on the array). A probe pair consists of a 25-mer 'perfect match' (PM) oligonucleotide derived from a 3' region of the original coding strand of the gene. This is accompanied in an adjacent microarray feature by a 25-mer 'mismatch' (MM) sequence, which has a nucleotide change at position 13 of the sequence. A 'signal' value representing transcript abundance is derived for each probe set via a process involving: background subtraction, noise correction and a comparison of the hybridisation signal for the PM and MM probes. The latter comparison enables the analysis algorithm to account for cross hybridisation and stray signal, which may affect quantitation of the transcript. During this process, a detection algorithm calculates a detection p-value and generates a 'present', 'marginal' or 'absent' (P, M or A) value for each transcript.

Before comparing two arrays, data were normalised to correct for technical variations between arrays. In this study, all arrays were normalised by scaling the overall intensity of the arrays to an arbitrary value of 100. This method assumes that the overall intensity of the arrays is identical and the majority of genes do not change in expression.

After normalisation, scaling factors for all the arrays were within an acceptable range (i.e. within 3 fold of each other) (Robertson, K., personal communication).

4.2.5. Microarray Quality Control

In the Rat Expression Set 230 a set of 'housekeeping' genes (e.g. GAPDH, beta actin, hexokinase 1) are included on the array. These genes are represented by probe sets derived from the 3', middle and 5' regions of the gene. By calculating a 3'/5' signal ratio, the user is able to assess whether full-length cDNA transcripts have been produced during the reverse transcription step of the labelling process. Optimal cDNA synthesis will produce a ratio value of around 1. To assess the sensitivity of the hybridisation, signal and detection values for Affymetrix spiked transcripts (i.e. bioB, bioC, bioD and cre) were noted. For all arrays, the spike transcript at lowest concentration (bioB, concentration 1.5 pM) was detected indicating that the hybridisation, washing, staining and scanning were optimal.

The performance of the arrays was further assessed prior to data analysis, which was being carried out with the help of Dr. Kevin Robertson. A scatter plot comparing the two arrays using the default expression measure provided by Affymetrix Microarray Suite 5.1 (MAS) was produced using S-PLUS software (Insightful Corporation), which allows exploratory data analysis and statistical modelling. Result is shown in Figure 4.4A. The scatter plot confirmed that the data had a symmetrical 'flared' distribution and showed a dynamic uninterrupted range of expression values from low to high signal values. The flared distribution occurs as a result of variation increasing as signal levels

decrease and is entirely typical of data normalised in the manner described above. Most of the variation between the two groups exists at the lower end of the gene expression levels. This suggests that the variability is in part due to array sensitivity and consequently, differences in low intensity genes may be unreliable.

To further investigate the signal distribution across the arrays, a 'box-and-whiskers' representation of the data was produced in S-PLUS (Figure 4.5). This figure confirmed that after normalisation the data was symmetrical and the decision was made to proceed with the data analysis.

4.2.6. Comparison of Uninfected and Infected Samples and Identification of Differentially Expressed Genes

In this study, control and infected samples were hybridised to two independent Affymetrix GeneChip Rat Expression Set 230A arrays. In order to detect and quantify changes in gene expression, a pair-wise comparison was undertaken in MAS 5.1. In this analysis, one array was designated as the baseline (uninfected) and the other as the experimental sample of interest (infected).

The Affymetrix MAS comparison algorithm was used to compare the difference values (PM-MM) for each probe pair on the baseline array with its corresponding probe pair on the experimental array. This process generates a change p-value which indicates the probability that there was a difference in transcript expression between the two samples. The process also produces a change value (up, down or unchanged). A second

algorithm is used by the software to produce a 'Signal Log Ratio' (SLR) value, which indicates the magnitude of change. In this system, the log scale used is base 2, which ensures that the output of the analysis is intuitive. A SLR of 1.0 indicates a 2-fold increase in transcript expression and a SLR of -1.0 indicates a 2-fold decrease in expression. A SLR of zero would indicate no change. In this analysis, data were sorted and filtered using a combination of the output values described above. To increase the likelihood that genes identified in this analysis were valid, an arbitrary signal threshold value of 50 was selected.

During the course of this study, an expression measure motivated by a log scale linear additive model was reported to provide more consistent estimates of fold change and improvement in detecting differentially expressed genes compared to the MAS algorithm (Irizarry et al. 2003). This summary statistic is referred to as the log scale robust multi-array analysis (RMA). In order to validate the methods described above, this method of analysis was also adopted in the study. As can be seen in Figure 4.4B, the data seemed to be less variable at low levels of expression. Figure 4.6 shows a diagram of the comparison of genes obtained from MAS and RMA. Since RMA provides more consistent estimates of fold change and significantly reduce variation at low level of expression, only 7 genes were found to be significantly regulated by the two methods and they were shown in Figure 4.7.

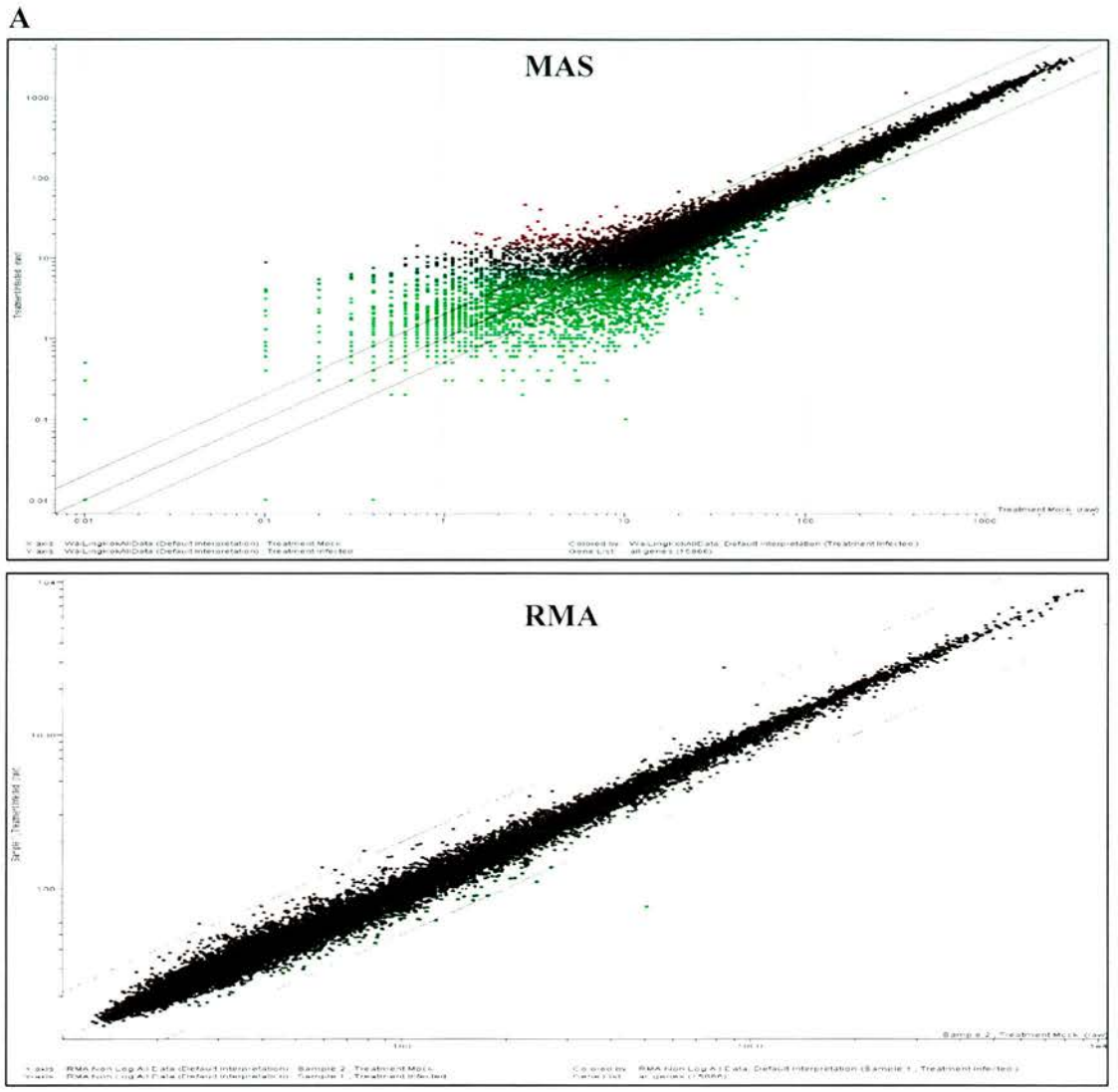

Figure 4.4 Representative scatter plot of overall expression level data from the GeneChip Rat Expression Set 210A experiment with two different normalisation methods. The control (uninfected) is plotted on the x-axis while the experiment (infected) is plotted on the y-axis. (A) Note the tight clustering of most data about y=x but a 'flare' distribution is obvious as the signal intensity decreases when data were analysed with MAS. A cut-off of 50 for the signal intensity was applied to the dataset in order to increase the stringency of the selection of probe sets for further analysis. (B) Data analysed with RMA, showing a better precision for lower expression values.

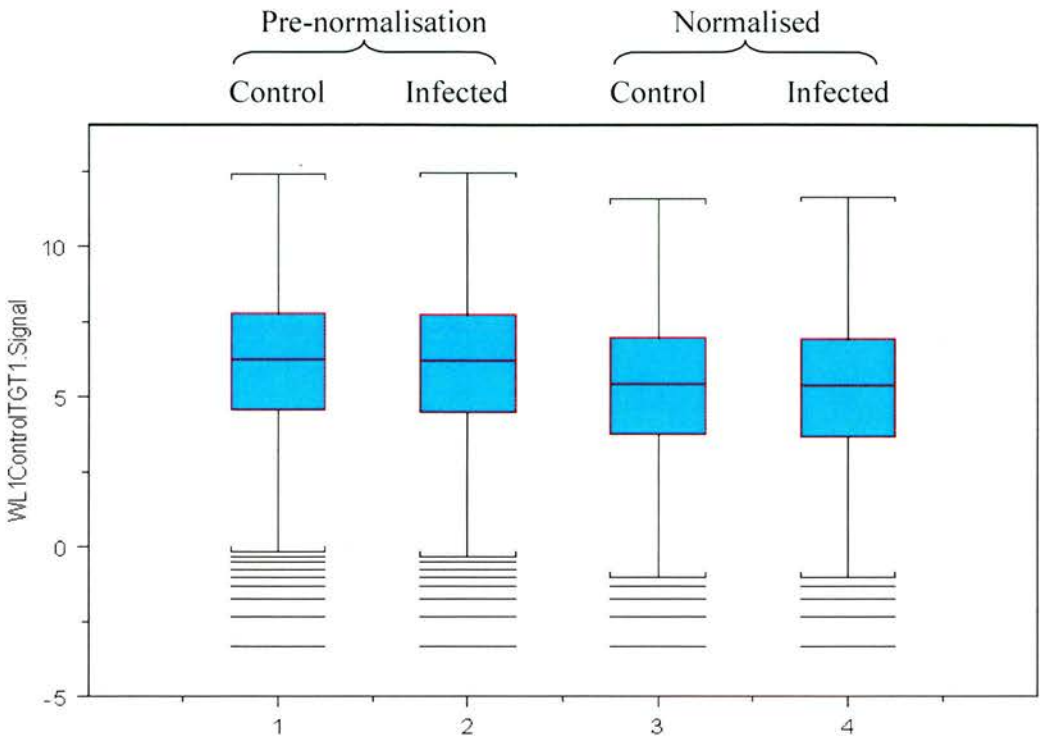

Figure 4.5 Box and whiskers plots show the distribution of the data before and after normalisation. Data was symmetrical after normalisation. The median value is represented by the central line inside the box. Above this line are data in the third quartile and below this line are data in the first quartile. The upper and lower quartiles are the 75th and 25th percentiles, respectively.

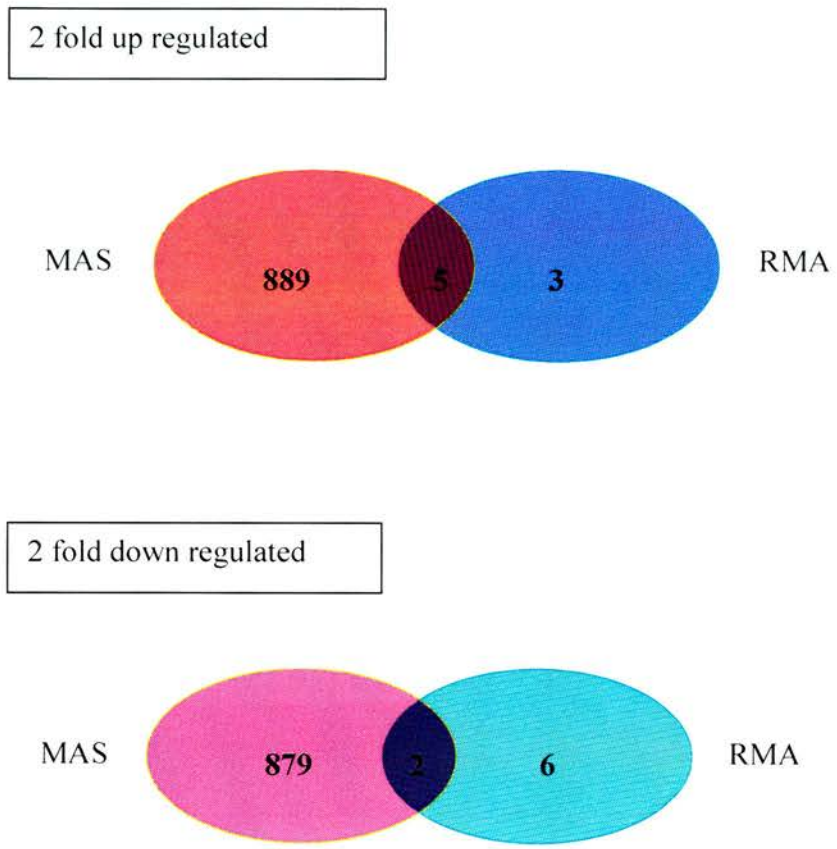

Figure 4.6 A comparison of genes found regulated by MAS and RMA analyses. There are a total of 15866 transcripts represented on the RAE230A GeneChip. Out of this figure, 894 and 881 genes were found to be up and down regulated more than 2 fold by MAS, respectively. Only 8 genes were expressed more than two fold either up or down regulated by RMA. There were 5 genes found to be up regulated and 2 genes down regulated more than 2 fold by both methods.

4.2.7. Identification of Significantly Regulated Genes

Individual control and infected samples were analysed on an array. Each gene was given a present (P), absent (A) or marginal (M) call and a value of signal intensity after an array analysis using the MAS 5.1 software. This study is based on a mixed population of cells with less than 100% of cells infected, therefore a small fold change in the expression might represent a large change in the real biological system.

Of the 15866 probe sets represented on the RAE 230A GeneChip, 5295 probe sets were not detected (33%) on either array (A to A) and were removed from the analysis. 9556 genes were detected in both samples (P to P), of which 332 had altered expression with 57 of them showing an increase in expression. Of the 57 increased in expression, there were 32 with a signal of > 50, which is the cut-off value selected for filtering and only 5 had a fold change of greater than 2. From the pool of P to P genes, there were 260 genes decreased in expression and only 2 were significantly down regulated.

There were 320 genes found to go from absent to present (A to P) after infection of which only 3 met the cut-off of 50 and were up regulated 2 fold or more. 692 genes went from present to absent (P to A) after infection and 2 of them met the cut-off of 50 and were down regulated more than 2 fold.

Figure 4.7 shows significantly regulated genes, which have a fold change of greater than 2 (SLR>1). These genes included prostaglandin D_2 synthase (Ptgds), S100 calcium-binding protein A9 (S100a9), cholinergic receptor (Chrna6), vitronectin (Vtn),

transthyretin (Ttr), phosphatidilinositol-3 kinase (Pik3r1) and heat shock 70 kD protein 1A (Hspa1a).

A

Probe Set ID	Control	Infected	*SLR	Fold Change	Gene Title
1367851_at	362.9	1143.7	1.5	3.151556903	prostaglandin D_2 synthase (Ptgds)
1387125_at	19.8	67.7	1.2	3.419191919	S100 calcium-binding protein A9 (S100a9)
1367598_at	23.3	53.7	1.2	2.30472103	transthyretin (Ttr)
1369845_at	51.3	105.8	1	2.062378168	cholinergic receptor, alpha polypeptide 6 (Chrna6)
1368380_at	25.8	56.7	1	2.197674419	vitronectin (Vtn)
1371776_at	272.6	54.4	-2.4	-5.011029412	phosphatidylinositol 3-kinase (Pik3r1)
1368247_at	127.9	65.4	-1	-1.955657492	heat shock 70kD protein 1A (Hspa1a)

* Signal log ratio (SLR) was determined by comparison of the signal intensities for the baseline (control) and the experimental (infected) array. This is computed using a one-step Tukey's Biweight method by taking a mean of the log ratios of probe pair intensities across the two arrays.

B

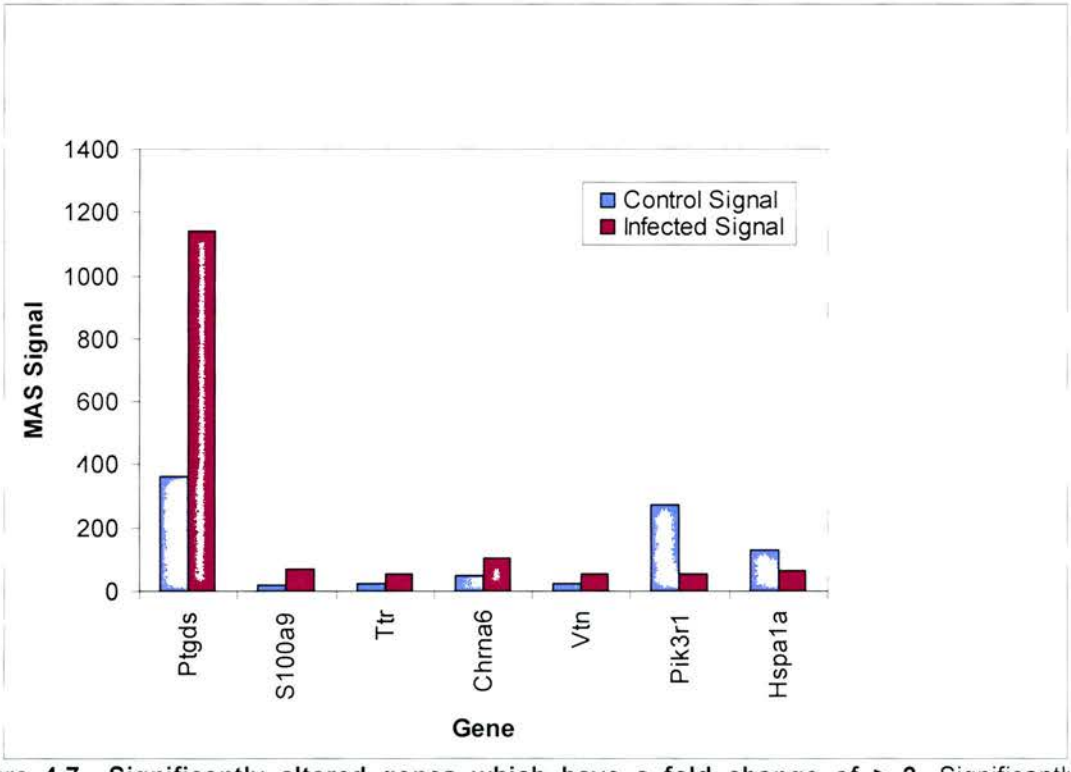

Figure 4.7 Significantly altered genes which have a fold change of > 2. Significantly regulated genes (A) which met the filtering criteria of having signal intensity greater than 50 and SLR >1 are shown in the graph (B).

4.2.8. Sorting of Data based on Biological Functions

In order to identify biologically novel and interesting differentially expressed transcripts, genes were assigned into various functional groups. The functional categories included cell-cell communication and signalling, inflammation and immune, growth, transcription factors, ion channel, neuropeptide, synapse and genes involved in tissue maintenance. Table 4.1 shows genes having signal of > 50 categorised into different functional groups.

Genes that may indirectly regulate the excitability of sensory neurones include ion transporters, neuropeptides, receptors, signalling molecules and proteins with synaptic functions. Multiple ion channel genes that may directly contribute to alter excitabilities of ipsilateral sensory neurons were observed to be regulated in the ipsilateral DRG. Down regulated ion channels include potassium channel (Kv9.3) and voltage-gated sodium channel (Scn11a). There were a number of genes known to be expressed in neurons. Many of the genes whose expression was altered play a definite role in neuronal physiology. These included genes encoding neurotransmitter receptors such as G protein-coupled receptor 56 and cholinergic receptor and proteins involved in signalling, including neuregulin which is essential for neuronal development by regulating the composition of neurotransmitter receptor in maturing synapses. Down regulation of synaptic proteins was also observed e.g. vesicle-associated membrane protein 2. Several genes involved in cell growth and development were down regulated such as insulin-like growth factor 2. Viral regulation of these genes may be important for viral replication and growth. Genes important in transcription are mostly down regulated

i.e. activating transcription factor 5 and transcription factor 8. Other genes that are regulated can be broadly categorised as genes that are important for tissue maintenance, remodelling and plasticity. For example, solute carrier family 7, member 1, which is involved in amino acid transport activity is down regulated. However, genes involved in neuroinflammation and immune activation were found to be up regulated e.g., prostaglandin D_2 synthase and CD74 antigen.

Due to the mixed heterogeneity of the sample, it was also important to look at those genes with low signal intensity. Genes from 'Present' to 'Absent' or vice versa with signal less than 50 in different functional groups are shown in Appendix 4.1 and 4.2. As there were too many from the 'Present' to 'Present' list with signal less than 50 and many of them were ESTs, therefore they were not analysed further. There were too many genes in each list to be discussed within the scope of this study. Even though most of them have low signal, it is more important to look at the magnitude of changes in expression before and after infection rather than to focus on the simple fold change. The low signal in these genes potentially limit the confidence with which one can interpret the data as true but when factors of heterogeneity of the samples were taken into account and the fact that not all cells were infected, then the small changes in expression might be important. These genes might be interesting to look at in the future.

Table 4.1 Functional Analysis of the Genes having Signal Intensity > 50 in the Microarray Analysis

Probe Set ID	Gene	Control	Infected	SLR	Fold Change
Inflammation, cytokine, immune					
1367679_at	CD74 antigen (invariant polpypeptide of MHC II antigen-associated)	123.3	222.9	0.7	1.8
1388138_at	thrombospondin 4	151.7	114.3	-0.5	-1.3
1370234_at	fibronectin 1	178.4	132.2	-0.7	-1.3
1371776_at	phosphatidylinositol 3-kinase, regulatory subunit, polypeptide 1	272.6	54.4	-2.4	-5
1367851_at	prostaglandin D2 synthase	362.9	1143.7	1.5	3.2
1367568_at	matrix Gla protein	510.7	776.6	0.6	1.5
Growth					
1367598_at	transthyretin	23.3	53.7	1.2	2.3
1367631_at	connective tissue growth factor	31	67	0.4	2.2
1367571_at	insulin-like growth factor 2	49.2	64.3	0.7	1.3
1388469_at	Rat insulin-like growth factor I mRNA, 3' end of mRNA	72	46.1	-0.5	-1.6
1371527_at	epithelia membrane protein 1	93.7	65.6	-0.4	-1.4
1387306_at	early growth response 2	98.5	69	-0.5	-1.4
1368005_at	inositol 1, 4, 5-triphosphate receptor 3	100.1	86.4	-0.3	-1.2
1370607_at	neuregulin 1	121.3	233.6	0.8	1.9
1368359_at	VGF nerve growth factor inducible	160.6	121.3	-0.4	-1.3
1377821_at	avian erythroblastosis oncogene B 3	184.7	124.5	-0.4	-1.5
1368391_at	solute carrier family 7, member 1	186.1	130.1	-0.4	-1.4
1369001_at	cholinergic receptor, nicotinic, alpha polypeptide 3	263.5	212.2	-0.2	-1.2
1370290_at	tubulin, beta 5	314.2	287.4	-0.2	-1.1
1373812_at	cyclin-dependent kinase inhibitor 1B	363.2	329	-0.3	-1.1
1371245_at	Rat hemoglobin beta-chain mRNA	368.1	192.8	-0.5	-1.9
1367882_at	microtubule-associated protein 1 A	371.5	316.2	-0.3	-1.2
1370057_at	cysteine and glycine-rich protein 1	381	322.4	-0.2	-1.2
1367846_at	S100 calcium-binding protein A4	611.7	547.2	-0.5	-1.1
1389533_at	fibulin 2	724.4	576.2	-0.3	-1.3

		Control	Infected	SLR	Fold Change
Transcription					
1370541_at	nuclear receptor subfamily 1, group D, member 2	88.9	72.6	-0.3	-1.2
1387306_at	early growth response 2	98.5	69	-0.5	-1.4
1370965_at	transcription factor 8	103.9	63	-0.7	-1.6
1368175_at	zinc-fingers and homeoboxes 1	112	92.3	-0.2	-1.2
1372601_at	activating transcription factor 5	132.5	118.1	-0.3	-1.1
1371979_at	sterol regulatory element binding protein 2	196.6	148.6	-0.4	-1.3
Ion channel					
1369845_at	cholinergic receptor, nicotinic, alpha polypeptide 6	51.3	105.8	1	2.1
1369638_at	eukaryotic elongation factor-2 kinase	90.7	61.2	-0.6	-1.5
1368005_at	inositol 1, 4, 5-triphosphate receptor 3	100.1	86.4	-0.3	-1.2
1370555_at	voltage gated channel like 1 (Vgcnl1)	139.3	110	-0.2	-1.3
1371979_at	sterol regulatory element binding protein 2	196.6	148.6	-0.4	-1.3
1369001_at	cholinergic receptor, nicotinic, alpha polypeptide 3	263.5	212.2	-0.2	-1.2
1368751_at	Shab-related delayed-rectifier K+ channel (Kv9.3)	335.7	453.3	0.4	1.4
1368768_at	sodium channel, voltage-gated, type11, alpha polypeptide (Scn11a)	487.2	418.6	-0.2	-1.2
Maintenance					
1367598_at	transthyretin	23.3	53.7	1.2	2.3
1367571_at	insulin-like growth factor 2	49.2	64.3	0.7	1.3
1371527_at	epithelial membrane protein 1	93.7	65.6	-0.4	-1.4
1368005_at	inositol 1, 4, 5-triphosphate receptor 3	100.1	86.4	-0.3	-1.2
1368391_at	solute carrier family 7, member 1	186.1	130.1	-0.4	-1.4
1369001_at	cholinergic receptor, nicotinic, alpha polypeptide 3	263.5	212.2	-0.2	-1.2
1370290_at	tubulin, beta 5	314.2	287.4	-0.2	-1.1
1368751_at	Shab-related delayed-rectifier K+ channel (Kv9.3)	335.7	453.3	0.4	1.4
1367851_at	prostaglandin D2 synthase	362.9	1143.7	1.5	3.2

Probe Set ID	Gene	Control	Infected	SLR	Fold Change
1373812_at	cyclin-dependent kinase inhibitor 1B	363.2	329	-0.3	-1.1
1371245_at	Rat hemoglobin beta-chain mRNA	368.1	192.8	-0.5	-1.9
1367882_at	microtubule-associated protein 1 A	371.5	316.2	-0.3	-1.2
1370057_at	cysteine and glycine-rich prote n 1	381	322.4	-0.2	-1.2
1387040_at	myelin and lymphocyte protein	412.7	299.8	-0.5	-1.4
Neural factor					
1371696_at	G protein-coupled receptor 56	350.2	262.5	-0.3	-1.3
1368359_at	VGF nerve growth factor inducible	160.6	121.3	-0.4	-1.3
1373098_at	band 83	246.7	165.8	-0.3	-1.5
1369001_at	cholinergic receptor, nicotinic, alpha polypeptide 3	263.5	212.2	-0.2	-1.2
1369845_at	cholinergic receptor, nicotinic, alpha polypeptide 6	51.3	105.8	1	2.1
1388644_at	monoglyceride lipase	159.1	129.3	-0.3	-1.2
1369974_at	vesicle-associated membrane protein 2	247.9	164.2	-0.4	-1.5
1387040_at	myelin and lymphocyte protein	412.7	299.8	-0.5	-1.4

4.2.9. Grouping Genes into Related Pathways- Pathway Analysis

It is recognised that genes and gene-products rarely, if ever, function in isolation within a biological system. Most commonly, they function as components within a cascade of networks. As a result, it is important to analyse microarray data in the context of signalling pathways and gene networks which it is hoped will lead to a higher level of understanding of the system. Ingenuity pathway analysis is an application that utilises the Ingenuity Pathways Knowledge Base (IPKB) to computationally analyse experimentally derived genomic or proteomic datasets to identify gene or protein networks of interest. IPKB is the world's largest curated database of biological networks created from millions of individually modelled relationships between proteins, genes, complexes, cells, tissues, drugs, and diseases. It can be used to concurrently analyse multiple datasets across different experimentation platforms and identify key functions and pathways that distinguish biological states.

To learn more about the biological function of genes changing in expression in response to infection, transcripts with a signal of greater than 50 in one or both of the samples were imported into Ingenuity Pathway Analysis software (Ingenuity Systems, Mountain View, CA). This filtering step was employed to exclude genes on or below an arbitrary level of detection in both groups and enable a focussed analysis of genes which have reliably detected by the array. The Ingenuity Pathway Analysis program uses the IPKB to relate gene products with each other, based on their interaction and function. Thus the knowledge base consists of associations extracted from literature, lists of canonical pathways and functions for individual genes. The Ingenuity Pathway Analysis

suite identifies dynamically generated biological networks, global canonical pathways and global functions. Highly regulated biological networks are dynamically identified using association rules among focus genes in a particular experiment. Each of these networks are ranked by a score based on negative log of *p*-value computed using a right-tailed Fisher's exact test that tests for the proportion of regulated genes in a particular network over competing networks. The score is the probability that a collection of genes equal to or greater than the number in a network could be achieved by chance alone. A score of 3 indicates that there is a 1/1000 chance that the focus genes are in a network due to random chance. Therefore, scores of 3 or higher have 99.9% confidence level of not being generated by random chance alone. This score was used as the cut-off for identifying gene networks.

There were four groups of networks found after the analysis but only one showed a high possibility that it was true with a score of 14 as illustrated in Figure 4.8. Network 1 has a group of 7 focus genes involving in cancer, cellular movement and reproductive system disease. Focus genes (shown in bold) are the genes designated as being differentially expressed in this study and which directly interact with other genes or gene products in the IPKB. Genes included in this network were insulin-like growth factor 2 (Igf2), vitronectin (Vtn), calcium/calmodulin-dependent protein kinase II alpha subunit (Camk2a), phosphatidylinositol 3-kinase (Pik3r1), cholinergic receptor (Chrna6), heat shock 70kD protein (Hspa1a) and creatine kinase (Ckm). Interactions between the focus genes and other genes in the network were not clearly related but the focus genes will be discussed further in section 4.3.2.

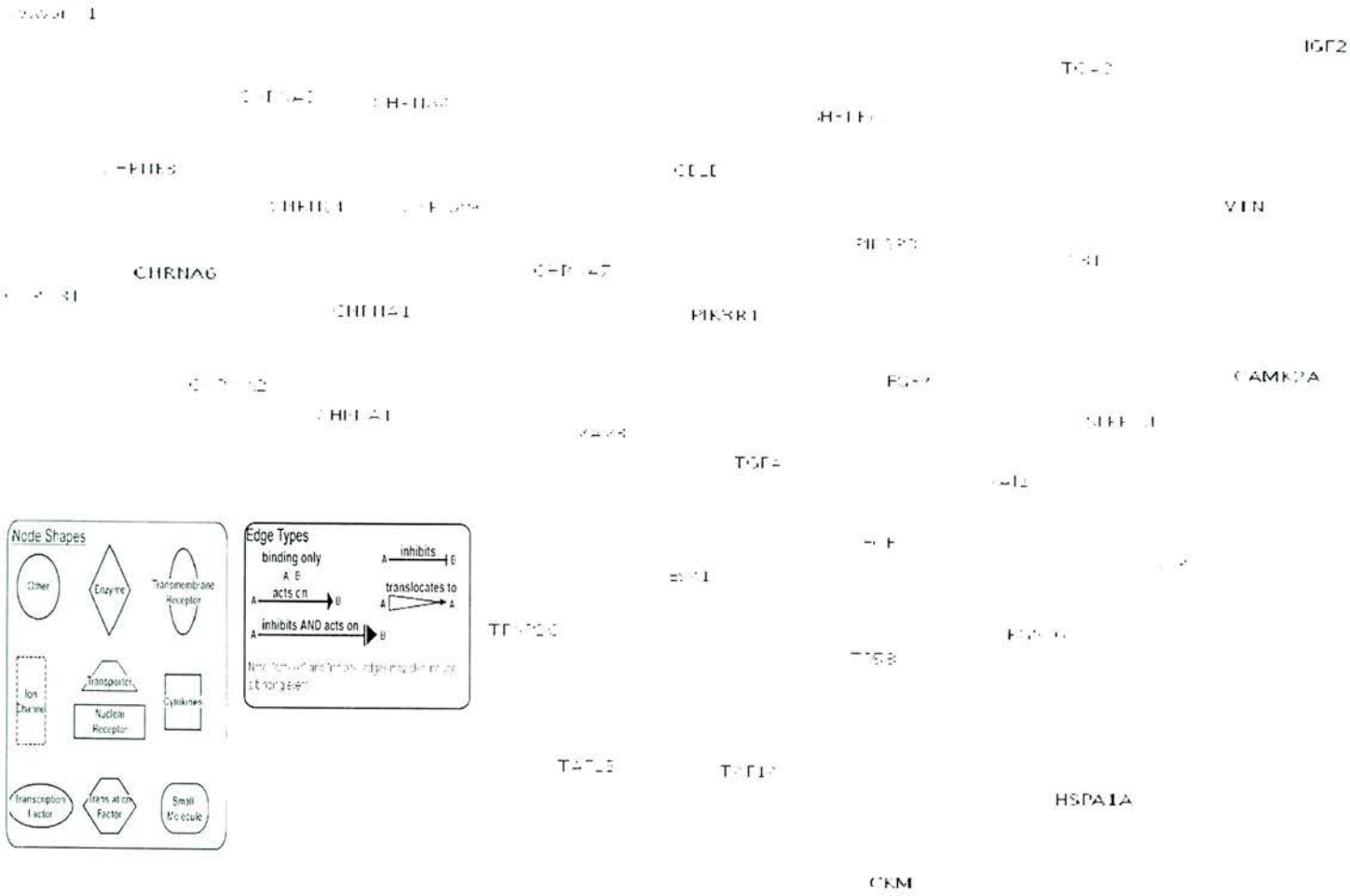

Figure 4.8 Network 1 from Ingenuity pathways analysis. There are 7 focus genes (in bold) in this network with top functions in cancer, cellular movement and reproductive system disease.

4.2.10. Validations of Selected Gene by Quantitative Real-Time RT-PCR

After candidate genes were identified in a microarray experiment, independent confirmation experiment using real time PCR or other techniques should be performed. Due to time constraints, only prostaglandin D_2 synthase (Ptgds) was validated here using quantitative real time PCR because of its striking difference in expression after infection and separate immunohistochemical studies within the group which had also showed that related proteins in the prostaglandin pathway, Cox-2 and PGE_2 were upregulated (Grant, D. and Dalziel, RG, personal communication). Beta actin was chosen as a housekeeping gene to correct for sample to sample variations in RT-PCR efficiency and errors in sample quantitation.

4.2.10.1. Construction of a Ptgds Clone

A cDNA clone containing Ptgds was constructed to be used as positive control in real-time PCR. Since Ptgds is localised in the central nervous system and male genital organs of various mammals (Urade and Hayaishi 2000), rat brain was used to extract RNA with a RNeasy Mini kit. RT-PCR was carried out as outlined in section 2.4.4. The amplified products were analysed on an agarose gel as shown in Figure 4.9. A clear distinct band of 136 bp was seen on the gel showing that the primers are specific and beta actin confirmed the integrity of the template and RT reaction.

After confirming the size was correct, the PCR product was purified and cloned into pGEM-T Easy vector as described in section 2.2.8. Four white colonies were

selected and grown overnight in 5 ml of culture containing ampicillin. Plasmids were extracted from the cultures and digested with *EcoR*I in order to check for positive recombinants. Figure 4.10 shows all four clones selected containing the insert with the right size after restriction digest with *EcoR*I. One of the positive clones was also sequenced and was used for further experiments.

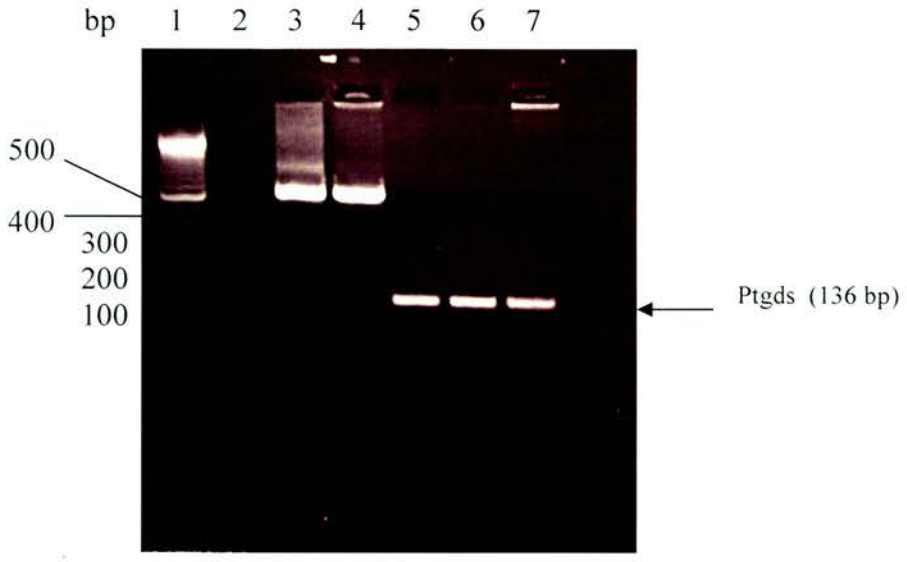

Figure 4.9 RT-PCR of Ptgds. Lane 1, 100 bp marker; 2, negative control without reverse transcriptase; 3, positive control for beta actin; 4, RT-PCR with beta actin primers; 5, 6, 7, RT-PCR with Ptgds primers.

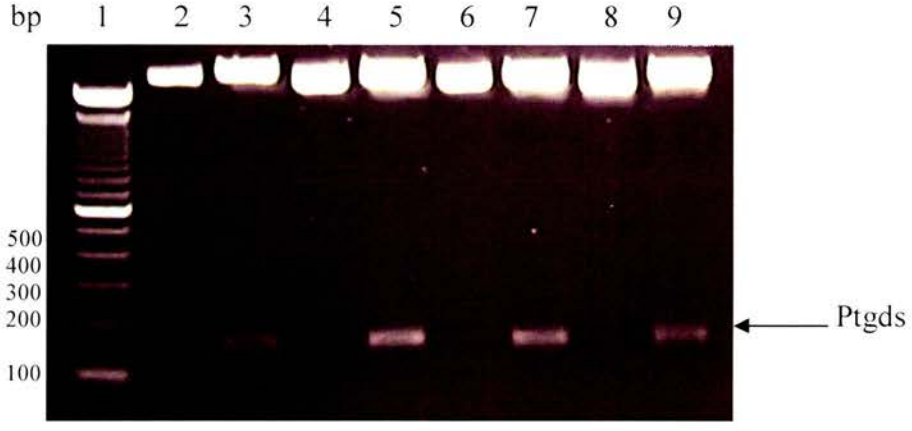

Figure 4.10 Restriction enzyme analysis to select for positive Ptgds clones. Plasmids were digested with *EcoRI* to check if they contained the Ptgds insert. Lane 1, 100 bp marker; lanes 2, 4, 6, 8, undigested plasmid; lanes 3, 5, 7, 9 digested plasmid.

4.2.10.2. Construction of Standard Curve

A standard curve for Ptgds was generated by preparing 10-fold serial dilutions of Ptgds plasmid from 10^4 to 1 copy (Figure 4.11A). The real-time PCR amplification of the Ptgds standard was linear over the range from 10^4 to 1 copy (r^2=0.9956).

Optimised PCR reaction mixtures used contained H_2O (11.7 µl), 10× PCR buffer without Mg (2 µl), Mg (3 mM; 2.4 µl), dNTP mix (10 mM each dNTP; 0.4 µl), forward primer (0.3 µM; 0.4 µl), reverse primer (0.3 µM; 0.4 µl), FastStart Taq (2 U, 0.2 µl), SYBR Green I (1:1000; 0.5 µl) and template DNA (2 µl) in a 20 µl reaction. A 40 cycles programme was used in a real-time PCR machine (Rotorgene 3000) with conditions as follow: 10 min at 95°C, 20 s at 94°C, 20 s at 57°C and 20 s at 72°C. Melting curve analysis was performed to ensure the production of a specific product. Figure 4.11B shows a specific product for Ptgds and further verification on an agarose gel shows the right size (Figure 4.11C).

A relative qRT-PCR quantitation was performed where Ptgds transcripts were normalised to cellular beta actin transcripts in the same cDNA preparation in control and infected DRG. Beta actin was shown in the microarray experiment to have a constant expression in the control and infected DRG. It was suggested that three or more housekeeping genes should be used for normalisation, as no one housekeeping gene is the best (Vandesompele et al. 2002). However, due to time limitation, the transcripts expression was only normalised against beta actin. Replicates of each sample were included and repeated with different priming methods, i.e. oligo dT and gene specific primers (GSP). The fold change difference from both methods was comparable,

indicating a high reproducibility of the results. Although the absolute qRT-PCR values were not identical to the microarray data due to the intrinsic differences between the two techniques, the results from qRT-PCR showed the same relative regulation of transcription and therefore corroborate the microarray data (Figure 4.12). The finding that prostaglandin D_2 synthase was upregulated in the infected DRG in microarray was confirmed by qRT-PCR with a fold change of 2.5-3.

A

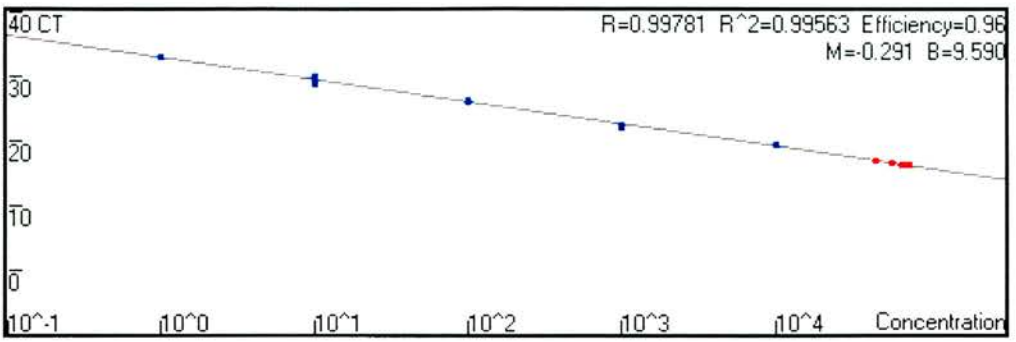

B

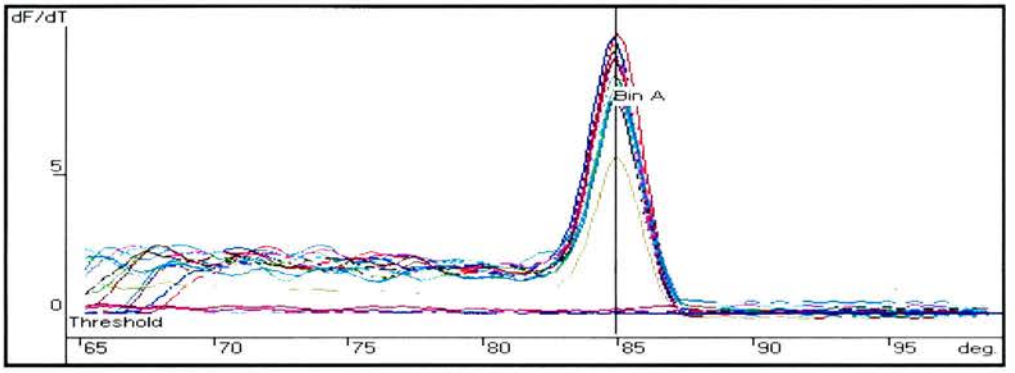

C

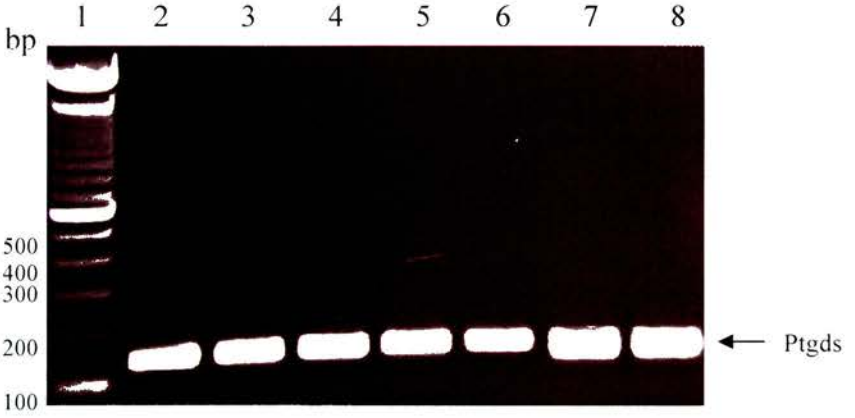

Figure 4.11 Real-time PCR assay set up for Prostaglandin D_2 synthase (Ptgds). (A) Standard curve for Ptgds. (B) Melting curve analysis shows a single distinct peak. (C) Post real-time PCR analysis of the Ptgds genes to confirm the correct size. Lane 1, 100 bp marker; 2-6, samples with Ptgds primers; lanes 7-8, positive controls for Ptgds. Beta actin was expressed in all samples tested.

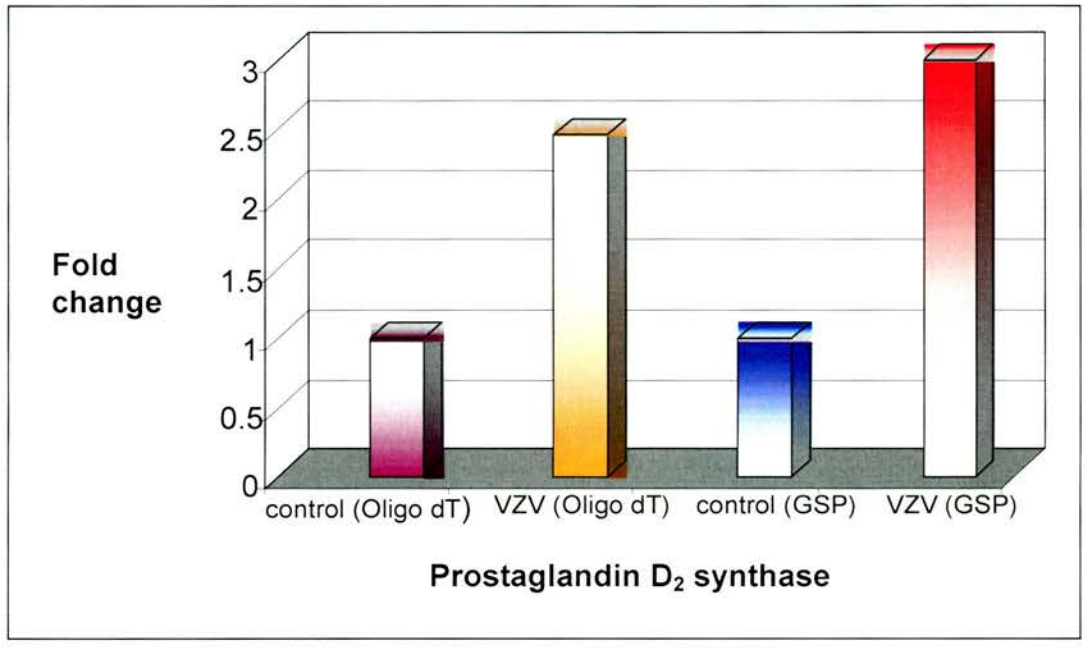

Figure 4.12 Validation of prostaglandin D_2 synthase (Ptgds) with real time PCR. Fold change differences of transcripts from two different priming methods (oligo dT and gene specific primer, GSP). Ptgds is shown to be upregulated in VZV infected DRG compare to control tissue corroborating to the result from microarray.

4.3. Discussion

This work represents a global analysis of the transcriptional responses of host cells following VZV-induced allodynia in a rat model. Affymetrix Rat Expression Set 230A oligonucleotide arrays were used to screen for changes in gene expression in DRG following development of allodynia in the VZV infected and mock-infected rats. The microarray data reflect changes in gene expression in the entire infected DRG, which is a heterogeneous tissue, composed of many different types of cells, such as neurons, glia, and connective tissue cells. It is important to note that since neurons are only ~10% of the ganglion cell population (Stevens 1989) and only a small fraction of cells in the DRG harbour latent VZV, even large differences in gene expression in individual infected cells might give rise to very small differences in expression on a whole ganglion basis.

4.3.1. Changes in Host Gene Expression in Infected DRG

Of the changes observed, more genes were down regulated than up regulated in the different functional groups. Many genes encoding ion channels and receptors, cell-cell communication and signalling pathways and proteins related to neurotransmission showed decreased, rather than increased expression after infection. This may be indicative of overall suppression of gene expression in injured DRG neurons. However, genes associated with inflammation and immune markers were shown to be up regulated.

The alterations in expression of neuron-specific genes observed in this study could represent a direct effect of VZV on cellular gene expression in the DRG. Alternatively, the virus may act indirectly on cellular gene expression e.g., by inducing neuronal injury which would then alter host gene expression. The expression of several genes with known roles in neurotransmission and signalling is altered in the infected DRG, some of this genes including G protein-coupled receptor 56 and potassium voltage-gated channel, affect neuronal excitability in an interconnected manner (Massengill et al. 1997), (Davis et al. 2002), (Kramer et al. 2003). This may suggest that presence of VZV in the DRG could lead to changes in neuronal physiology and could alter sensation consistent with the altered behavioural changes in the rat model after VZV infection.

A number of ion channels whose expression was altered in the infected DRG were also identified. These include the down regulation of potassium channel (Kv9.3) and voltage-gated sodium channel (Scn11a) consistent with findings from other array studies of neuropathic pain models (Wang et al. 2002), (Valder et al. 2003). Electrophysiological recordings have previously demonstrated that C-fibers and A fibers develop abnormal excitability following peripheral nerve injury, a phenomenon which implicates changes in gene and protein expression of ion channels. Post-injury changes in the distribution and activity of sodium channels within the DRG and the site of injury has the ability to regulate a state of hyperexcitability (Cummins et al. 2000).

Comparison of the global lists of regulated genes between this study and other reports are complicated by the different experimental conditions, biological system and variable criteria used to identify regulated genes in the different studies. However, there were similarities in gene regulation identified in this study to other separate array studies

looking at the effects of peripheral nerve injury on DRG gene expression in different neuropathic pain models (Wang et al. 2002), (Costigan et al. 2002), (Valder et al. 2003). Wang et al., (2002) reported on regulation of immediate early genes, ion channels and signalling molecules that contributed to the excitability of neurones and genes involved in neuroinflammation in a spinal nerve ligation model of neuropathic pain. A similar trend of gene regulation was also found in this study. Costigan and workers found reorganisation of cell structural components, activation of genes expressed by immune and inflammatory cells and downregulation of genes involved in neurotransmission in a model of sciatic nerve transection. Similar regulation of injury-responsive genes identified in injured DRG were reported by Valder et al., (2003) and they also demonstrated that injury-induced changes occurred not only in neurons but also in non-neuronal cells.

There are several reports on the global analysis of the transcriptional response of host cells to VZV infection (Cohrs et al. 2003b), (Jones and Arvin 2003), (Jones and Arvin 2005), (Kennedy et al. 2005). Studies by Cohrs, et al., (2003b) and Kennedy, et al., (2005) were investigating the gene expression profile of VZV lytic infection in tissue culture. Jeremy and Arvin (2003) reported a study on transcriptional changes in cellular genes after VZV infection of human T cells and fibroblasts *in vitro* and human skin xenografts in SCIDhu mice *in vivo*. They found no significant differences in gene regulation between pOka (VZV parental Oka strain) and vOka (VZV vaccine strain) in any of the cell types. However, significant changes in cellular gene regulation were observed between the three differentiated human cell types, suggesting specific differences in the biological consequences of VZV infection related to the target cell.

The classification of genes that were affected included those involved in immune and stress responses, cell adhesion, cell structure, signal transduction, cell cycle, apoptosis and other cell functions. Interferon response was found markedly induced in T cells. More recently, Jones and Arvin (2005) had investigated on the viral and cellular gene transcription in fibroblasts infected with VZV small plaque mutants using 42K human cDNA microarrays. They found that infection of fibroblasts with wild type or small plaque VZV mutants was associated with down regulation of NF-κB and interferon responsive genes, down regulation of TGF-β responsive genes accompanied by reduced amounts of fibrotic or wound healing response genes, activation of cellular proliferation genes, alteration of neuronal growth markers and cellular genes encoding proteins important in protein and vesicle trafficking. In the study reported in this thesis, not many interferon responsive genes were found significantly regulated either because the change is small or gene expression occurs in a small number of cells, which are below the level of sensitivity of this assay. Thrombospondin 4, which is a major activator of LTGF-β (latent form of TGF-β), was found to be down regulated in this study (Table 4.1). Transforming growth factor-beta (TGF-β) signalling pathway controls multiple cell processes including fibrotic or wound healing responses and it must be activated from its latent form (Jones and Arvin 2005). Down regulation of thrombospondin 4 reflected that the signalling through this pathway might be inhibited. Since TGF-β inhibits cell cycle progression, blocking this inhibition should enhance viral replication. Limiting the wound healing response could enhance the spread of the virus by inhibiting the repair of damaged cells.

4.3.2. Significantly Regulated Genes and their Functions

The microarray results presented in this present study do not include an exhaustive list of differentially expressed genes affected by VZV-induced allodynia in the rat model. This is mainly due to the different biological system used, i.e. most of the studies reported had been carried out in a tissue culture system where 100% infection could be assured while this study involved a complex tissue with mixed heterogeneity. Seven genes were found to be significantly regulated in this study.

Phosphoinositide 3-Kinases (PI3Ks) are proteins coupled to a variety of cell surface receptors and play a key role in signal transduction cascade regulating fundamental cellular functions such as transcription, proliferation, and survival (Maurel and Salzer 2000). PI3Ks also are important in disease processes such as inflammation and cancer.

Transthyretin, a plasma protein that functions as a transporter of thyroxine and retinol, mainly synthesised by the liver and choroid plexus of the brain. Altered transthyretin level in the cerebrospinal fluid has been linked to neuronal dysfunction such as Alzheimer's disease (Nunes et al. 2005).

S100 calcium-binding protein A9 or calgranulin B is a small calcium-binding protein that is highly expressed in neutrophil and monocyte cytosol and is found at high levels in the extracellular milieu during inflammatory conditions. It has been reported as a potent inducer of neutrophils and involved in neutrophil migration to inflammatory sites (Ryckman et al. 2003).

Heat shock proteins (HSP) are essential for the repair or removal of defective proteins as a result of various mechanical or chemical stresses, including oxidative free radicals and toxic metals, and plays major role during normal growth and differentiation of mammalian cells (Linquist 1986). HSP is also associated with the immune response, i.e. it helps the endogenous antigen process that guides the antigenic peptides to immunorecognition (Suto and Srivastava 1995).

Vitronectin, also called serum spreading factor or complement S-protein, is a 75-kD glycoprotein in plasma and tissue. A multifunctional protein, it promotes attachment and spreading of animal cells *in vitro*, inhibits cytolysis by the complement C5b-9 complex, and modulates antithrombin III-thrombin action in blood coagulation (Fink et al. 1992).

Nicotinic acetylcholine receptors are a family of ligand-gated, pentameric ion channels. The main function of this receptor family is to transmit signals for the neurotransmitter acetylcholine at neuromuscular junctions and in the central and peripheral nervous systems (Marubio and Changeux 2000).

Due to time constraint, only prostaglandin D_2 synthase was chosen to be validated and this gene will be discussed in detail in section 4.3.4.

4.3.3. Validation of Microarray Results

Genes identified by a single microarray experiment as having a more than 2-fold expression difference cannot be generally accepted as true without a repetition of the experiment or by validation and genes identified with differences less than 2-fold should not be eliminated as false positives without repetition or powerful validation (Rajeevan et al. 2001).

Validation of expression differences is accomplished with alternate methods such as Northern blot hybridisation or RNase protection assay. However, these assays are time-consuming, labour intensive and require large amounts of RNA (>5 μg total RNA). Conventional RT-PCR can be done with smaller amounts of RNA (20-40 ng) but quantification is difficult and relies on endpoint analysis of the PCR product. These limitations can be largely overcome by incorporating high throughput real-time PCR into the study. qRT-PCR is well suited to validate and confirm microarray results because it is rapid, fully quantitative and require less than 1000 fold RNA than the microarray experiment. For verification a relative quantification strategy was applied, which is based on the expression levels of a target gene versus a reference gene and is adequate for investigation of physiological changes in gene expression levels. Housekeeping genes are present in all nucleated cell types since they are necessary for basic cell survival. Mostly mRNA synthesis of these genes is considered to be stable in various tissues. Here, prostaglandin D_2 synthase (Ptgds) was validated and found to be upregulated, corroborating to the microarray analysis.

4.3.4. Prostaglandin D_2 Synthase

Prostaglandins (PGs) are the major arachidonic acid metabolite released from phospholipid membranes by phospholipase A_2. Different molecular species are produced by different synthetases after conversion to prostaglandin H_2 by two isoforms of the cyclooxygenase (Cox) enzyme, namely Cox-1 and Cox-2 (Larsen and Henson 1983), (Goodwin 1989). The actions of prostaglandin D_2, prostaglandin E_2, prostaglandin $F_{2\alpha}$, prostaglandin I_2 and thromboxane A_2 are mediated by stimulation of prostanoid DP, EP_{1-4}, FP, IP and TP receptors, respectively (Coleman et al. 1994). PGD_2 is formed from the product of Cox activity, PGH_2, by two distinct PGD synthases, the lipocalin-type synthase (L-Ptgds) and the glutathione-dependent hematopoietic PGD synthase (H-Ptgds). Figure 4.13 shows the prostaglandin metabolism pathway and the genes that have been either found to be regulated in microarray or immunohistochemisty.

PGD_2 is the most abundant PG in brain and regulates sleep, temperature and nociception (Urade and Hayaishi 2000). It signals through two distinct G protein-coupled receptors, DP1 and DP2 that have opposing effects on cyclic AMP (cAMP) production. Activation of DP1 receptor, which is positively coupled to cAMP, resulted in protection of neurones whereas activation of the DP2 receptor, which is negatively coupled to cAMP induced toxicity (Sawyer et al. 2002). Recent work has shown that the DP1 receptor of PGD_2 mediates neuronal protection in *in vitro* neuronal cultures (Liang et al. 2005). The unexpected finding that PGD_2 confers neuroprotection is similar in effect with PGE_2 EP2 and EP3 receptors. The dependence on cAMP-mediated signaling for this neuroprotective effect suggests that other PG receptors that are similarly couple

to cAMP may also protect neurones. These data could support an emerging new hypothesis that prostaglandin may have a neuroprotective role and may present a novel potential new therapeutic strategies that target specific PG receptors pathway.

Previous work in the lab has shown that Cox–2 and PGE_2 was upregulated in the infected DRG by immunohistochemistry. These observations coupled with the upregulation of Ptgds in the microarray experiment and real-time PCR, may suggest that the PG synthesis pathway is activated in the VZV-induced allodynic rats. There is a likelihood that Ptgds might play a similar neuroprotective role in the neurons, preventing damage incurred by VZV in the rat model. Cox-2 inhibitor such as Celebrex has been tested in the rat model and showed to alleviate allodynia (Dalziel, R.G., personal communication). Further studies will be interesting to look at the involvement of prostaglandins in modulation of pain and its function in conferring protection.

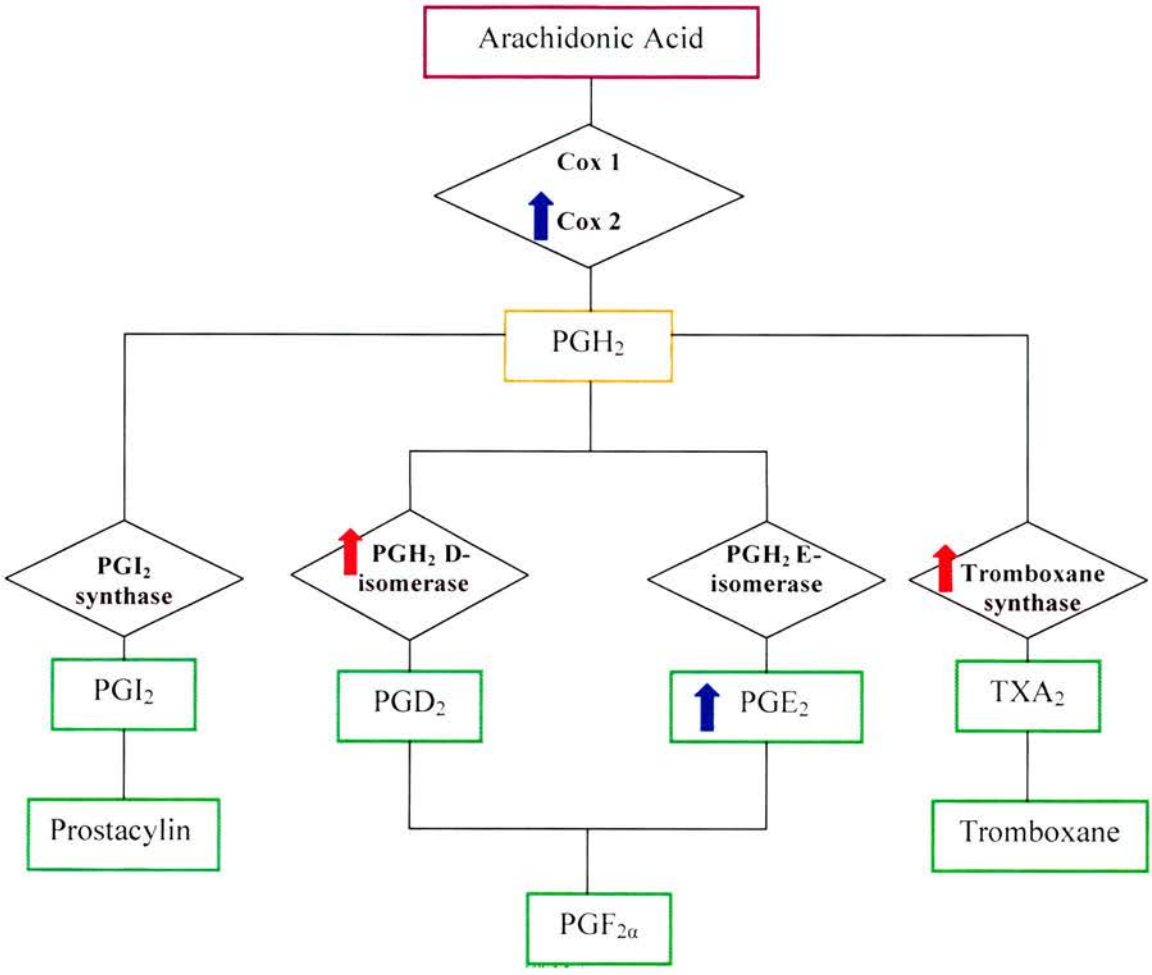

Figure 4.13 A schematic diagram of the prostaglandin metabolism pathway. Arachidonic acid, the most abundant precursor of prostaglandins in mammals, is transformed into PGH_2 by the action of Cox-1 and Cox-2. Further enzymatic conversion of PGH_2 by prostacylin synthase, various isomerases and thromboxane synthase leads to the prostanoids, i.e. the functionally important prostaglandins and thromboxanes. Red arrow shows genes found upregulated in microarray and blue arrow shows genes and products upregulated using immunohistochemistry.

4.3.5. Limitations of Microarray

The great value of microarrays lies in the large number of transcripts that can be assayed simultaneously. However, microarrays can have several limitations. Microarrays require more RNA than quantitative real-time PCR (qRT-PCR). Errors in identification of regulated transcripts (false positive or false negative) depend on the threshold to identify a transcript as regulated as well as on the complexity of the tissue source.

One of the limitations at the time when the microarray data analysis is carried out is that our knowledge of the rat genome is limited and the functions of the identified gene are incomplete. Although the RAE 230A GeneChip contains 15866 probe sets, it has an abundance of expressed sequence tags (EST). Not all of these probe sets can be definitively mapped to a physiologic pathway and therefore their assessment in MAS is limited. Given the rapidity with which genomics is expanding, it is only a matter of time before more complete data are available. However, this limited knowledge impeded a true representation of the physiologic pathways changed in the infected neurones.

Another problem with oligonucleotide arrays is sensitivity. Some group of transcripts that are expressed in the DRG might fall below the microarray detection threshold. Lack of sensitivity may result from technical issues such as poor probe performance or low copy number transcripts. Tissue heterogeneity and neuronal subpopulation restricted gene expression, may lower the concentration of a transcript in the total RNA sample to below detection threshold (Mirnics et al. 2001). Finally, the cost of the effort involved in microarray assays introduces practical constraints in the

number of RNA samples that can be analysed, thereby reducing the number of replicate experiments and the statistical power of the results (Wurmbach et al. 2002).

4.4. Conclusion

The microarray results presented here do not include an exhaustive list of genes affected by VZV infection, however genes associated with inflammation, immune and cytokine tended to be up-regulated, whereas genes involved in membrane excitability (ion channels) or neurotransmission (neurotransmitters and vesicle trafficking genes) tended to be down-regulated. The facts that infection might not be 100% following VZV inoculation into the rats and that DRG is a complex tissue represented in a mixed population of cells has reduced the number of significant genes being detected. As there are no array replicates in this experiment, all array values should only be considered as indicative of a real biologically relevant alteration in transcript level unless further validation has been done. Elucidating the specific role of genes regulated in sensory neurons after VZV infection will provide insight into many major biological issues including cell survival, growth, intercellular communication and the factors contribute to sensory abnormalities as in PHN. Microarray technology provides a powerful tool for beginning this analysis in a high throughput mode by revealing the extent of change in neuronal gene expression. In effect, this pilot study has proved that the Affymetrix array could be used to study the differential expression of genes in the pathogenesis of VZV-induced allodynia.

CHAPTER FIVE

RESULTS AND DISCUSSION

5.1. Introduction

After 15 years of clinical trials, a live attenuated VZV vaccine (Oka-Merck; VARIVAX) was licensed in the United States in 1995 (Krause and Klinman, 1995). The live attenuated varicella vaccine, the Oka strain (vOka) was originally a wild-type VZV isolate referred to as the parent Oka (pOka). POka was isolated from a child with varicella and passaged 6 times in human foreskin fibroblasts and stored at –70°C (Takahashi et al. 1974). The varicella vaccine was generated by passaging pOka 11 times in human embryonic lung cells, 12 times in guinea pig embryo fibroblasts, once in WI-38 cells and 9 times in MRC-5 cells (Takahashi et al. 1974). This procedure resulted in attenuation when susceptible children were inoculated with vOka (Johnson et al. 1997). While most healthy children and adults who are given the varicella vaccine develop immunity without experiencing any signs of disease, the virologic basis for this clinical attenuation of vOka however is not known.

The virulence of vOka in human skin xenografts in SCID mouse skin has been shown to be diminished as measured by a reduced yield of infectious virus, decreased viral protein synthesis, failure to invade the dermis and a slower destruction of epidermal cells compared to pOka (Moffat et al. 1998). This provided the first evidence of virologic basis of the clinical attenuation of vOka. Sequencing of the pOka and vOka genomes indicates variations in many of the ORFs, some of which are predicted to alter viral proteins, precluding a simple genetic explanation for the attenuation of vOka (Gomi et al. 2001), (Gomi et al. 2002).

In order to investigate the role in PHN of the latently expressed VZV genes in the DRG, it will be necessary to construct viruses that lack these genes and analyse their

phenotype in the rat model. Due to the difficulties in obtaining VZV virion DNA for transfection and in obtaining cell-free virus to plaque purify VZV mutants from wild-type virus, one way of generate recombinant VZV genomes has been using cosmid DNA (Cohen and Seidel 1994). The cosmid system based on the Oka strains has proved useful for studying the role of the viral gene in *in vitro* experiments. The aims of this experiment were:

- To investigate if there was any changes in the behavioural response in the rat model caused by pOka, vOka and VZV Ellen strains. VZV Ellen is a standard laboratory strain used to infect rats during the course of this work.
- To investigate the possibility of using the Oka strains to generate mutant viruses using cosmid DNAs. If the Oka viruses cause allodynia in the rats then mutant viruses could be constructed and tested to see if there is any effect of the deleted gene(s) in the rat model.

An outline of this experiment is shown in Figure 5.1.

5.1.1. *In vivo* Experiment

VZV Ellen, pOka and vOka were propagated in CV-1 cells as described in section 2.5.4. Cells and virus-infected cells were checked for their growth on a regular basis. Viruses were harvested when cells showed 80% cytopathic effect (CPE). Each T175 flask of virus-infected cells were harvested and resuspended in 150 µl of medium. Six animals were used for each group of virus strain.

Pre-testing and randomisation of animals was as described in section 2.6.4. Each animal was injected subcutaneously into the left hind paw with 50 µl of the suspension containing approximately 4×10^6 VZV infected cells or control non-

infected CV-1 cells. Animals were then tested at days 3, 7 and 10 post infection for the development of allodynia (section 2.6.4). Lumbar DRGs L1 to L6 ipsilateral and contralateral to the side of injection were obtained for PCR analysis.

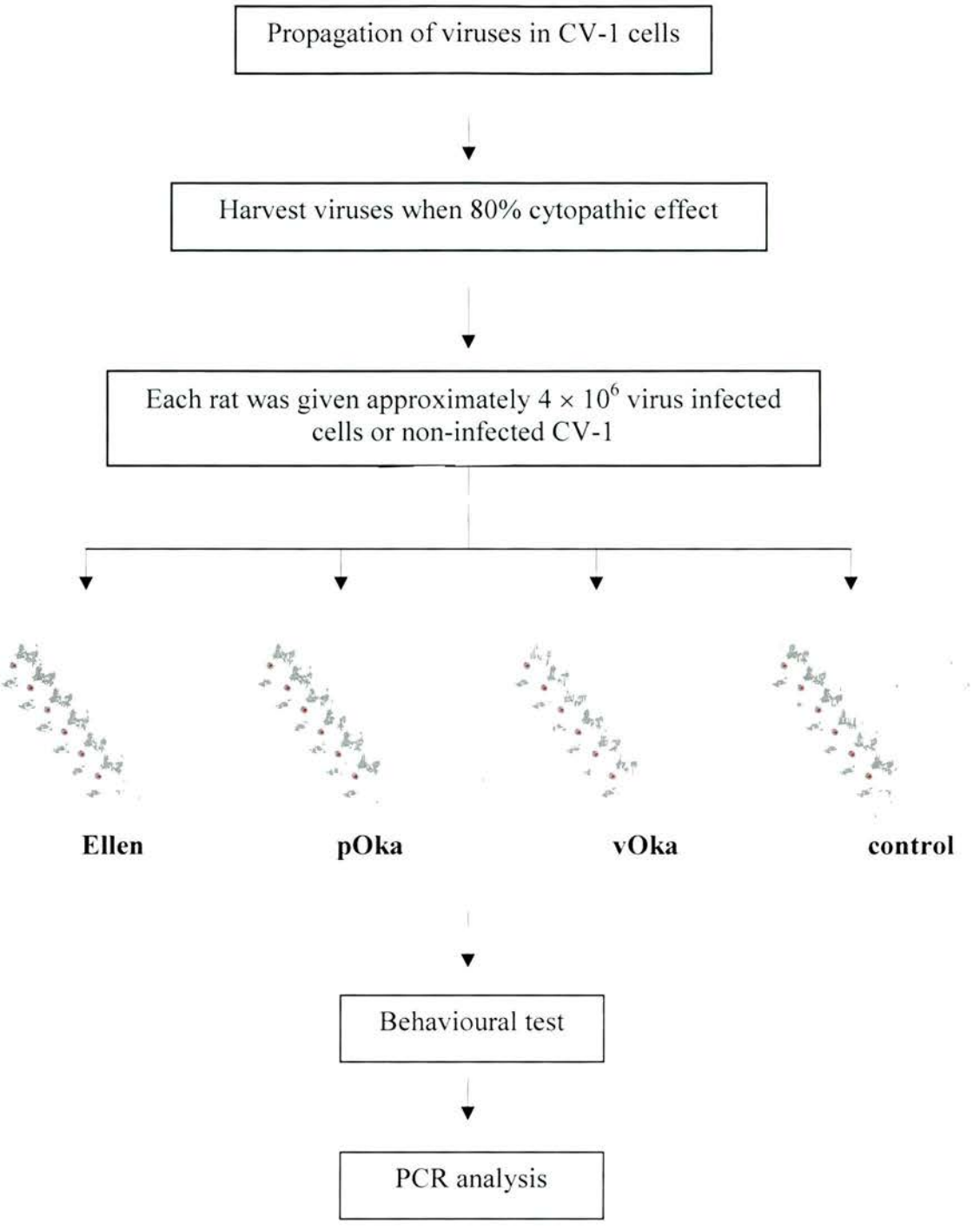

Figure 5.1 Flow chart showing the experiment carried out to investigate the effect of different strains of VZV in the rat model. Three groups of six rats were injected with VZV Ellen, pOka and vOka, respectively. Animals were tested for allodynia at specific days post infection. At the end of the study, tissues from these animals were collected for PCR analysis.

5.2. Results

5.2.1 Altered Behavioural Response in the Rats

Figure 5.2 shows the comparison of the development of allodynia in rats following infection with different VZV strains. The graphs show a summary of two independent experiments, which were carried out as described in section 5.1.1. The results of these experiments were represented as percentage of positive and negative responses to allodynia. A positive response is defined as paw withdrawal threshold (PWT) equal to or less than 15 g and a negative response is defined as PWT of greater than 15 g. 15 g was chosen as a cut-off point based on previous observations (Dalziel et al. 2004).

From these experiments, 67% of rats infected with VZV Ellen were found to develop allodynia at days 3, 7 and 10 post infection. However, in the pOka and vOka groups, the figure drops to 50% and 17%, respectively. The difference in the percentage of rats developing allodynia suggests that pOka and vOka do not induce allodynia as readily as VZV Ellen. This may indicate that there is a decrease in 'pathogenicity' of pOka and vOka in the rat model. The failure of vOka and pOka to reproducibly produce long term allodynia in the rats may be due to the genetic differences between these strains and VZV Ellen or could reflect a lack of spread to the DRG.

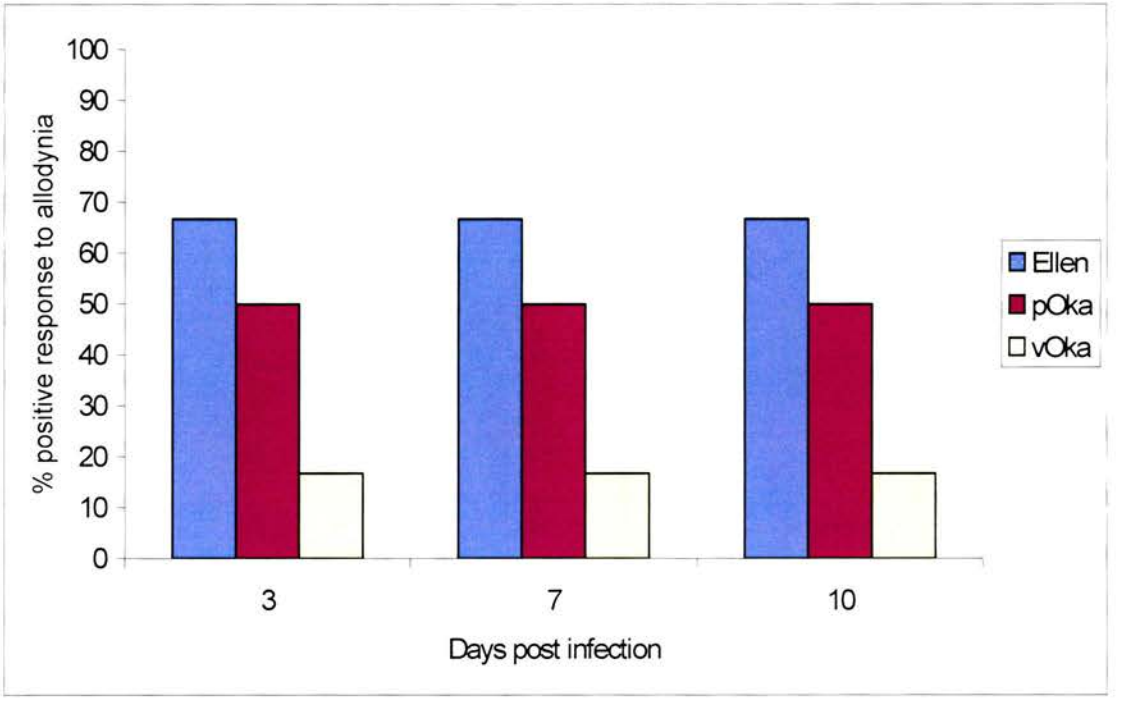

Figure 5.2 Graph bars show the overall sensitivity of the animals when infected with different strains of VZV. Three groups of six rats each were injected with either VZV Ellen, pOka or vOka. The animals were tested at 3, 7 and 10 days post infection for development of allodynia. Shown are animals with a positive response (PWT =< 15 g).

5.2.2 PCR analysis

In order to investigate if the changes in the behavioural responses in the rats infected with the different strains of VZV were related to the presence of VZV genome, PCR analysis were carried out on the lumbar DRG of these animals. Only tissues from one study were analysed here. The design and development of the nested-PCR assay using VZV63 primers were as described as in section 3.2.1. Table 5.1 shows that VZV DNA could be detected in rats developing allodynia (with a PWT =< 15 g) after infected with Ellen. No viral DNA was detected in pOka infected rats, which did not develop allodynia. A single rat in the vOka group developed allodynia and this animal was positive for the presence of VZV DNA in the DRG. The results here show that when animals did not develop allodynia, there is no viral genome being detected in the DRG. Presence of VZV DNA in vOka infected rats suggested that the virus was able to reach the DRG.

Table 5.1 Detection by PCR of VZV DNA in the rat DRG infected with different VZV strains. PCR analysis was carried out with primers specific for gene 63. PWT = paw withdrawal threshold; + = positive; - = negative.

Animal	Virus strain	Ipsilateral PWT (g)	VZV Gene 63
932	Ellen	15	+
1781	Ellen	60	-
1277	Ellen	11.7	+
1740	vOka	60	-
1742	vOka	11.7	+
1703	pOka	60	-
1705	pOka	60	-

5.3 Discussion

This study has provided some early information on the ability of the different strains of VZV to cause allodynia in the rat model. The results show that the standard laboratory strain, VZV Ellen is more capable of inducing allodynia in rats than are pOka and vOka. The Oka viruses were less 'pathogenic' in this model compared to the VZV Ellen strain and the duration of allodynia in vOka infected rats was less than in either pOka or Ellen infected rats during the 10 days of the study.

5.3.1 Effects of Different Strains of VZV in the Altered Behavioural Changes in the Rat Model

Both VZV Oka viruses have been shown in this study to cause the development of allodynia in the rat model, however, the percentage of vOka rats developing allodynia were more than two fold less than the number of pOka rats. This might be due to the genetic variation in the genomes of these viruses rather than their ability to replicate *in vitro* since it has been shown that pOka and vOka have similar growth effects in tissue culture (Moffat et al. 1998), (Zerboni et al. 2005). Comparison of the complete DNA sequences of vOka and pOka reveals that as many as 15 base substitutions, representing 8 amino acid differences were found in the gene 62 region alone (Gomi et al. 2002). An infectious centre assay of a plaque-purified clone (S7-01) of vOka containing 8 amino acid substitutions in ORF62 showed smaller plaque formation and less efficient virus spreading activity than did pOka in human embryonic lung cells (Gomi et al. 2002). Another clone (S-13) with only 5 substitutions in ORF62 spread slightly faster than S7-01 but not as effectively as pOka. Transient luciferase assays in 293 cells showed that transactivational activities

of the IE62 products of S7-01 and S7-13 were lower than that of pOka. Based on these results, it appears that amino acid substitutions in ORF62 are implicated in virus growth and spread from infected to uninfected cells. The IE62 product of vOka, which contained all eight amino acid substitutions, had less activity than the parental IE62 in activating all three kinetic classes of VZV promoters in CV-1 cells (Gomi et al. 2001). This data might also suggest that the substitutions in IE62, which is a major transactivator, play an important role in the differences in the replication and the attenuation of VZV.

VZV Ellen had been passaged more than 100 times since its isolation in 1964 (Straus et al. 1981). Prolonged passage in tissue culture cells appear to induce changes that have a significant impact on VZV virulence for human epidermal and dermal cells *in vivo*, since only the low passage clinical isolates like pOka were shown to be fully virulent in skin implants (Moffat et al. 1998). Both Ellen and vOka have been found to replicate to lower titres in SCIDhu mice with epithelial implants (Moffat et al. 1998). In contrast, the results shown in the present study suggested that VZV Ellen caused allodynia more readily than pOka or vOka in the rats. This might be caused by the lab adapted strain, VZV Ellen replicate more efficiently in tissue culture and produce more infectious virus. However, in this experiment, the viral titres were not determined for each virus before inoculation, therefore further work has to be done to investigate this possibility.

Recently, the attenuation of vOka in skin xenografts in the SCIDhu mouse model was investigated by using chimeric pOka and vOka recombinant viruses generated from cosmid DNAs (Zerboni et al. 2005). These workers have shown that vOka attenuation is multi-factorial and can be produced by genes from different regions of

the vOka genome. Others studies using recombinants made from cosmids in the SCIDhu model have demonstrated that VZV infectivity in skin can be diminished even by a single amino acid substitution, such as disrupting ORF47 kinase function in the mutant or altering C-terminal residues in gE (Besser et al. 2003), (Moffat et al. 2004). These findings indicate that VZV attenuation in skin can be achieved by very restricted alterations in the genome sequence.

The PCR analyses of the DRG infected with the different VZV strains in this study shows that viral DNA could be detected in the infected DRG in VZV Ellen infected rats which developed allodynia. Presence of vOka genome in the DRG could also be detected, indicating that this virus has reached the DRG. However it is difficult to draw any conclusion here due to the limited availability of rats developing allodynia in these groups. Therefore, in this study, it is speculated that besides the genetic variations, the less efficient viral spreading to the DRG might have caused the Oka strains to be less pathogenic in the development of allodynia compare to Ellen strain in the rat model.

5.4 Conclusion

VZV Ellen induced allodynia more readily than the Oka vaccine strain or its parental virus. The reasons for these observations were not clearly understood but the difference in the pathogenicity of vOka and pOka might be due to the multiple nucleotide differences between them that are predicted to change amino acid residues. These changes have been identified that could affect all three putative kinetic classes of VZV proteins, including immediate early regulatory proteins, early proteins and the late glycoproteins. The lack of viral spread to the DRG might be

another possible explanation for these viruses to be less capable of inducing allodynia in the rats. These experiments shows that the approach of using the Oka viruses to generate mutant viruses in a cosmid system which, could then be tested on the rat model might not be feasible if the Oka viruses did not induce allodynia in the rats readily.

Overall Discussion

The mechanism that leads to post-herpetic neuralgia (PHN) is not clearly understood. Until recently, research has been hampered by the lack of suitable animal models due to the species-specific nature of the virus. The introduction of a rat model of VZV persistent infection (Sadzot-Delvaux et al. 1990) with striking changes in behavioural responses (Fleetwood-Walker et al. 1999) which mimic the human situation has allowed the use of this model to study the mechanisms underlying PHN. The rat model is characterised by a limited expression of immediate early and early genes while late genes remain silent, mimicking the situation seen in human latency in terms of restricted viral gene expression (Grinfeld et al. 2004).

This study was intended to determine if the changes in the behavioural responses in the rats correlated with gene expression in the DRG. In agreement with previous findings, rats inoculated subcutaneously with VZV in the footpad harbour VZV DNA in their DRG (Sadzot-Delvaux et al. 1995), (Kennedy et al. 2001), (Grinfeld et al. 2004). However, it is difficult to draw any correlation between findings of viral DNA in specific DRG with the development of allodynia in the rats since there is no clear pattern of the distribution of VZV DNA in the lumbar DRG. VZV DNA could be found in the DRG of most rats developing allodynia. This suggests that the behavioural changes in the infected rats may be due to the presence of VZV in the DRG but the extent of gene expression could not be determined due to the low level of viral transcripts. Replicating virus has not been demonstrated in this model and so the observed allodynia is unlikely to be associated with ongoing virus replication as would be seen in the acute phase of herpes zoster (Sadzot-Delvaux et al. 1990), (Sadzot-Delvaux et al. 1995), (Fleetwood-Walker et al. 1999). This hypothesis is supported by the report that treatment of VZV-

infected rats with valaciclovir, an antiviral drug, does not block the development of allodynia (Dalziel et al. 2004), suggesting that continued lytic virus replication is not required for induction of allodynia by VZV.

When the viral load of the DRG was quantified, there was difference in the viral burden in each ganglion. This could suggest a variable susceptibility of diverse neuronal populations to viral infection and difference in the efficiency of viral spread in the DRG. However, further studies would need to be conducted to address this hypothesis. A study carried out to quantitate HSV viral load in human cranial nerve ganglia has found no significant correlation among ganglia from the same individual (Vrabec and Alford 2004). Their results supported the hypothesis that neuronal subpopulations have variable susceptibility to HSV infection.

Following peripheral nerve injury, it has been reported that phenotypic changes occur in peptide expression in DRG that may contribute to sensory sensitisation and chronic pain (Hokfelt et al. 1994), (Cummins et al. 2000), (Woolf and Salter 2000). Dramatic changes in gene expression of ion channels and signaling molecules that directly affect the excitability of neurons in the DRG and the spinal cord have been reported (Wang et al. 2002). Upregulation of neuropeptides such as NPY and galanin in the DRG of VZV infected rats has also been reported (Garry et al. 2005). Although the underlying pathophysiological mechanisms may be similar to other forms of neuropathic pain, it is unclear how latent VZV infection interacts with the nervous system to induce these changes. The question of whether VZV-induced allodynia affects neuronal gene expression was addressed by using microarray transcript profiling of host gene expression in ganglia from latently infected versus mock infected rat DRG.

Results from the microarray analyses have shown that many genes encoding ion channels and receptors, cell-cell communication and signalling pathways and proteins related to neurotransmission were down regulated after VZV infection, indicating an overall suppression of gene expression in injured DRG neurons. Genes associated with inflammation and immune markers were shown to be up regulated. It is expected that the markers for inflammation are up regulated in the DRG, since DRG axons are the primary infection site where cells of monocyte origin can be recruited. Among the significantly regulated genes, prostaglandin D_2 synthase was found to be highly up regulated and this observation was validated by real time PCR. A new hypothesis has suggested a neuroprotective role of prostaglandins in the central nervous system (Liang et al. 2005).

The patterns of changes in gene expression reported in this study are in consistent with the literature. Some genes that have been found to be regulated in the DRG in neuropathic pain models are not among those reported here because either the regulation is small or gene expression changes were not detected. Analysis of gene expression in infected DRG using microarray technology can be complicated greatly by cellular heterogeneity. Latent VZV genomes reside in the nuclei of neuron cell bodies in the DRG. However, DRG comprise not only clusters of sensory neurons and their nerve fibers but also nerve fibers derived from cells located outside the DRG that pass through or terminate within the ganglion and small glial cells called satellite cells that completely envelop the neuronal cell bodies (Lazarov 2002). Also contained in DRG are Schwann cells, endothelial cells of the microvasculature, blood cells and motor neurons. The level of change of any transcript in the RNA samples from a complex tissue is likely to be

much lower than that observed in a homogenous tissue. Any particular gene of interest may only be expressed in a small subset of cells, leading to a signal for that gene on the array that is difficult to measure reliability. These limitations are referred to as 'dilution effects' (Wurmbach et al. 2002).

One way to dissect the tissue heterogeneity problem might be to use a simple biological system, such as a cell line or purified cell populations. Sampling from simple systems is more likely to represent the expression level for the particular cell i.e. infected neurons in our study as compare to a complex system where there is a diversity of cellular substructures and mixed cellularity. Subdissection techniques, such as, laser capture microdissection of individual cells or tissue substructures are being increasingly adopted to provide specificity to sampling from complex systems. These approaches have enormous potential to improve resolution in microarray studies but generally only limited amount of RNA are obtained from these microdissected samples which are often too little for conventional labelling strategies.

Recent developments in mRNA amplification techniques are also providing a solution to this problem (Klur et al. 2004). Reports have shown that neuronal subtypes could be isolated by combining LCM and gene profiling with cDNA microarray (Luo et al. 1999) (Wang et al. 2005). It might be a good approach to integrate the technologies of laser capture microdissection and T7-based RNA amplification with DNA microarrays. This approach not only could minimise the 'dilution effect' but could generate information on the viral burden in single VZV infected cells since the ability to quantify viral load at the level of single cells is essential for understanding many aspects of latency and reactivation (Sawtell 1997). Individual cell types in the DRG could be

then studied, as there are differentially expressed genes in the different cell types e.g., small versus large neurones or neuronal versus non-neuronal cells. RNA could be linearly amplified an estimated 10^6 fold using T7 RNA polymerase which is sufficient for probe labelling if micorarray experiment is to be carried out.

Some other possible approaches could be implemented to the experimental design of the microarray study if it would be taken further in the future. Studying the time dependent changes in transcription after VZV-induced allodynia in the rats might generate important data since it has been reported that genes show diverse patterns of regulation in response to nerve injury in neuropathic pain models (Costigan et al. 2002). If cost permits, replication of the microarray experiment is desirable to obtain the variation in the gene expression for statistics calculation. It has been suggested that each microarray experiment should be performed in triplicate to increase data reliability (Lee et al. 2000).

In order to investigate the functions of latent VZV genes in the development of allodynia in the rat model, it is necessary to be able to generate mutant viruses that could be tested *in vivo*. Although the idea of generating mutant viruses with cosmid DNA derived from the Oka viruses might not be workable due to their reduced pathogenicity in the rat model, cloning the VZV genome into a bacterial artificial chromosome (BAC) might be another alternative to study the function of VZV-encoded genes by mutagenesis. The genomes of a number of herpesviruses have been cloned into a BAC (Borst et al. 1999), (Adler et al. 2000), (Zhou et al. 2002). Recently, the complete genome of VZV pOka strain has been cloned as a BAC and successful reconstitution of recombinant virus from the full-length VZV BAC genome (Nagaike et al. 2004). This

bacterial genetics method allows the stable maintenance of the viral genome in *Escherichia coli* and the introduction of mutations into the genome. This method will considerably speed up the construction of VZV mutants and allow studies on the functional role of VZV genes in host-virus interactions. This approach might be adapted but with cloning of a different VZV strain such as Ellen since this virus was able to cause the development of allodynia in the rat model.

The work presented in this thesis has provided some insights into the molecular mechanism that underlie the changes in the behavioural responses in the rat model. Further work has to be done so that advance in the study of pathogenesis of PHN could be achieved.

Abendroth, A., Slobedman, B., Lee, E., Mellins, E., Wallace, M. and Arvin, A.M. (2000) Modulation of major histocompatibility class II protein expression by varicella zoster virus. Journal of virology 74(4), 1900-1907.

Adler, H., Messerle, M., Wagner, M. and Koszinowski, U.H. (2000) Cloning and mutagenesis of the murine gammaherpesvirus 68 genome as an infectious bacterial artificial chromosome. Journal of Virology 74, 6964-6974.

Ahmed, M., Lock, M., Miller, C. and Fraser, N.W. (2002) Regions of the herpes simplex virus type 1 latency-associated transcript that protect cells from apoptosis in vitro and protect neuronal cells in vivo. Journal of Virology 76, 717-729.

Annunziato, P., LaRussa, P., Lee, P., Steinberg, S., Lungu, O., Gershon, A.A. and Silverstein, S. (1998) Evidence of latent varicella-zoster virus in rat dorsal root ganglia. The Journal of Infectious Disease 178, S48-51.

Arvin, A.M. (1996) Varicella-zoster virus: overview and clinical manifestations. Seminars in Dermatology 15(2 Suppl 1), 4-7.

Arvin, A.M. (1999) Chickenpox. In: M.H. Wolff, S. Schunemann and A. Schmidt (Eds), Varicella-zoster virus. Molecular Biology, Pathogenesis and Clinical Aspects, Vol. 3, Basel Karger, pp. 96-110.

Arvin, A.M. (2005) Aging, immunity and the varicella-zoster virus. New England Journal Of Medicine 352, 2266-2267.

Arvin, A.M. and Gershon, A.A. (1996) Live attenuated varicella vaccine. Annu Rev Microbiol 50, 59-100.

Arvin, A.M., Moffat, J.F. and Redman, R. (1996) Varicella-zoster virus: aspects of pathogenesis and host response to natural infection and varicella vaccine. Adv Virus Res 46, 263-309.

Attal, N., Jazat, F., Kayser, V. and Guilbaud, G. (1990) Further evidence for 'pain-related' behaviours in a model of unilateral peripheral mononeuropathy pain. Pain 41, 235-251.

Baiker A, Bagowski C, Ito H, Sommer M, Zerboni L, Fabel K, Hay J, Ruyechan W and Arvin AM. (2004) The immediate-early 63 protein of Varicella-Zoster virus: analysis of functional domains required for replication in vitro and for T-cell and skin tropism in the SCIDhu model in vivo. Journal of Virology 78(3), 1181-1194.

Balfour, H.H.J. (1999) Antiviral drugs. New England Journal of Medicine 340, 1255-1268.

Banchereau, J. and Steinman, R.M. (1998) Dendritic cells and the control of immunity. Nature 19, 245-252.

Berry, J.D. and Petersen, K.L. (2005) A single dose of gabapentin reduces acute pain and allodynia in patients with herpes zoster. Neurology 65(3), 444-7.

Besser, J., Sommer, M.H., Zerboni, L., Bagowski, C.P., Ito, H., Moffat, J., Ku, C.C. and Arvin, A.M. (2003) Differentiation of varicella-zoster virus ORF47 protein kinase and IE62 protein binding domains and their contributions to replication in human skin xenografts in the SCID-hu mouse. Journal of Virology 77, 5964-5974.

Bontems, S., Di Valentin, E., Baudoux, L., Rentier, B., Sadzot-Delvaux, C. and Piette, J. (2002) Phosphorylation of varicella-zoster virus IE63 protein by casein kinases influences its cellular localization and gene regulation activity. J Biol Chem 277(23), 21050-60.

Borst, E.M., Hahn, G., Koszinowski, U.H. and Messerle, M. (1999) Cloning of the human cytomegalovirus (HCMV) genome as an infectious bacterial artificial chromosome in Escherichia coli: a new approach for construction of HCMV mutants. Journal of Virology 73, 8320-8329.

Branco, F.J. and Fraser, N.W. (2005) Herpes simplex virus type 1 latency-associated transcript expression protects trigeminal ganglion neurons from apoptosis. Journal of Virology 79, 9019-9025.

Brechtbuehl, K., Whalley, S.A., Dusheiko, G.M. and Saunders, N.A. (2001) A rapid real-time quantitative polymerase chain reaction for hepatitis B virus. Journal of Virological Methods 93, 105-113.

Brown, P.O. and Botstein, D. (1999) Exploring the new world of the genome with DNA microarrays. Nature Genetics 21, 33-37.

Browne, E.P., Wing, B., Coleman, D. and Shenk, T. (2001) Altered cellular mRNA levels in human cytomegalovirus-infected fibroblasts: viral block to the accumulation of antiviral mRNAs. Journal of Virology 75, 12319-12330.

Butcher, S.J., Aitken, J., Mitchell, J., Gowen, B. and Dargan, D.J. (1998) Structure of the human cytomegalovirus B capsid by electron cryomicroscopy and image reconstruction. J Struct Biol 124(1), 70-6.

Campbell, M.E., Palfreyman, J.W. and Preston, C.M. (1984) Identification of herpes simplex virus DNA sequences which encode a trans-acting polypeptide responsible for stimulation of immediate early transcription. J Mol Biol 180(1), 1-19.

Carter, K.L., Cahir-McFarland, E. and Kieff, E. (2002) Epstein-barr virus-induced changes in B-lymphocyte gene expression. Journal of Virology 76, 10427-10436.

Cesarman, E., Chang, Y., Moore, P.S., Said, J.W. and Knowles, D.M. (1995) Kaposi's sarcoma-associated herpesvirus like DNA sequences in AIDS related body cavity based lymphomas. New England Journal of Medicine 332, 1186-1191.

Chang, Y., Cesarman, E., Pessin, M.S., Lee, F., Culpepper, J., Knowles, D.M. and Moore, P.S. (1994) Identification of herpesvirus-like DNA sequences in AIDS-associated Kaposi's sarcoma. Science 266, 1865-1869.

Chen, J.J., Zhu, Z., Gershon, A.A. and Gershon, M.D. (2004) Mannose 6-phosphate receptor dependence of varicella-zoster virus infection in vitro and in the epidermis during varicella and zoster. Cell 119, 915-926.

Chidiac, C., Bruxelle, J. and Daures, J.P. (2001) Characteristics of patients with herpes zoster on presentation to practitioners in France. Clinical infectious disease 33, 62-69.

Choo, P.W., Donahue, J.G., Manson, J.E. and Platt, R. (1995) The epidemiology of varicella and its complication. Journal of Infectious Disease 172, 706-712.

Clarke, P., Beer, T., Cohrs, R. and Gilden, D.H. (1995) Configuration of latent varicella-zoster virus DNA. J Virol 69(12), 8151-4.

Cohen, J.I., Cox, E., Pesnicak, L., Srinivas, S. and Krogmann, T. (2004) The varicella-zoster virus open reading frame 63 latency-associated protein is critical for establishment of latency. Journal of Virology 78, 11833-11840.

Cohen, J.I., Krogmann, T., Ross, J.P., Pesnicak, L. and Prikhod'ko, E.A. (2005) Varicella-zoster virus ORF4 latency-associated protein is important for establishment of latency. Journal of virology 79(11), 6969-6975.

Cohen, J.I., Moskal, T., Shapiro, M., Purcell, R.H. (1996) Varicella in chimpanzees. Journal of Medical Virology 50, 289-92.

Cohen, J.I. and Nguyen, H. (1998) Varicella zoster ORF61 deletion mutants replicate in cell culture, but a mutant with stop codons in ORF61 reverts to wild-type virus. Virology 246, 306-316.

Cohen, J.I. and Seidel, K. (1994) Varicella-zoster virus (VZV) open reading frame 10 protein, the homolog of the essential herpes simplex virus protein VP16, is dispensable for VZV replication in vitro. Journal of Virology 68, 7850-7858.

Cohen, J.I. and Straus, S.E. (2001) Varicella-zoster virus and its replication. In: D.M. Knipe and P.M. Howley (Eds), Fields Virology (Fourth Edition), Vol. 2, Lippincott Williams and Wilkins, pp. 2707-2730.

Cohrs, R.J., Barbour, M. and Gilden, D.H. (1996) Varicella-zoster virus (VZV) transcription during latency in human ganglia: detection of transcripts mapping to genes 21, 29, 62, and 63 in a cDNA library enriched for VZV RNA. J Virol 70(5), 2789-96.

Cohrs, R.J., Barbour, M.B., Mahalingam, R., Wellish, M. and Gilden, D.H. (1995) Varicella-zoster virus (VZV) transcription during latency in human ganglia: prevalence of VZV gene 21 transcripts in latently infected human ganglia. J Virol 69(4), 2674-8.

Cohrs, R.J., Gilden, D.H. and Mahalingam, R. (2004) Varicella zoster virus latency, neurological disease and experimental models: an update. Frontiers in Bioscience 9, 751-762.

Cohrs, R.J., Gilden, D.H., Kinchington, P.R., Grinfeld, E., Kennedy, P.G.E. (2003) Varicella-zoster virus gene 66 transcription and translation in latently infected human ganglia. Journal of Virology 77, 6660-6665.

Cohrs, R.J., Hurley, M.P. and Gilden, D.H. (2003) Array analysis of viral gene transcription during lytic infection of cells in tissue culture with varicella-zoster virus. Journal of Virology 77, 11718-11732.

Cohrs, R.J., Randall, J., Smith, J., Gilden, D.H., Dabrowski, C., van der Keyl, H. and Tal-Singer, R. (2000) Analysis of individual human trigeminal ganglia for latent herpes simplex virus type 1 and varicella-zoster virus nucleic acids using real-time PCR. Journal of Virology 74, 11464-11471.

Cohrs, R.J., Srock, K., Barbour, M.B., Owens, G., Mahalingam, R., Devlin, M.E., Wellish, M. and Gilden, D.H. (1994) Varicella-zoster virus (VZV) transcription during latency in human ganglia: construction of a cDNA library from latently infected human trigeminal ganglia and detection of a VZV transcript. J Virol 68(12), 7900-8.

Cohrs, R.J., Wischer, J., Essman, C. and Gilden, D. (2002) Characterisation of varicella-zoster virus gene 21 and 29 proteins in infected cells. Journal of Virology 76, 7228-7238.

Coleman, R.A., Smith, W.L. and Narumiya, S. (1994) VIII International union of pharmacology classification of prostaglandin receptors:properties, distribution and structure of the receptors and their subtypes. Pharmacology Review 46, 205-229.

Colvin, L.A., Mark, M.A. and Duggan, A.W. (1996) Bilaterally enhanced dorsal horn postsynaptic currents in a rat model of peripheral mononeuropathy. Neuroscience Letter 207, 29-32.

Costigan, M., Befort, K., Karchewski, L., Griffin, R.S., D'Urso, D., Allchorne, A., Sitarski, J., Mannion, J.W., Pratt, R.E. and Woolf, C.J. (2002) Replicate high-density rat genome oligonucleotide microarrays reveal hundreds of regulated genes in the dorsal root ganglion after peripheral nerve injury. BMC Neuroscience 3 : 16, 1-18.

Crawford, D.H. (2004) Epstein-Barr virus. In: A.J. Zuckerman, J.E. Banatvala, J.R. Pattison, P.D. Griffiths and B.D. Schoub (Eds), Pinciples and Practice of Clinical Virology, John Wiley & Sons, pp. 123-145.

Croen, K.D., Ostrove, J.M., Dragovic, L.J. and Straus, S.E. (1988) Patterns of gene expression and sites of latency in human nerve ganglia are different for varicella-zoster and herpes simplex viruses. Proc Natl Acad Sci U S A 85(24), 9773-7.

Croen, K.D. and Straus, S.E. (1991) Varicella-zoster virus latency. Annu Rev Microbiol 45, 265-82.

Cummins, T.R., Dib-Hajj, S.D., Black, J.A. and Waxman, S.G. (2000) Sodium channels and the molecular pathophysiology of pain. Progress in Brain Research 129, 3-19.

Dalziel, R.G., Bingham, S., Sutton, D., Grant, D., Champion, J.M., Dennis, S.A., Quinn, J.P., Bountra, C., Mark, M.A. (2004) Allodynia in rats infected with varicella zoster virus- a small animal model for post herpetic neuralgia. Brain Research Reviews 46(2), 234-242.

Davis, A.M., Henion, T.R. and Tobet, S.A. (2002) Gamma-aminobutyric acid receptors and the development of the ventromedial nucleus of the hypothalamus. Journal of Comparative Neurology 449, 270-280.

Davison, A.J. (2002) Evolution of the herpesviruses. Veterinary Microbiology 86, 69-88.

Davison, A.J. and Scott, J.E. (1986) The complete DNA sequence of varicella-zoster virus. Journal of General Virology 67, 1759-1816.

Debrus, S., Sadzot-Delvaux, C., Nikkels, A.F., Piette, J. and Rentier, B. (1995) Varicella-zoster virus gene 63 encodes an immediate-early protein that is abundantly expressed during latency. J Virol 69(5), 3240-5.

Defechereux, P., Debrus, S., Baudoux, L., Rentier, B. and Piette, J. (1997) Varicella-zoster virus open reading frame 4 encodes an immediate-early protein with posttranscriptional regulatory properties. Journal of Virology 71, 7073-7079.

Defechereux, P., Debrus, S., Baudoux, L., Schoonbroodt, S., Merville, M.P., Rentier, B. and Piette, J. (1996) Intracellular distribution of the ORF4 gene product of varicella-zoster virus is influenced by the IE62 protein. Journal of General Virology 77, 1505-1513.

Defechereux, P., Melen, L., Baudoux, L., Merville-Louis, M.P., Rentier, B. and Piette, J. (1993) Charcaterization of the regulatory functions of the varicella-zoster virus open reading frame 4 gene product. Journal of Virology 67, 4379-4385.

Dhiman, N., Bonilla, R., O'Kane, D. and Poland, G.A. (2002) Gene expression in microarrays: a 21st century tool for directed vaccine design. Vaccine 20, 22-30.
Disney, G.H. and Everett, R.D. (1990) A herpes simplex virus type 1 recombinant with both copies of the VMw175 coding sequences replaced by homologous varicella-zoster virus open reading frame. Journal of General Virology 71, 2681-2689.
DiValentin, E., Bontems, S. and Habran, L. (2005) Varicella zoster virus IE63 protein represses the basal transcription machinery by disorganising the pre-initiation complex. Biological Chemistry 386, 255-267.
Dixon, R.A. and Schaffer, P.A. (1980) Fine-structure mapping and functional analysis of temperature-sensitive mutants in the gene encoding the herpes simplex virus type 1 immediate early protein VP175. Journal of Virology 36, 189-203.
Dueland, A.N., Ranneberg-Nilsen, T. and Degre, M. (1995) Detection of latent varicella zoster virus DNA and human gene sequences in human trigeminal ganglia by in situ amplification combined with in situ hybridization. Arch Virol 140(11), 2055-66.
Dunkel, E.C., Geary, P.A., Pavan-Langston, D., Piatak, M., Zhu, Q. (1995) Varicella-zoster ocular infection in the rabbit: a model of human zoster ophthalmicus. Neurology 45, S21-S28.
Dworkin, R.H., Portenoy, R.K. (1996) Pain and its persistence in herpes zoster. Pain 67(2-3), 241-251.
Efstathiou, S., Minson, A.C., Field, H.J., Anderson, J.R. and Wildy, P. (1986) Detection of herpes simplex virus-specific sequences in latently infected mice and in humans. Journal of Virology 57, 446-455.
Emmert-Buck MR, Bonner RF, Smith PD, Chuaqui RF, Zhuang Z, Goldstein SR, Weiss RA and Liotta L. (1996) Laser capture microdissection. Science 274, 998-1001.
Enright, A.M. and Prober, C. (2003) Antiviral therapy in children with varicella zoster virus and herpes simplex virus infections. Herpes 10, 32-36.
Farrell, M.J., Margolis, T.P., Gomes, W.A. and Feldman, L.T. (1994) Effect of the transcription start region of the herpes simplex virus type 1 latency-associated transcript promoter on expression of productively infected neurons in vivo. Journal of Virology 68, 5337-5343.
Fink, T.M., Jenne, D.E. and Lichter, P. (1992) The human vitronectin (complement S-protein) gene maps to the centromeric region of 17q. Human Genetics 88, 569-572.
Fleetwood-Walker, S.M., Quinn, J.P., Wallace, C., Blackburn-Munro, G., Kelly, B.G., Fiskerstrand, C.E., Nash, A.A. and Dalziel, R.G. (1999) Behavioural changes in the rat following infection with varicella zoster virus. Journal of General Virology 80, 2433-2436.
Flint, S.J., Enquist, L.W., Racaniello, V.R. and Skalka, A.M. (2004) Patterns of infection, Principles of Virology, ASM Press, pp. 597-621.
Forghani, B., Mahalingam, R., Vafai, A., Hurst, J.W. and Dupuis, K.W. (1990) Monoclonal antibody to immediate early protein encoded by varicella-zoster virus gene 62. Virus Research 16, 195-210.
Gabel, C.A., Dubey, L., Steinberg, S.P., Sherman, D., Gershon, M.D. and Gershon, A.A. (1989) Varicella-zoster virus glycoprotein oligosaccharides are phosphorylated during posttranslational maturation. J Virol 63(10), 4264-76.
Galer, B.S., Rowbotham, M.C., Perander, J. and Friedman, E. (1999) Topical lidocaine patch relieves postherpetic neuralgia more effectively than a vehicle topical patch: results of an enriched enrollment study. Pain 80(3), 533-8.
Gann, J.W. and Whitley, R.J. (2002) Herpes zoster. New England Journal of Medicine 347, 340-346.
Garber, D.A., Schaffer, P.A. and Knipe, D.M. (1997) A LAT-associated function reduces productive-cycle gene expression during acute infection of murine sensory neurons with herpes simplex virus type 1. Journal of Virology 71, 5885-5893.
Garry, E.M., Delaney, A., Anderson, H.A., Sirinathsinghji, E.C., Clapp, R.H., Martin, W.J., Kinchington, P.R., Krah, D.L., Abbadie, C. and Fleetwood-Walker, S.M. (2005) Varicella zoster virus induces neuropathic changes in rat dorsal root ganglia and behavioral reflex

sensitisation that is attenuated by gabapentin or sodium channel blocking drugs. Pain 118, 97-111.
Gavin, M., Barry, S., Anthony, L.C. and Allison, A. (2003) Varicella-Zoster Virus Productively Infects Mature Dendritic Cells and Alters Their Immune Function. Journal of Virology 77, 4950-4959.
Gershon, A.A., Sherman, D.L., Zhu, Z., Gabel, C.A., Ambron, R.T. and Gershon, M.D. (1994) Intracellular transport of newly synthesised varicella-zoster virus: final envelopment in the trans-Golgi network. Journal of Virology 68, 6372-6390.
Gilden, D.H., Devlin, M., Wellish, M., Mahalingam, R., Huff, C., Hayward, A. and Vafai, A. (1988) Persistence of varicella-zoster virus DNA in blood MNCs of patients with varicella or zoster. Virus Genes 2, 299-305.
Gilden, D.H., Kleinschmidt-DeMasters, B.K., LaGuardia, J.J., Cohrs, R.J. and et al. (2000) Neurologic complications of the reactivation of varicella-zoster virus. New England Journal of Medicine 342, 635-645.
Gilden, D.H., Mahalingam, R., Dueland, A.N. and Cohrs, R. (1992) Herpes zoster: pathogenesis and latency. Prog. Med. Virol. 39, 19-75.
Gilden, D.H., Rozenman, Y., Murray, R., Devlin, M., Vafai, A. (1987) Detection of varicella-zoster virus nucleic acid in neurons of normal human thoracic ganglia. Ann Neurol 22, 377-380.
Gilden, D.H., Wright, R.R., Schneck, S.A., J.M., G. and Mahalingam, R. (1994) Zoster sine herpete, a clinical variant. Ann Neurol 35, 530-533.
Gomi, Y., Imagawa, T., Takahashi, M. and Yamanishi, K. (2001) Comparison of DNA sequence and transactivation activity of open reading frame 62 of Oka varicella vaccine and its parental viruses. Archive of Virology Supplement 17, 49-56.
Gomi, Y., Sunamachi, H., Mori, Y., Nagaike, K., Takahashi, M. and Yamanishi, K. (2002) Comparison of the complete DNA sequences of the Oka varicella vaccine and its parental virus. Journal of Virology 76, 11447-11459.
Goodwin, J.S. (1989) Immunomodulation by eicosanoids and anti-inflammatory drugs. Current Opinion in Immunology 2, 264-268.
Gray, W.L. (2004) Simian varicella: a model for human varicella-zoster virus infections. Rev Med Virol 14(6), 363-81.
Grinfeld, E., Sadzot-Delvaux, C. and Kennedy, P.G.E. (2004) Varicella-zoster virus proteins encoded by open reading frames 14 and 67 are both dispensable for the establishment of latency in a rat model. Virology 323, 85-90.
Grose, C. (1981) Variation on a theme by Fenner: the pathogenesis of chickenpox. Pediatrics 68, 735-737.
Grose, C. and Ng, T.I. (1992) Intracellular synthesis of varicella-zoster virus. Journal of Infectious Disease 166(Suppl 1), S7-S12.
Grose, C., Tyler, S., Peters, G., Hiebert, J., Stephens, G.M., Ruyechan, W.T., Jackson, W., Storlie, J. and Tipples, G.A. (2004) Complete DNA sequence analyses of the first two varicella-zoster virus glycoprotein E (D150N) mutant viruses found in North America: Evolution of genotypes with an accelerated cel spread phenotype. Journal of Virology 78(13), 6799-6807.
Grose, C., Ye, M. and Padilla, J. (2000) Pathogenesis of primary infection. In: A.M. Arvin and A.A. Gershon (Eds), Varicella zoster virus. Virology and Clinical management, Cambridge University Press, pp. 105-122.
Grunewald, K., Desai, P., Winkler, D.C., Heymann, J.B., Belnap, D.M., Baumeister, W. and Steven, A.C. (2003) Three-dimensional structure of herpes simplex virus from cryo-electron tomography. Science 302, 1396 1398.
Harson, R. and Grose, C. (1995) Egress of varicella-zoster virus from the melanoma cell: A tropism for the melanocyte. Journal of Virology 69, 4994-5010.
He, H., Boucaud, D., Hay, J. and Ruyechan, W.T. (2001) Cis and trans elements regulating expession of the varicella zoster virus gI gene. Archives of Virology Suppl 17, S57-S70.
Hill, J.M., Gebhardt, B.M., Bouterie, A.M., Thompson, H.W., O'Callaghan, R.J., Halford, W.P. and Kaufman, H.E. (1996) Quantitation of herpes simplex virus type 1 DNA and latency

associated transcripts in rabbit trigeminal ganglia demonstrates a stable reservoir of viral nucleic acids during latency. Journal of Virology 70, 3137-3141.

Hokfelt, T., Zhang, X. and Wiesenfeld-Hallin, Z. (1994) Messenger plasticity in primary sensory neurons following axotomy and its functional implications. Trends in Neuroscience 17, 22-30.

Holland, P.M., Abramson, R.D. et al. (1991) Detection of specific polymerase chain reaction product by utilizing the 5'-3' exonuclease activity of Thermus aquaticus DNA polymerase. Proceedings of the National Academia of Sciences USA 88, 7276-7280.

Hope Simpson, R.E. (2001) Some early investigations into the nature of herpes zoster and postherpetic neuralgia. In: C.P.N. Watson and A.A. Gershon (Eds), Herpes Zoster and Postherpetic Neuralgia, Pain Research and Clinical Management, Vol. 11, Elsevier Science, pp. 1-12.

Hope-Simpson, R.E. (1965) The nature of herpes zoster: a long term study and a new hypothesis. Proceeding of the Royal Society of Medicine 58, 2-20.

Hope-Simpson, R.E. (1975) Post herpetic neuralgia. J. R. Coll. Gen.Pract. 25, 571-575.

Howe, J.G. and Shu, M.D. (1993) Upstream basal promoter element important for exclusive RNA polymerase III transcription of the EBER 2 gene. Molecular Cell Biology 13, 2655-2665.

Hyman, R.W., Ecker, J.R. and Tenser, R.B. (1983) Varicella-zoster virus RNA in human trigeminal ganglia. Lancet 2, 814-816.

Inchauspe, G. and Ostrove, J.M. (1989) Differential regulation by varicella zoster virus and herpes simplex virus type 1 trans-activating genes. virology 173, 710-714.

Ito, H., Sommer, M.H., Zerboni, L., He, H., Boucaud, D., Hay, J., Ruyechan, W. and Arvin, A.M. (2003) Promoter sequences of varicella-zoster virus glycoprotiein I targeted by cellular transactivating factors Sp1 and USF determine virulence in skin and T cells in SCIDhu mice in vivo. Journal of Virology 77, 489-498.

Irizarry RA, Bolstad BM, Collin F, Cope LM, Hobbs B and Speed TP (2003) Summaries of Affymetrix GeneChip probe level data. Nucleic Acids Research 31(4), 1-8.

Jackers, P., Defechereux, P., Boudoux, L. and et al. (1992) Characterisation of regulatory functions of the varicella-zoster virus gene 63-encoded protein. Journal of Virology 66, 3899-3903.

Johnson, C.E., Stancin, T., Fattlar, D., Rome, L.P. and Kumar, M.L. (1997) A long term prospective study of varicella vaccine in healthy children. Pediatrics 100, 761-766.

Johnson, R.W. (2002) Consequences and management of pain in herpes zoster. Journal of Infectious Disease 186, S83-S90.

Jones, J.O. and Arvin, A.M. (2003) Microarray analysis of host cell gene transcription in response to varicella-zoster virus infection of human T cells and fibroblasts in vitro and SCIDhu skin xenografts in vivo. Journal of Virology 77, 1268-1280.

Jones, J.O. and Arvin, A.M. (2005) Viral and cellular gene transcription in fibroblasts infected with small plaque mutants of varicella-zoster virus. Antiviral Research 68, 56-65.

Kanazi, G.E., Johnson, R.W. and Dworkin, R.H. (2000) Treatment of postherpetic neuralgia. Drugs 59(5), 1113-1126.

Katz, J.P., Bodin, E.T. and Coen, D.M. (1990) Quantitative polymerase chain reaction analysis of herpes simplex virus DNA in ganglia of mice infected with replication-incompetent mutants. Journal of Virology 64, 4288-4295.

Kennedy, P.G., Grinfeld, E., Craigon, M., Vierlinger, K., Roy, D., Forster, T. and Ghazal, P. (2005) Transcriptomal analysis of varicella-zoster virus infection using long oligonucleotide-based microarrays. Journal of General Virology 86, 2673-2684.

Kennedy, P.G., Grinfeld, E. and Gow, J.W. (1998) Latent varicella-zoster virus is located predominantly in neurons in human trigeminal ganglia. Proc Natl Acad Sci U S A 95(8), 4658-62.

Kennedy, P.G. and Steiner, I. (1994) A molecular and cellular model to explain the differences in reactivation from latency by herpes simplex and varicella-zoster viruses. Neuropathol Appl Neurobiol 20(4), 368-74.

Kennedy, P.G.E. (2002) Key issues in varicella-zoster virus latency. Journal of Neurovirology 8 (Suppl 2), 80-84.
Kennedy, P.G.E., Grinfeld, E. and Bell, J.E. (2000) Varicella-zoster virus gene expression in latently infected human trigeminal ganglia. Journal of Virology 74, 11893-11898.
Kennedy, P.G.E., Grinfeld, E., Bontems, S. and Sadzot-Delvaux, C. (2001) Varicella-zoster virus gene expression in latently infected rat dorsal root ganglia. virology 289, 218-223.
Kennedy, P.G.E., Grinfeld, E. and Gow, J.G. (1999) Latent Varicella-zoster virus in human dorsal root ganglia. Virology 258, 451-454.
Kinchington, P.R., Bookey, D. and Turse, S.E. (1995) The transcriptional regulatory proteins encoded by varicella-zoster virus open reading frames (ORFs) 4 and 63, but not ORF 61, are associated with purified virus particles. J Virol 69(7), 4274-82.
Kinchington, P.R., Fite, K., Seman, A. and Turse, S.E. (2001) Virion association of IE62, the varicella-zoster virus (VZV) major transcriptional regulatory protein, requires expression of the VZV open reading frame 66 protein kinase. Journal of Virology 75, 9106-9113.
Kinchington, P.R., Fite, K., Turse, S.E. and et al. (2000) Nuclear accumulation of IE62, the varicella-zoster virus (VZV) major transcriptional regulatory protein, is inhibited by phosphorylation mediated by the VZV open reading frame 66 protein kinase. Journal of Virology 74, 2265-2277.
Kinchington, P.R., Hougland, J.K., Arvin, A.M., Ruyechan, W.T. and Hay, J. (1992) The varicella-zoster virus immediate-early protein IE62 is a major component of virus particles. J Virol 66(1), 359-66.
Kinchington, P.R. and Turse, P.R. (1998) Regulated nuclear localization of the Varicella-zoster virus major reguatory protein, IE 62. The Journal of Infectious Diseases 178((suppl)), S16-S21.
Klur, S., Toy, K., Williams, M.P. and Certa, U. (2004) Evaluation of procedures for amplification of small-size samples for hybridisation on microarrays. Genomics 83, 508-517.
Kost, R.G. and Straus, S.E. (1996) Postherpetic neuralgia-pathogenesis treatment and prevention. New England Journal Of Medicine 335, 32-42.
Kramer, M.F., Cook, W.J., Roth, F.P., Zhu, J., Holman, H., Knipe, D.M. and Coen, D.M. (2003) Latent herpes simplex virus infection of sensory neurons alters neuronal gene expression. Journal of Virology 77, 9533-9541.
Krause, P.R. and Klinman, D.M. (1995) Efficacy, immunogenecity, safety, and use of live attenuated chicken pox vaccine. Journal of Paediatrics 127, 518-525.
Ku, C.C., Zerboni, L., Ito, H., Wallace, M., Graham, B. and Arvin, A.M. (2004) Transport of varicella-zoster virus to skin by infected CD4 T cells and modulation of viral replication by epidermal cell interferon-alpha. Journal of Experimental Medicine 200, 917-925.
LaGuardia, J.J., Cohrs, R.J. and Gilden, D.H. (1999) Prevalence of varicella-zoster virus DNA in dissociated human trigeminal ganglion neurons and nonneuronal cells. J.Virol 73, 8571-8577.
Larsen, B.L. and Henson, P.M. (1983) Mediators inflammation. Annual Review in Immunology 1, 335-359.
LaRussa, P. (2000) Clinical manifestations of varicella. In: A.M. Arvin and A.A. Gershon (Eds), Varicella-zoster virus. Virology and Clinical Management, Cambridge University Press, pp. 206-219.
Lazarov, N.E. (2002) Comparative analysis of the chemical neuroanatomy of the mammalian trigeminal ganglion and mesencephalic nucleus. Progress in Neurobiology 66, 19-59.
Lee, M.L. and et al. (2000) Importance of replication in microarray gene expression studies: statistical methods and evidence from repetitive cDNA hybridisations. Proceedings of the National Academy of Sciences 97, 9834-9839.
Lehner, P. and Trowsdale., J. (1998) Antigen presentation: coming out gracefully. Curr. Biol. 8, R605-R608.
Lekanne Deprez RH, Fijnvandraat AC, Ruijter JM and Moorman AF (2002). Sensitivity and accurary of quantitative real-time polymerase chain reaction using SYBR green I depends on cDNA synthesis conditions. Analytical Biochemistry 307, 63-69.

Levin, M.J., Cai, G.Y., Manchak, M.D. and Pizer, L.I. (2003) Varicella-zoster virus DNA in cells isolated from human trigeminal ganglia. Journal of virology 77, 6979-6987.
Liang, X.B., Wu, L.J., Hand, T. and Andreasson, K. (2005) Prostaglandin D2 mediates neuronal protection via the DP1 receptor. Journal of Neurochemistry 92, 477-486.
Linquist, S. (1986) The heat shock response. Annual Review in Biochemistry 55, 1511-1191.
Lipshutz, R., Fodor, S., Gingeras, T. and Lockart, D. (1999) High density synthetic oligonucleotide arrays. Nature Genetics 21 (Suppl), 20-24.
Lockhart, D.J., Dong, H., Byrne, M.C., Follettie, M.T., Gallo, M.V. and Chee, M.S. (1996) Expression monitoring by hybridisation to high-density oligonucleotide arrays. Nature Biotechnology 14, 1675-1680.
Lowry, P.W., Sabella, C. and Koropchek, C. (1993) Investigation of the pathogenesis of varicella-zoster virus infection in guinea pigs by using polymerase chain reation. Journal of Infectious Disease 167, 78-83.
Lowry, P.W., Solem, S., Watson, B.N., Koropchak, C.M., Thackray, H.M., Kinchington, P.R., Ruyechan, W.T., Ling, P., Hay, J. and Arvin, A.M. (1992) Immunity in strain 2 guinea-pigs inoculated with vaccinia virus recombinants expressing varicella-zoster virus glycoproteins I, IV, V or the protein product of the immediate early gene 62. J Gen Virol 73(Pt 4), 811-9.
Lungu, O., Annunziato, P.W., Gershon, A., Staugaitis, S.M., Josefson, D., LaRussa, P. and Silverstein, S.J. (1995) Reactivated and latent varicella-zoster virus in human dorsal root ganglia. Proc Natl Acad Sci U S A 92(24), 10980-4.
Lungu, O., Panagiotidis, C.A., Annunziato, P.W., Gershon, A.A. and Silverstein, S.J. (1998) Aberrant intracellular localization of varicella-zoster virus regulatory proteins during latency. Proc Natl Acad Sci U S A 95(12), 7080-5.
Luo, L., R.C., S., Guo, H., Bittner, A., Joy, K.C., Galindo, J.E., Xiao, H., Rogers, K.E., Wan, J.S., Jackson, M.R. and Erlander, M.G. (1999) Gene expression profiles of laser-captured adjacent neuronal subtypes. Nature Medicine 5(1), 117-122.
Mador, N., Goldenberg, D., Cohen, O., Panet, A. and Steiner, I. (1998) Herpes simplex virus type 1 latency-associated transcripts suppress viral replication and reduce immediate-early gene mRNA levels in a neuronal cell line. Journal of Virology 72, 5067-5075.
Maggioncalda, J., Mehta, A., Su, Y.H., Fraser, N.W. and Block, T.M. (1996) Correlation between herpes simplex virus type 1 rate of reactivation from latent infection and the number of infected neurons in trigeminal ganglia. Virology 225, 72-81.
Mahalingam, R., Kennedy, P.G.E., Gilden, D.H. (1999) The problems of latent varicella zoster virus in human ganglia: precise cell location and viral content. Journal of Neurovirology 5, 445-448.
Mahalingam, R., Wellish, M., Cohrs, R., Debrus, S., Piette, J., Rentier, B. and Gilden, D.H. (1996) Expression of protein encoded by varicella-zoster virus open reading frame 63 in latently infected human ganglionic neurons. Proc Natl Acad Sci U S A 93(5), 2122-4.
Mahalingam, R., Wellish, M., Gilden, D.H. (1995) Persistence of varicella-zoster virus DNA in elderly patients with postherpetic neuralgia. Journal of Neurovirology 1, 130-133.
Marubio, L.M. and Changeux, J.P. (2000) Nicotinic acetylcholine receptor knockout mice as animal models for studying receptor function. European Journal of Pharmacology 393, 113-121.
Massengill, J.L., Smith, M.A., Son, D.I. and O'Dowd, D.K. (1997) Differential expression of K4-AP currents and Kv3.1 potassium channel transcripts in cortical neurons that develop distinct firing phenotypes. Journal of Neuroscience 17, 3136-3147.
Maurel, P. and Salzer, J.L. (2000) Axonal regulation of Schwann cell proliferation and survival and the initial events of myelination requires PI 3-kinase activity. Journal of Neuroscience 20, 4635-4645.
Mayne, M., Cheadle, C., Soldan, S.S., Cermelli, C., Yamano, Y., Akhyani, N., Nagel, J.E., Taub, D.D., Becker, K.G. and Jacobson, S. (2001) Gene expression profile of herpesvirus-infected T cells obtained using immunomicroarrays induction of proinflammatory mechanisms. Journal of Virology 75, 11641-11650.

McKee, T.A., Disney, G.H., Everett, R.D. and Preston, C.M. (1990) Control of expression of the varicella-zoster virus major immediate early gene. Journal of General Virology 71, 897-906.

McNamee, E.E., Taylor, T.J. and Knipe, D.M. (2000) A dominant-negative herpesvirus protein inhibits intranuclear targeting of viral proteins: effects on DNA replication and late gene expression. Journal of Virology 74, 10122-10131.

Meier, J.L., Holman, R.P., Croen, K.D., Smialek, J.E. and Straus, S.E. (1993) Varicella-zoster virus transcription in human trigeminal ganglia. Virology 193(1), 193-200.

Meier, J.L. and Straus, S.E. (1995) Interactions between varicella-zoster virus IE62 and cellular transcription factor USF in the coordinate activation of genes 28 and 29. Neurology 45(12 Suppl 8), S30-2.

Mettenleiter, T.C. (2000) Aujeszky's disease (pseudorabies) virus: The virus and molecular pathogenesis-state of the art, June 1999. Veterinary Research 31, 99-115.

Michael, E.J., Kuck, K.M. and Kinchington, P.R. (1998) Anatomy of the varicella-zoster virus open-reading frame 4 promoter. Journal of Infectious Diseases 178, S27-S33.

Millhouse, S. and Wigdahl, B. (2000) Molecular circuitry regulating herpes simplex virus type 1 latency in neurons. Journal of Neurovirology 6, 6-24.

Minson, A.C., Davison, A.J., Eberle, R., Desrosiers, R C., Fleckenstein, B., McGeoch, D.J., Roizman, B., Studdert, D.M.J., ed. (2000) Herpesviridae. Virus Taxonomy. Edited by M.H.V. van Regenmortel, Fauquet, C.M., Bishop, D.H.L., Carstens, E.B., Estes, M.K., Lemon, S.M., Maniloff, J., Mayo, M.A., McGeoch, D.J., Pringle, C.R., Wickner, R.B. Academic Press, New York.

Mirnics, K., Middleton, F.A., Lewis, D.A. and Levitt, P. (2001) Analysis of complex brain disorders with gene experssion microarrays: schizophrenia as a disease of the synapse. Trends in Neuroscience 24, 479-486.

Moffat, J., Mo, C., Cheng, J.J., Sommer, M.H., Zerboni, L., Stamatis, S. and Arvin, A.M. (2004) Functions of the C-terminal domain of varicella-zoster virus glycoprotein E in viral replication in vitro and skin and T cell tropism in vivo. Journal of Virology 78, 12406-12415.

Moffat, J.F., Zerboni, L., Kinchington, P.R., Grose, C., Kaneshima, H. and Arvin, A.M. (1998) Attenuation of the vaccine Oka strain of varicella-zoster virus and role of glycoprotein C in alphaherpesvirus virulence demonstrated in the SCID-hu mouse. J Virol 72(2), 965-74.

Moriuchi, H., Moriuchi, M. and Cohen, J., I. (1994a) The RING finger domain of the varicella-zoster virus open reading frame 61 protein is required for its transregulatory functions. Virology 205, 238-246.

Moriuchi, H., Moriuchi, M., Straus, S.E. and Cohen, J.I. (1993a) Varicella-zoster virus (VZV) open reading frame 61 protein transactivates VZV gene promoters and enhances the infectivity of VZV DNA. Journal of Virology 67, 4290-4295.

Moriuchi, H., Moriuchi, M., Straus, S.E. and Cohen, J.I. (1993b) Varicella-zoster virus open reading frame 10 protein, the herpes simplex virus VP16 homolog, transactivates herpesvirus immediate-early gene promoters. Journal of Virology 67, 2739-2746.

Moriuchi, M., Moriuchi, H. and Cohen, J.I. (1995) The varicella-zoster virus immediate-early 62-promoter contains a negative regulatory element that binds transcriptional factor NF-Y. Virology 214, 256-258.

Moriuchi, M., Moriuchi, H., Straus, S.E. and Cohen, J.I. (1994b) Varicella-zoster virus (VZV) virion-associated transactivator open reading frame 62 protein enhances the infectivity of VZV DNA. Virology 200, 297-300.

Moses, A.V., Jarvis, M.A., Raggo, C., Bell, Y.C., Ruhl, R., Luukkonen, B.G., Griffith, D.J., Wait, C.L., Druker, B.J., Heinrich, M.C., Nelson, J.A. and Fruh, K. (2002) Kaposi's sarcoma-associated herpesvirus-induced upregulation of the c-kit proto-oncogene, as identified by gene expression profiling, is essential for the transformation of endothelial cells. Journal of Virology 76, 8383-8399.

Myers, M.G. and Conelly, B.L. (1992) Animal models of varicella. Journal of Infectious disease 166 (Suppl 1), S48-50.
Myers, M.G., Connelly, B.L., Stanberry, L.R. (1991) Varicella in hairless guinea pigs. Journal of Infectious Disease 163, 746-751.
Myers, M.G., Stanberry, L.R., Edmond, B.J. (1985) Varicella-zoster virus infection of strain 2 guinea pigs. Journal of Infectious Disease 151, 106-113.
Nagaike, K., Mori, Y., Gomi, Y., Yoshii, H., Takahashi, M., Wagner, M., Koszinowski, U. and Yamanishi, K. (2004) Cloning of the varicella-zoster virus genome as an infectious bacterial artificial chromosome in Escherichia coli. Vaccine 22, 4069-4074.
Nudel, U., Zakut, R., Shani, M., Neuman, S., Levy, Z. and Yaffe, D. (1983) The nucleotide sequence of the rat cytoplasmic beta-actin gene. Nucleic Acids Res 11(6), 1759-71.
Nunes, A.F., Saraiva, M.J. and Sousa, M.M. (2005) Transthyretin knockouts are a new mouse model for increased neuropeptide Y. FASEB(Nov 1).
Oxman, M.N. (2000) Clinical manifestations of herpes zoster. In: A.M. Arvin and A.A. Gershon (Eds), Varicella-zoster virus: virology and clinical management, Cambridge University Press, pp. 246-275.
Oxman, M.N.e.a. (2005) A vaccine to prevent herpes zoster and postherpetic neuralgia in older adults. The New England Journal of Medicine 352, 2271-2284.
Pass, R.F. (2001) Cytomegalovirus. In: E.M. Knipe, Howley, P.M. (Ed), Fields Virology, Fourth Edition, Vol. 2, Lippincott Williams and Wilkins, Philadelphia, pp. 2675-2705.
Pease AC, Solas D, Sullivan EJ, Cronin MT, Holmes CP and Fodor SP (1994) Light-generated oligonucleotide arrays for rapid DNA sequence analysis. Proceedings of the National Academia of Sciences USA 91, 5022-5026.
Perera, L.P., Kaushal, S., Kinchington, P.R., Mosca, J.D., Hayward, G.S. and Straus, S.E. (1994) Varicella-zoster virus open reading frame 4 encodes a transcriptional activator that is functionally distinct from that of herpes simplex virus homology ICP27. J Virol 68(4), 2468-77.
Perera, L.P., Mosca, J.D., Ruyechan, W.T. and Hay, J. (1992) Regulation of varicella-zoster virus gene expression in human T lymphocytes. Journal of Virology 66(5298-5304).
Perng, G.C., Dunkel, E.C., Geary, P.A., Slanina, S.M., Ghiasi, H., Kaiwar, R., Nesburn, A.B. and Wechsler, S.L. (1994) The latency-associated transcript gene of herpes simplex virus type 1 (HSV-1) is required for the efficient in vivo spontaneous reactivation of HSV-1 from latency. Journal of Virology 68, 8045-8055.
Peterson, C.L., Vugia, D. and Meyers, H. (1996) Risk factors for invasive group A streptococcal infections in children with varicella: a case-control study. Pediatrics and Infectious Disease 15, 151-156.
Pevenstein, S.R., Williams, R.K., McChesney, D., Mont, E.K., Smialek, J.E., Straus, S.E. (2000) Quantitation of latent varicella-zoster virus and herpes simplex virus genomes in human trigeminal ganglia. Journal of Virology 73(12), 10514-10518.
Pieters, J. (1997) MHC class II restricted antigen presentation. Current opinion in immunology 9, 89-96.
Portenoy, R.K., Duma, C. and Foley, K.M. (1986) Acute herpetic and postherpetic neuralgia: clinical review and current management. Ann Neurol 20(6), 651-64.
Provost, P.J., Keller, P.M., Banker, F.S., Keech, B.J., Klein, H.J., Lowe, R.S., Morton, D.H., Phelps, A.H.,McAleer, W.J., Ellis, R.W. (1987) Successful infection of the common marmoset (Callithrix jacchus) with human varicella-zoster virus. Journal of Virology 61, 2951-2955.
Rajeevan, M.S., Vernon, S.D., Taysavang, N. and Unger, E.R. (2001) Validation of array-based gene expression profiles by real-time (kinetic) RT-PCR. J Mol Diagn 3(1), 26-31.
Ramakrishnan, R., Fink, D.J., Jiang, G., Desai, P., Glorioso, J.C. and Levine, M. (1994) Competitive quantitative PCR analysis of herpes simplex virus type 1 DNA and latency associated transcript RNA in latently infected cells of the rat brain. Journal of Virology 68, 1864-1873.
Ramsay, G. (1998) DNA chips: state-of-the-art. Nature Biotechnology 16, 40-44.

Roizman, B. (1996) Herpesviridae. In: B.N. Fields, Knipe, D.M., Howley, P.M., Channock, R.M., Melnick, J.L., Roizman, B., Straus, S.E. (Ed), Fields Virology, Lippencott-Raven, Philadelphia, New York.

Roizman, B., Desrosiers, R. C., Fleckenstein, B., Lopez, C., Minson, A.C, Studdert, M.J. (1992) The family Herpesviridae: an update. Archive of Virology 123, 425-449.

Roizman, B. and Pellett, P.E. (2001) The Family Herpesviridae: A Brief Introduction. In: D.M.a.H. Knipe, P.M. (Ed), Fields Virology, Fourth ed, Vol. 2, Lippincott Williams & Wilkins, Philadelphia, USA, pp. 2381-2397.

Roizman, B. and Sears, A.E. (1995) The replication of herpes simplex viruses. In: R.J. Whitley and C. Lopez (Eds), The Human Herpesviruses, Raven Press, New York.

Rowbotham, M.C. (2001) What is a 'clinically meaningful' reduction in pain. Pain 94, 131-132.

Rowbotham, M.C. and Fields, H.L. (1996) The relationship of pain, allodynia and thermal sensation in postherpetic neuralgia. Brain 119, 347-354.

Ruyechan, W.T. and Hay, J. (2000) DNA replication. In: A.M. Arvin, Gershon, A.A. (Ed), Varicella-zoster virus: Virology and Clinical Management, Cambridge University Press, pp. 51-73.

Ryckman, C., Vandal, K., Rouleau, P., Talbot, M. and Tessier, P.A. (2003) Proinflammatory Activities of S100: Proteins S100A8, S100A9, and S100A8/A9 Induce Neutrophil Chemotaxis and Adhesion. Journal of Immunology 170, 3233-3242.

Sabella, C., Lowry, P.W., Abbruzzi, G.M., Koropchak, C.M., Kinchington, P.R., Sadegh-Zadeh, M., Hay, J., Ruyechan, W.T., Arvin, A.M. (1993) Immunization with the immediate-early tegument protein (open reading frame 62) of varicella-zoster virus protects guinea pigs against virus challenge. Journal of Virology 67, 7673-7676.

Sadzot-Delvaux, C., Debrus, S., Nikkels, A., Piette, J. and Rentier, B. (1995) Varicella-zoster virus latency in the adult rat is a useful model for human latent infection. Neurology 45(12 Suppl 8), S18-20.

Sadzot-Delvaux, C., Merville-Louis, M.P., Delree, P., Marc, P., Piette, J., Moonen, G. and Rentier, B. (1990) An in vivo model of varicella-zoster virus latent infection of dorsal root ganglia. J Neurosci Res 26(1), 83-9.

Sadzot-Delvaux, C. and Rentier, B. (2000) Animal models of infection. In: A.M. Arvin and A.A. Gershon (Eds), Varicella-Zoster virus-Virology and Clinical Management, Cambridge University Press, pp. 169-183.

Sadzot-Delvaux, C. and Rentier, B. (2001) The role of varicella zoster virus immediate early proteins in latency and their potential use as components of vaccines. Archive of Virology Supplement 17, 81-89.

Santos, R.A., Padilla, J.A., Hatfield, C. and Grose, C. (1998) Antigenic variation of varicella zoster virus Fc receptor gE: loss of a major B cell epitope in the ectodomain. Virology 249, 21-31.

Sato, H., Pesnicak, L. and Cohen, J.I. (2003) Varicella-zoster virus ORF47 protein kinase, which is required for replication in human T cells and ORF66 protein kinase, which is expressed during latency are dispensable for establishment of latency. Journal of Virology 77, 11180-11185.

Sawtell, N.M. (1997) Comprehensive quantification of herpes simplex virus latency at the single-cell level. Journal fo Virology 71, 5423-5431.

Sawtell, N.M. (1998) The probability of in vivo reactivation of herpes simplex virus type 1 increases with the number of latently infected neurons in the ganglia. Journal of Virology 72, 6888-6892.

Sawtell, N.M., Poon, D.K., Tansky, C.S. and Thompson, R.L. (1998) The latent herpes simplex virus type 1 genome copy number in individual neurons is virus strain specific and correlates with reactivation. Journal of Virology 72(7), 5343-5350.

Sawtell, N.M. and Thompson, R.L. (1992) Herpes simplex virus type 1 latency-associated transcription unit promotes anatomical site-dependent establishment and reactivation from latency. Journal of Virology 66, 2157-2169.

Sawyer, N., Cauchon, E., Chateauneuf, A., Cruz, R.P., Nicholson, D.W., Metters, K.M., O'Neill, G.P. and Gervais, F.G. (2002) Molecular pharmacology of the human prostaglandin D2 receptor, CRTH2. British Journal of Pharmacology 137, 1163-1172.

Schaible, H.G. and Richter, F. (2004) Pathophysiology of pain. Current concepts in clinical surgery 389, 237-243.

Schena, M., Shalon, D., Davis, R.W. and Brown, P.O. (1995) Quantitative monitoring of gene expression patterns with a complementary DNA microarray. Science 270, 467-470.

Sederati, F., Izumi, K.M., Wagner, E.K. and Stevens, J.G. (1989) Herpes simplex virus type 1 latency-associated transcription plays no role in establishment or maintenance of a latent infection in murine sensory neurons. Journal of Virology 63, 4455-4458.

Sharp, M., K. Terada, A. Wilson, S. Nader, P. E. Kinchington, W. T. Ruyechan, J. Hay and Arvin, A.M. (1992) Kinetics and viral protein specificity of the cytotoxic T lymphocyte response in healthy adults immunized with live attenuated varicella vaccine. Journal of Infectious Disease 165, 852-858.

Shelton, L.S., Albright, A.G., Ruyechan, W.T. and Jenkins, F.J. (1994) Retention of the herpes simplex virus type 1 (HSV-1) UL37 protein on single-stranded DNA columns requires the HSV-1 ICP8 proteins. Journal of Virology 68, 521-525.

Silverstein. S., S., S.E. (2000) Pathogenesis of latency and reaction. In: A.M.G. Arvin, A.A. (Ed), Varicella-Zoster Virus- Virology and Clinical Management, Cambridge University Press, pp. 123-141.

Sommer, M.H., Zagha, E., Serrano, O.K., Ku, C.C., Zerboni, L., Baiker, A., Santos, R., Spengler, M., Lynch, J., Grose, C., Ruyechan, W., Hay, J. and Arvin, A.M. (2001) Mutational analysis of the repeated open reading frames, ORFs 63 and 70 and ORFs 64 and 69, of varicella-zoster virus. J Virol 75(17), 8224-39.

Spear, P.G., Eisenberg, R.J. and Cohen, G.H. (2000) Three classes of cell surface receptors for alphaherpesviruses entry. virology 275, 1-8.

Spear, P.G. and Longnecker, R. (2003) Herpesvirus entry: an update. Journal of Virology 77, 10179-10185.

Spengler, M., Ruyechan, W. and Hay, J. (2000) Physical interaction between two varicella zoster virus regulatory proteins, 1E4 and IE62. Virology 272, 375-381.

Stankus, S.J., Dlugopolski, M. and Packer, D. (2000) Management of herpes zoster (shingles) and postherpetic neuralgia. Am Fam Physician 61(8), 2437-44, 2447-8.

Steiner, I. (1996) Human herpes viruses latent infection in the nervous system. Immunol Rev 152, 157-73.

Stevens, J.G. (1989) Human herpesviruses: a consideration of the latent state. Microbiol. Rev 53, 318-332.

Stevens, J.G., Wagner, E.K., Devi-Rao, G.B., Cook, L., Felman, L.T. and et al. (1987) RNA complementary to a herpesvirus alpha gene mRNA is prominent in latently infected neurons. Science 235, 1056-1059.

Straus, S., Aulakh, H.S., Ruyechan, W.T., Hay, J., Casey, T.A., Vande Woude, G.F., Owens, J. and Smith, H.A. (1981) Structure of varicella-zoster virus DNA. Journal of Virology 40, 516-525.

Sturm, R.A., Das, G. and Herr, W. (1988) The ubiquitous octamer-binding protein Oct-1 contains a POU domain with a homeo box subdomain. Genes Development 2, 1582-1599.

Suarez-Quian CA, Goldstein SR, Pohida T, Smith PD, Peterson JI, Wellner E, Ghany M and Bonner RF (1999) Laser capture microdissection of single cells from complex tissues. Biotechniques 26, 328-335.

Suto, R. and Srivastava, P.K. (1995) A mechanism for the specific immunogenicity of heat shock protein-chaperoned peptides. Science 269, 1585-1588.

Takahashi, M., Okuno, Y., Otsuka, T., Osame, J., Takamizawa, A. and et al. (1975) Development of a live attenuated varicella vaccine. Biken Journal 18, 25-33.

Takahashi, M., Otsuka, T., Okuno, Y., Asano, Y. and Yazaki, T. (1974) Live vaccine used to prevent the spread of varicella in children in hospital. Lancet ii, 1288-1290.

Tipples, G.A., Stephens, G., Sherlock, C., Bowler, M., Hoy, B., Cook, D. and Grose, C. (2002) New variant of varicella-zoster virus. Emerging Infectious Disease 8, 1504-1505.

Trus, B.L., Gibson, W., Cheng, N. and Steven, A.C. (1999) Capsid structure of simian cytomegalovirus from cryoelectron microscopy: evidence for tegument attachment sites. J Virol 73(3), 2181-92.

Tyagi S and Kramer FR (1996) Molecular beacons: probes that fluoresce upon hybridization. Nature Biotechnology 14(3), 303-308.

Tyring, S., Barbarash, R.A., Nahlik, J.E., Cunningham, A., Marley, J., Heng, M., Jones, T., Rea, T., Boon, R. and Saltzman, R. (1995) Famciclovir for the treatment of acute herpes zoster; effects on acute disease and postherpetic neuralgia: a randomised, double-blind, placebo-controlled trial. Annual International Medicine 123, 89-96.

Urade, Y. and Hayaishi, O. (2000) Biochemical, structural, genetic, physiological, and pathophysiological features of lipocalin-type prostaglandin D synthase. Biochimica et Biophysica Acta 1482, 259-271.

Vafai, A., Wellish, M. and Gilden, D.H. (1988) Expression of varicella-zoster virus in blood mononuclear cells of patients with postherpetic neuralgia. Proceedings of the National Academia of Sciences USA 85, 2767-2770.

Valder, C.R., Liu, J.J., Song, Y.H. and Luo, Z.D. (2003) Coupling gene chip analyses and rat genetic variances in identifying potential target genes that may contribute to neuropathic allodynia development. Journal of Neurochemistry 87, 560-573.

Vandesompele J, De Preter K, Pattyn F, Poppe B, Van Roy N, De Paepe A and Speleman F. (2002) Accurate normalization of real-time quantitative RT-PCR data by geometric averaging of multiple internal control genes. Genome Biology 3(7), RESEARCH0034.

Volmink, J., Lancaster, T., Gray, S. and Silagy, C. (1996) Treatments for postherpetic neuralgia--a systematic review of randomized controlled trials. Fam Pract 13(1), 84-91.

Vrabec, J.T. and Alford, R.L. (2004) Quantitative analysis of herpes simplex virus in cranial nerve ganglia. Journal of Neurovirology 10, 216-222.

Wagenpfeil, S., Neiss, A. and Wutzler, P. (2004) Effects of varicella vaccination on herpes zoster incidence. Clin Microbiol Infect 10(11), 954-60.

Wagner, E.K. and Bloom, D.C. (1997) Experimental investigation of herpes simplex virus latency. Clinical Microbiology Review 10, 419-443.

Wang, H., Sun, H., Della Penna, K., Benz, R.J., Xu, J., Gerhold, D.L., Holder, D.J. and Koblan, K.S. (2002) Chronic neuropathic pain is accompanied by global changes in gene expression and shares pathobiology with neurodegerative diseases. Neuroscience 114, 529-546.

Wang, K., Lau, T.Y., Morales, M., Mont, E.K. and Straus, S.E. (2005) Laser-capture microdissection: refining estimates of the quantity and distribution of latent herpes simplex virus 1 and varicella-zoster virus DNA in human trigeminal ganglia at the single-cell level. Journal of Virology 79, 14079-14087.

Wang, Z.H., Gershon, M.D., Lungu, O., Zhu, Z. and Gershon, A.A. (2001) Essential role played by the C-terminal domain of glycoprotein I in envelopment of varicella-zoster virus in the trans-Golgi network: interactions of glycoproteins with tegument . Journal of Virology 75, 323-340.

Watson, C.P. (1989) Postherpetic neuralgia. Neurol. Clin. 7, 231-248.

Watson, C.P. and Babul, N. (1998) Efficacy of oxycodone in neuropathic pain: a randomized trial in postherpetic neuralgia. Neurology 50(6), 1837-41.

Weidmann, M., Meyer-Konig, U. and Hufert, F.T. (2003) Rapid detection of herpes simplex virus and varicella-zoster virus infections by real-time PCR. Journal of Clinical Microbiology 41, 1565-1568.

Weller, T.H. (1996) Varicella: Historical perspective and clinical oerview. Journal of Infectious Disease 174, S306-S309.

Whitcombe D, Theaker J, Guy SP, Brown T and Little S (1999) Detection of PCR products using self-probing amplicons and fluorescence. Nature Biotechnology 17(8), 804-807.

White, T.M.e.a., Mahalingam, R., Kolhatkar, G. and Gilden, D.H. (1997) Identification of simian varicella virus homologues of varicella zoster virus genes. Virus Genes 15(3), 265-9.

Whitley, R.J. (2000) Treatment of varicella. In: A.M. Arvin and A.A. Gershon (Eds), Varicella-zoster virus: Virology and Clinical Management, Cambridge University Press, pp. 385-395.

Whitley, R.J. (2001) Herpes zoster: natural history, diagnosis and therapy. In: C.P.N.G. Watson, A.A. (Ed), Herpes Zoster and Postherpetic Neuralgia, Pain Research and Clinical Management, Vol. 11, Elsevier Science B. V., pp. 65-78.

Wittwer, C.T., Herrmann, M.G., Moss, A.A. and Rasmussen, R.P. (1997) Continuous fluoresence monitoring of rapid cycle DNA amplification. BioTechniques 22, 130-138.

Wood, M. (2002) Understanding pain in herpes zoster: an essential for optimising treatment. The Journal of Infectious Disease 186, S78-82.

Wood, M.J., Kay, R. and Dworkin, R.H. (1996) Oral acyclovir therapy accelerates pain resolution in patients with herpes zoster: a meta-analysis of placebo-controlled trials. Clinical of Infectious Disease 22, 341-347.

Woolf, C.J. and Salter, M.W. (2000) Neuronal plasticity: increasing the gain in pain. Science 288, 1765-1769.

Wroblewska, Z., Valyi-Nagy, T., Otte, J., Dillner, A., Jackson, A., Sole, D.P. and Fraser, N.W. (1993) A mouse model for varicella-zoster virus latency. Microb Pathog 15(2), 141-51.

Wu, C.A., Nelson, N.J., McGeoh, D.J. and Challberg, M.D. (1988) Identification of herpes simplex virus type 1 genes required for origin-dependent DNA synthesis. Journal of Virology 62, 435-443.

Wu, G., Ringkamp, M., Hartke, T.V., Murinson, B.B., Campbell, J.N., Griffin, J.W. and Meyer, R.A. (2001) Early onset of spontaneous activity in uninjured C-fiber nociceptors after injury to neighboring nerve fibers. Journal of Neuroscience 21, 1-5.

Wurmbach, E., Gonzalez-Maeso, J., Yuen, T., Ebersole, B.J., Mastaitis, J.W., Mobbs, C.V. and Sealfon, S.C. (2002) Validated genomic approach to study differentially expressed genes in complex tissues. Neurochemistry Research 27, 1027-1033.

Xia, D., Srinivas, S., Sato, H., Pesnicak, L., Straus, S.E. and Cohen, J.I. (2003) Varicella-zoster virus open reading frame 21, which is experssed during latency, is essential for virus replication but dispensable for establishment of latency. Journal of Virology 77, 1211-1218.

Zerboni, L., Hinchliffe, S., Sommer, M.H., Ito, H., Besser, J., Stamatis, S., Cheng, J., DiStefano, D., Kraiouchkine, N., Shaw, A. and Arvin, A.M. (2005) Analysis of varicella zoster virus attenuation by evaluation of chimeric parent Oka/vaccine Oka recombinant viruses in skin xenografts in the SCIDhu mouse model. Virology 332, 337-346.

Zhou, F.C., Zhang, Y.J. and Deng, J.H. (2002) Efficient infection by a recombinant Kaposi's sarcoma-associated herpesvirus cloned in a bacterial artificial chromosome: application for genetic analysis. Journal of Virology 76, 6185-6196.

Zhu, Z., Gershon, M.D., Hao, Y., Ambron, R.T., Gabel, C.A. and Gershon, A.A. (1995) Envelopment of varicella-zoster virus: targeting of viral glycoproteins to the trans-Golgi network. Journal of Virology 69(12), 7951-7959.

Appendix 4.1 Present to Absent Gene List in Different Functional Groups

Mock	Infected	Fold Change	Gene Title
Cell adhesion and structure			
3.1	2.9	-1.068965517	procollagen, type XI, alpha 1
9.4	4.7	-2	Pleckstrin homology domain containing
10.8	9.4	-1.14893617	protocadherin 3
13	8.8	-1.477272727	Opioid-binding protein/cell adhesion molecule-like
14.5	9.6	-1.510416667	kinesin family member 6
14.5	7.7	-1.883116883	tenascin R
18.1	9.1	-1.989010989	vitamin D receptor
18.9	8.8	-2.147727273	inhibin beta-A
23.7	25	-0.948	inhibin alpha
25.9	21.9	-1.182648402	keratin complex 2, basic, gene 5
27.7	17.2	-1.610465116	slit homolog 1 (Drosophila)
30.4	26.3	-1.155893536	Kinesin light chain 3
40.7	25.2	-1.615079365	procollagen, type II, alpha 1
40.9	55.8	-0.73297491	AE binding protein 1 (predicted)
52.5	42.6	-1.232394366	sushi-repeat-containing protein
Cell cycle, apoptosis, development			
5.8	5.7	-1.01754386	angiotensin II receptor, type 2
7.6	10.4	-0.730769231	Fas-associated factor 1
9.8	9.4	-1.042553191	checkpoint kinase 1 homolog (S. pombe)
10.5	5.3	-1.981132075	Roundabout homolog 1 (Drosophila)
11.3	10.8	-1.046296296	tumor-associated calcium signal transducer 1
11.4	10.7	-1.065420561	Similar to DNA polymerase alpha catalytic subunit
13	9.7	-1.340206186	myosin 5B
14.9	6.7	-2.223880597	B-cell leukemia/lymphoma 2 related protein A1
16.9	15.7	-1.076433121	glypican 2 (cerebroglycan)
19	19.1	-0.994764398	Unc-5 homolog B (C. elegans)
19.4	7	-2.771428571	paraoxonase 1
20.5	15.9	-1.289308176	large (Drosophila) homolog-associated protein 1
24.1	20.5	-1.175609756	Polymerase (DNA-directed), delta 3
25.1	16.8	-1.494047619	polymerase (DNA directed), gamma
27.5	31.2	-0.881410256	G0/G1 switch gene 2 (predicted)
49.8	61.1	-0.815057283	plexin domain containing 2 (predicted)
70	38.3	-1.82767624	calcium/calmodulin-dependent protein kinase II alpha subunit
Signal transduction: receptors, kinases, phosphatases, G-proteins			
8.3	11.3	-0.734513274	taste receptor, type 2, member 16
8.6	13.3	-0.646616541	wingless-type MMTV integration site 5A
8.6	6.4	-1.34375	angiotensin II type-1 receptor
9	8.5	-1.058823529	protein tyrosine phosphatase, receptor type, Q
9	8.5	-1.058823529	protein tyrosine phosphatase, receptor type, Q
10.2	5.2	-1.961538462	protein phosphatase 1
10.6	17.4	-0.609195402	tensin like C1 domain containing phosphatase
10.9	5	-2.18	thyroid stimulating hormone, beta subunit
11.2	3.3	-3.393939394	membrane-spanning 4-domains, subfamily A
11.5	6.7	-1.71641791	insulin receptor substrate 1
12	12.5	-0.96	Rho guanine nucleotide exchange factor 7
13.8	13.4	-1.029850746	olfactory receptor 1278
14.3	16.7	-0.856287425	growth factor receptor bound protein 7
14.4	12.4	-1.161290323	lectin, galactoside-binding, soluble, 4 (galectin 4)

15.3	10.9	-1.403669725	MAS-related G protein-coupled receptor, member B4
15.6	19.4	-0.804123711	olfactory receptor 1500
15.7	8.4	-1.869047619	membrane-spanning 4-domains
18.5	11.4	-1.622807018	arginine vasopressin receptor 2
19.8	28.5	-0.694736842	thyrotropin releasing hormone receptor
20.6	22.5	-0.915555556	phosphodiesterase 4D
20.6	18.1	-1.138121547	corticotropin releasing hormone receptor 2
23.6	18.4	-1.282608696	apelin, AGTRL1 ligand
26.6	22.2	-1.198198198	protein phosphatase 1
32.9	17.1	-1.923976608	Suppressor of variegation 4-20 homolog 1
37.9	34.6	-1.095375723	gap junction membrane channel protein alpha 4
50	35.9	-1.39275766	Plexin B1 (predicted)
54.1	29.5	-1.833898305	somatostatin receptor 3
65.5	90	-0.727777778	similar to cornichon-like protein (predicted)
74.9	91.9	-0.815016322	preproenkephalin, related sequence

Neural factor

11.5	6.8	-1.691176471	loop tail associated protein (predicted)
21.3	15.7	-1.356687898	synaptonemal complex protein SC65
24.4	15	-1.626666667	solute carrier family 1
61.5	51.5	-1.194174757	huntingtin-associated protein 1
107.5	93	-1.155913978	internexin, alpha

Immune, inflammatory and stress

6.2	1.4	-4.428571429	prostaglandin-endoperoxide synthase 2
12.5	20.5	-0.609756098	interleukin 18
13.5	12.4	-1.088709677	prostaglandin-endoperoxide synthase 1
16.8	15.6	-1.076923077	complement component 3
20.7	28.8	-0.71875	interleukin 2 receptor, beta chain
25.3	33.9	-0.746312684	sequestosome 1
26.5	21.7	-1.221198157	interleukin 2 receptor, gamma
29.4	14.8	-1.986486486	carbonic anhydrase 3
45.6	29	-1.572413793	Lymphocyte antigen 68

Cell cyle

12.4	13.9	-0.892086331	hemogen
12.8	11.6	-1.103448276	epiregulin
15.8	16	-0.9875	cell division cycle 20 homolog (S. cerevisiae)
20.4	5.4	-3.777777778	fibroblast growth factor 7
22.8	33	-0.690909091	myelocytomatosis viral oncogene homolog (avian)
23.6	31.9	-0.739811912	murine thymoma viral (v-akt) oncogene homolog 2
25.9	17.2	-1.505813953	wee 1 homolog (S. pombe) (predicted)
26.4	17.8	-1.483146067	betacellulin
28.2	25.7	-1.097276265	RAD50 homolog (S. cerevisiae)
37.1	32.1	-1.15576324	v-ets erythroblastosis virus E26 oncogene homolog 1
37.5	32.7	-1.146788991	CCA2 protein
40.8	36.2	-1.127071823	brain expressed myelocytomatosis oncogene

Replication, transcription, protein modification, degradation machinery

7.1	7.3	-0.97260274	ATP-binding cassette, sub-family B (MDR/TAP)
7.6	4.8	-1.583333333	MAD homolog 7 (Drosophila)
9.2	7.4	-1.243243243	epidermal growth factor
9.2	6.6	-1.393939394	paternally expressed 3 (predicted)
9.2	1.3	-7.076923077	similar to KIAA1074 protein (predicted)
9.6	7.5	-1.28	spermatogenesis associated 9 (predicted)

10.9	19.9	-0.547738693	RAR-related orphan receptor alpha (predicted)
11	11	-1	Isoleucine-tRNA synthetase (predicted)
11.1	15.6	-0.711538462	matrix metallopeptidase 3
11.4	13.8	-0.826086957	Double-stranded RNA-binding protein p74
11.9	9.9	-1.202020202	peptidylglycine alpha-amidating monooxygenase
12.1	9.6	-1.260416667	Ubiquitin specific protease 25 (predicted)
13.1	12.3	-1.06504065	Ring finger protein 149 (predicted)
13.2	14.6	-0.904109589	meprin 1 alpha
13.5	17.8	-0.758426966	transcription factor 12
14	9.7	-1.443298969	nuclear receptor subfamily 1, group D, member 2
14.4	21.9	-0.657534247	WD repeat domain 10 (predicted)
14.4	13	-1.107692308	serum amyloid P-component
14.6	16.8	-0.869047619	receptor-interacting serine-threonine kinase 3
14.7	9.2	-1.597826087	Upstream transcription factor 2
15.4	14.8	-1.040540541	DnaJ (Hsp40) homolog, subfamily C
16.5	9.3	-1.774193548	similar to 1500031N24Rik protein (predicted)
16.6	10.5	-1.580952381	thyroid hormone responsive protein
17.4	11.4	-1.526315789	Sp1 transcription factor
17.4	6.1	-2.852459016	Protocadherin 1 (cadherin-like 1) (predicted)
17.9	16.2	-1.104938272	carboxypeptidase X 1 (M14 family) (predicted)
18.9	19.6	-0.964285714	GATA binding protein 4
19.5	8.5	-2.294117647	protein tyrosine phosphatase, non-receptor type 6
19.6	17.2	-1.139534884	ankyrin repeat and SOCS box-containing protein 2
19.6	15.8	-1.240506329	discs, large homolog 4 (Drosophila)
19.8	11.5	-1.72173913	caspase 1
20	10.7	-1.869158879	a disintegrin and metalloprotease domain 2
21.2	24.6	-0.861788618	protein serine kinase H1 (predicted)
21.4	13.7	-1.562043796	Glycogen synthase kinase 3 alpha
21.9	24	-0.9125	mannan-binding lectin serine peptidase 1
22.3	21.4	-1.042056075	amyloid beta (A4) precursor protein-binding
22.6	23.5	-0.961702128	early growth response 3
22.8	22.7	-1.004405286	putative regulation protein GS3
23	16.7	-1.377245509	endothelin 1
23.2	18.7	-1.240641711	upstream binding transcription factor
23.3	21.4	-1.088785047	RNA polymerase 1-2
23.5	27.6	-0.851449275	Rab geranylgeranyl transferase, a subunit
23.5	21.3	-1.103286385	serine/threonine kinase 38 (predicted)
23.7	26	-0.911538462	Ubiquitin-conjugating enzyme E2Q (putative)
24.5	11	-2.227272727	POU domain, class 2, transcription factor 3
25.8	9	-2.866666667	nuclear receptor subfamily 4, group A, member 2
26.2	21.3	-1.230046948	potassium voltage-gated channel
26.8	20.4	-1.31372549	T-box 2 (predicted)
26.8	17.8	-1.505617978	tripartite motif protein 47 (predicted)
29	21.4	-1.355140187	Similar to E430002G05Rik protein (predicted)
29.2	25.1	-1.163346614	signal transducer and activator of transcription 5B
29.5	23.7	-1.244725738	SNF1-like kinase
29.7	40.1	-0.740648379	Copine V (predicted)
30.4	21.6	-1.407407407	peptidyl arginine deiminase, type I
32.8	28	-1.171428571	myeloid/lymphoid or mixed-lineage leukemia
39	38.5	-1.012987013	TAP binding protein
40.3	34.5	-1.168115942	a disintegrin-like and metalloprotease
42.4	33.7	-1.258160237	protein kinase C binding protein 1 (predicted)
43.9	56.8	-0.772887324	signal transducer and activator of transcription 5A
46.6	41.9	-1.112171838	Forkhead box K2 (predicted)
47.7	28.2	-1.691489362	membrane metallo endopeptidase

56.3	36.1	-1.559556787	similar to RIKEN cDNA 1110020A23 (predicted)
56.4	26.8	-2.104477612	ankyrin repeat domain 10 (predicted)
61.1	53.5	-1.142056075	Transcription elongation factor B (SIII)
75.7	73.5	-1.029931973	dual specificity phosphatase 14 (predicted)
80.9	71.1	-1.137834037	tissue specific transplantation antigen P35B
85.3	103.8	-0.82177264	general transcription factor III C 1

Synthesis, transport, biochemical pathway

2.8	4.4	-0.636363636	ATPase, Na+/K+ transporting, beta 3 polypeptide
7.1	1.4	-5.071428571	Similar to hypothetical protein CL25084 (predicted)
9.9	5.9	-1.677966102	Solute carrier family 6
11.1	6	-1.85	ATP-binding cassette
11.4	1.4	-8.142857143	solute carrier family 9, member 4
11.7	10.3	-1.13592233	gamma-aminobutyric acid receptor, subunit beta 2
11.9	13.8	-0.862318841	Tetratricopeptide repeat domain 8 (predicted)
12.5	8.5	-1.470588235	gap junction membrane channel protein alpha 1
12.7	8.6	-1.476744186	ataxia, cerebellar, Cayman type (caytaxin)
13.3	6.4	-2.078125	solute carrier family 4
13.5	12.8	-1.0546875	Sorting nexin associated golgi protein 1 (predicted)
14	14.2	-0.985915493	solute carrier family 9, member 3
14.4	8.6	-1.674418605	solute carrier family 7
14.7	9	-1.633333333	potassium voltage gated channel
16	13.4	-1.194029851	potassium channel, subfamily K, member 15
16.9	9.6	-1.760416667	ATP-binding cassette
17.5	17.1	-1.023391813	chloride channel 2
17.5	9.4	-1.861702128	sorting nexin associated golgi protein 1 (predicted)
17.8	25.8	-0.689922481	solute carrier family 12
18.4	17.1	-1.076023392	solute carrier family 26 (sulfate transporter)
20.1	9.6	-2.09375	ATP-binding cassette, sub-family C (CFTR/MRP)
20.3	29.1	-0.697594502	ATPase, Ca++ transporting, plasma membrane 2
22.7	13.4	-1.694029851	potassium inwardly-rectifying channel
23.7	18.5	-1.281081081	potassium inwardly-rectifying channel
25.1	12	-2.091666667	glutamate receptor, ionotropic, kainate 2
27.1	22.9	-1.183406114	potassium inwardly-rectifying channel
28.1	21.3	-1.319248826	cadherin 17
30	22.4	-1.339285714	potassium intermediate/small conductance calcium-activated channel
34.2	26.5	-1.290566038	activin A receptor, type 1
34.2	24	-1.425	glutamate receptor, ionotropic, kainate 5
35.4	52.8	-0.670454545	potassium inwardly-rectifying channel
40.1	27	-1.485185185	potassium inwardly-rectifying channel
56.7	46.8	-1.211538462	insulin-like growth factor 2 receptor
58.1	50.3	-1.155069583	potassium voltage gated channel

Miscellaneous

3.5	2	-1.75	glutamate oxaloacetate transaminase 2
6.2	7.4	-0.837837838	dimethylglycine dehydrogenase precursor
7.8	8.1	-0.962962963	Cytochrome P450 IIA1
8.4	9.6	-0.875	leptin receptor
8.5	3.4	-2.5	arylacetamide deacetylase (esterase)
9.2	7.4	-1.243243243	epidermal growth factor
9.3	9.9	-0.939393939	Similar to helicase-like protein NHL isoform 2
9.5	10.6	-0.896226415	FMS-like tyrosine kinase 1
9.8	9	-1.088888889	solute carrier family 2 (facilitated glucose transporter)
10.2	11.7	-0.871794872	Similar to KIAA1161 protein (predicted)
10.4	15.2	-0.684210526	hematopoietically expressed homeobox

10.7	13.9	-0.769784173	similar to RIKEN cDNA 1700073K01 (predicted)
11.5	5.9	-1.949152542	solute carrier family 6 (neurotransmitter transporter)
12.5	9.5	-1.315789474	paired box gene 6
12.6	22.5	-0.56	desmin
12.8	12.3	-1.040650407	troponin T3, skeletal, fast
12.9	4.5	-2.866666667	cytochrome P450, family 2, subfamily c, polypeptide 7
13.5	11.7	-1.153846154	Coagulation factor XIII, A1 subunit
13.6	13	-1.046153846	KH-type splicing regulatory protein
13.8	8.1	-1.703703704	solute carrier family 34 (sodium phosphate)
14.2	9.8	-1.448979592	20 alpha-hydroxysteroid dehydrogenase
14.4	10.6	-1.358490566	triadin
14.5	1.9	-7.631578947	nucleoporin 133 (predicted)
15.9	14.8	-1.074324324	dopa decarboxylase
16	13.2	-1.212121212	cytochrome P450, family 4
16.7	12.9	-1.294573643	regenerating islet-derived 3 alpha
16.8	17.7	-0.949152542	neuraminidase 3
16.8	4.5	-3.733333333	zinc finger, FYVE domain containing 20 (predicted)
17.2	17.7	-0.971751412	thyroglobulin
17.5	23	-0.760869565	tropomodulin 4 (predicted)
18.7	9.1	-2.054945055	phosphoribosyl pyrophosphate synthetase 2
18.8	15.7	-1.197452229	Similar to flavoprotein oxidoreductase MICAL2
19.2	21.5	-0.893023256	exostoses (multiple)-like 3
20.6	32.3	-0.637770898	polycystic kidney disease 1 homolog
21.1	15.6	-1.352564103	fructose-1,6-bisphosphatase 2
21.3	22.9	-0.930131004	ATP-binding cassette, sub-family B (MDR/TAP)
21.7	19.4	-1.118556701	cytosolic acyl-CoA thioesterase 1
22.2	15.3	-1.450980392	Similar to PS1D protein
22.8	7.3	-3.123287671	insulin receptor
24.8	14.3	-1.734265734	kynureninase (L-kynurenine hydrolase)
27.6	28.1	-0.982206406	3-hydroxybutyrate dehydrogenase
27.6	10.9	-2.532110092	phospholipase A2, group X
30.5	16.6	-1.837349398	similar to 2610033H07Rik protein (predicted)
32.1	24.9	-1.289156627	CUG triplet repeat,RNA-binding protein 2
32.2	23.1	-1.393939394	intersectin 1
32.3	33.3	-0.96996997	SH3-domain GRB2-like 1
34.3	24.1	-1.423236515	Synaptonemal complex protein 3
35.1	20.2	-1.737623762	activating transcription factor 3
36.9	23.2	-1.590517241	RNA binding motif protein 7 (predicted)
37.1	40	-0.9275	similar to RIKEN cDNA 0610042E07 (predicted)
37.7	45.5	-0.828571429	spermatogenesis associated 2
37.8	29.6	-1.277027027	N-deacetylase/N-sulfotransferase
38.2	22.1	-1.728506787	B7 homlog 3
38.5	37.5	-1.026666667	UDP-Gal:betaGlcNAc beta 1,4- galactosyltransferase
39.6	34.4	-1.151162791	Cdc42 guanine nucleotide exchange factor (GEF) 9
40	30.5	-1.31147541	phosphorylase kinase alpha 1
40.2	50.3	-0.799204771	phosphoenolpyruvate carboxykinase 2
42.9	18	-2.383333333	folate receptor 1 (adult)
43.4	35.7	-1.215686275	SECIS binding protein 2
43.8	41.8	-1.04784689	Best5 protein
44.9	30.5	-1.472131148	trimethyllysine hydroxylase, epsilon
45.2	44.5	-1.015730337	protein phosphatase 1
48.3	47.8	-1.010460251	dynein, axonemal, light chain 4 (predicted)
48.4	36.9	-1.311653117	cystathionine beta synthase
50.1	48.7	-1.028747433	low density lipoprotein receptor-related protein 1
58.2	36.9	-1.577235772	creatine kinase, muscle

68	41	-1.658536585	ABO blood group (transferase A)
81.3	62.9	-1.292527822	Lysosomal phospholipase A2
91	51.1	-1.780821918	dentatorubral pallidoluysian atrophy

Appendix 4.2 Absent to Present Gene List in Different Functional Groups

Mock	Infect	Fold Change	Gene Title
Cell adhesion and structure			
3.9	9	2.307692308	nephrosis 1 homolog, nephrin (human)
13.5	11.9	0.881481481	keratin complex 1, acidic, gene 19
26.8	42	1.567164179	dynein, cytoplasmic, light intermediate chain 1
28.7	35	1.219512195	epithelial V-like antigen (predicted)
29.4	44.8	1.523809524	opioid-binding protein
31.9	32.6	1.021943574	LOC498010
50.5	41.4	0.81980198	scavenger receptor class B, member 1
54.6	62	1.135531136	breast cancer anti-estrogen resistance 1
Signal transduction: receptors, kinases, phosphatases, G-proteins			
5.3	13.1	2.471698113	glutamate receptor, metabotropic 8
9.4	15.8	1.680851064	rhodopsin
9.9	12.6	1.272727273	phosphodiesterase 11A
12.6	10.9	0.865079365	gastrin releasing peptide receptor
13.1	15.7	1.198473282	olfactory receptor 857 (predicted)
15.1	20.4	1.350993377	somatostatin receptor 5
15.3	18.4	1.202614379	angiotensin II receptor, type 1 (AT1A)
19.8	22.6	1.141414141	5-hydroxytryptamine (serotonin) receptor 4
21	17	0.80952381	prostaglandin F receptor
21.7	23	1.059907834	inositol 1,4,5-trisphosphate 3-kinase A
22.1	24	1.085972851	smoothened homolog (Drosophila)
33.8	22.4	0.662721893	regulator of G-protein signaling 12
41.2	54.8	1.330097087	protein tyrosine phosphatase
41.8	50.4	1.205741627	guanine nucleotide binding protein
103.8	129.4	1.246628131	phosphatidylinositol 3-kinase
Immune and stress response			
7.3	10.8	1.479452055	phospholipid scramblase 1
11.6	10.9	0.939655172	inducible T-cell co-stimulator
18.8	20.4	1.085106383	Fc receptor, IgG, low affinity III
25.8	56.7	2.197674419	vitronectin
Neural factor			
6.2	9	1.451612903	synaptosomal-associated protein 29
8.4	10.7	1.273809524	gamma-aminobutyric acid (GABA) receptor
19.1	13.7	0.717277487	Lactalbumin, alpha
Cell cycle, development, apoptosis, transcription factors			
7.7	15.4	2	RAS guanyl releasing protein 2
8.4	21.5	2.55952381	aurora kinase B
10.1	12.3	1.217821782	Bcl2-like 1
13.2	13.9	1.053030303	pro-platelet basic protein
14	13	0.928571429	protein kinase, cGMP-dependent, type II
20.5	28.4	1.385365854	phosphatidylinositol 3-kinase
25.1	30.9	1.231075697	cell division cycle 20 homolog
25.2	34	1.349206349	biregional cell adhesion molecule-related
27.6	37.8	1.369565217	TNFRSF1A-associated via death domain
36.1	51	1.412742382	histone deacetylase 7
37.2	46	1.23655914	Murine thymoma viral (v-akt) oncogene

Replication, transcription, protein modification

5	13.4	2.68	clock homolog (mouse)
5.1	8.6	1.68627451	SMAD, mothers against DPP homolog 5
6.1	17.4	2.852459016	forkhead box E1
6.3	13.8	2.19047619	PHD finger protein 7 (predicted)
7.6	23.7	3.118421053	zinc finger protein 535 (predicted)
8.5	13.3	1.564705882	camello-like 3
8.8	12.9	1.465909091	Similar to Myosin light chain kinase 2
10.5	16.6	1.580952381	Actin related protein 2/3 complex
11.1	12	1.081081081	nuclear receptor subfamily 0, group B
11.9	13	1.092436975	transcription factor 7, T-cell specific
12.5	13.5	1.08	Ribophorin II
12.6	12.1	0.96031746	transient receptor protein 6
12.8	16.7	1.3046875	calcium/calmodulin-dependent protein kinase IV
15.9	26.2	1.647798742	Janus kinase 3
18	25.7	1.427777778	protein phosphatase 1F
18.1	18.8	1.038674033	polymerase (DNA directed), alpha 2
19.8	19.7	0.994949495	cell division cycle 34 homolog
20.8	22.9	1.100961538	protein tyrosine phosphatase
22.5	18.5	0.822222222	Mitogen activated protein kinase 2
27.2	31.7	1.165441176	transcription elongation factor A (SII)
29.6	26.6	0.898648649	secreted frizzled-related protein 4
30.4	31	1.019736842	ATPase family, AAA domain containing 3A
34.7	46.8	1.34870317	Leucyl-tRNA synthetase, mitochondrial
35.2	51.2	1.454545455	transmembrane 4 superfamily member 7
36	47.6	1.322222222	Fas death domain-associated protein
39.5	53.1	1.344303797	nucleoporin 54
41.6	54.9	1.319711538	heparanase
42.8	34.1	0.796728972	forkhead box D4
49.5	44.9	0.907070707	protein tyrosine phosphatase
49.6	37	0.745967742	TATA element modulatory factor 1
62.8	68.4	1.089171975	myeloid ecotropic viral integration site-related gene 2
68.2	42.3	0.620234604	glucocorticoid modulatory element binding protein 2
68.2	42.3	0.620234604	glucocorticoid modulatory element binding protein 2

Synthesis, transport and biochemical pathways

5.2	10.2	1.961538462	cation channel, sperm associated 2
5.5	13.8	2.509090909	KH-type splicing regulatory protein
5.7	5.9	1.035087719	potassium voltage gated channel
11.3	16.4	1.451327434	hephaestin
12.7	12.3	0.968503937	potassium voltage gated channel
13	20.1	1.546153846	gamma-aminobutyric acid (GABA-A) receptor
13.8	10.4	0.753623188	syntaxin 17
15.6	12.5	0.801282051	glutamate receptor, ionotropic
16.8	17.2	1.023809524	aquaporin 6
19.9	29.4	1.477386935	Solute carrier family 14 (urea transporter)
23.6	36.6	1.550847458	Solute carrier family 6
23.7	34.9	1.47257384	potassium channel, subfamily K
23.8	28	1.176470588	solute carrier family 31 (copper transporters)
33.3	34.3	1.03003003	Solute carrier family 22
33.8	26.1	0.772189349	glutamate receptor, ionotropic, 2
38.8	38.5	0.992268041	ATP-binding cassette
51.3	105.8	2.062378168	cholinergic receptor, nicotinic

Miscellaneous

2.8	46	16.42857143	ubiquitin-activating enzyme E1-domain
5.5	7.2	1.309090909	lipase, hepatic
5.7	8.2	1.438596491	3-alpha-hydroxysteroid dehydrogenase
6.7	15	2.23880597	SNM1-like
7	14.6	2.085714286	acyl-Coenzyme A oxidase 2
7.4	13	1.756756757	homeo box A2
7.8	9.1	1.166666667	cd36 antigen
8.1	18.2	2.24691358	alpha-2-HS-glycoprotein
9.1	8.3	0.912087912	surfactant, pulmonary-associated protein A1
10.4	12.7	1.221153846	cytochrome P450, subfamily 2G
11.4	20.4	1.789473684	phosphorylase kinase gamma 1
14.5	15.6	1.075862069	enolase 3, beta
14.8	9.7	0.655405405	Similar to RN49018 (predicted)
16.1	23.4	1.453416149	FtsJ homolog 2 (E. coli) (predicted)
16.3	20.9	1.282208589	growth hormone receptor
17.6	30.5	1.732954545	RAS-related C3 botulinum substrate 2
17.7	22.3	1.259887006	cytochrome b-245, beta polypeptide
19.4	32.6	1.680412371	fibromodulin
21.3	26.8	1.258215962	peroxisomal biogenesis factor 6
22.3	16.2	0.726457399	elastin
22.3	25.6	1.147982063	beta-1,3-glucuronyltransferase 1
30.1	31.9	1.059800664	stanniocalcin 1
30.9	45.9	1.485436893	thioredoxin reductase 2
37.2	28.1	0.755376344	Hexosaminidase B (predicted)
40.8	39.1	0.958333333	cytochrome P450 4F6
51	47.7	0.935294118	THO complex 3 (predicted)
65.7	77.5	1.179604262	fatty acid desaturase 2
68.4	61.3	0.89619883	RNA, U3 small nucleolar interacting protein 2
96	79.9	0.832291667	carnitine palmitoyltransferase 2